“Analysis of the rice response to suboptimal temperatures: an integrated approach”

Student: Ayelén Gázquez

Supervisor from UNLP: Andrés Alberto Rodríguez

Supervisor from UA: Gerrit T.S. Beemster

Year: 2017

THESIS PRESENTED AS PART OF A DOUBLE PHD TO OBTAIN THE DIPLOMAS OF:

-**Doctor de la Facultad de Ciencias Exactas** – Área Ciencias Biológicas [Doctor from the Faculty of Exact Sciences – Biologic Sciences area] (UNIVERSIDAD NACIONAL DE LA PLATA)

-**Doctor in de wetenschappen: biologie** [Doctor of Science: Biology] (UNIVERSITEIT ANTWERPEN)

FACULTAD DE CIENCIAS EXACTAS

DEPARTAMENTO DE CIENCIAS BIOLÓGICAS

Trabajo de Tesis Doctoral:

"Análisis de la respuesta del arroz a temperaturas subóptimas: un enfoque integrado"

Tesista: *Ayelén Gázquez*

Director: *Andrés Alberto Rodríguez*

Director: *Santiago Javier Maiale*

Co-Directora: *Mónica Laura Casella*

Año: *2017*

The present doctoral thesis to obtain the degrees of: ***Doctor de la Facultad de Ciencias Exactas – Área Ciencias Biológicas***; and ***Doctor in de wetenschappen: biologie***; has been majorly realized at the **Instituto de Investigaciones Biotecnológicas – Instituto Tecnológico de Chascomús (IIB-INTECH)** in the group **Laboratorio de Fisiología del Estrés Abiótico en Plantas** in Argentina. A year of the research has been done at the **Department of Biology** of the **Universiteit Antwerpen** in the group **Inegrated Molecular Plant Physiology Research (IMPRES)** in Belgium. The participation in both groups lead to a **double PhD** agreement between the **UNLP** and the **UA**. This work was done under the supervision of Andrés Alberto Rodriguez and Santiago Javier Maiale and the co-supervision of Mónica Laura Casella at the UNLP, and the supervision of Gerrit T.S. Beemster at the UA.

CONICET

UNIVERSIDAD NACIONAL DE SAN MARTÍN

IIB-INTECH

Universiteit Antwerpen

ACKNOWLEDGMENTS

At the end of my Thesis, I have to pleasantly thank many people that contributed in many ways in order this work to be successful. I cannot start with others than my family and friends who sometimes supported me from more than a thousand kilometers away and sometimes even more. It was not without them and the strong support of my country, Argentina, that I could have studied Biotechnology. In that way, I have to be grateful to my home University, the *Universidad Nacional de La Plata* (UNLP), and particularly the *Facultad de Ciencias Exactas*, where I grow up for many years and where I found the ones that now I call my best friends and to whom I also am really grateful. The UNLP is more than the place where I studied, it is also the place where I work and where I became the professional I am now. I have to thank a lot to the chair where I teach, *Química Analítica Instrumental*, where I learned a lot and where I found support along my PhD studies. Special thanks have to be given to Mónica Casella, who is not only the Professor in charge but it was also my co-Supervisor in this Thesis. Besides, she was always my support by all ways means, as researcher, as a Professor, and as a counselor. Of course I cannot leave aside my partners, and my students –sorry for my mistakes!

During my PhD my Supervisors became also part of my family. Andrés Rodríguez and Santiago Maiale welcomed me some time ago around 2011 in the *Laboratorio del Estrés Abiótico en Plantas* at the IIB-INTECH. I cannot be more thankful to find you since you have guide me through this process in the best way a supervisor can do it. You always supported me in all of my decisions, even if they were wrong –quiet often by the way!-. I never felt uncomfortable in the lab and we have great anecdotes to tell. Of course I have to thank all the crew in the lab! Without you it would not have been that fun! And of course thanks for your inputs in my Thesis! I cannot forget about Ana Menéndez and Oscar Ruíz that always supported me and help me with everything I needed, even if it had nothing to do with science.

The *Univesrity of Antwerp* (UA) was my second University, where I also found lots of great people and, of course, people that I sum up to my best friends list. Being in another country is not easy, but Prof. Gerrit T.S. Beemster welcomed me in his lab. The IMPRES group is not only a great place to work where you can learn lot of stuff, but also where you can find the best people from all around the world. I have my best memories with you! Thank you guys! Не ме пипай! I know we will see each other again.

My PhD could not have been possible without the support of CONICET that gave me the grant to make it. I hope my country never gives up on science because it is the only way we can improve our quality life. Many other institutions have helped me through this process with other grants and I have to thank them: the *Agencia Nacional de Promoción y Tecnología* (PICT 2010-1066; PICT Start Up 2013-0399) for founding my research; the *Academic Mobility for Inclusive Development in Latin America ERASMUS Mundus Action 2* that gave a fellowship for doing my research at the UA; the UA for giving me another grant, DOCPRO, to finish that research; IIB-INTECH for letting me do my research there and even live there for a while. Many people also helped me with different parts of my research, I am thankful to all of you. I cannot forget someone that helped me a lot, someone that opened the portals of knowledge and made them free: Alexandra Elbakyan, without you no Thesis is possible nowadays!

Last but not least, I thank you that are reading my Thesis. You have to be included in this list because it was not other than for you that I wrote this big long manuscript. I hope you enjoy it and find answers and doubts along it. And remember…

"…the works of the imagination always have a point of contact with the reality"

La mujer de piedra in *Rimas y leyendas*, Gustavo Adolfo Bécquer (1871)
(from the original *"las obras de la imaginación tienen siempre algún punto de contacto con la realidad"*)

This Thesis has been partially published in the next journals and congress proceedings:

2017. Gázquez A and Beemster GTS. *What determines organ size differences between species? A meta-analysis of the cellular basis*. New Phytologyst. **doi**: 10.1111/nph.14573

2016. Gázquez A, Checovich ML, Maiale S, Rodríguez A, Beemster G. *Diferentes estrategias del crecimiento de hojas de cultivares de arroz a temperaturas subóptimas: un punto de vista celular.* Summary and poster in XXXI Reunión Argentina de Fisiología Vegetal, Corrientes, Argentina.

2015. Gázquez A, Maiale SJ, Rachoski MM, Vidal A, Ruíz OA, Menéndez AB, and Rodriguez AA. *Physiological response of multiple contrasting rice (Oryza sativa L.) cultivars to suboptimal temperatures*. J Agron Crop Sci **201**: 117–127

2014. Gázquez A, Maiale SJ, Bezus R, Menéndez AB, and Rodriguez AA. *Análisis transcripcional de la respuesta al estrés por temperaturas subóptimas en arroz (Oryza sativa, L.) en dos cultivares contrastantes*. Summary and poster in XV Congreso Latinoamericano de Fisiología Vegetal - XXX Reunión Argentina de Fisiología Vegetal (XV CLAFV – XXX RAFV), Buenos Aires, Argentina.

2014. Gázquez A, Maiale SJ, Vidal A, Ruíz OA, Menéndez AB, y Rodriguez AA. *Análisis del comportamiento fisiológico de múltiples cultivares de arroz contrastantes en condiciones de temperaturas subóptimas*. Summary and poster in XV Congreso Latinoamericano de Fisiología Vegetal -XXX Reunión Argentina de Fisiología Vegetal (XV CLAFV – XXX RAFV), Buenos Aires, Argentina.

2012. Gázquez A, Bonfiglio N, Rodriguez A, Maile S, Bezus R, Vidal A, and Ruíz O. *Caracterización fisiológica y molecular de germoplasma de arroz (Oryza sativa) de uso en Argentina sometido a estrés por frío*. Summary and poster in XXIX Reunión Argentina de Fisiología Vegetal (XXIX RAFV), Buenos Aires, Argentina.

SUMMARY

Rice (*Oryza sativa* L.) is one of the most important cereal crops in the global food system feeding nearly half the world's population and its cultivation, processing and trade represents one of the biggest economic activities on Earth. During the months of culture the temperatures are optimal (28-30 °C) for rice but high frequencies of suboptimal temperatures are observed. Although some early studies demonstrated that rice growth rate and metabolism are noticeably inhibited in the range of 15-20 °C, the physiological bases for rice growth delay by suboptimal temperatures remain fairly unexplored. Hence, the aim of this Thesis was to study the response of rice seedlings from contrasting cultivars to suboptimal temperatures of growth at different organization levels and elucidate some mechanisms related with tolerance.

In order to achieve our goal we designed a screening method for detecting variability in sensitivity among rice cultivars at the seedling stage subjected to suboptimal temperatures usually found in the field (13/21 °C d/n, Entre Ríos, Argentina). This method was based on the reduction of the growth of the third leaf and it had some advantages, for instance, it was specifically designed for testing suboptimal temperatures, it was a quick method easy to set up in a growth chamber where multiple cultivars can fit at once, and it is quantitative. It is noteworthy that the measurements done in growth chambers were highly correlated with the ones in the field, pointing out that the proposed system was able to predict what happened in the field and so it works as a model system of the stress.

The main characteristic of the suboptimal temperatures stress was the reduction of the seedling growth at the shoot as well as at the leaf level. The growth analysis of the fourth leaf together with the transcriptome, proteome and redox system analyses accorded that processes related with cell division were inhibited and that damage occurred in the division zone so enzymatic antioxidant systems were triggered in this zone as a response. The diminution of growth was associated with a detriment of the Photosystem II evidenced in fast-transient chlorophyll analyses that impacted also in the photosynthetic rate and stomata conductance. Besides, carbon assimilation, storage and usage were also compromise. Different comparative analysis between tolerant and sensitive cultivars allowed us to distinguish some responses to the stress that could be associated with its variability in sensitivity. Hence, we associated the tolerance against suboptimal temperatures stress with the capacity of maintaining a healthy photosynthetic apparatus, the protection of the meristematic zone that leads cell division rate, and the balance between carbon storage and usage. For first time we

here described the major effects of the suboptimal temperatures stress in rice seedlings and detected possible mechanism of tolerance that should be further studied. This work will help to design future strategies for stacking tolerant mechanisms that will help in the obtaining of high yield cultivars that perform better under this stress. The creation of new marker assisted breeding programs could be a good way to address this issue and, hence, genome-wide association studies based on the described mechanism could help for finding new markers.

RESUMEN

El arroz (*Oryza sativa* L.) es uno de los cultivos de cereales más importantes en el sistema de alimentos mundial alimentando cerca de la mitad de la población del mundo y su cultivo, procesado y comercio representa una de las actividades económicas más importantes en la Tierra. Durante los meses de cultivo las temperaturas son óptimas (28-30 °C) para el arroz pero altas frecuencias de temperaturas subóptimas son observadas. A pesar de que algunos estudios tempranos demostraron que la velocidad de crecimiento del arroz y su metabolismo son notablemente inhibidos en el rango de 15-20 °C, las bases fisiológicas del retraso del crecimiento del arroz permanecen bastante inexploradas. Por lo tanto, el objetivo de esta Tesis fue estudiar la respuesta de plántulas de arroz de cultivares contrastantes a temperaturas subóptimas de crecimiento a diferentes niveles organizacionales y dilucidar algunos mecanismos relacionados con su tolerancia.

Con el fin de lograr nuestro objetivo, diseñamos un método de *screening* para detectar variabilidad en sensibilidad entre cultivares de arroz en el estadío de plántula sometidos a temperaturas subóptimas típicamente encontradas en el campo (13/21 °C d/n, Entre Ríos, Argentina). Este método se basó en la reducción del crecimiento de la tercer hoja y tuvo algunas ventajas, por ejemplo, fue específicamente diseñado para probar temperaturas subóptimas, fue un método rápido fácil de montar en una cámara de crecimiento donde múltiples cultivares pueden caber a la vez, y es cuantitativo. Es de destacar que las mediciones realizadas en las cámaras de crecimiento fueron sumamente correlacionadas con las realizadas en el campo, destacando que el sistema propuesto pudo predecir lo que sucedió en el campo y por lo tanto funciona como un sistema modelo del estrés.

La principal característica del estrés por temperaturas subóptimas fue la reducción del crecimiento de la plántula a nivel de vástago como así también a nivel de la hoja. El análisis de crecimiento de la cuarta hoja junto con los análisis del transcriptoma, proteoma y sistema redox coincidieron en que los procesos relacionados con la división celular fueron inhibidos y que el daño ocurrió en la zona de división generando la activación de sistemas antioxidantes enzimáticos en esta zona como respuesta. La disminución del crecimiento fue asociada con el daño del fotosistema II evidenciado en el análisis rápido de fluorescencia transiente de la clorofila y que impactó, además, en la velocidad de fotosíntesis y la conductancia estomática. Por otra parte, la asimilación, almacenamiento y uso de carbono estuvieron comprometidos. Diferentes estudios comparativos entre cultivares tolerantes y sensibles nos permitieron distinguir algunas

respuestas al estrés que pudieron ser asociadas con su variabilidad en sensibilidad. Por lo tanto, nosotros vinculamos la tolerancia al estrés por temperaturas subóptimas con la capacidad de mantener un aparato fotosintético son, la protección de la zona meristemática que realiza la división celular, y el balance entre la asimilación de carbono, su almacenamiento y su uso. Por primera vez aquí describimos los efectos más importantes del estrés por temperaturas subóptimas en plántulas de arroz y pudimos detectar posibles mecanismos asociados a su tolerancia que deberían ser más ampliamente estudiados. Este trabajo ayudará en el diseño de futuras estrategias para apilar mecanismos de tolerancia que permitirán obtener cultivares de alto rendimiento con mejor desempeño bajo este estrés. La creación de nuevos programas de mejoramiento asistido por marcadores podría ser un buen modo para abordar esta problemática y, en consecuencia, los estudios basados en la asociación del genoma completo en base a los mecanismos descriptos podrían ayudar en encontrar nuevos marcadores.

SAMENVATTING

Globaal gezien is rijst (*Oryza sativa* L.) is één van de belangrijkste graangewassen. Het voorziet bijna de helft van de wereldpopulatie van voedsel en de teelt, verwerking en handel behoren tot één van de grootste economische activiteiten op aarde. Tijdens het teeltseizoen zijn de temperaturen voor rijst optimaal (28-30°C), maar toch worden er vaak suboptimale temperaturen waargenomen. Hoewel eerdere studies aantoonden dat de groeisnelheid en het metabolisme van rijst geïnhibeerd worden in de temperatuurrange van 15-20°C, is de fysiologische basis voor deze verminderde groei bij suboptimale temperaturen nog niet echt bestudeerd. Daarom werd in deze thesis het effect van suboptimale temperaturen op de groei van rijstzaailingen van verschillende cultivars bestudeerd en dit in verschillende stadia van ontwikkeling. Hierdoor zullen de onderliggende mechanismen gerelateerd aan stress tolerantie beter begrepen worden.

Hiervoor werd een screening methode ontwikkeld die de variatie in de gevoeligheid voor de typische suboptimale temperaturen die in het veld te meten zijn (13/21°C d/n, Entre Ríos, Argentina) detecteert tijdens het zaailingstadium van verschillende rijstcultivars. Deze methode is gebaseerd op de afname in groei van het derde blad en heeft enkele voordelen. Zo is het specifiek ontwikkeld om suboptimale temperaturen te testen, is het kwantitatief en is het een snelle methode die men gemakkelijk in een groeikamer kan gebruiken waarin verschillende cultivars tegelijkertijd kunnen groeien. Belangrijk op te merken is dat de metingen die gebeurden in de groeikamer een sterke correlatie vertonen met degenen in het veld. Dit duidt erop dat het voorgestelde systeem in staat was om te voorspellen wat er in het veld zou gebeuren en daarom werkt het als een modelsysteem voor deze stress.

Het opmerkelijkste kenmerk voor suboptimale temperatuurstress in zaailingen was de afname in de groei van zowel scheut als blad. De groeianalyse van het vierde blad, samen met de transcriptoom-, proteoom- en redoxsysteemanalyse, wezen op een inhibitie van celdeling gerelateerde processen. Verder werd schade vooral in de delingszone toegebracht waardoor in deze zone het enzymatische antioxidantsysteem werd getriggerd. De vermindering in groei was geassocieerd met schade aan Photosysteem II, wat werd aangetoond door fast-transient chlorofylanalyses. Deze schade had op zijn beurt een invloed op de fotosynthesesnelheid, stomatale geleidbaarheid, koolstof assimilatie, -opslag en -verbruik. Uit verschillende vergelijkende analyses tussen tolerante en gevoelige cultivars, konden we observeren hoe de respons op de stress geassocieerd was met de variatie in sensitiviteit. Hieruit

konden we besluiten dat de tolerantie ten opzichte van suboptimale temperaturen samenhangt met de capaciteit om een goed functionerend fotosynthetisch apparaat te onderhouden, om de meristematische zone te beschermen en om de balans tussen koolstofopslag en -gebruik te onderhouden. We beschrijven hier voor het eerst de belangrijkste effecten van stress ten gevolge van suboptimale temperaturen op zaailingen van rijst en beschrijven mogelijke mechanismen voor tolerantie die verder bestudeerd moeten worden. Dit werk zal helpen bij de ontwikkeling van toekomstige strategieën om verschillende tolerantiemechanismen samen te voegen om zo cultivars te ontwikkelen die een hogere opbrengst hebben tijdens deze vorm van stress. De ontwikkeling van merker-geassisteerde kweekprogramma's zou hiervoor een goede aanpak kunnen vormen en hiermee samenhangend zouden genoomwijde associatiestudies die gebaseerd zijn op het beschreven mechanisme kunnen helpen bij het vinden van nieuwe merkers.

Table of contents

ABBREVIATIONS

ABA	Absicic acid
ABS	Absorbed energy
ANOVA	Analysis of variance
APX	Ascorbate peroxidase
ASC	Ascorbate
ATP	Adenosine triphosphate
BLAST	Basic Local Alignment Search Tool
BRs	Brassinosteroids
CAT	Catalase
CDD	Conserve Domain Database
Chl	Chlorophyll
CS	Cross-section
CSD	Cold Shock Domain
DAPI	4',6-diamidino-2-phenylindole
DEG	Differentially expressed gene
DET	Differentially expressed transcripts
DHAR	Dehydroascorbate reductase
DI_0	Dissipated energy
DNA	Deoxyribonucleic acid
DTT	Dithiotreitol
EC	Enzyme Commission numbers
EDTA	Ethylenediaminetetraacetic acid
ET_0	Electrons transported
ET	Ethylene
EZ	Elongation zone
EZ-MaZ	Transition zone between the elongation and the mature zone
FC	Fold change
FDR	False Discovery Rate
FLL	Final leaf length
FRAP	Ferric Reducing Ability of Plasma
FW	Fresh weight
GA	Galic acid
GCS	Glycine cleavage system
GDD	Growing degree days
GO	Gene ontology
GOBP	Gene ontology biological process
GOCC	Gene ontology cellular component
GOMF	Gene ontology molecular function
GPX	Glutathione peroxidase
GR	Glutathione reductase
GRx	Glutaredoxin
Gs	Stomatal conductance
GS/MS	Gas chromatography-mass spectrometry
GSH	Glutathione

GSSC	Glutathione disulfide
HPLC	High performance liquid chromatography
IS	Internal standard
iTRAQ	Isobaric tags for relative and absolute quantification
JA	Jasmonic acid
JIP test	Non-invasive chlorophyll fluorescence fast-transient test
LED	Light Emitting Diode
LER	Leaf elongation rate
M	Meristem zone
MaZ	Mature zone
MDA	Malondialdehyde
MDAR	Monodehydroascorbate reductase
MDHA	Monodehydroascorbate
M-EZ	Transition zone between the meristem and the elongation zone
mRNA	Messenger ribonucleic acid
MS	Mass spectrometry
MS/MS	Tandem mass spectrometry
NADP	Nicotinamide adenine dinucleotide phosphate (oxidaze)
NADPH	Nicotinamide adenine dinucleotide phosphate (reduced
NBT	Nitro Blue tetrazodium
OEC	Oxygen Evolving Complex
OT	Optimal temperatures of plant growth
PAR	Photosynthetically active radiation
PCA	Principal components analysis
PMSF	Phenylmethane sulfonyl fluoride
Pn	Net photosynthesis rate
POX	Peroxidase
PQ	Plastoquinone
PSI	Photosystem I
PSII	Photosystem II
PUFA	Polyunsaturated fatty acid
Q_A	Quinone A
Q_B	Quinone A
QE	Quercetin
qPCR	Quantitative polymerase chain reaction
RC	Reaction center
RNA	Ribonucleic acid
ROS	Reactive oxygen species
Rubisco	Ribulose-1,5-bisphosphate carboxylase/oxygenase
RWC	Relative water content
SD	Standard deviation
SE	Standard error
SIM	Selected Ion Monitoring
SOD	Superoxide dismutase
ST	Suboptimal temperatures of plant growth
tASC	Total ascorbate
TBA	Thiobarbituric acid
TCA	Tricloroacetic acid

TEM	Transmition electron microscope
tGSH	Total glutathione
TR_0	Transferred energy
TRx	Thioredoxin

INTRODUCTION

The importance of rice

Rice (*Oryza sativa* L.) is one of the most important cereal crops in the global food system feeding nearly half the world's population, and it's cultivation, processing and trade represents one of the biggest economic activities on Earth (GRiSP, 2013; FAO, 2016). 159 million ha of rice are harvested each year destine only for human consumption, accounting for 78% of its production in 2009, a great percentage compared with 64% for wheat and only 14% for maize (GRiSP, 2013). The main producer of rice is by far Asia with 90% of the global production, followed by Americas with 5% and only small contributions from Africa, Europe and Oceania (FAO, 2016). Global food demand increases rapidly and as a consequence it is predicted that an extra 116 million tons of rice will be needed annually by 2035. Since in Asia arable lands are declining due to urbanization, climate change, and competition from other high-value agriculture, it is expected that America and Africa will have to augment their production, specially Brazil and Argentina (GRiSP, 2013; Flachsbarth et al., 2015). In Latin America and the Caribbean, rice is the second source of daily calories for many countries. The increase of rice production in an efficient and sustainable way in this region is of great importance to achieve global food demand in the future and assure the continuity of the rice market in the zone (Benavidez, 2006; Zorrilla et al., 2013; Laurance et al., 2014). In the process, efficient management practices and attainment of high yield on existing croplands will lead to minimal environmental damage.

Besides its importance for human consumption and global economy, rice has the smallest genome of the major cereal crops and it has been completely sequenced (Eckardt, 2000; International Rice Genome Sequencing Project, 2005; Livore, 2006a; Jackson, 2016). The great amount of genetic resources developed for rice makes it a great model plant especially for comparative genomics and molecular marker assisted plant breeding (Shimamoto and Kyozuka, 2002; Jena and Mackill, 2008; Das and Rao, 2015; Hasan et al., 2015; Wijerathna, 2015). In the last 10 years more than 3,000 rice cultivars have been sequenced and open access resources for rice breeding based on genome-wide association mapping have been developed (The 3000 Rice Genomes Project, 2014; McCouch et al., 2016). Rice has also its advantages over other crops regarding proteome analysis, since large databases of proteins sequences are also available (Kosová et al., 2011; Singh and Jwa, 2013). Rice has then become the first cereal crop that has such amount of genetic tools allowing it to be the model for monocot crop plants in this research area.

The problem of low temperatures for rice culture

Oryza sativa has evolved in tropical and subtropical areas and hence it is vulnerable to cold weather (Quintero, 2009). Several million ha of rice cultivation are affected globally by low temperature every year, resulting in annual yield losses of 1–3.9 t/ha (Jena and Hardy, 2012). Since water is not usually a problem in Argentina, soil quality is good and radiation supply is assured, the most relevant limiting factor for incrementing rice yield in the region is temperature (Quintero, 2009). For rice, the minimum temperature of growth is around 8-12 °C, the optimum temperature of growth is 28-30 °C, and the maximum temperature of growth is 42-45 °C (Quintero, 2009).

The production is concentrated in the humid region of the country where the climate varies from temperate to humid subtropical, this includes the provinces Corrientes (40%), Entre Ríos (38%), Santa Fé (16%), Formosa (3%), and Chaco (3%; Villanova and Albornoz, 2006; GRiSP, 2013). Rice is usually sown between September and December and it is harvested between February and March. During these months the temperatures are optimal but high frequencies of temperatures under the optimum are observed in Entre Ríos during September and October, and the end of January and beginning of February, affecting this way the seedling and the flowering stages (Quintero, 2009). Therefore, the presence of low temperatures conditionates the early-sowing and affects the capture of resources generating great consequences in the achieved rice yield (Arguissain, 2006; Brizuela, 2006; Quintero, 2009). This phenomena not only affects Argentina but it also has similar consequences in the early-sowing of other areas, *e.g.*, central China (Wang et al., 2016).

Cold stress in rice

Plant physiologists use the term freezing to mean temperatures below 0 °C, chilling for temperatures between 0 °C and the minimum temperature for growth, and suboptimal temperatures of growth (ST) for those between the former and the optimum temperature (Menéndez et al., 2013). Under field conditions, rice seedlings are exceptionally subjected to freezing periods, more regularly they endure chilling, whereas the most common situation is ST that persists for the most part of the vegetative stage (Greaves, 1996; Allen and Ort, 2001; Morsy et al., 2005; Zhang et al., 2012). Many plant species have developed an array of mechanisms that enable them to minimize the negative effects of cold stress. The ability to cold acclimate, *i.e.*, to increase cold tolerance, is a multigenic trait that results from a complex process involving a number of physiological and biochemical changes. This includes changes in gene expression, membrane structure and function, and contents of water, proteins,

lipids, and primary and secondary metabolites (Basuchaudhuri, 2014). Numerous authors have focused on morphological, biochemical and molecular responses to chilling and freezing in this crop (Bertin et al., 1996; Rabbani et al., 2003; Peng and Ismail, 2004; Cheng, 2006; Bonnecarrère et al., 2011; Zhang et al., 2012; Wang et al., 2013; Basu and Roychoudhury, 2014). Besides, some early studies demonstrated that rice growth rate and metabolism are noticeably inhibited in the range of 15-20 °C (Kabaki, 1983; Takanashi et al., 1987), differently to chilling that completely stops the seedling growth (Allen and Ort, 2001; Aghaee et al., 2011). However, the physiological bases for rice growth delay by ST remain fairly unexplored.

Cold stress usually occurs during the seedling stage or panicle development. Although ST induces spikelet sterility of rice when subjected during the panicle development, part of this sterility could be explain by ST during the seedling stage (Shimono et al., 2007; Quintero, 2009). Temperatures of 18-19 °C during early stages of growth can increase the susceptibility of the plant to ST sterility during the reproductive stages, even though the physiological mechanism remains unknown. The effect of ST during the seedling stage could be of great importance in Argentina because in order to avoid ST episodes during the flowering season, rice is usually sown early in September-October when ST is frequent. Quintero (2009) analyzed the factors that limit the growth and productivity of rice in Argentina, particularly in Entre Ríos, and found that although good agronomical practices would increase rice yield, the development of cultivars that are tolerant to cold stresses at the seedling stage is essential to achieve better yield. The importance of genetic improvement was already described as a decisive factor that contributed 74.0% of the total increase yield in China between 1980 and 2012 (Yu et al., 2012). Hence, new breeding programs that try to achieve cold tolerant high yield cultivars need to be designed and for that research on the response to ST is needed to unravel the characteristics of this stress at the seedling stage.

While generally sensitive to low temperatures, considerable variation in the extent to this stress injury is exhibited by seedlings of different rice germoplasm accessions. Of the two major *O. sativa* subspecies, japonica cultivars, typically grown in both tropical and temperate zones, are usually more cold tolerant than indica cultivars, mostly grown in tropical lowland areas (Yoshida, 1981; Livore, 2006b; Kim and Tai, 2011). However, indica cultivars are usually more efficient in absorbing energy, they have an excellent vigor and fast emergence when temperatures are above the optimum (Livore, 2006b). Hence, there is a potential use of japonica germoplasm to

improve high yield indica cultivars so they can tolerate ST stress (Negrão et al., 2008). The availability of cultivars with contrasting response to low temperatures gives an opportunity to use them to identify potential mechanisms associated with its tolerance.

Hypothesis and main goal

From what was described above and based on the known information in this issue, the next **hypothesis** was drawn up: *"there is a differential response to suboptimal temperatures among seedlings from different rice cultivars (Oryza sativa* L.*)"*. In order to test this hypothesis here it was proposed to *"study the response at different levels of contrasting rice cultivars (Oryza sativa* L.*) to suboptimal temperatures of growth subjected during the seedling stage"* as the **main goal** of this thesis.

CHAPTER 1: Phenotypic analysis of contrasting rice cultivars to suboptimal temperatures

1.1 INTRODUCTION

Breeding and genetic manipulation to increase crop yields require of rapid and reliable procedures to select the best adapted among numerous cultivars. It has been suggested that specific selection techniques under controlled conditions would be useful to speed up the development of cultivars with higher chilling tolerance (Wery et al., 1994; Bertin et al., 1996; Strauss et al., 2006). Many methods already exist that try to distinguish tolerant from sensitive cultivars to cold stress. For instance, the most popular one is the Standard Evaluation System (IRRI, 1988), a protocol that needs 30 days for the evaluation and it is based in visual rating. Thus, diminishing the time of evaluation and obtaining quantitative data for statistical testing should be preferred over visual or subjective measurements for cultivar selection. Finding rice cultivars with objective contrasting responses to ST could contribute to the breeding or biotechnological development of cultivars with improved ST tolerance, and also to increase the current knowledge of this growth constraint.

Photosystem II (PSII) has been demonstrated to be an important component determining sensitivity to low temperature stress (Strauss et al., 2006; Strauss et al., 2007; Pagter et al., 2008). Among major effects of chilling on rice plants during early vegetative growth is the inhibition of electron transport through PSII and consequent photoinhibition (Gesch and Heilman, 1999; Jeong et al., 2002). Chilling tolerance was associated with a reduced level of photoinhibition and oxidative damage (Bonnecarrère et al., 2011). Low temperature may also affect chlorophyll (Chl) fluorescence of PSII in several other species (Long and Humphries, 1994; Strasser et al., 1995). The ratio of variable to maximal Chl fluorescence or maximum quantum efficiency of PSII (F_V/F_M) decreased in plants subjected to low temperatures (Renaut et al., 2005; Pagter et al., 2008). Therefore, this ratio has been widely used and proved useful as parameter to screen for chilling tolerance (Neuner and Larcher, 1990; Sthapit et al., 1993; Agati et al., 1995; Fracheboud et al., 1999) and thus could also be useful as well to screen rice plants under ST stress.

1.1.1 Transient fluorescence of chlorophyll *a*

Chl-*a* fluorescence emitted by plants reflects photosynthetic activities that can be measured by the non-invasive chlorophyll fluorescence fast-transient test (JIP test; Strasser et al., 2000). The JIP test defines the maximal (subscript “0”) energy fluxes in the energy cascade (Figure 1-1): light is absorbed by the antenna molecules within the photosynthetic membrane (ABS), this absorbed energy is transferred as excitation energy and is either trapped (TR_0) at a reaction center (RC) and electrons are

transported (ET_0) to do chemically useful work generating ATP and NADPH, or dissipated (DI_0) mainly as heat and less as emitted fluorescence. Based on the fluorescence in response to a saturating light pulse, the specific energy fluxes (per RC) and the phenomenological energy fluxes (per excited cross-section, CS), as well as for the flux ratios or yields, can be derived.

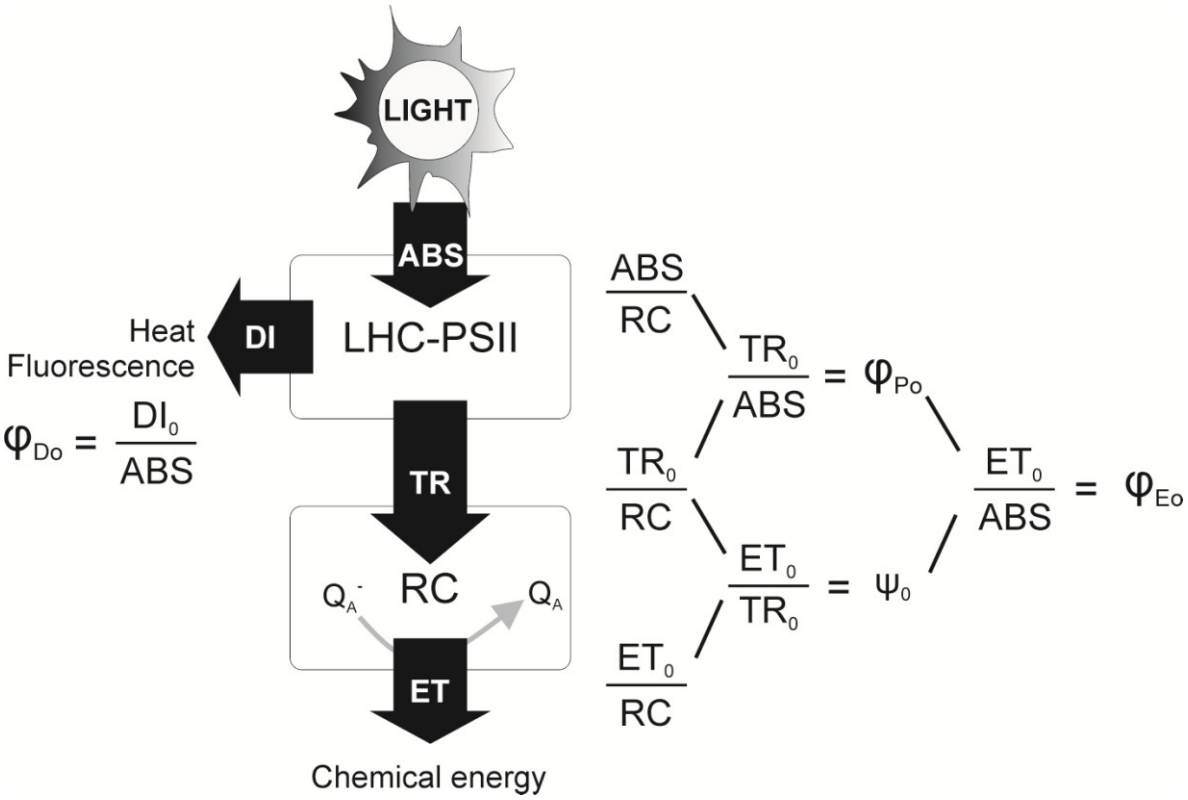

Figure 1-1. Simplified model of energy fluxes in the photosynthetic apparatus. Energy is absorbed (ABS) by the antenna molecules of the Photosystem II (LHC-PSII). Part of this energy is trapped (TR) by the reaction center (RC) and electrons are transported (ET) via quinone A acceptor (Q_A) to generate chemical energy, or is dissipated (DI) as heat and fluorescence. Specific energy fluxes (per RC) and flux yields (ψ and φ) are described in the figure. Subscript "0" denotes maximal energy fluxes. Figure adapted from González Moreno et al., (2008).

If a sample is pre-adapted to darkness and suddenly illuminated, the fluorescence of Chl increase with time reflecting the reduction of the RC from the PSII giving information of the photochemical activity. The kinetic of fluorescence emission plotted in function of time presents four points named O-J-I-P that can be used to calculate the fluxes and yields described above. Shortly, these points are marked in Figure 1-2 and represent (Stirbet and Govindjee, 2011):

— at the beginning all the electron acceptors are mostly in the oxidized state so the centers are open and the fluorescence intensity is at its minimum, F_0, represented as “O” in the curve for “origin” (usually at 20 μs);

— from O to J the fluorescence raises very fast, it is known as the photochemical phase and depends strongly on the intensity of the exciting light (J or F_J usually at 2 ms);

— J to I (I or F_I usually at 20 ms) and I to P are known as thermal phases and they are much slower, they represent the partial reduction of the quinone A (Q_A) and the quinone B (Q_B) ;

— when the fluorescence reaches the peak P, usually called F_M, when the exciting light is saturating, all Q_A molecules are completely reduced (PSII centers are closed) and electrons have reached the plastoquinone (PQ), due to the reduction of the entire linear electron transport chain;

— when fluorescence decrease it is called the steady-state and it is symbolized as S.

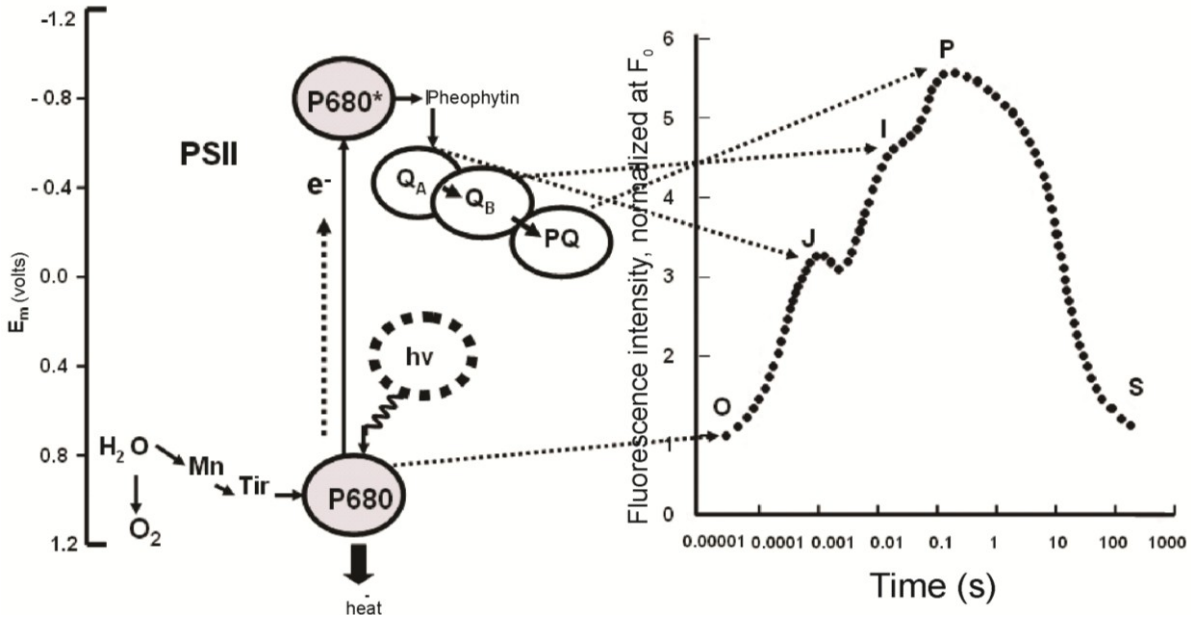

Figure 1-2. Example of kinetic of fluorescent emission of Chl-*a* from PSII of a pre-darkened sample and its relation to reactions in the electron chain. Letters and steps are explained in the text. Figure adapted from González Moreno et al., (2008).

These points of the OJIP curve are then used to calculate different parameters that are useful to describe the photochemical activity and are listed in Table 1-1.

Table 1-1. Summary of the OJIP test formulae (Strasser et al., 2000; González Moreno et al., 2008; Stirbet and Govindjee, 2011).

Extracted and technical fluorescence parameters	
F_0	= fluorescence intensity at 20 μs
F_{250}	= fluorescence intensity at 250 μs
F_J	= fluorescence intensity at the J-step (at 2 ms)
F_M	= maximal fluorescence intensity
t_{fmax}	= time to reach F_M, in ms
V_J	= $(F_J - F_0) / (F_M - F_0)$
Area	= area between fluorescence curve and F_M
M_0	= $4 . (F_{250} - F_0) / (F_M - F_0)$
S_m	= Area / $(F_M - F_0)$; normalized complementary area related to the number of electron carriers per electron carriers chain or energy needed to close all reaction centres.
ABS	= absorbed energy flux
TR_0	= trapped energy flux at time F_0
ET_0	= electron transport energy flux at time F_0
DI_0	= dissipated energy flux at time F_0
RC	= reaction centre
CS_0	= excited cross-section CS at time F_0
RC/ABS	= number of Q_A reducing RC per PSII antenna Chl
RC/ CS_0	= number of RC per CS_0
Quantum efficiencies	
TR_0/ABS	= $(1 - F_0) / (F_M)$; or F_v/F_M; maximum quantum yield of primary PSII photochemistry
DI_0/ABS	= 1- (TR_0/ABS); maximum dissipated quantum yield of PSII
ET_0/TR_0	= 1 - V_J; probability that trapped exciton move an electron into the electron chain beyond quinone A (Q_A)
ET_0/ABS	= $(1 - F_0) / (F_M) . (1/ ET_0/TR_0)$; Quantum yield for electron transport
Specific energy fluxes	
ABS/RC	= $M_0 . (1/V_J) . (1/ TR_0/ABS)$ or energy absorbed per reaction centre
TR_0/RC	= $M_0 . (1/V_J)$
ET_0/RC	= $M_0 . (1/V_J) . (ET_0/TR_0)$
DI_0/RC	= (ABS/RC) – (TR_0/RC)
Phenomenological energy fluxes	
ABS/CS_0	= F_0 or energy absorbed a T_0 per excited cross section
DI_0/CS_0	= (ABS/CS_0) - (TR_0/CS_0)
TR_0/CS_0	= (TR_0/ABS) . (ABS/Cs)
ET_0/ CS_0	= (TR_0/ABS) . (ET_0/TR_0) . (ABS/Cs)
Vital indices	
PI_{ABS}	= (RC/ABS)*(TR_0/ABS /1- TR_0/ABS)*(ET_0/TR_0/1- ET_0/TR_0); performance index for energy conservation from photons absorbed by PSII antenna to the reduction of Q_B

1.2 AIMS

The aim of this chapter was to gain insight into the physiological response of rice to ST and to detect rice cultivars with contrasting performance under a ST range. For this purpose, plant growth, PSII functioning and photosynthetic gas exchange parameters, among others, of several rice cultivars were characterized when confronting the ST condition.

1.3 MATERIALS AND METHODS

1.3.1 Plant material

Rice cultivars Koshihikari, IR24, IR28, IR50, Japonesito 3 meses, Japonesito 8 meses, Japonesito Prolifico, General Rossi, H313-1-2, H313-26-2, Bombilla, Cini 754, Cnia 948, CT-6742-10-10-1, Oro, Cala PA, Ayasmi, Honezhaosen were kindly provided by the Rice Breeding Program of the Universidad Nacional de La Plata, Argentina. Seeds of these cultivars were placed within Petri plates on two layers of Whatman Nº 5 filter paper rinsed with 7 mL Carbendazim 0.025 %p/v (Yoshida, 1981) and incubated in growth chamber at 30 °C in darkness until germination. The resultant seedlings were transplanted to different substrates for laboratory and outdoor assays.

1.3.2 Laboratory assays

The following A and B assays were performed in a growth chamber with 12 h photoperiod, 80% humidity and 200 µmol photons m^{-2} s^{-1} of photosynthetically active radiation (PAR). The day/night temperatures for ST and optimal temperatures of growth (OT) were 21/13 and 28/24 ºC, respectively.

A) Short-term assay: Seedlings were hydroponically cultured at OT by transplanting them on plastic net frames placed over a 4 L black tray containing 3 L distilled water. After three days of culture, the water was replaced by 3 L Yoshida solution (Gregorio et al., 1997). Thereafter, the Yoshida solution was renewed every three days until the end of the experiment. When the third leaf (Yoshida, 1981) emerged (T_0 stage), half of the seedlings were transferred to the ST condition. Seedlings were further cultivated for another 3 d under the OT or ST conditions (Figure 1-3 A).

B) Long-term assays: Seedlings were transplanted to 0.5 L plastic pots, containing sterile organic soil extract as substrate. Pots were inundated within 4 L trays with 3 L distilled water and kept either at ST or OT during 24 d. Water was periodically added to the trays in order to maintain the water level invariable during the time lapse

experiments. In the case of plants maintained at OT, at the 25th experimental day temperature was kept at 24 °C during 2 h starting at the begging of the photoperiod, and then it was gradually diminished, until reaching 11.5 °C after 3 h in order to measure gas exchange parameters at different temperatures (Figure 1-3 B).

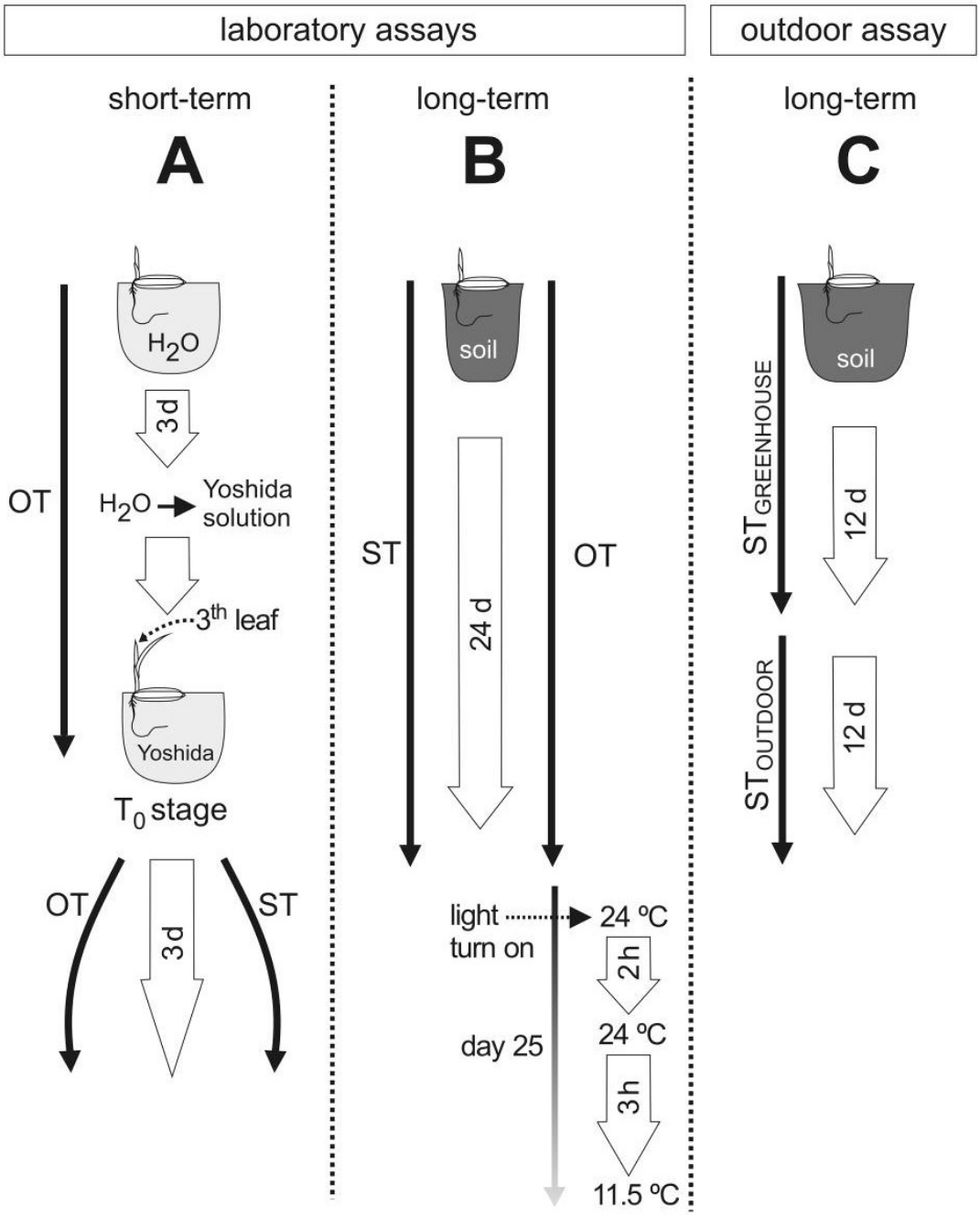

Figure 1-3. Sketch of the laboratory and outdoor experimental setups.

1.3.3 Outdoor assay

Seedlings were transplanted to 4 L pots with holes in the bottom and filled with sterile organic soil extract. Pots were placed in 10 L trays and inundated with 5 L

distilled water (Figure 1-3 C). Trays were kept in a greenhouse, with 21/13 ± 2 °C day/night, 550 PAR, for 12 d. Afterwards, trays were transferred outside in the open, where plants were further grown for another 12 d, under the temperature and PAR conditions depicted in Figure 1-4.

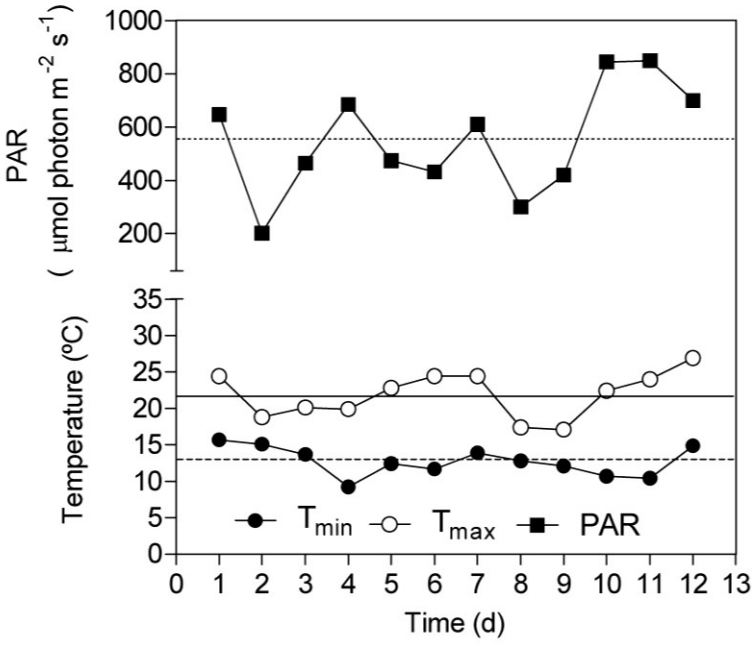

Figure 1-4. Environmental PAR and air temperature of the outdoor experiment. Graphic represents the PAR and the air temperature registered from the 12th to the 24th day of the experiment. Dotted, solid and dashed lines represent the average of PAR, maximum and minimum temperatures respectively.

1.3.4 Plant growth analysis in the short-term laboratory assay

Seedlings from the hydroponic culture were scanned at 600 ppi resolution (HP PSC 1510 Hewlett Packard Development Company, LP, USA) at the T_0 stage and after three days of culture under OT or ST. The digitalized images were analyzed with the software package Optimas (Optimas 6.1, Corporation. Bothell, WA) to determine the third leaf length. Net leaf elongation was calculated from the equation:

Net leaf elongation = length at day 3 – length at T_0 stage

1.3.5 Chlorophyll fluorescence fast-transient test

Non-invasive chlorophyll fluorescence fast-transient test (JIP test) was performed on blades of expanded leaves with a portable chlorophyll fluorometer (Pocket PEA, Hansatech Instrument, UK) in laboratory and outdoor experiments. For this purpose, leaves were covered with leaf-clips to adapt them to darkness for 20 min. Then leaf-clips were opened and samples were exposed during 3 s to 3500 µmol photons m^{-2} s^{-1} (637 nm peak wavelength). The pocket PEA software (PEA plus v1.1, Hansatech Instrument Ltd., UK) was used to analyze PSII properties according to Strasser et al.,

2000. The JIP analyzed parameters were: RC/CS_0, RC/ABS, F_V/F_M, ABS/RC, DI_0/RC and PI_{ABS}. Their definitions were described in Table 1-1.

1.3.6 Determination of chlorophyll content

Chl content was measured on blades of expanded leaves of plants grown outdoor with a non-invasive portable chlorophyll spectrophotometer (Clorofilio, Cavadevices, BA, Arg.). Data were expressed in SPAD units.

1.3.7 Determination of gas exchange parameters

The gas exchange parameters, net photosynthesis rate (Pn), stomatal conductance (Gs) and internal CO_2 concentration (Ci) were measured in blades of expanding leaves at light saturation (1200 µmol photons m^{-2} s^{-1} illumination, LED light) at the same air temperature of each particular experimental conditions, using a portable photosynthesis system (TPS-2 Portable Photosynthesis System, MA, USA).

1.3.8 Determination of relative water content

The relative water content (RWC) was estimated on the leaf blade. For this purpose, tissue was weighed fresh, after being floated for 24 h and achieve turgidity, and after oven-dried at 70 ºC for 48 h. RWC was calculated from the equation:

$$RWC = [(\text{fresh weight} - \text{dry weight}) / \text{turgid weight} - \text{dry weight}] \times 100$$

1.3.9 Statistical analyses

Data was subjected to ANOVA and *post-hoc* analyses, DGC test (Balzarini and Di Rienzo, 2012) and T test using the Infostat statistical software package (Di Rienzo et al., 2016).

1.4 RESULTS AND DISCUSSION

1.4.1 Screening of rice growth performance under suboptimal and optimal temperatures conditions

We carried out a screening to identify rice cultivars with contrasting growth performance under ST. For this purpose, a short-term, a hydroponic culture system was established at the laboratory, subjecting seedlings during the expansion of their third leaf to ST or OT conditions. Results revealed variations among the 18 different cultivars regarding the net leaf elongation of seedling grown under ST during three days (Figure 1-5 A). The percentage of net leaf elongation reduction, related to that registered at OT, averaged 70% for all cultivars (Figure 1-5 B). Cultivars Cnia 948, Oro, Cini 745, IR28, General Rossi, Japonesito Prolífico, CT-6742-10-10-1 and Koshihikari presented the lowest percentage of net leaf elongation reduction, in that order, whereas the sequence with cultivars presenting the highest values of this parameter was Honezhaosen, H313-1-2, Japonesito 8 meses, IR24, H 313-26-2, Cala P.A. IR50 and Bombilla.

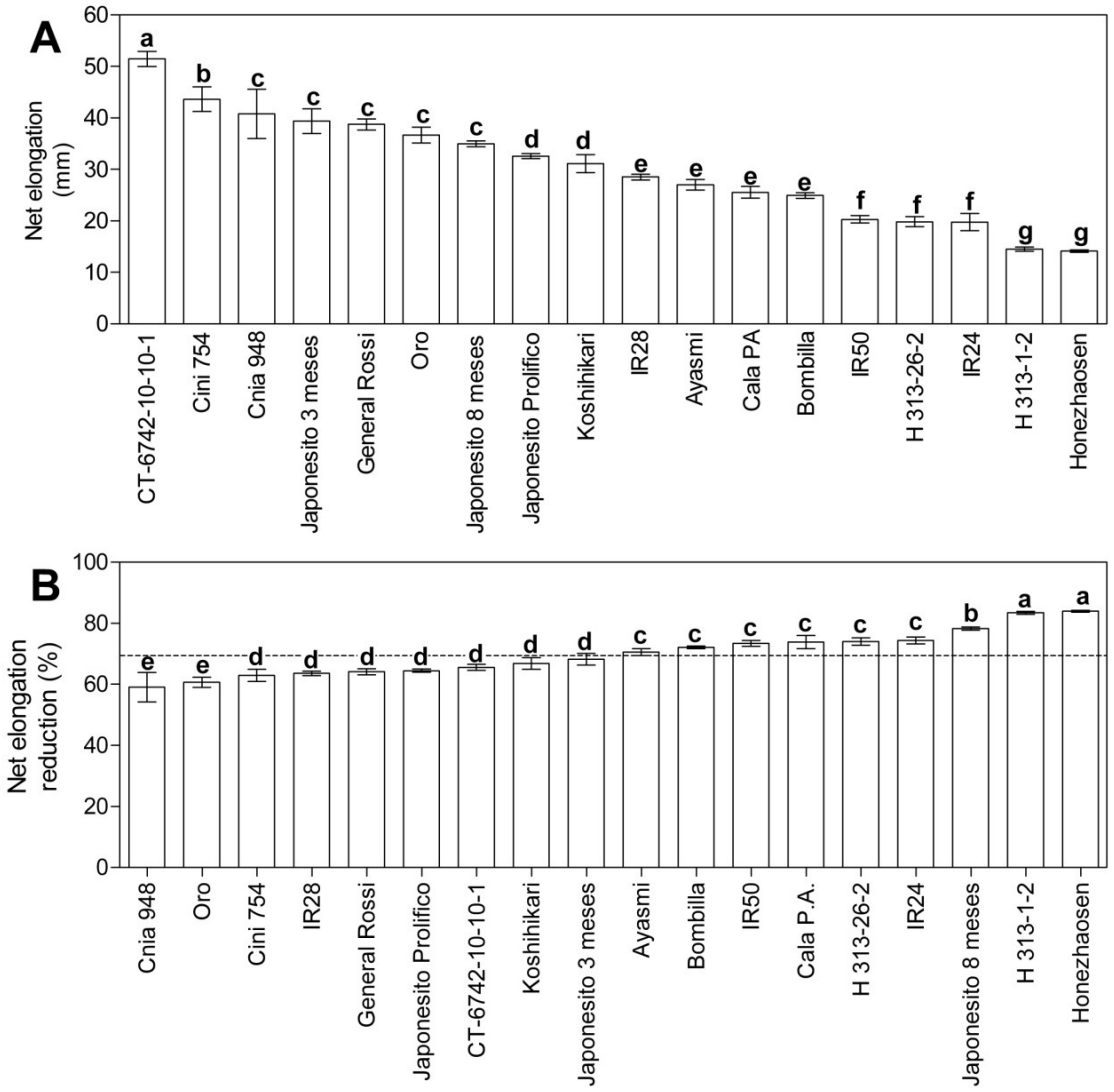

Figure 1-5. Net leaf elongation in rice cultivars. Seedlings were grown hydroponically under ST and OT in short-term laboratory assays. Net leaf elongation of the third leaf was determined by the analysis of digitalized images of shoots. **A)** Net leaf elongation under ST. **B)** Percentage of net leaf elongation reduction of plant grown under ST with respect to that elongation in plant grown under OT. Dashed line represents the mean percentage of net leaf elongation reduction across all cultivars. Bars with the same letter are not statistically different (DGC test; $P < 0.01$; data represents mean ± SE; n = 15).

Afterwards, plants of eight cultivars representative of the two groups delimited by this average (above and below) were subjected to ST conditions in two long-term (24 d) experiments, performed either at the laboratory or outdoor. Results from the last experiments showed that rice cultivars varied their shoot height response to ST (Figure 1-6), being the pattern of this variation similar to that found for net leaf elongation values in the former experiment (Figure 1-5): cultivars IR24, Honezhaosen, and IR50

(hereafter, the L group) presented lower shoot heights and net leaf elongation than CT-6742-10-10-1, General Rossi, Bombilla, Koshihikari, and Cnia 948 (hereafter, the H group).

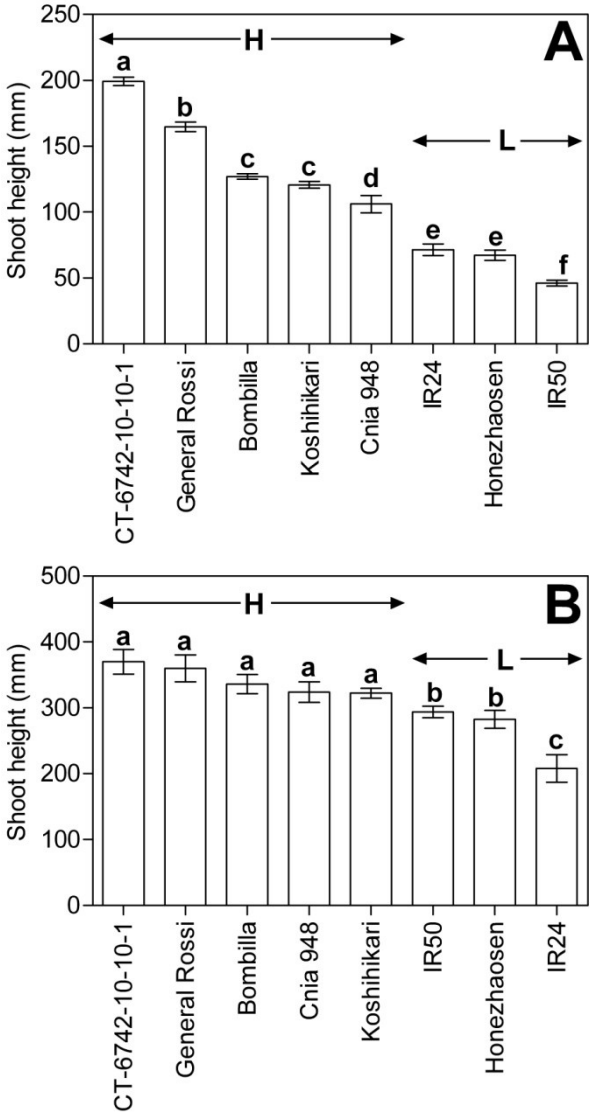

Figure 1-6. Shoot height of selected rice cultivars. Seedlings were grown under **A)** laboratory and **B)** outdoor ST conditions in long-term experiments. H: H group of cultivars; L: L group of cultivars. Bars with the same letter are not statistically different (DGC test; $P < 0.01$; data represents mean ± SE; n = 15).

1.4.2 Effect of suboptimal temperatures treatment on the Photosystem II performance

We then performed a laboratory experiment where F_V/F_M, RC/ABS, PI_{ABS}, RC/CS_0, ABS/RC and DI_0/RC parameters were evaluated with the JIP test at 10 and 24 days after temperature treatments were initiated. Cultivars of the H group displayed F_V/F_M values mostly falling within the optimum range (0.75 - 0.85, according to Bolhàr-Nordenkampf et al., 1989) until the end of the experiment (with the exception of a slight decrease observed in cultivar Cnia 948 at day 24). In contrast, cultivars of the L group

presented F_V/F_M values equal or lower than the optimum value of 0.75 at day 10 (Figure 1-7 A), with the exception of cultivar IR24. However, at day 24 all cultivars from the L group showed F_V/F_M values below that limit. Our results revealed that the RC/ABS decreased overtime for all cultivars with the exception of Koshihikari, for which an increase of this ratio was found (Figure 1-7 B). The performance index PI_{ABS} combines structural and functional criteria of the PSII, so it is a good vital index (González Moreno et al., 2008). The PI_{ABS} decreased over time for cultivars Cnia 948, Honezhaosen and IR50, whereas it increased in Koshihikari, and did not change significantly in the remaining cultivars (Figure 1-7 C). On other hand, for all cultivars of the L group the RC/CS_0 lowered over time (Figure 1-7 D), whereas for cultivars from the H group it did not change significantly, indicating that RCs inactivation may have occurred in the first, but not in the second cultivar group. Under ST stress, all cultivars increased their ABS/RC ratio over time (Figure 1-7 E). However, these increments tended to be lower in the H group, compared with those of the L group. The ABS/RC is dependent on the ratio of active to non-active reaction centers and representative of the average antenna size (Strasser et al., 2000). Such results, along with those of the RC/CS_0 ratio (Figure 1-7 D) would indicate an inactivation of some RCs in the L group. Likewise, the DI_0/RC ratio, which is indicative of the amount of energy absorbed that is not trapped by the RC, but dissipated, tended to increase in both cultivar groups, although the magnitude of the increment was higher in the L than in the H group (Figure 1-7 F). Next, the F_V/F_M, RC/ABS, PI_{ABS}, RC/CS_0, ABS/RC, and DI_0/RC were measured on these same cultivars subjected to ST, in an outdoor, long-term experiment, at final time (day 24, Figure 1-8). Again, F_V/F_M values were optimal for group H and suboptimal for group L (Figure 1-8A). Besides, group H showed higher RC/ABS and PI_{ABS} values than group L (Figure 1-8 B and C). Inversely, the ABS/RC, and DI_0/RC values in the H group of cultivars were lower than those of the L group (Figure 1-8 E and F), whereas both cultivars groups could not be separated by their RC/CS_0 (Figure 1-8 D). Interestingly, high and significant correlation coefficients were found between values obtained at the laboratory and outdoor experiments for growth data and for most of the above measured JIP parameters (Table 1-2).

In contrast to the chlorophyll fluorescence, Chl content did not show significant differences among cultivars in this outdoor assay (Figure 1-9).

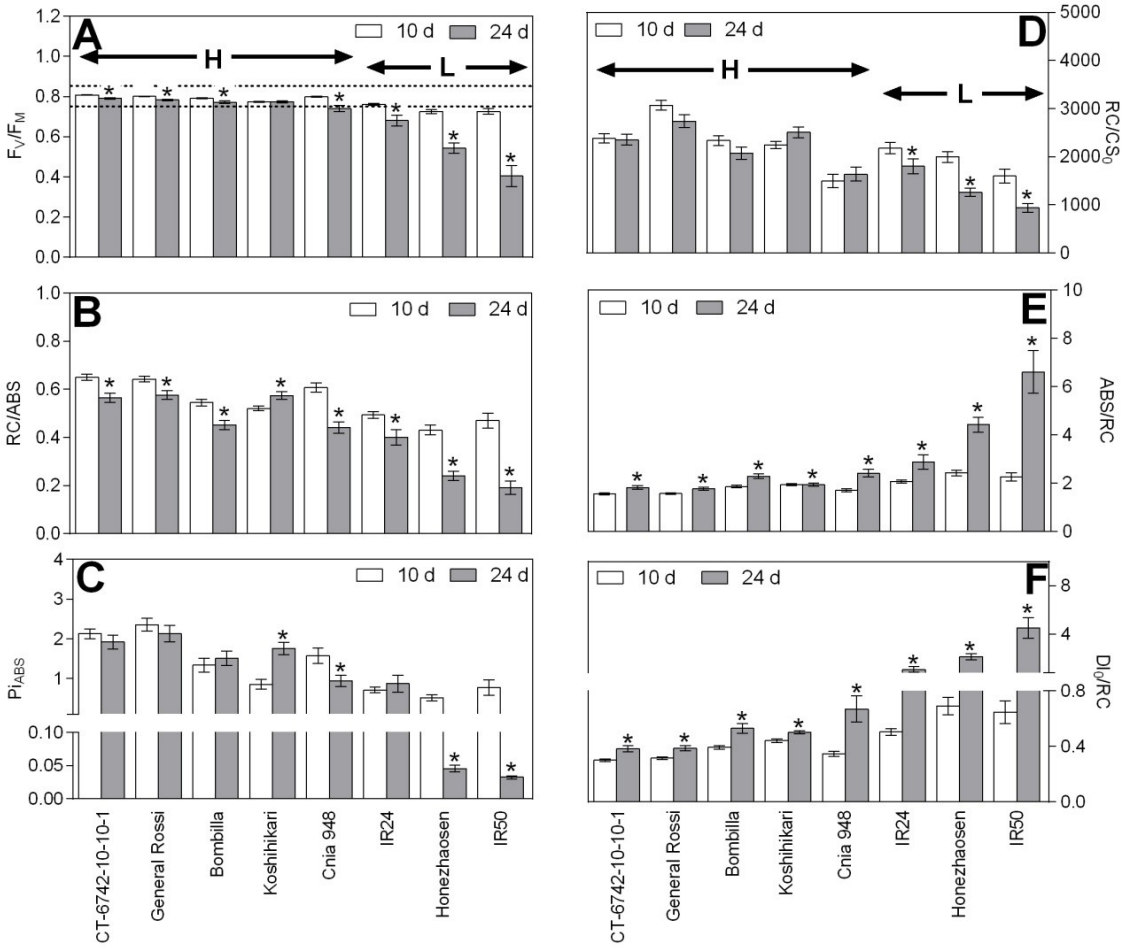

Figure 1-7. JIP test in selected rice cultivars grown under ST condition, in laboratory experiment. Seedlings were grown during 24 d. JIP test was done with a portable chlorophyll fluorometer at the 10th and 24th days. The JIP analyzed parameters were: **A)** F_V/F_M, **B)** RC/ABS, **C)** PI_{ABS}, **D)** RC/CS_0, **E)** ABS/RC and **F)** DI_0/RC. Dashed lines in A, represent the maximum (0.85) and minimum (0.75) F_V/F_M optimum values. H: H group of cultivars; L: L group of cultivars. Bars (mean ± SE; n = 15) with the same letter are not statistically different (DGC test; $P < 0.01$). White and grey letters correspond to 10th and 24th days, respectively. Asterisks represent significant differences between the sampling days (T test; $P < 0.01$).

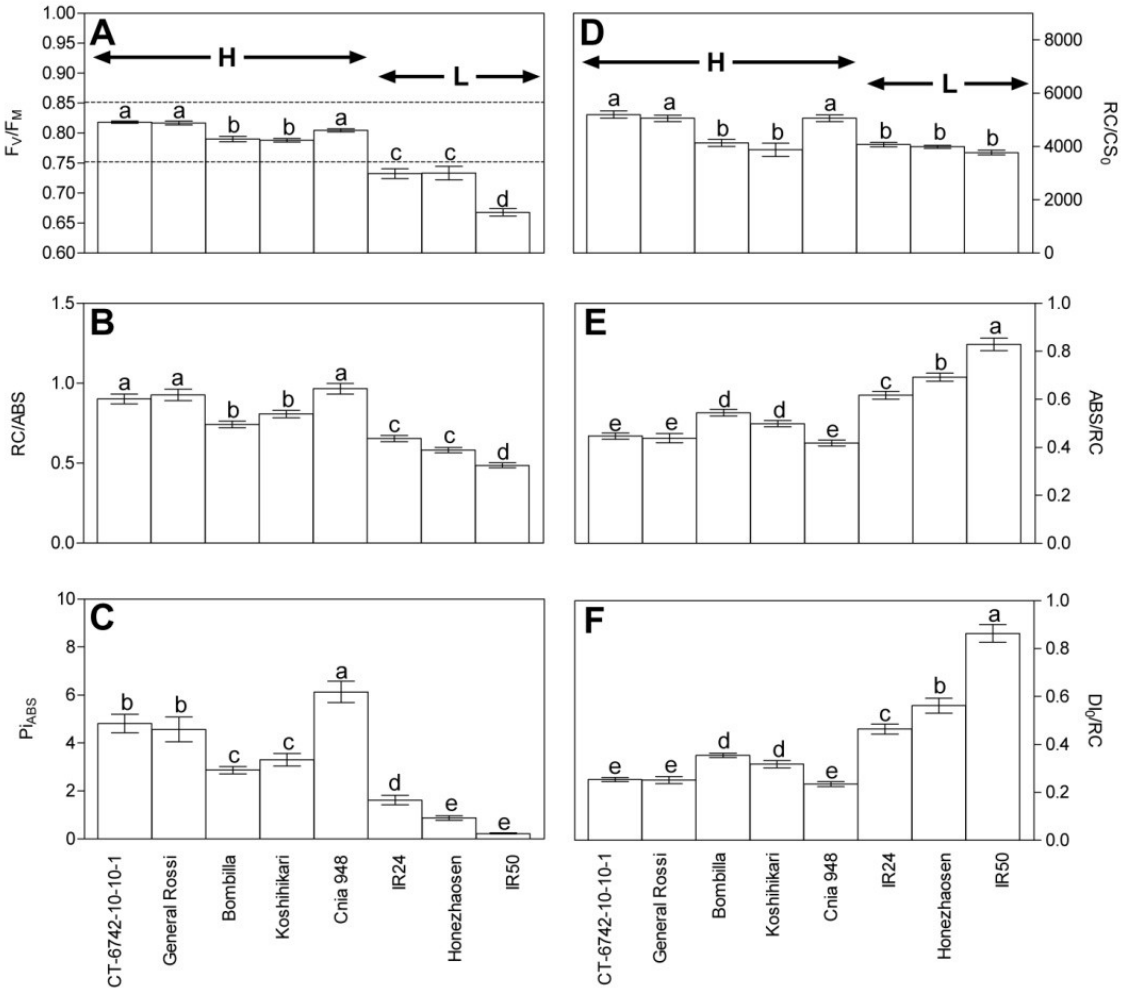

Figure 1-8. JIP test in selected cultivars under ST condition, in outdoor experiment. JIP test was done with portable chlorophyll fluorometer at the end of the assay (24 d). The JIP analyzed parameters were: **A)** F_V/F_M, **B)** RC/ABS, **C)** PI_{ABS}, **D)** RC/CS_0, **E)** ABS/RC and **F)** DI_0/RC. Dashed lines in A, represent the maximum (0.85) and minimum (0.75) F_V/F_M optimum values. H: H group of cultivars; L: L group of cultivars. Bars with the same letter are not statistically different (DGC test; $P < 0.01$; data represents mean ± SE; n = 15).

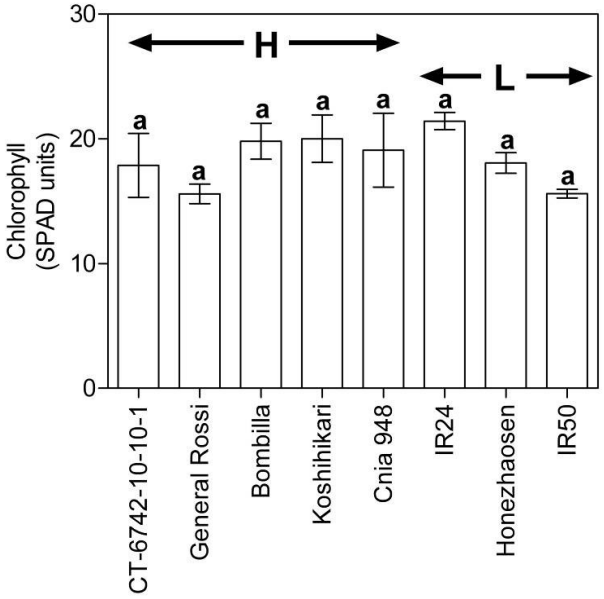

Figure 1-9. Chlorophyll (Chl) content in selected rice cultivars under ST in outdoor experiment. Chl content was determined with a portable chlorophyll spectrophotometer at the end of the assay (24 d). H: H group of cultivars; L: L group of cultivars. Bars with the same letter are not statistically different (DGC test; $P < 0.01$; data represent mean ± SE; n = 15).

Table 1-2. Correlation between values obtained at the laboratory and outdoor experiments for shoot height and JIP parameters.

Parameter	Pearson R	P value
Shoot height	0.78	0.0160
F_V/F_M	0.94	0.0005
RC/ABS	0.86	0.0160
PI_{ABS}	0.70	0.0350
RC/CS_0	0.49	0.2210
ABS/RC	0.94	0.0006
DI_0/RC	0.97	<0.0001

1.4.3 Influence of suboptimal temperatures treatment on gas exchange parameters

Gas exchange analyses were performed in the outdoor experiment, on seedlings of the same selected set of contrasting cultivars as above. Gs and Pn differently varied among cultivars: under ST conditions, cultivars from to the L group had significantly higher Gs values than those of the H group (Figure 1-10 A), whereas both cultivars

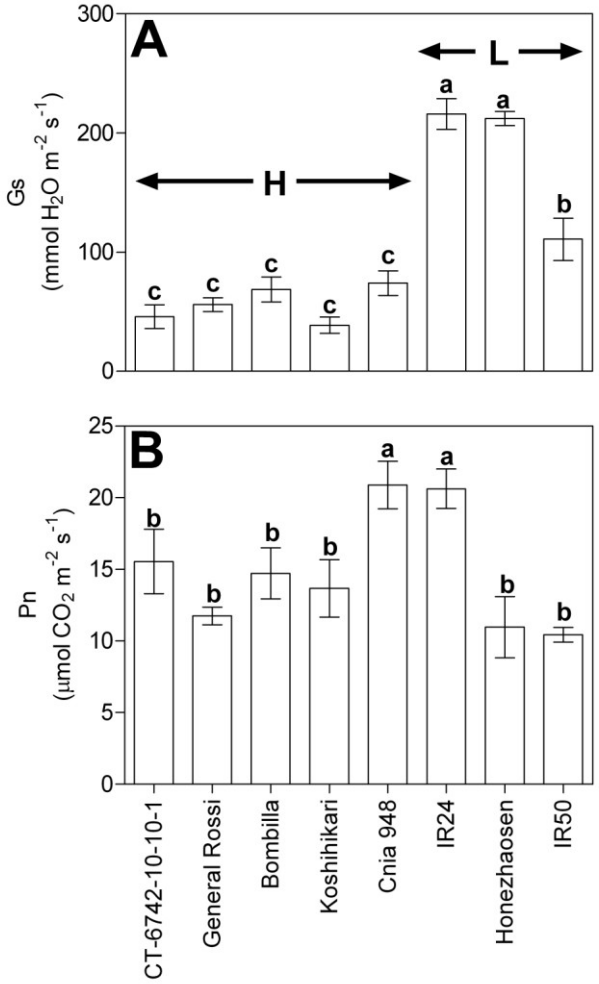

Figure 1-10. Gas exchange parameters in selected rice cultivars grown under ST condition, in outdoor experiment. Gs **(A)** and Pn **(B)** were determined with a portable photosynthesis system at the end of assay (24 d). H: H group of cultivars; L: L group of cultivars. Bars with the same letter are not statistically different (DGC test; P < 0.01; data represents mean ± SE; n = 15).

groups could not be separated by their Pn (Figure 1-10 B), Ci and RWC (Figure 1-11). An additional laboratory, long term assay was performed in order to describe gas exchange ST range. Seedlings of groups H and L were grown under OT during 24 days. At the 25th day, at the beginning of the photoperiod, the temperature was set at 24 °C during 2 h and then gradually lowered to 11.5 °C over a period of 3 h. Our results showed that Gs tended to decrease in parallel with the temperature and again, cultivars of the H group had lower Gs values than those of the L group, across the entire temperature range (Figure 1-12 A). On other hand, Pn values also tended to decrease in all cultivars with decreasing temperature and, as in the outdoor assay, groups H and L could not be clearly distinguished (Figure 1-12 B).

Finally, we calculated the instant water use efficiency (WUE_i= Pn/Gs, Ripullone et al., 2004) in our rice plants based on values obtained in former outdoor (Figure 1-10) and laboratory (Figure 1-12) assays. Results from the outdoor assay indicated that cultivars from the H group, presented higher WUE_i values than those of the L group, which is related to the fact that they had a reduced Gs, compared with the L cultivar group (Figure 1-13 A). Accordingly, the

laboratory assay showed that the WUE_i was progressively increased by temperatures below 20 °C, but only in cultivars of the H group (Figure 1-13 B).

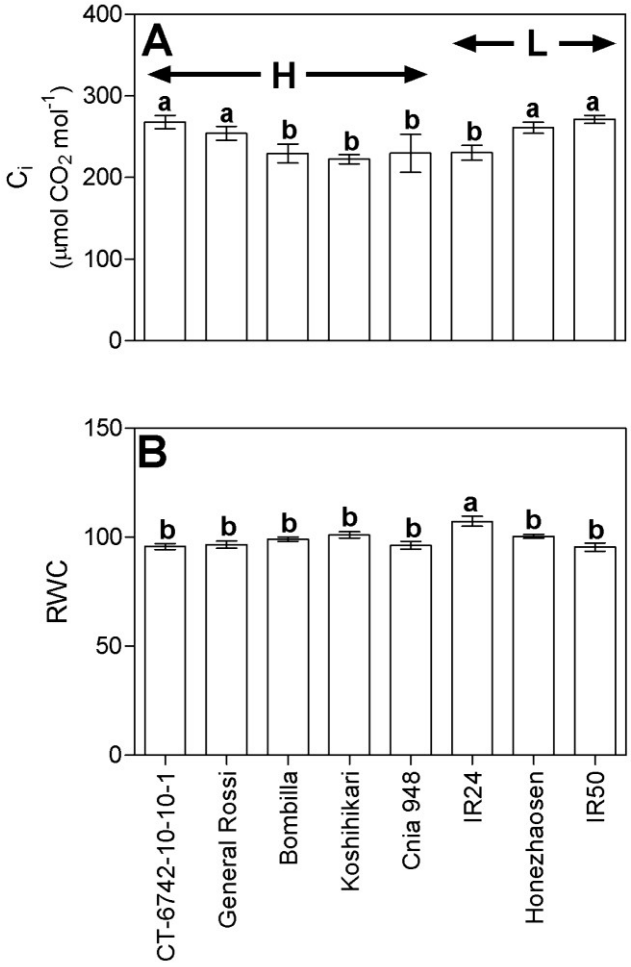

Figure 1-11. Intercellular CO_2 concentration and relative water content in selected rice cultivars grown under ST condition, in outdoor experiment. C_i **(A)** and RWC **(B)** were determined at the end of assay (24 d). H: H group of cultivars; L: L group of cultivars. Bars with the same letter are not statistically different (DGC test; $P < 0.01$; data represents mean ± SE; n = 15).

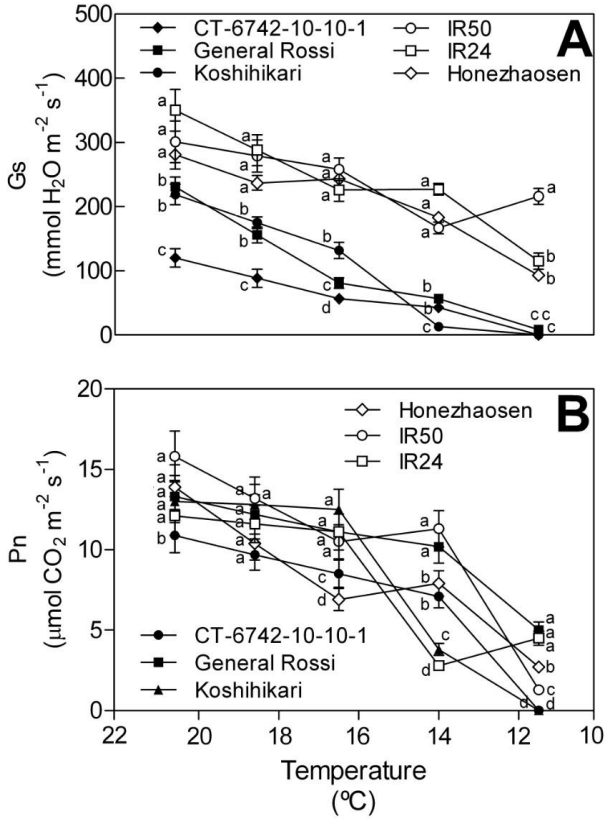

Figure 1-12. Gas exchange parameters in selected rice cultivars grown under a ST range, in a laboratory experiment. Seedlings were grown during 24 d under OT condition. At day 25, the temperature of the growth chamber was diminished gradually during 3 h from 24 ºC to 11.5 ºC. Gs **(A)**, Pn **(B)** were determined in the 21-11.5 ºC range. Different letters represent significant differences among cultivars at each temperature (DGC test; $P < 0.01$; data represents mean ± SE; n = 6).

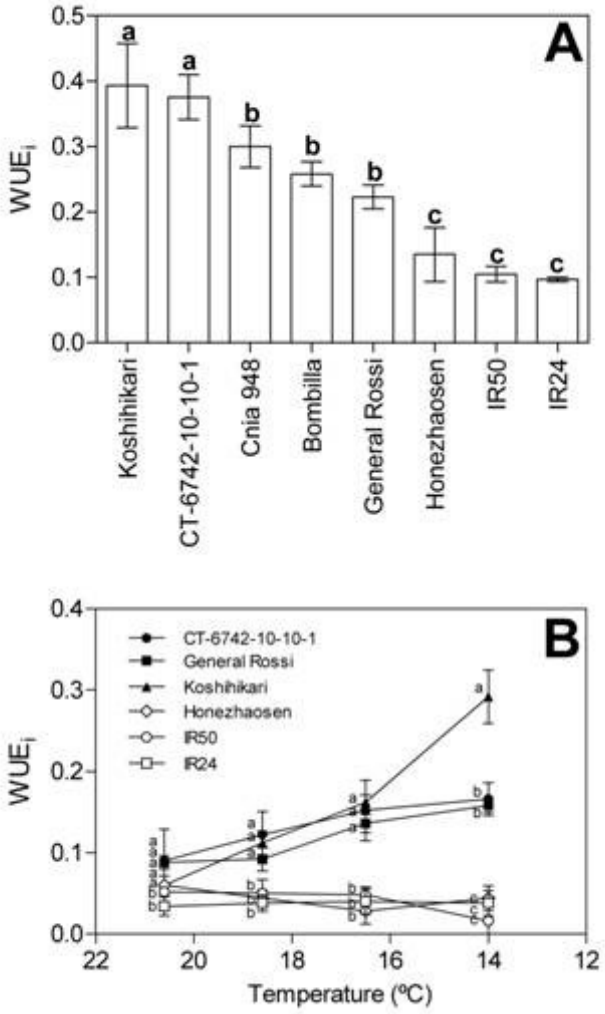

Figure 1-13. Instantaneous water use efficiency in selected rice cultivars grown under laboratory **(A)** and outdoor **(B)** ST at long-term experiments. WUEi was calculated from Gs and Pn data (Figure 1-10 and Figure 1-12). H: H group of cultivars; L: L group of cultivars. Bars with the same letter are not statistically different in A. Different letters represent significant differences among cultivars at each temperature in B (DGC test; $P < 0.01$; data represents mean ± SE; n = 15 and 6 for A and B, respectively).

1.5 CONCLUSIONS

One of the aims of the present work was to detect rice cultivars with contrasting performance under ST conditions. Our results showed that across the 18 cultivars tested there was significant variation in extent of the ST-induced growth reduction, allowing us to assigned the more extreme cultivars to an H (high shoot height under ST conditions) and an L (low shoot height) group of cultivars, which we then considered as tolerant and sensitive, respectively. This grouping was supported by most of the JIP parameters measured under both laboratory and outdoor experiments, which

suggested a higher ST-derived detrimental effect on the PSII functionality in the L, compared with the H group of cultivars. On one hand, the outcome of measurements from the laboratory experiment indicated that the PSII performance of the L group of cultivars, in contrast with those of the H group, tended to decrease from days 10 to 24 when treated with ST. On the other hand, results on F_V/F_M, Chl content, RC/ABS, PI_{ABS}, RC/CS_0, ABS/RC and DI_0/RC, obtained in the outdoor experiment, indicated that the amount of active chlorophyll progressively declined with decreasing temperature. The fact that such reduction was more obvious in the L group most likely contributes to its lower tolerance to ST.

Our F_V/F_M results from laboratory and outdoor experiments are in line with previous works in chilled rice reporting higher F_V/F_M values in tolerant than in sensitive cultivars (Guo-li and Zhen-fei, 2005; Li et al., 2010b; Bonnecarrère et al., 2011), although in contrast with other reports indicating that F_V/F_M is frequently insensitive to chilling (van Heerden et al., 2003). Also in contrast with our results, reductions in the Chl content in sensitive, but not in tolerant rice cultivar grown under chilling stress, were previously reported (Li et al., 2010b; Kim et al., 2012). Such apparent contradictions between our and other results could be attributed to the different physiological nature of chilling and ST treatments.

Results from our outdoor and laboratory experiments show that the two groups of cultivars (L and H) could be discriminated on the base of their F_V/F_M, RC/ABS, PI_{ABS}, ABS/RC and DI_0/RC. Interestingly, cultivars ranked in a very similar way for each measured parameter (Figure 1-7 and Figure 1-8), what stimulated us to propose that laboratory measurements of these parameters would be a valid method to predict the response of rice cultivars to ST in the field. In this regard, the positive and significant coefficients found in a correlation analyses between laboratory and outdoor results suggested that this method might be valid. Likewise, both groups of cultivars could be clearly discriminated by their Gs but not Pn, Ci and RWC profiles. The fact that in the outdoor assay, cultivars from the H group showed higher WUE_i values than those of the L group suggests that WUE_i adjustment through Gs reduction could be part of the mechanisms contributing in these cultivars to growth sustainment during ST constrain.

Screening methods frequently identified japonica and indica cultivars, respectively, as tolerant and susceptible to cold (Mackill and Xiaomao, 1997). Our results suggest that japonica cultivars also have a better performance under the ST constraint than indica ones. Thus, Koshihikari and Bombilla, described as japonica cultivars (Takeuchi et al., 2001; Giarrocco et al., 2007) were included within the group of cultivars most

tolerant to ST, whereas IR50 and IR24, typical indica cultivars (Andaya and Mackill, 2003), which were regarded as sensitive to cold stress (Ghosh and Singh, 1983; Andaya and Mackill, 2003; Guo-li and Zhen-fei, 2005; Kim and Tai, 2011; Kim et al., 2012) were among the most sensitive to ST.

Gs measurements over a range of temperatures denoted intrinsic differences between tolerant and sensitive cultivars since Gs was already higher for the L group than for the H group in temperatures near the optimum. This could be further explained on the genotypic nature of the cultivars since indica cultivar usually have high stomatal density and high Gs while japonica cultivars show the opposite pattern (Chen et al., 1990). Besides, it has been reported that high Gs measurements correlate with high stomatal density in rice (Ohsumi et al., 2007) but it was also revealed that genotypic difference between japonica and indica in Gs rely more in stomata aperture (Maruyama and Tajima, 1990). However, our results showed that differences between the groups of cultivars increased when lowering the temperature so mechanisms for controlling Gs should be different between them. In parallel, the Gs results here obtained are in line with a report showing that stomata of chilling-sensitive maize cultivars remain open, while those of chilling-tolerant cultivars close under chilling stress (Aroca et al., 2003). A similar phenomenon was observed in chilling sensitive and tolerant tomato cultivars subjected to chilling stress (Bloom et al., 2004). Last reports are congruent with the notion that low temperature provokes leaf dehydration in sensitive plants (Pardossi et al., 1992; Janowiak and Markowski, 1994; Aroca et al., 2011). Therefore, it is possible that in cultivars of the H group, a higher ability to reduce Gs may have led to improved water balance and lower sensitivity under the ST conditions. Unfortunately, there are relatively few reports on the effect of low temperature on Gs and Pn in rice, and these are specific of chilling stress (e.g.: Li et al., 2010; Aghaee et al., 2011; Hassibi et al., 2011), preventing us from further discussion of our results.

Koshihikari is the leading variety in Japan (40 %; Uehara, 2003) and it is used in breeding as donor of cold tolerance trait (Ashikari et al., 2007). Interestingly, we detected at least two cultivars, CT-6742-10-10-1 and General Rossi, with superior tolerance than Koshihikari to the ST condition, which could be used as parents or tolerance donors in breeding for new crop varieties. We also propose that these cultivars, along with the more sensitive cultivars here studied (e.g.: Honezhaosen or IR50) could also be useful for further studies orientated to elucidate the physiological mechanisms leading to improved growth under ST conditions.

CHAPTER 2: Analysis of plant growth

This chapter consists of two different parts that discuss the same issue but at different levels: plant organ growth. The first part is focused on the regulation of the plant organ size between species. In order to address the question how cell division and cell expansion contribute to size differences across species, a meta-analysis of growth parameters of roots, monocotyledonous and dicotyledonous leaves was done. Kinematic analysis of organ growth was used in this meta-analysis as a quantitative method to unravel the cellular basis of differences in organ growth rates. The second part is focused on the cellular basis of the growth response of the rice leaf to suboptimal temperatures stress and the same approach of kinematic analysis is used. Overall, the first part gives a good introduction of kinematic analysis in a wider context and the second part describes directly what happens with the theme of interest in this Thesis: the effect of suboptimal temperatures stress on rice seedlings.

CHAPTER 2 PART 1: What determines organ size differences between species? A meta-analysis of the cellular basis

2.1 INTRODUCTION

How plants regulate growth is a central question in plant development. Differences in the size of organs between species are staggering: leaves of *Arabidopsis thaliana* are only 10-20 mm^2 (Kalve et al., 2014a), whereas those of *Helianthus annuus* become 18.000 - 30.000 mm^2 (Granier and Tardieu, 1998b); 1500 times larger. Superimposed on this, ontogenetic and environmental effects cause substantial differences even in a single genotype: The fifth leaf of wheat seedlings is only 3x the length of the first (Beemster and Masle, 1996) and leaves of bonsai trees are up to 25x smaller than those of the same species grown under normal conditions (Körner et al., 1989).

Cells are the building blocks of the plant body and therefore an obvious question to ask is “which cellular process is primarily responsible and how is it modulated to cause differences in organ size?” To address this question, it is crucial to examine cell division and expansion in parallel. Linear, steady-state growing organs, such as root tips and *Graminae* leaves have been analyzed for decades (Goodwin and Stepka, 1945) using a rigorous quantitative framework (Silk and Erickson, 1979). In these linear systems, organ growth rate is a direct consequence of the number of cells produced per unit of time by cell division (cell production, P) and the length of cells entering the mature part of the organ (l_{mat}; Table 2-1, Eqs. 2 & 3). Moreover, P is determined by the number of cells in the division zone (N_{div}) and average cell division rate (D; Table 2-1, Eq. 4), while l_{mat} is defined by the length of cells leaving the meristem (l_{div}), the average rate (RER) and duration of cell expansion (T_{el}; Table 2-1, Eq. 5).

Although Eudicotyledonous leaves also exhibit a spatial developmental gradient (Donnelly et al., 1999; Kazama et al., 2010; Andriankaja et al., 2012), they do not grow steady-state and are more conveniently described on a temporal basis considering the leaf as a whole, essentially ignoring variations in developmental patterns across the leaf (Das Gupta and Nath, 2015). Mature leaf blade area (LBA) is a function of the cell number (N_{mat}) and the cell area at maturity (A_{mat}; Table 2-1, Eq. 7). N_{mat}, in turn, is determined by the initial number of cells that are recruited in the primordium (N_{prim}), the duration of the division phase (T_{div}), and the average rate of cell division (D; Table 2-1, Eq. 8). Similarly, A_{mat} is a function of the area of cells exiting the division phase (A_{div}), the duration of the cell expansion phase (T_{exp}), and the average (relative) rate of cell expansion (RER; Table 2-1, Eq. 9).

The relationships between these cellular parameters and whole organ growth have been used to study genetic differences, environmental conditions and physiological

treatments in single species. Across these studies, no single parameter can be found that is responsible for the observed differences in organ size, indicating that the treatments and genotypic differences differentially affect the growth process. However, these studies allow us to identify the main parameters that determine differences between species, across a wider range of organ sizes than the individual studies. Therefore we extracted the data from all kinematic studies we could find for three types of organs, root tips, *Graminae* and Eudicotyledonous leaves, and performed a meta-analysis to determine the cellular mechanisms controlling the characteristic differences in organ size between plant species.

Table 2-1. Formulas and parameters used for kinematic analysis of different organ types.

Kinematic analysis of growth parameters	Symbol	Relationship between parameters	Equation N°
Roots and *Graminae* leaves			
Final leaf length (mm)	FLL	$=LER.T_{LE}$	Equation 1
Time of leaf elongation (h)	T_{LE}		
Leaf elongation rate ($mm.h^{-1}$)	LER	$=(P.l_{mat})/1,000$	Equation 2
Overall root elongation rate ($mm.h^{-1}$)	LER	$=(P.l_{mat})/1,000$	Equation 3
Cell production rate ($cells.h^{-1}$)	P	$=N_{div}.D$	Equation 4
Number of cells in the division zone	N_{div}		
Relative division rate ($cell.cell^{-1}.h^{-1}$)	D		
Mature cell length (µm)	l_{mat}	$=l_{div}.e^{RLI}$	Equation 5
Relative length increase	RLI	$=RER.T_{el}$	Equation 6
Relative expansion rate ($µm.µm.h^{-1}$)	RER		
Length of cells leaving the meristem (µm)	l_{div}		
Cells residence time in elongation zone (h)	T_{el}		
Eudicotyledonous leaves			
Leaf blade area (cm^2)	LBA	$=(N_{mat}.A_{mat})/1e^{8}$	Equation 7
Mature cell number	N_{mat}	$=N_{prim}.e^{Tdiv.D}$	Equation 8
Number of cells in the primordium	N_{prim}		
Time that cells expend dividing (h)	T_{div}		
Relative division rate ($cell.cell^{-1}.h^{-1}$)	D		
Mature cell area ($µm^2$)	A_{mat}	$=A_{div}.e^{RLA}$	Equation 9
Relative area increase	RLA	$=RER.T_{exp}$	
Area of cells in division ($µm^2$)	A_{div}		
Time that cells expend expanding (h)	T_{exp}		
Relative expansion rate ($µm^2.µm^2.h^{-1}$)	RER		

2.2 AIMS

The aim of this work was to detect the cellular processes that are primarily responsible for the size of roots and leaves from *Graminae* and Eudicotyledonous species.

2.3 MATERIALS AND METHODS

2.3.1 Data extraction

We extracted quantitative cellular parameters (Table 2-1) from the main texts, tables and figures of the published kinematic studies. If they were not explicitly given, we calculated them, based on kinematic equations and the data in the same article (showed in red in the supplementary tables). In total, 21 manuscripts were analyzed for roots (Supplementary Table 1), 20 for *Graminae* leaves (Supplementary Table 2), and 17 for Eudicotyledonous leaves (Supplementary Table 3).

2.3.2 Statistical analysis

We performed Multiple Linear Regression analyses to investigate the relationships between cellular and whole organ growth parameters (Table 2-1) with SPSS statistical software for Windows (v22.0, SPSS Inc., Chicago, IL, USA). The equations 1 to 9 described in Table 2-1 were linearized by log-transformation constituting equation 10 to 16, respectively, that were fitted to the data obtained or derived from the literature.

For roots tips (using data in Suppl. Table 1):

$$\log(\mathrm{ORER}) = C_0 + C_1 \times \log(\mathrm{P}) + C_2 \times \log(l_{mat}) \quad \text{(Equation 10)}$$

$$\log(\mathrm{P}) = C_0 + C_1 \times \log(N_{div}) + C_2 \times \log(\mathrm{D}) \quad \text{(Equation 11)}$$

$$\log(l_{mat}) = C_0 + C_1 \times \log(l_{div}) + C_2 \times \mathrm{RLI} \quad \text{(Equation 12)}$$

$$\log(\mathrm{RLI}) = C_0 + C_1 \times \log(\mathrm{RER}) + C_2 \times \log(T_{el}) \quad \text{(Equation 13)}$$

For *Graminae* leaves (using data in Suppl. Table 2):

$$\log(\mathrm{FLL}) = C_0 + C_1 \times \log(\mathrm{LER}) + C_2 \times \log(T_{LE}) \quad \text{(Equation 14)}$$

$$\log(\mathrm{LER}) = C_0 + C_1 \times \log(\mathrm{P}) + C_2 \times \log(l_{mat}) \quad \text{(Equation 15)}$$

Equations 11, 12 and 13 were also used for *Graminae* leaves.

For Eudicotyledonous leaves (using data in Suppl. Table 3):

$$\log(\mathrm{LBA}) = \mathrm{C}_0 + \mathrm{C}_1 \times \log(\mathrm{N}_{\mathrm{mat}}) + \mathrm{C}_2 \times \log(\mathrm{A}_{\mathrm{mat}}) \quad \text{(Equation 16)}$$

The data and regressions were plotted using the OriginPro software package for Windows (v9.1.0, OriginLab Corporation, Northampton, MA, USA).

2.4 RESULTS

2.4.1 Roots

The linear, indeterminate development of roots is ideally suitable to study the cellular basis of organ growth differences. Consequently, the earliest studies, as well as the largest total number of kinematic studies (21; see Supplementary Table 1), have been performed on root tips. These included six different species: *Allium cepa*, *Arabidopsis thaliana*, *Solanum lycopersicum*, *Phleum pratense*, *Triticum aestivum* and *Zea mays*. Although data for metaxylem and epidermal cells were reported in some studies, the majority of the data involved cortical cells.

We first determined the contributions of variations in mature cell length (l_{mat}) and cell production (P) to differences in the overall root elongation rates (ORER; Table 2-1, Eq. 3). As these two parameters directly determine organ growth rate, variation in l_{mat} and P accounted for 100% of the variation across species and cell types (Eq. 10; Supplementary Figure 1 A). Both parameters contributed significantly, but the standardized coefficients (Beta) suggested that impact of P on ORER was larger than that of l_{mat}. To compare their contributions in more detail, we analyzed the models of ORER vs. l_{mat} and P, separately. As different cell types have characteristic differences in cell length, they were analyzed separately. For all three cell types represented in the data set, there was a strong positive correlation between P and ORER (R^2 between 0.78 and 0.90; Figure 2-1 A). In contrast, the correlation between l_{mat} and ORER was only significant for cortical cells (R^2 of 0.33; Figure 2-1 B). There was no correlation between P and l_{mat}, suggesting that cell production and expansion are independent and high cell production does not lead to smaller cells or that both vary in parallel (data not shown). Thus, these results show that differences in root growth rate between species are primarily driven by variations in the number of cells produced in the meristem.

Cell production (P) in turn is directly determined by the number of dividing cells (N_{div}) and the rate at which these cells are dividing (D), allowing us to performed a similar regression analysis (Table 2-1, Eq. 4). Because there was insufficient data for

the other cell types, we restricted this analysis to the cortical cells. As expected, N_{div} and D together explained 99% of the variation in P (Eq. 11; Supplementary Figure 1 B). Both parameters contributed significantly and roughly equally. Consistently, N_{div} explained 73% and D 74% of the variation in P (Figure 2-1 C and D). Since the number of cells in the meristem largely determines the length of the meristem (L_{mer}, the distance between the stem cells and the position where cells of a given cell type stop dividing and start expanding), the length of the meristem was also positively correlated with P (R^2 of 0.67; inset in Figure 2-1 C). There was no correlation between average cell division rate and number of cells in the meristem (data not shown). These results indicate that variations in rates of cell division and number of dividing cells contribute equally and independently to differences in overall cell production.

Although not contributing much to the variation in ORER, there were significant differences in l_{mat}. Therefore we explored the basis of this variation, focusing on cortical cells, using the relationship between l_{mat}, the length of the cells exiting the meristem (l_{div}) and the relative length increase in the elongation zone (RLI; Table 2-1, Eq. 5). Indeed, these two parameters accounted for 100% of the variance in mature cell length (Eq. 12; Supplementary Figure 1 C). Both l_{div} and RLI contributed significantly, but RLI had a higher Beta coefficient. However, individually the length of cells leaving the meristem did not show a significant correlation (Figure 2-1 E), whereas RLI was positively correlated and explained 39% of the variance in l_{mat} (Figure 2-1 F). Interestingly, l_{div} and RLI were negatively correlated (R^2 = 0.80; Supplementary Figure 1 D). Since most of the variation in l_{mat} was explained by RLI, which in turn is a function of RER and T_{el} (Table 2-1, Eq. 6), we further investigated the relationship between the latter three parameters. As expected, RER and T_{el} explained 100% of the variance in RLI and both parameters had a comparable impact (Eq. 13; Supplementary Figure 1 E). However, only T_{el} showed a significant correlation with RLI, although the correlation was weak (R^2 of 0.21; Figure 2-1 G and H). Together, these results show that differences in mature cell size are mostly explained by the time cells continue to expand and that small cells typically expand for a longer period.

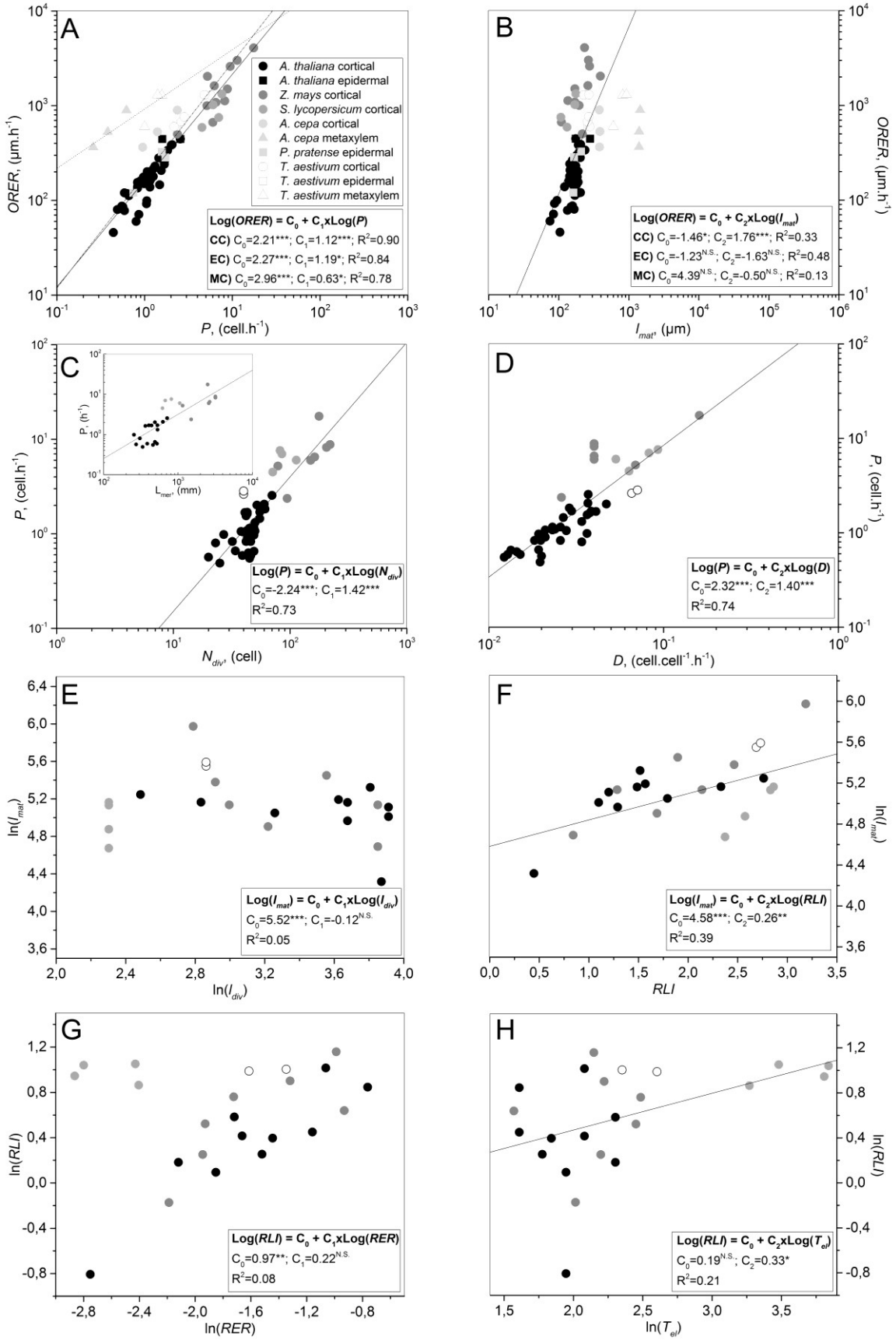

Figure 2-1. The cellular basis of differences in root growth rate across a range of species. **A)** the relationship between root elongation rate (ORER) and cell production (P). **B)** the

relationship between ORER and mature cell length (l_{mat}). **C)** the relationship between P and number of cells in the meristem (N_{div}). **D)** the relationship between P and average cell division rate (D). **E)** the relationship between l_{mat} and length of cells at the end of the meristem (l_{div}). **F)** the relationship between l_{mat} and relative length increase (RLI). **G)** the relationship between RLI and relative elongation rate (RER). **H)** the relationship between RLI and time of cells in the elongation zone (T_{el}). Figures A and B show models for cortical cells (CC), epidermal cells (EC), and mesophyll cells (MC). Inset in figure C shows the correlation between P and length of the meristem (L_{mer}). Details of the regression parameters are shown in each figure: C_0, C_1, and C_2 are the partial coefficients; R^2 the coefficient of correlation. n = 63 for CC, 6 for EC and MC in A and B; 47 in figures C and D; 27 in inset of figure C; and 23 in figures E, F, G and H. Significance: * 0.01<*p*-value<0.05; ** 0.001<*p*<0.01; *** *p*<0.001; NS, *p* not significant. T-test.

2.4.2 Graminae leaves

The growth of *Graminae* leaves has strong similarities with that of root tips: It is linear and cells are organized files with a spatial gradient of proliferating, expanding and mature cells. Although the growth of these leaves, in contrast to roots, is determinate, after emergence there usually is a phase of steady-state growth that has been extensively used for kinematic analyses. To study the differences in leaf length and leaf growth rates between *Graminae* species, we extracted data from 20 published kinematic studies, involving twelve different species: *Aegilops caudata*, *Aegilops tauschii*, *Festuca arundinacea*, *Lolium perenne*, *Lolium multiflorum*, *Oryza sativa*, *Poa annua*, *Poa trivialis*, *Poa compressa*, *Poa alpine, Triticum aestivum*, and *Zea mays* (Supplementary Table 2). Across these studies two different types of cells were most frequently analyzed: epidermal cells in the file adjacent to stomata (sister cells); and cells located more centrally between stomatal files that are substantially larger (Beemster and Masle, 1996).

To explain differences in FLL, we first analyzed the contribution of leaf elongation rate (LER) and the duration of that elongation (T_{LE}; Table 2-1, Eq. 1). In accordance with Eq.1, LER and T_{LE} together accounted for 100% of the variance in FLL (Eq. 14). Both parameters contributed to variation in FLL, although the Beta coefficients suggest the effect of LER was stronger (Supplementary Figure 2 A). Consistently, LER alone explained 94% of the variation in FLL and T_{LE} only 40% (Figure 2-2). This analysis suggests that differences in mature leaf size are primarily correlated with differences in leaf growth rate, with a minor contribution of duration of the growth process.

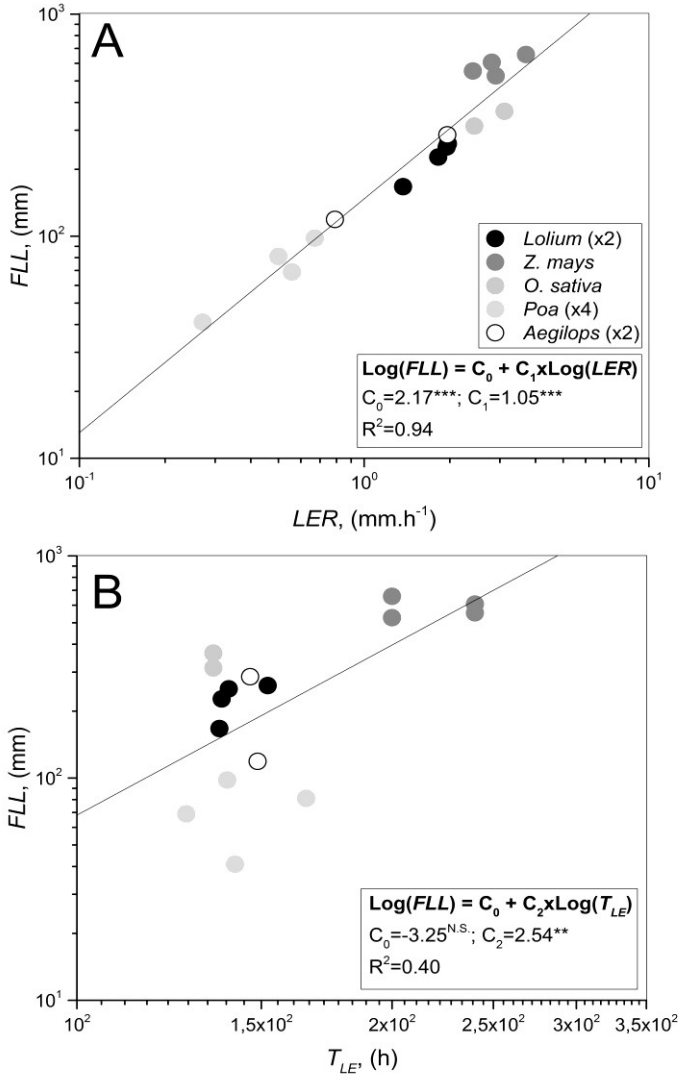

Figure 2-2. The difference in growth pattern determining leaf size across a range of *Graminae* species. **A)** the relationship between FLL and LER. **B)** the relationship between FLL and T_{LE}. Details of the regression parameters are shown in each figure: C_0, C_1, and C_2 are the partial coefficients; R^2, coefficient of correlation; n = 16. Significance: * 0.01<*p*-value<0.05; ** 0.001<*p*<0.01; *** *p*<0.001; NS, *p* not significant. T-test.

Based on the kinematic data we then investigated the role of cell production and mature cell length in determining variation in LER. Analogous to roots, cell production (P) and mature cell length (l_{mat}) together fully accounted for variation in LER (Eq. 15; Supplementary Figure 2 B). Although both parameters significantly contributed to leaf elongation rate, the Beta coefficients suggested that impact of cell production was larger. Indeed, cell production of sister cells and elongated cells between stomatal files by itself explained 89% and 47 % of the variation in LER, respectively (Figure 2-3 A), while no significant correlation was found for mature cell length of either type (Figure 2-3 B). No evidence was found to suggest that l_{mat} and P correlated (data not shown). Thus, analogous to the observations in the root tip, differences in leaf growth rate between species are largely controlled by cell production in the meristem.

To investigate if the analogy between the two organs extends to the underlying mechanisms, we investigated the relationship between P, N_{div} and D across *Graminae* leaves (see Table 2-1), focusing on the sister cells for which sufficient data were

available. As expected, N_{div} and D together fully accounted for the variation in cell production (Eq. 11; Supplementary Figure 2 C). Although both parameters significantly contributed to cell production, N_{div} had a higher Beta coefficient than D. Consistently, N_{div} by itself accounted for 67% of the variance in cell production (Figure 2-3 C). In contrast to what was found for the root tips, D was not significantly correlated with P in *Graminae* leaves (Figure 2-3 D). Since the size of the meristem is related to the number of cells in it, L_{mer} explained 79% of the variation in P (inset in Figure 2-3 C). No correlation was found between the N_{div} or L_{mer} and D (data not shown). Together these data indicate that in *Graminae* leaves, the size of the meristem (and hence the number of dividing cells) is the main determinant of leaf growth rate and ultimately leaf size.

Although variation in l_{mat} did not significantly contribute to LER, we analyzed cell expansion parameters in detail to understand if cell size variation in the leaf is achieved in a similar way as in the root. Similar to the root tip, l_{div} and RLI together accounted for 100% of the variation in l_{mat} (Table 2-1, Eq. 5) and although both parameters had a significant effect, that of RLI was stronger than that of l_{div} (Eq. 12; Supplementary Figure 2 D). This was confirmed with the partial models (Figure 2-3 E and F): While the correlation between l_{mat} and l_{div} was not significant, RLI explained 65% of the variation in l_{mat}. In analogy with roots, we found a negative correlation between l_{div} and RLI (Supplementary Figure 2 E). Finally, as expected, the variation in RLI was fully explained by RER and T_{el} (Eq. 13; Supplementary Figure 2 F). Similar to the situation in root tips, only T_{el} explained 64% of the variation in RLI, whereas RER did not correlate (Figure 2-3 G and H). These results show that also in *Graminae* leaves differences in mature cell size are due to variations in duration of the expansion phase and cells that are small when leaving the meristem expand for a longer period to compensate.

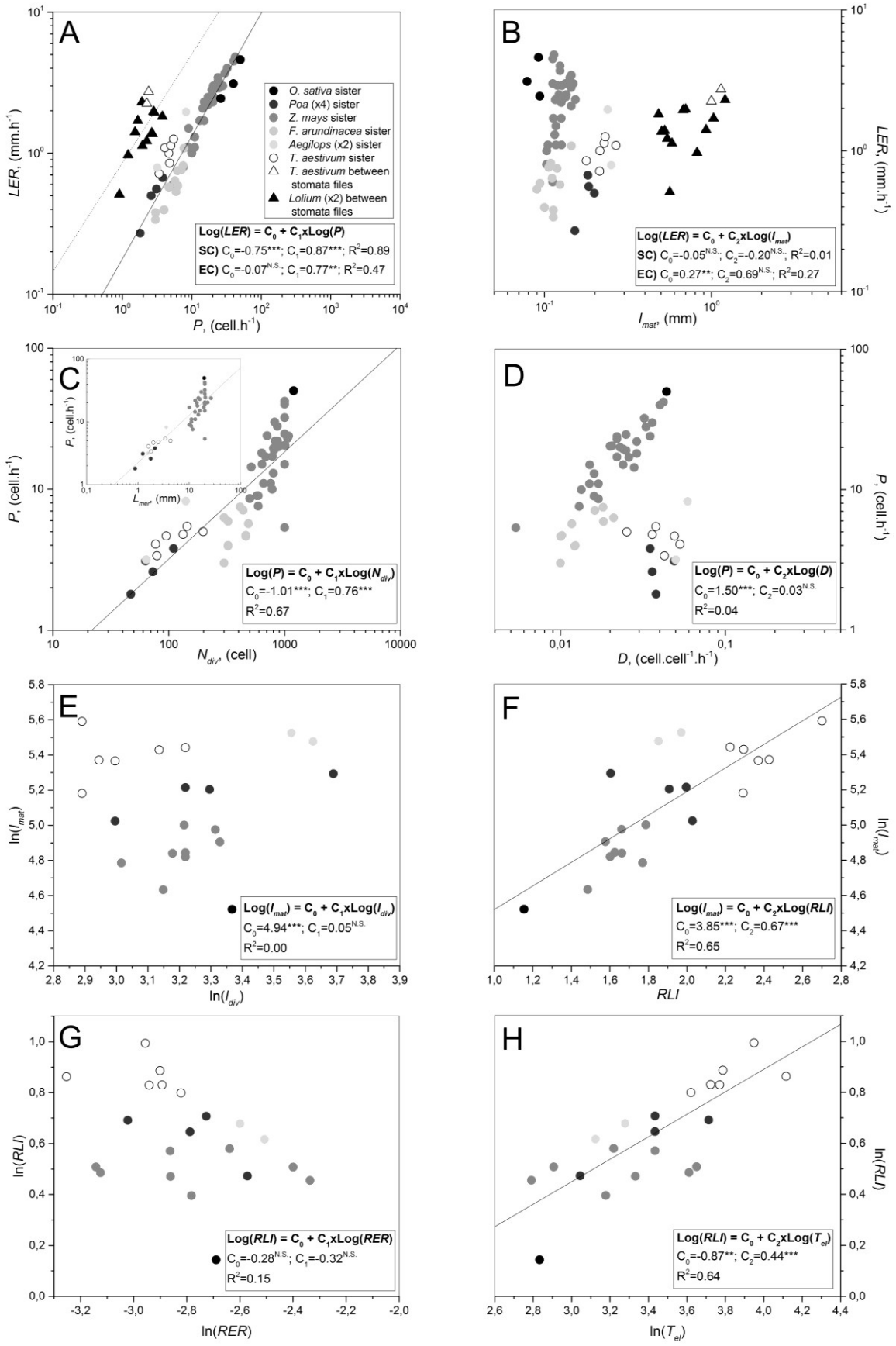
A
LER, (mm.h-1)
P, (cell.h-1)
O. sativa sister
Poa (x4) sister
Z. mays sister
F. arundinacea sister
Aegilops (x2) sister
T. aestivum sister
T. aestivum between stomata files
Lolium (x2) between stomata files
Log(LER) = C0 + C1xLog(P)
SC) C0=-0.75***; C1=0.87***; R2=0.89
EC) C0=-0.07N.S.; C1=0.77**; R2=0.47
B
LER, (mm.h-1)
Imat, (mm)
Log(LER) = C0 + C2xLog(Imat)
SC) C0=-0.05N.S.; C2=-0.20N.S.; R2=0.01
EC) C0=0.27**; C2=0.69N.S.; R2=0.27
C
P, (cell.h-1)
Ndiv, (cell)
Lmer, (mm)
Log(P) = C0 + C1xLog(Ndiv)
C0=-1.01***; C1=0.76***
R2=0.67
D
P, (cell.h-1)
D, (cell.cell-1.h-1)
Log(P) = C0 + C2xLog(D)
C0=1.50***; C2=0.03N.S.
R2=0.04
E
ln(Imat)
ln(Idiv)
Log(Imat) = C0 + C1xLog(Idiv)
C0=4.94***; C1=0.05N.S.
R2=0.00
F
ln(Imat)
RLI
Log(Imat) = C0 + C2xLog(RLI)
C0=3.85***; C2=0.67***
R2=0.65
G
ln(RLI)
ln(RER)
Log(RLI) = C0 + C1xLog(RER)
C0=-0.28N.S.; C1=-0.32N.S.
R2=0.15
H
ln(RLI)
ln(Tei)
Log(RLI) = C0 + C2xLog(Tei)
C0=-0.87**; C2=0.44***
R2=0.64

Figure 2-3. The cellular basis of differences in leaf elongation rate across a range of *Graminae*. **A)** the relationship between leaf elongation rate (LER) and cell production (P). **B)** the relationship between LER and mature cell length (l_{mat}). **C)** the relationship between P and number of cells in the meristem (N_{div}). **D)** the relationship between P and average cell division rate (D). **E)** the relationship between l_{mat} and length of cells at the end of the meristem (l_{div}). **F)** the relationship between l_{mat} and relative length increase (RLI). **G)** the relationship between RLI and relative elongation rate (RER). **H)** the relationship between RLI and time of cells in the elongation zone (T_{el}). Figures A and B show models for sister cells (SC), and elongated cells between stomata files cells (EC). Inset in figure C shows the correlation between P and length of the meristem (L_{mer}). Details of the regression parameters are shown in each figure: C_0, C_1, and C_2 are the partial coefficients; R^2, coefficient of correlation; n = 60 for SC, and 14 for EC in A and B; 56 in figures C and D; 44 in inset of figure C; and 21 in figures E, F, G and H. Significance: * 0.01<*p*-value<0.05; ** 0.001<*p*<0.01; *** *p*<0.001; NS, *p* not significant. T-test.

2.4.3 Eudicotyledonous leaves

Kinematic analysis *sensu-strictu* is not useful to study the cellular basis of the growth of Eudicotyledonous leaves. Instead, measuring organ and cell size in function of time is a more efficient way to achieve this (Fiorani and Beemster, 2006). We found 17 papers on 4 species, including *Arabidopsis thaliana*, *Helianthus annuus*, *Manihot esculenta* and the hybrid *Populus x canascens* where such studies were performed (Supplementary Table 3). We focused on epidermal cells since palisade cells were only studied in one species (*A. thaliana* (Ferjani et al., 2007; Hisanaga et al., 2013)).

We first analyzed the contribution of the number of cells (N_{mat}) and mature cell area (A_{mat}) to the variation in leaf blade area (LBA; Table 2-1, Eq. 7). Together N_{mat} and A_{mat} accounted for 100% of the variance in LBA (Eq. 16; Supplementary Figure 3). Data points clustered into two groups, a group with low leaf area corresponded to data from *Arabidopsis thaliana* and the other group with high leaf area, including the other 3 species. Both N_{mat} and A_{mat} contributed to variations in leaf area since their partial coefficients were significant. However, the Beta coefficient of the N_{mat} was higher than the one of A_{mat}. Indeed, similar to the situation in roots and *Graminae* leaves, cell number was more important in determining organ growth than cell size, as N_{mat} explained 98% of the variance of leaf area (Figure 2-4 A). Curiously, A_{mat} correlated negatively with LBA accounting for 36% of the variation (Figure 2-4 B). No correlation was found between N_{mat} and A_{mat}, implying independence of the two parameters (data not shown). The relations between N_{mat}, N_{prim}, T_{div} and D, and A_{mat}, A_{div}, T_{exp} and RER could not be analyzed as these parameters were typically not determined. Only D for *Arabidopsis thaliana* and *Helianthus annuus* epidermal cells, could be correlated with

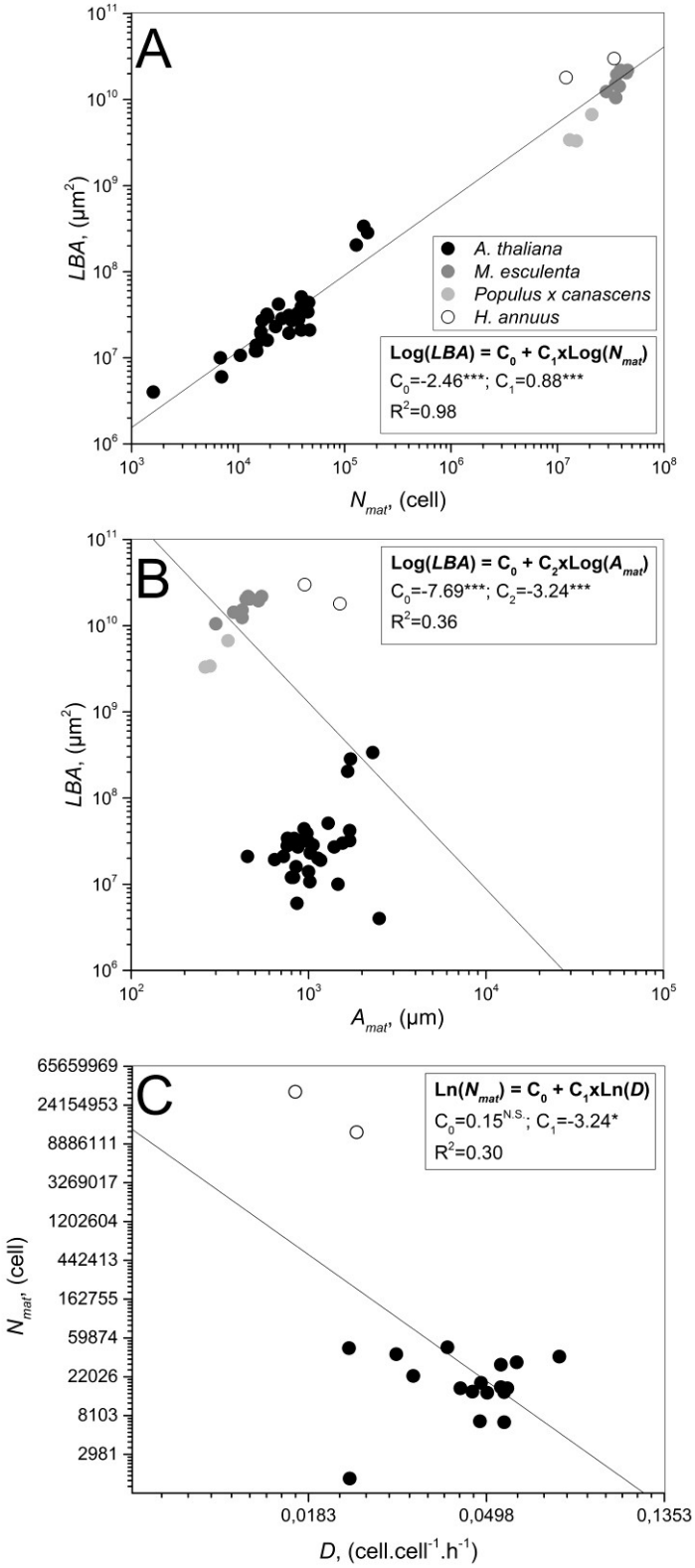

N_{mat} showing a significant, negative correlation, but with poor adjustment (Figure 2-4 C).

These data show that, consistent with the situation in roots and *Graminae* leaves, cell production rather than mature cell size determines variation in leaf size.

Figure 2-4. The cellular basis of differences in leaf size across a range of Eudicotyledonous species. **A)** the relationship between LBA and A_{mat}. **B)** the relationship between LBA and N_{mat}. **C)** the relationship between N_{mat} and D. Details of the regression parameters are shown in each figure: C_0, C_1, and C_2 are the partial coefficients; R^2, coefficient of correlation; n = 46 in A and B, n = 19 in C. Significance: * 0.01<*p*-value<0.05; ** 0.001<*p*<0.01; *** *p*<0.001; NS, *p* not significant. T-test.

2.5 DISCUSSION AND CONCLUSIONS

We addressed the question which cellular mechanisms determine the variation in organ sizes between plant species. To this end we performed a quantitative meta-analysis of kinematic data obtained for root tips and *Graminae* leaves, and developmental studies of Eudicotyledonous leaves available in the literature. Although data from different labs and different conditions were compared, variation in organ size between species exceeded experimental variation, so that interspecies differences could effectively be studied based on the combined data. By analyzing results from the three different organs across a wide range of species a consistent picture emerges: First of all, cell proliferation (variations in cell number) rather than cell expansion (the size of mature cells) determines the final size of plant organs. Second, the number of dividing cells (and meristem size) and not the rate at which cells divide, determines cell production. Third, cells that are small when leaving the meristem compensate by expanding for longer. Fourth, variations in mature cell size are primarily determined by the duration of cell expansion.

Thus, the cellular basis of organ size variation between species is remarkably similar for the three different organs. Studying the underlying molecular regulation of these parameters by comparing species has, to our knowledge, not been done to date. Nevertheless, findings within a single species provide us with a good basis. Firstly, such studies largely confirm the importance of the size of the meristem as the crucial control point in organ growth regulation both in root tips (Baskin, 2000; West et al., 2004) and in *Graminae* leaves (Bultynck et al., 2003; Barrôco et al., 2006; Powell and Lenhard, 2012; Czesnick and Lenhard, 2015). The importance of this control mechanism has been widely recognized and this has led to studies where the size of the meristem is the only cellular parameter that was determined (Ioio et al., 2008; Moubayidin et al., 2010; Tsukagoshi et al., 2010). Moreover, approaches to extract this parameter from cell length profile data (French et al., 2012; Bizet et al., 2014; Voorend et al., 2014), velocity profiles (van der Weele et al., 2003), the expression of cell cycle markers (Ferreira et al., 1994; Donnelly et al., 1999; West et al., 2004) and infra-red images (Bizet et al., 2014) have been developed. In dicotyledonous leaves it is virtually impossible to use meristem size as a basis to determine overall cell production, as the group of cells recruited at the SAM to form the leaf, exponentially grows during the proliferative development of the leaf. The equivalent to meristem size in linear systems therefore is the duration of the proliferative phase, as both parameters essentially represent the transition from proliferation to expansion. Indeed, kinematic studies in *Arabidopsis thaliana* have shown that across a range of genetic perturbations that

cause variations in leaf size, the duration of cell proliferation was most frequently involved (Gonzalez et al., 2012). This has facilitated the discovery of a hormonal network that controls the position where cells exit from proliferation. Interestingly, not only the cellular basis of organ growth is very similar in different organs, as we show here, also the molecular regulation shows strong similarities (Nelissen et al., 2016).

A recent modeling study demonstrated that cell autonomous regulation cannot account for observed growth patterns in root tips and that spatial control by hormones is required (De Vos et al., 2014). Auxin accumulates in proliferating tissues in root tips (Grieneisen et al., 2007; Brunoud et al., 2012) and in leaves of *Arabidopsis thaliana* and *Zea mays* (Nelissen et al., 2012), quickly dropping to low levels in expanding cells. Indeed, genetic perturbation of auxin signaling in root tips (Sabatini et al., 1999; Swarup et al., 2005) , *Zea mays* (Tsiantis et al., 1999; Guo et al., 2014) and *Arabidopsis thaliana* leaves (Schruff et al., 2006; Bilsborough et al., 2011; Kasprzewska et al., 2015) affects the transition from proliferation to cell expansion.

In the growth zone of *Zea mays* gibberellins show a striking accumulation pattern at the position where cells exit the proliferation zone (Nelissen et al., 2012). Indeed, altered levels of gibberellins result in marked differences in organ size, linked to meristem size (Nelissen et al., 2012). Again, also in *Arabidopsis thaliana* leaves, overproduction of gibberellins resulted in increased leaf size (Huang et al., 1998) that were related to increased cell production (although cell size was also enhanced (Gonzalez et al., 2010)) and also in the root tip gibberellins directly controls the transition from meristem to elongation zones in (Ubeda-Tomás et al., 2008; Achard et al., 2009; Perilli et al., 2012). Thus, it appears that the molecular signaling network controlling organ growth has a similar architecture in different organs. Therefore, an obvious question to address is if and how hormonal regulation is involved in the regulation of differences in organ size between species. Our results clearly demonstrate that such investigations should focus on the regulation of the exit from proliferation.

An interesting and unexpected finding was a strong negative correlation between the size of cells leaving the meristem and the duration of the subsequent phase of cell expansion. In theory, this could be due to a technical artifact related to the determination of the position of the end of the proliferation zone. In *Arabidopsis thaliana* root tips with very different sizes of the expansion zone, the duration is remarkably stable (Beemster and Baskin, 1998). However, the different methods employed to determine meristem size in the studies we used could easily result in over-

or underestimation of this boundary. This would lead to over- or underestimation of the cells that exit, as the cell size increases quickly in this region (Beemster and Baskin, 1998) , but also inversely affect the estimated size of the elongation zone and consequently, the residence time in it. However, it is also plausible that the mechanisms that control exit from cell proliferation and exit from expansion are completely independent. This implies that in some genotypes/species cells exit mitosis at a smaller size, but as the size of mature cells is independently regulated and rates of cell expansion do not contribute to size increase differences (Figs. 2-1 E and G), smaller cells would on average expand for a longer period.

In contrast to the transition between cell proliferation and expansion, very little is known about the regulation of the transition from expansion to maturity. One hypothesis could be that cell size itself is sensed and a trigger for termination of cell expansion. However, perturbations of cell division frequently lead to adjustment of mature cell size that counteract the effects on mature cell number, a phenomenon called compensation (Tsukaya, 2002; Beemster et al., 2003; Ferjani et al., 2007; Horiguchi and Tsukaya, 2011). Therefore, a second yet unknown spatial signal appears to be a more likely explanation.

Studies of the response to abiotic stresses suggests that the mechanism by which growth responds to abiotic stress depends on the duration of the exposure. In root tips of *Arabidopsis thaliana* transplanted to 0.5% NaCl, the adaptation involved two phases: First, a rapid transient inhibition of the cell cycle during which cyclin-dependent kinase (CDK) activity and CYCB1;2 promoter activity were reduced, resulting in fewer cells remaining in the meristem. However, after meristem size was adjusted, cell cycle duration returned to control values (West et al., 2004). Remarkably, a similar response was found in wheat seedlings responding to soil compaction. In the first leaf that was exposed, cell production was reduced due to cells in a normal size meristem dividing slower. However in subsequent leaves, a similar reduction in cell production was due to a reduced meristem size and cells divided at similar rates as control plants (Beemster et al., 1996). These findings indicate that short-term responses are primarily mediated by changes in the rate of division, whereas in the longer term the more structural response involves adjustment of meristem size, allowing a similar reduction in cell production with cells proliferating at control rates. These examples of contrasting cellular responses to the same adverse condition, that nevertheless result in similar overall growth responses, indicate the flexibility of the cellular growth parameters within a single plant. Inversely, increased cell expansion in response to mutations that inhibit

cell division demonstrates that these parameters can be adjusted to limit effects on overall organ size (Ferjani et al., 2007) under a given environmental condition. This flexibility within individual species highlights the importance of our study of variations occurring in the broader context of interspecies variation, where differences in growth are much larger than observed in a single species. Moreover, it allows to identify the parameters preferentially selected by evolution to determine organ growth differences and speculate on why this may be the case.

It could be hypothesized that at normal rates the cell division process is most efficient and has optimal possibilities to be adjusted in response to fluctuations in the environment. The same argument to some extent would account for cell size differences. Although often cell sizes are reduced by stress conditions, these changes are limited. Our finding that mature cell size does not contribute to size differences of the three types of organs we analyzed across a wide range of species also suggest that there is optimal cell size, probably for physiological functioning.

Another argument for the exit from proliferation being the primary control mechanism for organ size variation is that cell division is an exponential process. One additional round of cell division before starting to expand, doubles cell production at the organ scale, potentially doubling organ size.

For these reasons, the main outcome from this study, that meristem size/exit from proliferation is the main parameter controlling organ size, seems a logic solution from an evolutionary perspective.

CHAPTER 2 PART 2: Kinematic analysis of the leaf growth responses of rice cultivars with contrasting sensitivity to suboptimal temperatures

2.6 INTRODUCTION

In the previous chapter we described the main effects on rice subjected to suboptimal temperatures (ST) stress and demonstrated that different cultivars had different physiological responses. Particularly, the effect on leaf growth triggered the question of how rice regulates leaf growth under this stress and if this is different between cultivars. Here six representative cultivars with different performance were used, three from the tolerant group, Koshihikari, CT-6742-10-10-1 and General Rossi, and three from the sensitive group, IR50, IR24, and Honezhaosen. Koshihikari and IR50 were included because they are elite cultivars, Koshihikari is well known for its tolerance to cold stress and is a japonica cultivar (Takeuchi et al., 2001), while IR50 is sensitive to cold stress and belongs to the indica subspecies (Andaya and Mackill, 2003; Guo-li and Zhen-fei, 2005).

Cells are the building blocks of the plant body and the regulatory units that integrate locally perceived chemical and physiological signals by genetically encoded molecular regulatory networks that ultimately control the growth process (Gonzalez et al., 2012; Kalve et al., 2014b; Czesnick and Lenhard, 2015). At the cell level only two processes contribute to the growth of the organ: cell division (the act of duplicating the genome and forming a new cell wall during cytokinesis) and cell expansion (the increase in cell volume). It is important to note that dividing cells also undergo cell expansion in order to roughly double their size prior to cytokinesis (Green, 1976). The regulation of leaf growth in rice is therefore the result of the modulation of these cellular processes, resulting in differences in organ size. So the questions “how does rice regulate the growth of their leaves when subjected to ST stress?” and “if this is different between cultivars?” can be addressed by an examination of cell division and cell expansion parameters. Understanding how division and expansion are coordinated in the organ growth could lead us to unravel the mechanisms behind it. Kinematic analysis of leaves growth provides the mathematical framework to obtain these parameters.

The kinematic approach views organ growth in terms of motion of cells or “tissue elements”. Its advantage is that it enables the description of the growth process in a mathematical way in terms of the patterns of division and expansion. Cell division and cell expansion are independent processes, but they are often synchronized during development. Linear, steady-state growing organs, such as root tips and monocotyledonous leaves have been analyzed for decades (Goodwin and Stepka, 1945) using a rigorous quantitative framework (Silk and Erickson, 1979). In these linear systems, cells are typically organized in discrete files running along the length of the

organ. This allows to simplify the analysis to the perspective of a single representative row of cells, at the base (leaf) or tip (root) of which cells are actively dividing. Division drives a flow of cells across a boundary, where they stop dividing and start expanding until they cross a second boundary at which they stop expanding and hence have reached their mature size, creating a spatial gradient of development (Fiorani and Beemster, 2006; Figure 2-5). From this simplified perspective it can be easily seen that organ growth rate is a function of the number of cells produced by cell division in the meristematic region of each cell file and the mature cell length established by expansion in the elongation zone. In the case of monocotyledonous leaves, that have a determinate growth pattern, the final leaf length (FLL) is a function of the leaf elongation rate (LER) and the time that the leaf continues elongating (T_{LE}; Table 2-2, Eq. 1). LER is a function of the number of cells produced by cell division (cell production, P) and the length of cells entering the mature part of the organ (l_{mat}; Table 2-2, Eqs. 2). Moreover, P is a function of the number of cells in the division zone (N_{div}) and average cell division rate (D; Table 2-2, Eq. 3), while l_{mat} is determined by the length of cells leaving the meristem (l_{div}), the average rate (RER) and duration of cell expansion (T_{el}; Table 2-2, Eq. 4).

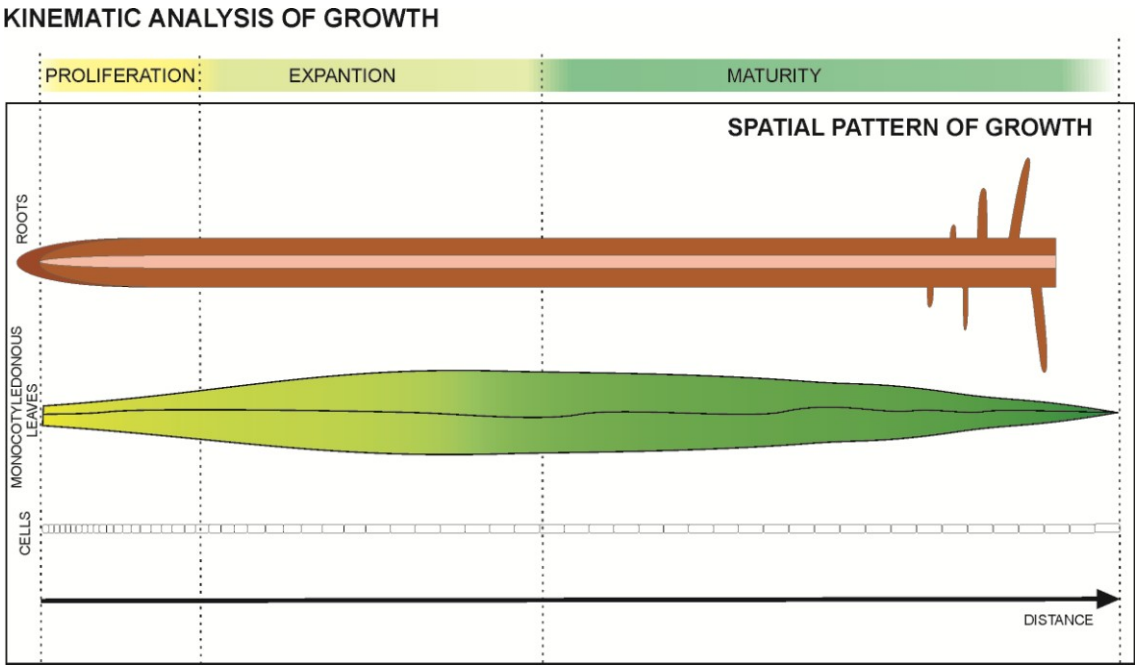

Figure 2-5. Schematic representation of growth pattern of leaves of monocotyledonous and roots.

Table 2-2. Equations and definitions used for kinematic analysis.

Kinematic analysis of growth parameters			
	Symbol	Relationship between parameters	Equation N°
Final leaf length (mm)	FLL	$=LER.T_{LE}$	Equation 1
Time of leaf elongation (h)	T_{LE}		
Leaf elongation rate ($mm.h^{-1}$)	LER	$=(P.l_{mat})/1{,}000$	Equation 2
Cell production rate ($cells.h^{-1}$)	P	$=N_{div}.D$	Equation 3
Number of cells in the division zone	N_{div}		
Relative division rate ($cell.cell^{-1}.h^{-1}$)	D		
Mature cell length (µm)	l_{mat}	$=l_{div}.e^{RER.T_{el}}$	Equation 4
Relative expansion rate ($\mu m.\mu m.h^{-1}$)	RER		
Length of cells leaving the meristem (µm)	l_{div}		
Cells residence time in elongation zone (h)	T_{el}		

The impact of temperature on plant development is usually modeled using thermal time concept that presupposes that the growth of a plant is linearly related to temperature or the total amount of heat to which it is exposed (Granier and Tardieu, 1998a; Granier et al., 2002). This theory provides a measure of physiological time that can be applied to the growth of seedlings, the inflorescence appearance, and any other stage of the plant. It is based on the assumption that a base temperature of growth exist and that the growth parameter being analyzed has a linear relationship with temperatures over the base one. The thermal time, or growing degree days (GDD), determines the optimum planting/harvesting/spraying dates (Trudgill et al., 2005). However, it has been also used to model the effect of climate conditions and hence it can be used to model the effect of ST stress on leaf growth of rice seedlings.

2.7 AIMS

This chapter aims to understand the mechanisms at the cell level that determine leaf growth of rice cultivars subjected to ST stress. To unravel this, a kinematic analysis of leaf growth was done to quantify changes in division, expansion and morphology of the rice leaf induced by ST. In order to distinguish between tolerant and sensitive mechanisms, two groups of representative cultivars were used: three tolerant, and three sensitive.

2.8 MATERIALS AND METHODS

2.8.1 Plant material and growth conditions

Rice seeds (*Oryza sativa*) from cultivars Koshihikari, CT-6742-10-10-1, General Rossi, IR50, IR24, and Honezhaosen were kindly provided by the Rice Breeding Program on the Universidad Nacional de La Plata, Argentina. Seeds of these cultivars were placed within Petri plates on two layers of Whatman N° 5 filter paper rinsed with 7 mL carbendazim 0.025 %p/v (Yoshida, 1981) and incubated in growth chamber at 30 °C in darkness until germination. The resultant seedlings were transplanted to peat potting medium (Jiffy, The Netherlands; volume of the pots: 1.6 l, dimensions: 13 cm high and 5" in diameter) and saturated with water. The seedlings were then grown in a growth chamber (Conviron, Adaptis A1000) under controlled conditions with 12 h photoperiod, 80% humidity and 350 µmol photons m^{-2} s^{-1} of photosynthetically active radiation (PAR). Day and night temperatures for optimal temperatures of growth treatment (OT) were 28 and 24 °C (d/n), respectively. When the third leaf (Yoshida, 1981) emerged, temperatures for the suboptimal temperatures of growth treatment (ST) were modified to 21 and 13 °C (d/n), respectively. Seedlings were further cultivated and harvested two days after the emergence of the fourth leaf, when leaf elongation was in steady-state.

2.8.2 Growth and kinematic analysis

In order to determine leaf elongation rate (LER) the length of the fourth leaf (Yoshida, 1981) was measured daily with a ruler, using top of the soil as a reference point. The measurements were carried out on 23 plants per cultivar/treatment 2 h after the start of the photoperiod throughout the growth of the fourth leaf, from its emergence till it reached its final length (FLL). Leaf elongation rates were calculated as the difference in leaf length divided by the time interval between successive measurements. A kinematic analysis was performed on the fourth leaf of five representative plants of each cultivar/treatment harvested on the second day after their emergence from the whorl of older leaves (during its steady-state growth) following the protocol described by Pettkó-Szandtner et al. (2015) and Rymen et al. (2010) with minor modifications. Briefly, the forth leaf was harvested after 48 h of its appearance by carefully removing the older leaves with the help of forceps and a scalpel. Imprints of the abaxial epidermis of the basal 4 and 5 cm of the leaf for the OT and ST conditions, respectively, were made with nail varnish. Taking special care not to damage the leaf, these were transferred to microscopy slides by means of

cellophane tape. The first two centimeters from the basal part of the same leaf that was used for imprints were further analyzed to determine meristem size. To this end they were cut with a scalpel and placed in 3:1 v/v absolute ethanol:acetic acid for fixation of cell walls and clearing chlorophyll. Samples were kept at 4 °C from 24 h up to several weeks before use. They were then washed for 20 min in wash buffer containing 0.05 M Tris-HCl pH 7.0 and 0.5% Triton X-100 and incubated with 1 μg.ml^{-1} DAPI (4',6-diamidino-2-phenylindole) in wash buffer for 5-7 min. Fluorescent nuclei were observed with a fluorescence microscope (AxioScope A1, Axiocam ICm1, Zeiss) at 20X magnification. The length of meristematic zone of the leaves was estimated by locating the most distal mitosis in the abaxial epidermal cells and then determining the distance between the base of the leaf and its position by counting the number of frames needed to cross that distance and multiply it by the corresponded width of that field (Fiorani et al., 2000). For cell length measurements the length of elongated cells next to stomata files (Luo et al., 2012) was measured at 1 mm intervals from the imprints of the leaf by light microscopy (Scope A1, Axiocam ICm1; Zeiss) using the online measurement module in the Axiovision (Rel. 4.8, Zeiss) software. For meristematic cells 40X and for the elongating and mature cells 20X (Plan) objectives were used. The raw data obtained from individual leaves were smoothed and interpolated to 1-mm spaced points using the kernel smoothing function locpoly of the Kern Smooth package (Wand and Jones, 1995) for the R statistical package (R Foundation for Statically Computing), which allowed averaging between leaves and comparison between cultivar/treatments. The calculations of cell division and expansion parameters were based on this data (Table 2-2), as described earlier (Rymen et al., 2010).

2.8.3 Thermal time calculation

Growing degree days parameter was calculated by daily integration of leaf temperatures according to Bonhomme (2000):

$$GDD = \left[\left[\frac{(T_{MAX} - T_{MIN})}{2}\right] - T_{BASE}\right]$$

Where T_{MAX} is the daily maximum air temperature, T_{MIN} is the daily minimum air temperature, T_{BASE} is the temperature below the leaf is not growing. T_{BASE} was set to 10 °C (Lee, 1979; Gao et al., 1992; Sánchez et al., 2014).

2.8.4 Statistical analysis

Statistical analysis was performed using ANOVA and post-hoc Tukey test with Infostat statistical software package (Di Rienzo et al., 2016).

2.9 RESULTS AND DISCUSSION

We studied the effect of cold stress on the growth of rice seedlings to determine the cellular basis of differences in the growth response between cultivars with contrasted tolerance. For this purpose, an analysis of growth of the fourth leaf of six different rice cultivars subjected to suboptimal (ST) and optimal temperatures (OT) was carried out (Supplementary Table 4). The general response of these cultivars to cold stress was described in the previous chapter, where studies on the growth of the third leaf of the cultivars led to define two groups with strongly different characteristics: Koshihikari, CT-6742-10-10-1 and General Rossi belong to the tolerant group (H: high growth); IR50, IR24 and Honezhaosen belong to the sensitive group (L: low growth). In this report, seedlings from the same cultivars were grown at 24/28 °C day/night till the third leaf emerged. At that stage, seedlings for the control treatment were kept growing under these temperatures while temperatures for seedlings under the suboptimal temperature treatment were shifted to 13/21 °C day/night.

2.9.1 The effect of suboptimal temperatures on leaf growth

The fourth leaf was analyzed because it is the first leaf to fully develop under stress conditions and because the third leaf was too small for kinematic analysis. The overall effect of ST stress on rice growth can be expressed by its effects on the final leaf length (FLL). The six cultivars studied here reduced their FLL of the fourth leaf -41% on average (Table 2-3) in response to ST stress. This change in FLL is determined by the leaf elongation rate (LER) and the time while the leaf is elongating (T_{LE}; Table 2-2, Eq. 1). Both parameters were affected in response to ST (Table 2-3): LER was reduced by -76%, whereas T_{LE} was increased by 98%, which largely compensates for the reduced LER. The coordination of lower leaf elongation rates with higher duration of elongation in response to low temperatures was already described for maize plants where in temperatures going from 28/23 °C to 13/8 °C day/night the reduction in LER was about 88% while T_{LE} was incremented more than seven times, so that the overall reduction in final leaf size was about 70% (Bos et al., 2000). Other stresses did not affect T_{LE} as much as cold temperatures. For example, phosphorus deficiency in *Lollium perenne* caused a diminution of LER of about 40% and the compensation with higher T_{LE} was only about 32% (Kavanová et al., 2006). Youssef et al. (2016) studied 14 genotypes of

Medicago truncatula hypocotyls growth response at optimal conditions (17 °C and O MPa), low temperatures (8 °C), and water deficit (-0.5 MPa) and found that while the reductions of final length of the hypocotyls were similar for low temperatures (20%) and water deficit (24%) stresses compared to the control, low temperatures produced higher reductions in the rate of growth -70%- with higher increments of the time they were growing -156%- than the water deficit -56% and 44%, respectively-. Another study done in maize showed that the reduction in FLL by drought stress was mainly due to a great reduction in LER with only partial compensation of the duration of the growth (Avramova et al., 2015). It is known that the spatial and temporal processes regulating growth are independent, implying that LER and T_{LE} are subjected to a different control mechanism (Nelissen et al., 2016). An analysis done in a maize populations linked the duration of growth to the transcriptome of the basal part of the division zone during steady state growth and found a complex network of genes that did not share many genes between the parameters LER and T_{LE} (Baute et al., 2015; Baute et al., 2016).

Next, the cellular basis of the effect of ST on LER was analyzed by kinematic analysis during steady-state growth of the leaf (Figure 2-6), which is based on measurements of the cell length profile (Supplementary Figure 4) along the growth zone and the length of the meristem determined by locating mitotic cells. The reduction of LER in response to ST was largely explained by a reduction of -67% in cell production rate (P), with only a minor reduction of -25% in mature cell length (l_{mat}; Table 2-2, Eq.2; Table 2-3). Similar results were found on maize when subjected to cold night stress (4 °C) where the reduction in LER was mainly due to reductions in division rate that affected the cell production and no differences in mature cell length were found (Rymen et al., 2007). Usually, it is cell proliferation what determines organ size no matter the organ that is being studied (leaf or root) or the species (see Part 1 of this chapter).

Table 2-3. Analysis of the effect of ST stress on the growth of the fourth leaf of rice. Data are average of six cultivars ± SD in OT and ST treatment. An ANOVA was used as statistical test with the factors *Treatment*, *Sensitivity*, and *Treatment*Sensitivity*, here only the *p*-value for the *Treatment* factor is shown for all parameters. When *p*-value< 0.05 is marked in bold and percentage change of ST over OT data is shown, otherwise marked as not significant (NS). A *post-hoc* Tukey test was conducted on the parameter T_{LE} since its interaction was significant (*p*-value = 0.0214), the rest of the parameters had *p*-value>0.05 for the interaction. Parameters: *FLL*, final leaf lengths; *LER*, leaf elongation rate; T_{LE}, time that leaf were elongating; *P*, cell production; l_{mat}, mature cell length; N_{div}, number of cells in the meristem; L_{mer}, length of the meristem; *D*, average cell division rate; T_C, cell cycle duration; T_{div}, resident time of cells in the meristem; l_{div}, length of the cells leaving the mersitem; *RER*, relative elongation rate; T_{el}, resident time of cells in the elongation zone; L_{gz}, length of the whole growth zone; L_{el}, length of the elongation zone; N_{gz}, number of cells in the whole growth zone; N_{el}, number of cells in the elongation zone.

Parameter	OT	ST	%	Treatment *p*-values
FLL (cm)	33.5 ± 8.3	19.7 ± 7.2	-41	**0.002**
LER ($mm.h^{-1}$)	2.9 ± 0.6	0.7 ± 0.2	-76	**<0.0001**
T_{LE} (d)	6.7 ± 0.6	13.3 ± 1.4	98	**<0.0001 ***
P ($cells.h^{-1}$)	38.38 ± 5.34	12.75 ± 2.08	-67	**<0.0001**
l_{mat} (µm)	75.51 ± 7.12	56.39 ± 6.00	-25	**0.0016**
N_{div} (cells)	520.30 ± 137.06	388.76 ± 59.63	NS	0.0731
L_{mer} (mm)	5.10 ± 0.95	4.07 ± 0.65	-20	**0.0274**
D ($cells.cells^{-1}.h^{-1}$)	0.07869 ± 0.02066	0.03529 ± 0.00755	-55	**0.0022**
T_C (h)	9.49 ± 2.35	21.75 ± 4.31	129	**0.0003**
T_{div} (h)	85.92 ± 24.39	187.85 ± 39.64	119	**0.0008**
l_{div} (µm)	15.07 ± 3.23	11.94 ± 1.26	NS	0.0809
RER ($µm.µm^{-1}.h^{-1}$)	0.09487 ± 0.01190	0.03063 ± 0.00244	-68	**<0.0001**
T_{el} (h)	17.78 ± 2.37	53.99 ± 5.84	204	**<0.0001**
L_{gz} (mm)	29.30000 ± 3.84240	21.60000 ± 4.87278	-26	**0.0064**
L_{el} (mm)	24.20057 ± 3.61432	17.53189 ± 4.35257	-28	**0.0106**
N_{gz} (cells)	1205.80 ± 222.37	1065.53 ± 191.72	NS	0.2520
N_{el} (cells)	685.50 ± 135.85	676.77 ± 148.98	NS	0.9068

* *post-hoc* Tukey test showed that the effect of the treatment differ in both tolerant and sensitive groups of cultivars and between cultivars with a *p*-value<0.05. There was no difference between cultivars in OT condition.

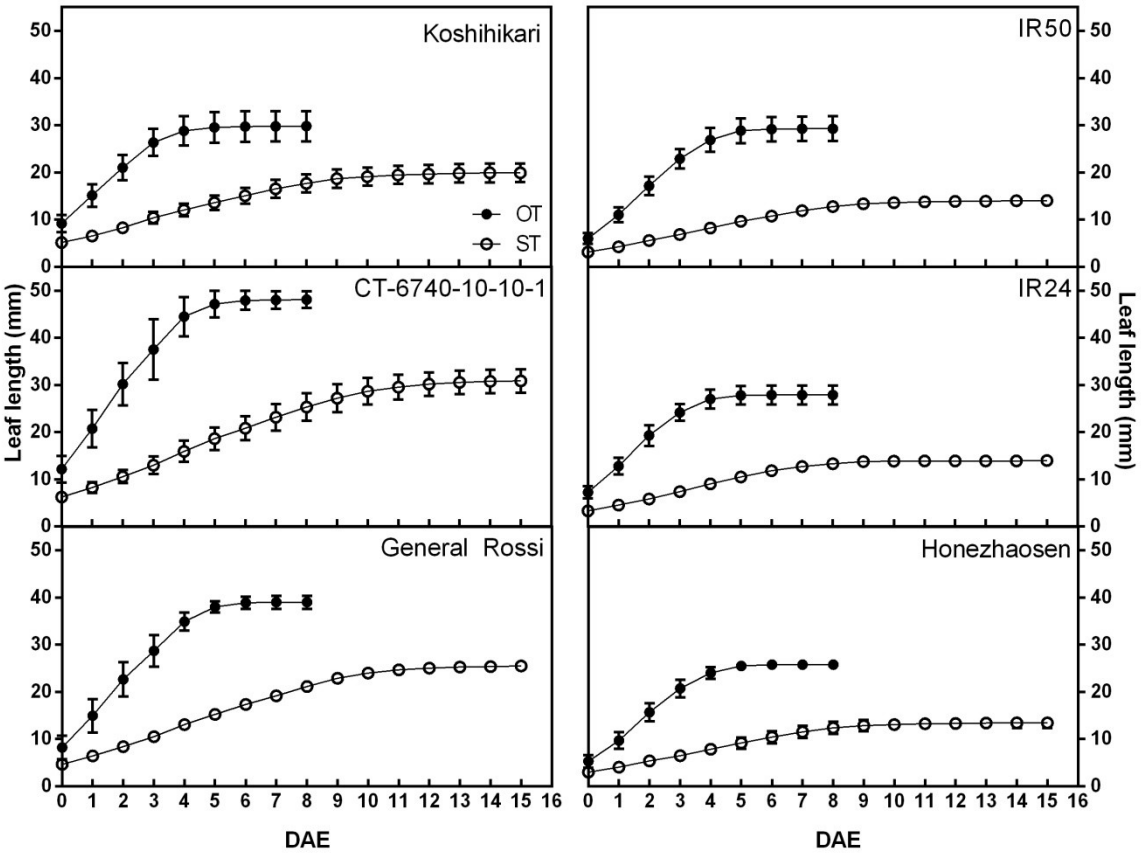

Figure 2-6. Leaf length during time of growth of the fourth leaf of the six rice cultivars. Filled circles represent measurements during OT condition; open circles represents measurements during ST conditions. Each point is media ± SE. n=23.

The parameters related with division processes, number of dividing cells (N_{div}) and average cell division rate (D), further explain changes in P (Table 2-2, Eq. 3). N_{div} was not significantly affected by ST stress (Table 2-3) but the length of the meristem (L_{mer}), which is largely determined by N_{div}, was slightly affected (-20%). P was highly influenced by the reduction of -55% in D. The time that cells reside in the meristem (T_{div}) was incremented a 119% in response to the stress to counteract the diminution of D. The expansion of the cells in the elongation zone depends on the length of the cells when they are leaving the meristem (l_{div}), the relative expansion rate (RER), and the time they expend elongating (T_{el}) to achieve l_{mat} (Table 2-2, Eq. 4). l_{div} was not affected by the ST treatment (Table 2-3). The main effect of ST regarding expansion of the cells was found on the RER that was reduced a -68%. T_{el} raised a 204% in response to ST to compensate this effect on RER. The length of the elongation zone (L_{el}) was slightly reduced -28% and its number of cells (N_{el}) was not modified. As a result, l_{mat} was only reduced -25% on average in all cultivar.

2.9.2 Different response of leaf growth from tolerant and sensitive cultivars to suboptimal temperatures

Although ST stress greatly affected FLL of the fourth leaf of rice seedlings, differences between tolerant and sensitive cultivars were found. While the sensitive cultivars reduced their FLL by -51%, the tolerant ones only had a -35% lower FLL (Table 2-4) confirming that differences in the sensitivity to the stress relate to the growth of the third leaf (Chapter 1). These differences in the reduction of FLL between the groups were partially explained by differences in the LER reduction: the tolerant cultivars decrease LER -74% while the sensitive ones did it -79%. The main cause of the difference of 16% in reduced FLL was T_{LE}, this parameter was increased 80% in the sensitive group and 116% in the tolerant group.

As discussed above, the general response of incrementing T_{LE} could be explained by the thermal time theory. Nevertheless, the difference in T_{LE} adjustment for reduced LER in response to ST conditions between tolerant and sensitive cultivars could not be explained by adjusting for thermal time since the GDD necessary to achieve FLL was lower for sensitive cultivars under ST than under OT condition and differ with tolerant cultivars (Table 2-5). The temperature summation that rice needs to achieve certain developmental stage is known to vary from cultivar to cultivar in part because temperature thresholds (T_{BASE}) for adapted varieties to warm climates are higher than in cold tolerant cultivars (Yoshida, 1981; Gao et al., 1992; Trudgill et al., 2005; Counce et al., 2015). Moreover, in maize the regulatory gene network that is behind LER and T_{LE} was proven to be different (Baute et al., 2015; Baute et al., 2016): at the gene level, LER was found more related to signaling while T_{LE} was to primary metabolism. Besides, the group of cultivars here analyzed performed different under ST stress regarding the PSII (Chapter 1), so it could be suggested that a possible different regulation in the balance between carbon supply and its utilization is leading the difference between the groups.

Table 2-4. Analysis of the effect of ST stress on the growth of the fourth leaf of tolerant and sensitive cultivars of rice. Data are average of three cultivars ± SD in OT and ST treatment. An ANOVA was used as statistical test with the factors *Treatment*, *Sensitivity*, and *Treatment*Sensitivity*, here only the *p*-value for the *Sensitivity* factor is shown for all parameters. When *p*-value< 0.05 is marked in bold. Percentage change of ST over OT data is shown for each group of cultivars if *Treatment p*-value was <0.05, otherwise marked as not significant (NS). A *post-hoc* Tukey test was conducted on the parameter T_{LE} since its interaction was significant (*p*-value = 0.0214), the rest of the parameters had *p*-value>0.05 for the interaction. Parameters: *FLL*, final leaf lengths; *LER*, leaf elongation rate; T_{LE}, time that leaf were elongating; *P*, cell production; l_{mat}, mature cell length; N_{div}, number of cells in the meristem; L_{mer}, length of the meristem; *D*, average cell division rate; T_C, cell cycle duration; T_{div}, resident time of cells in the meristem; l_{div}, length of the cells leaving the mersitem; *RER*, relative elongation rate; T_{el}, resident time of cells in the elongation zone; L_{gz}, length of the whole growth zone; L_{el}, length of the elongation zone; N_{gz}, number of cells in the whole growth zone; N_{el}, number of cells in the elongation zone.

Parameters	Tolerant cultivars		Sensitive cultivars		%		Sensitivity *p*-values
	OT	ST	OT	ST	T	S	
FLL (cm)	38.9 ± 9.0	25.5 ± 5.3	28.2 ± 1.9	13.9 ± 0.5	-35	-51	**0.0066**
LER ($mm.h^{-1}$)	3.3 ± 0.7	0.8 ± 0.1	2.6 ± 0.1	0.6 ± 0.0	-74	-79	**0.0373**
T_{LE} (d)	6.7 ± 0.8	14.4 ± 0.3	6.7 ± 0.5	12.1 ± 1.0	116	80	**0.0275 ***
P ($cells.h^{-1}$)	41.80 ± 5.59	14.47 ± 0.51	34.96 ± 2.22	11.02 ± 1.30	-65	-68	**0.0204**
l_{mat} (µm)	75.64 ± 6.44	58.76 ± 7.99	75.37 ± 9.23	54.01 ± 3.04	-22	-28	0.5554
N_{div} (cells)	566.29 ± 106.13	404.16 ± 68.90	474.31 ± 171.34	373.35 ± 58.59	NS	NS	0.3639
L_{mer} (mm)	5.78 ± 0.78	4.29 ± 0.88	4.42 ± 0.51	3.85 ± 0.35	-26	-13	**0.0463**
D ($cells.cells^{-1}.h^{-1}$)	0.07610 ± 0.01456	0.03872 ± 0.00760	0.08128 ± 0.02890	0.03187 ± 0.00703	-49	-61	0.9341
T_C (h)	9.48 ± 1.62	19.67 ± 3.15	9.49 ± 3.35	23.83 ± 4.85	108	151	0.3245
T_{div} (h)	86.83 ± 16.57	171.20 ± 31.50	85.01 ± 34.79	204.50 ± 45.87	97	141	0.4439
l_{div} (µm)	15.42 ± 3.31	11.69 ± 0.90	14.73 ± 3.84	12.19 ± 1.73	NS	NS	0.9554
RER ($µm.µm^{-1}.h^{-1}$)	0.09845 ± 0.00661	0.03016 ± 0.00303	0.09129 ± 0.01648	0.03111 ± 0.00224	-69	-66	0.5697
T_{el} (h)	16.59 ± 2.46	55.35 ± 8.62	18.97 ± 1.93	52.63 ± 2.31	234	177	0.9522
L_{gz} (mm)	31.53333 ± 4.62310	24.66667 ± 5.53655	27.06667 ± 0.75719	18.53333 ± 0.70238	-22	-32	**0.0358**
L_{el} (mm)	25.75263 ± 4.88644	20.37806 ± 4.77450	22.64851 ± 1.24668	14.68572 ± 0.51420	-21	-35	0.0601
N_{gz} (cells)	1266.21 ± 229.09	1194.18 ± 184.02	1145.38 ± 245.33	936.88 ± 91.53	NS	NS	0.1347
N_{el} (cells)	699.93 ± 185.58	790.02 ± 118.05	671.07 ± 105.22	563.53 ± 55.48	NS	NS	0.1149

* *post-hoc* Tukey test showed that the effect of the treatment differ in both tolerant and sensitive groups of cultivars and between cultivars with a *p*-value<0.05. There was no difference between cultivars in OT condition.

Table 2-5. Thermal time accumulated to achieve final leaf length (FLL) of the fourth leaf of rice. Data are average of three cultivars ± SD in OT and ST conditions. An ANOVA was used as statistical test with the factors *Treatment*, *Sensitivity*, and *Treatment*Sensitivity*, when *p*-value< 0.05 is marked in bold. A *post-hoc* Tukey test was conducted since the interaction was significant, averages with the same letter are not significantly different (*p*-value>0.05).

	Tolerant cultivars		Sensitive cultivars		Treatment *p*-value	Sensitivity *p*-value	Treatment* Sensitivity *p*-value
	OT	ST	OT	ST			
GDD to achieve FLL	106.7^{A} ± 13.4	100.8^{A} ± 1.9	107.7^{A} ± 7.2	**84.7^{B} ± 7.3**	**<0.0001**	**0.0012**	**0.0002**

The variations in LER were further studied with a kinematic analysis and found to be explained by variation in P (Table 2-4); the sensitive cultivars reduced P -68% while the tolerant ones did it -65%. The analysis also showed that the reduction of L_{mer} was -13% in the sensitive group and -26% in the tolerant one, and the effect on of the length of the total growth zone (L_{gz}) was -32% for the sensitive group and -22% for the tolerant one. Although not significant, the lower effect of ST on D in the tolerant cultivars compared to the sensitive ones might be the cause of the reduction in P.

2.10 CONCLUSIONS

Understanding the cellular basis of how the plant predictably and reproducibly regulates its growth in response to adverse environmental conditions provides a basis for further analyses into the molecular of this response and is therefore indispensable for the development of more tolerant crop varieties in the future. The final length of the fourth leaf was found greatly affected in response to ST, although big differences were found between the tolerant and the sensitive confirming what was found in the previous chapter on the growth of the third leaf. This difference was mainly due to differences in the capacity of the cultivars of incrementing the time the leaf was growing in response to ST. Although this could be partially explained by adjusting for thermal time, the differences in sensitivity needs more research. Unfortunately, T_{LE} is not so easily studied at the cellular level, as it is controlled by the activity of the leaf intercalary meristem deep inside the whorl of surrounding leaves. The mechanisms behind LER and T_{LE} are different and independently controlled by the plant (Baute et al., 2015; Baute et al., 2016; Nelissen et al., 2016) possibly explaining such a small difference in the effect of ST on LER between the sensitive and the tolerant group, and such a big difference in T_{LE}. The relationship of T_{LE} with carbohydrates balance in maize, and the fact that the rice sensitive cultivars here analyzed showed a poor performance of the

PSII (Chapter 1), suggests that the difference in sensitivity could rely on an imbalance between sources and sink affecting more the FLL of the sensitive group. Differences on T_{LE} could be further investigated obtaining cell length profiles at different times during the duration of the leaf elongation, for instance. Kinematic analysis was here used to determine the cellular bases of the LER reductions. The cell production rate was the main cause of the growth reduction in response to ST due to a great effect on the cell division rate. Besides, the effect of ST on cell production also differed between tolerant and sensitive genotypes being greater on the first ones. This difference could be attributed to different inhibition of the cell division rate. The mature size of the cells was not highly reduced in response to the stress. Although relative expansion rates were strongly reduced, there was a strong compensation with the time the cells expended elongating.

CHAPTER 3: Transcriptome analysis of the response to suboptimal temperatures in rice cultivars with contrasting sensitivity

3.1 INTRODUCTION

Many plant species have developed an array of mechanisms that enable them to minimize the negative effects of cold stress. The ability to withstand cold by acclimating, *i.e.*, to increase cold tolerance, is a multigenic trait that results from a complex process involving a number of physiological and biochemical changes. This includes changes in gene expression, membrane structure and function, and contents of water, proteins, lipids, and primary and secondary metabolites (Basuchaudhuri, 2014). Despite the fact that numerous gene expression studies on plant response to cold stress have been published (Rabbani et al., 2003; Cheng, 2006; Zhang et al., 2012; Basu and Roychoudhury, 2014), none of them have been focused on ST.

In the first chapter, two groups of cultivars were defined as sensitive and tolerant on the base of their growth and physiological parameters during plant response to ST stress, under laboratory and field conditions. Among the tolerant and sensitive groups were Koshihikari (*O. sativa* L. spp japonica; Takeuchi et al., 2001; Giarrocco et al., 2007) and IR50 (*O. sativa* L. spp indica; Andaya and Mackill, 2003), respectively, in line with their previous description as cold sensitive (IR50; Guo-li and Zhen-fei, 2005) and tolerant (Koshihikari; Takeuchi et al., 2001) cultivars. The present work provides a transcriptome perspective of the response of two representative contrasting cultivars against ST stress.

3.2 AIMS

This chapter aims to gain insight into the general transcriptome response of two contrasting cultivars against ST.

3.3 MATERIALS AND METHODS

3.3.1 Plant material and growth conditions

Rice cultivars Koshihikari and IR50 were kindly provided by the Rice Breeding Program of the Universidad Nacional de La Plata, Argentina. Seeds were placed within Petri plates on two layers of Whatman Nº 5 filter paper rinsed with 7 mL Carbendazim 0.025 %p/v (Yoshida, 1981) and incubated in growth chamber at 30 ºC in darkness until germination. Seedlings were transplanted to plastic net frames placed over a 4 L black tray containing 3 L distilled water. Black trays with seedlings of both cultivars were placed in two chambers for plant growing (Percival E-30B, Percival Scientific, IA, USA) with 12 h photoperiod, 80% humidity, and 400 µmol photons m^{-2} s^{-1} of

photosynthetically active radiation (PAR). Day and night temperatures for optimal temperatures of growth treatment (OT) were 28 and 24 °C, respectively. After three days of culture, the water was replaced by 3 L Yoshida solution (Rachoski et al., 2015). Therein, the Yoshida solution was renewed every three days until the end of the experiment. When the third leaf (Yoshida, 1981) emerged, day and night temperatures of one chamber were modified to 21 and 13 ºC, respectively (ST). Seedlings were further cultivated and harvested after 24 h of treatment.

3.3.2 Total RNA extraction

RNA extraction was made using a Spectrum™ Plant Total RNA kit (Sigma-Aldrich), according to the manufacturer's instructions. After 24 h of treatment, three seedling shoots of each cultivar and treatment were harvested, pooled and kept at -80 ºC until RNA extraction. Each pool of three plants represented a biological replicate. The integrity of the RNA extracted was visually verified on 1.5% agarose. The RNA quality was analyzed using a fluorometer (BioTek Synergy H1 Multi-Mode Reader with Take3 Micro-Volume Plate, VT, USA). Only high-quality total RNA (with ratio 260/280 = 1.7-2.1) was used.

3.3.3 Microarrays and data analysis

The RNA samples were analyzed by a microarray technique using Affymetrix microarray solutions. IR50 and Koshihikari RNA samples were processed using Affymetrix Rice Gene 1.0 ST arrays designed specifically for indica (RCnGene-1_0-st) and japonica (RJpGene-1_0-st) cultivars, respectively. RCnGene-1_0-st had 610,417 probes, 15 probes/gene, and 40,987 probe sets; and it was designed based on BGI genebuild. RJpGene-1_0-st had 521,299 probes, 17 probes/gene, and 29,664 probe sets; and it was designed based on RAP2 genebuild. Five biological replicates from the same experiment were used per cultivar and per treatment. Microarray analysis was performed according with Affymetrix protocols (GeneChip Expression Wash, Stain and Scan User Manual P/N 702731 Rev.3, GeneChip WT Terminal Labeling and Hybridization user manual P/N 702808 Rev. 6 and The Ambion WT Expression Kit protocol P/N 4425209C) using an Affymetrix GeneChip Scanner system (Affymetrix GeneChip Scanner 3000 7G with Fluidics Station 450, Hybridization Oven 645 and computer workstation with Affymetrix GeneChip Command Console Software, CA, USA). Raw data is available in Supplementary Data 1. Microarray datasets were normalized with the RMA algorithm using the Affymetrix Expression Console software v1.4.0. A *post-hoc* principal components analysis done with all datasets ruled out one dataset of ST treatments in both cultivars. The normalized datasets were analyzed and

filtered using the Affymetrix Transcriptome Analysis Console v2.0 software. Differentially expressed transcripts (DET) between the ST and OT samples were identified using one-way ANOVA with a FDR < 0.1. A fold change of ± 2 in transcript expression was used as the cut-off value.

3.3.4 Microarray validation

A qPCR analysis was used to validate microarray datasets. A DNase treatment and removal reagents were applied to all total RNA samples using the Ambion® DNA-free™ Kit (Life Technologies), according to the manufacturer's instructions. cDNA was synthesized using 2 µg of total RNA sample and 200 units of Promega M-MLV Reverse Transcriptase in a total reaction volume of 25 µL, according to manufacter's instructions. The qPCR reaction mixture contained 5 µL from a fivefold dilution of the cDNA stock, 7.5 µL of FastStart Universal SYBR Green Master Mix (ROX; Roche), 10 µL of 600 nM forward and reverse primers and dH_2O until final volume. Primers were designed by Primer3Plus (Untergasser et al., 2012; Supplementary Table 5) and checked for unespecificity via a BLAST search of Gramene database (Ware et al., 2002). qPCR reactions were performed using qPCR System (Applied Biosystems StepOnePlus™ Real Time PCR system, CA, USA). Relative quantification was performed by the comparative cycle threshold method using the InfoStat software (Di Rienzo et al., 2016) with *actine-1* gene (*ACT1*) as housekeeping, reported as the most suitable reference gene, together with *eIF-4a*, for qPCR in rice (Li et al., 2010a).

3.3.5 Gene ID assignation to differentially expressed transcripts

DET sequences were associated to gene locus (gene ID) and differentially expressed genes (DEG) were obtained from each DET via a BLAST offline technique according to Camacho et al., (2009). DET sequences from Koshihikari and IR50 were BLAST searched in the rice database files of the International Rice Genome Sequencing Project (IRGSP; Genome assembly IRGSP v.1/MSU7 based on *O. sativa* japonica group cv. Nipponbare; Sakai et al., 2013) and the Beijing Genome Institute (BGI; Genome assembly BGI-RIS ASM465 v.1 based on *O. sativa* indica group cv 93-11; Zhao et al., 2004), respectively. For the BLAST searches, the BLAST+ software (NCBI-BLAST v.2.2.31, ND, USA) and BLAST Command Line Applications User Manual (NCBI, ND, USA) were used. The BLAST searches included an algorithm, which was designed specifically with the following criteria for gene ID assignation: e value cut off $1e^{-9}$ and when two or more transcript clusters matched the same gene the transcript clusters were eliminated.

3.3.6 Gene annotation and functional enrichment

MapMan Bins were assigned to the protein sequences of the DEGs using the Mercator web application (Lohse et al., 2014). These sequences were obtained from GrameneMart tool of the Gramene database with IRGSP (in Koshihikari case) or BGI (in IR50 case) annotation lists, submitted to Mercator web application and searched against Arabidopsis TAIR proteins (release 10), Swiss Prot/UniProt Plant Proteins, TIGR5 rice proteins, Cluster of orthologous eukaryotic genes, and Conserve Domain database, blast cut-off was set in 80, and multiple bin assignments were allowed. UniProtKB/TrEMBL information from DEGs were obtained from UNIPROT database by searching DEGs genes IDs in IRGSP (for Koshihikari) or BGI (for IR50) annotation. GrameneMart description was obtained from BioMart, by searching the genes IDs in IRGSP (for Koshihikari) or BGI (for IR50) annotation. Batch web ConserveDomain-search tool from NCBI website (Marchler-Bauer et al., 2011) was used to search protein sequences from both arrays that were obtained from GrameneMart, E-Value cut-off was set in 0.01, composition-corrected scoring was allowed, low-complexity filter was not apply, maximum number of hits was set on 500 and the search was made against CDD 46675 PSSMs database. KEGG Orthology assignment (Tanabe and Kanehisa, 2012) was made using KAAS web application (Moriya et al., 2007), search of cDNA sequences of DEGs was made against *Arabidopsis thaliana*, *A. lyrata*, *Theobroma cacao*, *Glycine max*, *Fragaria vesca*, *Vitis vinifera*, *Solanum lycopersicum*, and *O. sativa* japonica KEGG database, using the bi-directional best hit BBH algorithm. With this information KEGG pathways were assigned to DEGs, this was manually curated using information from RiceCyc v3.3 (http://pathway.gramene.org/) and BRENDA (Chang et al., 2009) databases. A literature search was conducted for each DEG from its ID in IRGSP and BGI for both arrays using the search engines Ricewiki (Zhang et al., 2014) and Shigen (Kurata and Yamazaki, 2006). Functional assignment brief description was made integrating all this information.

DEGs from Koshihikari and IR50 were functionally analyzed using 1D annotation algorithm (Cox and Mann, 2012) with Perseus software (http://141.61.102.17/perseus_doku/doku.php?id=start; Version 1.5.5.3). Annotation files were downloaded from Perseus database (annotations.perseus-framework.org) based on Uniprot. The databases *Oryza sativa subsp. Japonica* and *Oryza sativa subsp. Indica* were used for Koshihikari and IR50, respectively. The manually curated networks and pathway classification from KEGG were also used for the analysis.

3.4 RESULTS AND DISCUSSION

3.4.1 Profiling of transcriptome

To comprehensively analyze the response of rice to ST, gene expression of two contrasting cultivars was evaluated. For this purpose, microarrays designed especially for indica and japonica cultivars were used. Samples from IR50 and Koshihikari seedlings were subjected to 24 h of ST and OT treatments and analyzed with microarray technique validated by qPCR. For the qPCR selected genes were analyzed (Supplementary Table 5). The average Pearson correlation coefficient between the microarray and the qPCR results was 0.86 and 0.92 for Koshihikari and IR50, respectively (Supplementary Figure 5).

The effect of ST on the seedlings caused 178 and 331 differentially expressed transcripts (DETs) in Koshihikari and IR50, respectively (Supplementary Table 6). Since Koshihikari belongs to japonica cultivars and IR50 to indica cultivars, gene annotation was done with two different gene models based on the different cultivars to obtain the differentially expressed genes (DEGs). In IR50, 327 DEGs were identified based on 2012-07-BGI (cv. 93-11, indica cultivar) while 175 were found in Koshihikari with the IRGSP-1.0/MSU7 genebuild (cv. Nipponbare, japonica cultivar). Approximately 40 DEGs were equally regulated in both cultivars. In order to show a global view of the DEGs, a functional classification was performed according to KEGG orthology. We were able to assign a function to 80% of the DEGs in each cultivar, on average. Besides, 198 and 92 DEGs of IR50 and Koshihikari, respectively, were also classified in a KEGG pathway category. The profile of the function distributions of these DEGs in each KEGG pathway (metabolism, environmental processing, genetic information processing, organismal systems, and cellular processes) was similar in both cultivars (Figure 3-1). Further description of the major metabolism was done since it was found to be the most represented category in both microarrays. Each subcategory of metabolism pathways showed great differences between cultivars, particularly in the case of carbohydrates, lipids and secondary metabolites.

To increase the power of the comparison of the results from both cultivars, an enrichment analysis was done with the 1D enrichment algorithm (Cox and Mann, 2012). The analysis showed 1 enriched term for Koshihikari transcriptome where receptor kinases were downregulated (Table 3-1). IR50 had 34 terms enriched, 17 of them were systematically upregulated and 17 were downregulated. Between the upregulated, some of them were related to carbohydrate metabolism, transport,

replication and repair, and cellular parts. The downregulated terms grouped ion binding, some receptors, and secondary metabolism. Overall, these results suggested large differences between the cultivars responses against ST that will be further described.

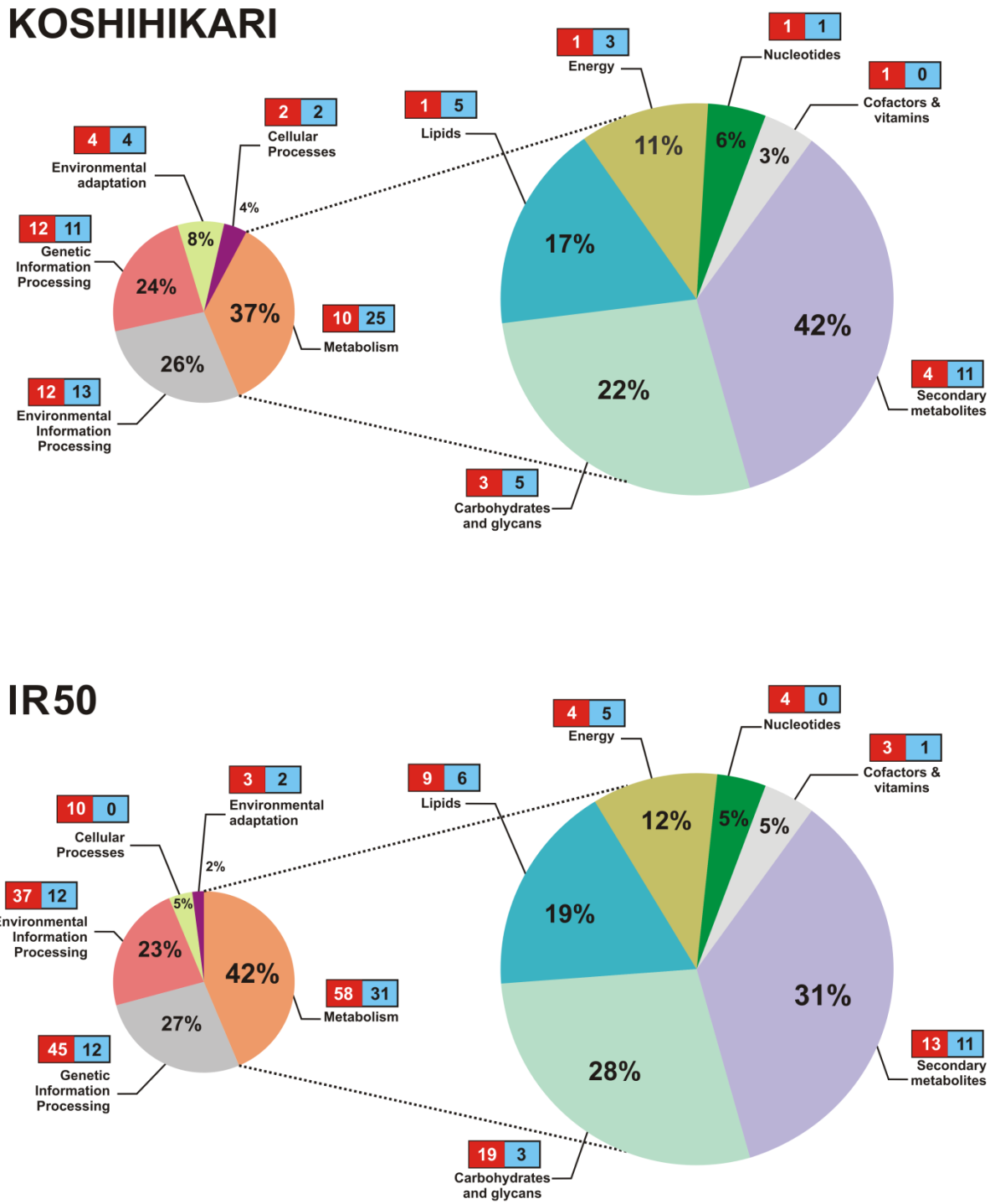

Figure 3-1. Distribution of DEGs among the different KEGG pathways and subpathways within KEGG pathway Metabolism. The percentage distribution of DEGs in each KEGG pathway

is shown on the left pie graph for each cultivar. The pie graph on the right represents the percentage distribution of DEGs in each subpathway within KEGG pathway Metabolism. Numbers in red and blue squares represent upregulated and downregulated DEGs, respectively.

Table 3-1. 1D functional enrichment analysis of transcriptome data from Koshihikari and IR50 rice cultivars subjected to ST stress. The next categories were used for the analysis: Mapman BINs name, KEGG molecular interaction and reaction networks, KEGG molecular interaction and reactions networks subclass, KEGG pathways, gene ontology (GO) biological processes (GOBP), GO molecular function (GOMF), and GO cellular component (GOCC). Only terms with FDR < 0.15 are in the table.

Category type	Name	Number of DEGs with the term	Score	*p*-value	FDR value	FC Mean
Koshihikari						
Mapman BINs name	receptor kinases	7	-0.754386	0.0007273	0.119277	-3.33
IR50						
GOMF name	nutrient reservoir activity	4	-0.931957	0.00135441	0.11016	-11.3
Mapman BINs name	leucine rich repeat VIII	5	-0.811656	0.00183824	0.09375	-4.67
Mapman BINs name	terpenoids	6	-0.751282	0.00161138	0.13697	-3.23
GOMF name	carbon-oxygen lyase activity	6	-0.751282	0.00161138	0.09829	-3.23
GOMF name	carbon-oxygen lyase activity. acting on phosphates	6	-0.751282	0.00161138	0.07864	-3.23
GOMF name	terpene synthase activity	6	-0.751282	0.00161138	0.06553	-3.23
GOCC name	extracellular region	8	-0.653251	0.00159518	0.05583	-5.92
GOMF name	iron ion binding	9	-0.582471	0.00287435	0.07793	-1.54
GOMF name	transition metal ion binding	15	-0.58038	0.00014553	0.03551	-3.62
Mapman BINs name	receptor kinases	18	-0.522009	0.00019545	0.04984	-2.09
Mapman BINs name	abiotic	13	-0.5	0.00224201	0.09529	-3.88
Mapman BINs name	secondary metabolism	16	-0.416071	0.0049845	0.12711	-1.03
Mapman BINs name	stress	22	-0.363636	0.00436902	0.12379	-2.64
GOMF name	metal ion binding	41	-0.296215	0.00213658	0.06517	-1.52
GOMF name	cation binding	42	-0.264294	0.00563862	0.13758	-1.39

GOMF name	ion binding	42	-0.264294	0.00563862	0.12508	-1.39
GOMF name	binding	112	-0.185217	0.00582279	0.1184	-0.25
GOCC name	membrane part	30	0.280731	0.0112119	0.13081	2.12
GOCC name	integral to membrane	29	0.312286	0.00546497	0.12752	2.272
GOCC name	intrinsic to membrane	29	0.312286	0.00546497	0.09564	2.272
GOCC name	cell part	82	0.312763	2.15E-05	0.00151	2.054
GOMF name	hydrolase activity	36	0.314218	0.00208175	0.07256	1.682
molecular interaction and reaction networks subclass	Membrane transport	31	0.32871	0.00258242	0.03745	2.389
GOMF name	transporter activity	18	0.386226	0.00585239	0.10985	2.471
GOCC name	Membrane	16	0.387302	0.00895236	0.12533	2.392
GOCC name	cytoplasmic part	14	0.392519	0.0129245	0.12925	2.339
molecular interaction and reaction networks subclass	Carbohydrate metabolism	17	0.442488	0.00211681	0.06139	2.419
molecular interaction and reaction networks subclass	Replication and repair	7	0.657848	0.00289865	0.02802	3.211
Mapman BINs name	transport	9	0.677019	0.00053077	0.06767	3.086
Mapman BINs name	major CHO metabolism	6	0.713333	0.00274866	0.10013	2.995
patwhay maps (or hierarchy)	Starch and sucrose metabolism	8	0.716331	0.00053694	0.04564	3.018
Mapman BINs name	ABC transporters and multidrug resistance systems	6	0.747179	0.0017091	0.10896	3.382
Mapman BINs name	sugars	5	0.778528	0.00280769	0.0895	3.558
Mapman BINs name	JUMONJI family	3	0.928862	0.00560694	0.12998	3.717

3.4.2 Synthesis and degradation of carbohydrates

On average, 25% of the DEGs within metabolism were categorized under carbohydrate and glycans metabolism in both cultivars (Figure 3-1). While Koshihikari downregulated the majority of its DEGs within this pathway (Figure 3-2), IR50 upregulated them (Figure 3-3). Koshihikari upregulated an isoamylase that degradates starch (EC 3.2.1.68) and downregulated an α-galactosidase (EC 3.2.1.22) involved in the galactose metabolism. The downregulation of α-galactosidase was relate with improved cold tolerance in petunia, apparently due to the accumulation of raffinose (Pennycooke, 2003). Furthermore, a chilling sensitive cultivar of rice was transformed with the galactinol synthase from wheat and presented enhanced tolerance to chilling stress (5 °C) related with accumulation of galactinol and raffinose (Shimosaka and Ozawa, 2015). Besides, the wild type of this cultivar increased raffinose content in response to long exposures to chilling (Saito and Yoshida, 2011). Another report on rice seedlings under chilling stress also showed increased galactose content in the tolerant cultivar (Morsy et al., 2007). The role of raffinose and galactinol is not clear but it was suggested that they act as osmoprotectants, stabilizers of cellular membranes, and as scavengers of reactive oxygen species (Nishizawa et al., 2008; Sengupta et al., 2015). The synthesis of starch was upregulated through a starch synthase in response to ST in IR50 (Figure 3-3). However, this cultivar also downregulated a DEG associated with the Calvin cycle closely related with the starch synthesis (fructose 1,6-biphosphate aldolase; EC 4.1.2.13). The sensitive cultivar also upregulated numerous DEGs from the carbohydrate degradation pathways, including the same isoamylase upregulated in Koshihikari. Many other DEGs of degradation from starch and sucrose, glycolysis and galactose metabolism were upregulated, agreeing with the downregulation of the enriched term *nutrient reservoir activity* and the upregulation of *hydrolase activity* (Table 3-1). These saccharides are the major energy storage molecules in leaves and its degradations products can serve as a carbon and energy source for growth if the plant needs it (Brouns et al., 2006; Ling et al., 2013). Besides, IR50 also upregulated the monodehydroascorbate reductase (EC 1.6.5.4) related with the redox response.

Cell wall modification was also regulated at the gene level in both cultivars. IR50 showed upregulation of DEGs from the degradation of cellulose, modification of xyloglucan network, and generation of pectin (Figure 3-3), whereas Koshihikari upregulated DEGs from pectin catabolism and downregulated the xyloglucan:xyloglucosyl transferase (Figure 3-2). Overall, this suggested a transformation of the cell wall.

3.4.3 Energy response

Plants growing under cold conditions need to conserve their capacity to perform photosynthesis (Huner et al., 1998). The photostasis is achieved through the balance between the energy supplied by the electrons generated by the oxygen evolving complex (OEC) and the energy consumed by the carbon dioxide assimilation in the Calvin cycle (Ensminger et al., 2006). Genes related to energy represented 11.5% of all DEGs on average in both cultivars (Figure 3-1). Both cultivars downregulated the PSII oxygen evolving enhancer protein 2 (PsbP), a protein that together with PsbQ constitute subunits of the OEC that facilitate the retention of Ca^{2+} and Cl^{-}, essential cofactors for water-splitting reaction in PSII (Seidler, 1996; Figure 3-2 ad Figure 3-3). IR50 also downregulated PsbR, a subunit of PSII that might be involved in the binding of PsbP to the PSII (Suorsa et al., 2006; Liu et al., 2009). All these events could have led to a decoupling and inactivation of the OEC. Furthermore, IR50 altered the expression of other three important genes related with the photosynthetic apparatus (Figure 3-3): **a)** downregulated the ferredoxin (PetF), the iron-sulfur protein of PSI that transfers electrons to ferredoxin-$NADP^{+}$-oxidoreductase; **b)** upregulated PsbS, a PSII subunit necessary for photoprotective thermal dissipation (qE) of excess absorbed light energy in plants (Ishida et al., 2011); **c)** downregulated the glutamyl-tRNA reductase (HemA, EC 1.2.1.70), an enzyme of a limiting step within chlorophyll biosynthesis. These events suggested that ST altered normal Photosystem functioning in IR50, which could have in turn reduced the electrons transport rate and NADPH production for the Calvin cycle. Besides, the downregulation of the aldolase described in the previous section could also compromised rate-limiting steps of the Calvin cycle since it is predicted that this enzyme have the potential to control photosynthetic carbon flux through the cycle (Uematsu et al., 2012).

Genes regarding oxidative phosphorylation were found upregulated only in the sensitive cultivar. Glutathione oxidation was genetically upregulated in IR50 while the tolerant cultivar downregulated it. Lastly, sulfur metabolism was regulated by ST only in Koshihikari.

3.4.4 Biosynthesis and degradation of fatty acids

The lipid metabolism subcategory grouped on average 18% of the DEGs from metabolism in both cultivars (Figure 3-1). One of the major effects of cold stress in plants is the remodeling of membrane fluidity by the alteration of its fatty acid composition (Upchurch, 2008). This effect is mainly regulated by the activity of fatty acid desaturases at the transcriptional and post-transcriptional levels (De Palma et al.,

2007; Upchurch, 2008). Polyunsaturated fatty acids (PUFA) synthesis was genetically enhanced by the upregulation of different desaturases genes in Koshihikari (Figure 3-2) as well as in IR50 (Figure 3-3). Many authors reported that cold tolerance in rice is related with an increase in unsaturated fatty acids (Majumder et al., 1989; Bertin et al., 1998; Maeda et al., 1999). Moreover, a positive relationship between the unsaturated fatty acid composition of the chloroplast membrane and the photosynthetic tolerance to chilling was reported (Peoples et al., 1978; Ariizumi et al., 2002; Zhu et al., 2007).

Besides, IR50 showed upregulation of genes associated with fatty acid degradation in endoplasmic reticulum and peroxisome (Figure 3-3). The peroxisomal β-oxidation pathway could be another strategy for obtaining extra energy in order to maintain the cellular homeostasis, as it was shown for starch-depleted Arabidopsis under extended darkness (Kunz et al., 2009). With regard of triacylglycerides, both cultivars exhibited downregulated DEGs in the degradation pathway (Figure 3-2 and Figure 3-3). Some of these genes were related with the production of jasmonic acid (JA).

3.4.5 Secondary metabolism

Secondary metabolism represented a great percentage of DEGs in both cultivars (Figure 3-1). IR50 displayed many DEGs related with flavonoids, isoflavonoids, citoplasmatic terpenoids and polyketides, and polyamines upregulated, while those related with plastid sesquiterpenoids were downregulated (Figure 3-3), agreeing with the enrichment result. The transcriptome analysis showed the downregulation of lutein biosynthesis in Koshihikari, supporting the idea previously discussed of a healthy PSII in Koshihikari, as a better performance of this Photosystem was reported for Arabidopsis mutants that were deficient in lutein when exposed to chilling stress (Pérez-Bueno and Horton, 2008). In addition, a DEG from a peroxidase that synthesizes lignin from phenylpropanoids was found downregulated in both cultivars (Figure 3-2 and Figure 3-3).

Polyamines are secondary metabolites known to be involved in many physiological processes such as cell growth and development, and the response against different environmental conditions (Calzadilla et al., 2014), including cold stress (Menéndez et al., 2013). It has been reported that different plant species –including rice- increase polyamines content under cold stress, particularly putrescine (Lee et al., 1997; Berberich et al., 2015). The relation between polyamines contents and the degree of tolerance of a plant is quite controversial in the literature although they have been linked to an increase antioxidant capacity in the redox homeostasis (Liu et al., 2015).

Our results showed that DEGs of polyamine biosynthesis pathway were upregulated in IR50. Since the *de novo* synthesis of polyamines usually causes an accumulation of polyamines in the plant and it is highly regulated at the transcript level, it could be that polyamines level increased in response to ST in the sensitive cultivar (Liu et al., 2015).

Regarding hormones, genes from ethylene (ET) production were found downregulated in both cultivars (Figure 3-2 and Figure 3-3). ET functions as a repressor of plant growth and development in the response to cold stress but whether it is usually increased or diminished is not well established yet (Eremina et al., 2016). When rice is subjected to cold stress, it rapidly elevates endogenous JA levels (Du et al., 2013). Our research showed that ST upregulated genes from the JA biosynthesis pathway only in IR50 (Figure 3-3). Interestingly, Wingler (2015) included the effects of JA in his model of signaling interactions that restrict growth at low temperatures mainly because of an inhibition of the cell division (Świątek et al., 2002; Noir et al., 2013). Besides, the results showed that IR50 upregulated DEGs of key enzymes within phytosterols and brassinosteroids (BRs) biosynthesis pathways. BRs are hormones implicated in the promotion of plant growth and development. They have shown along with its precursors, the phytosterols, to increase cold tolerance in plants (Kagale et al., 2007; Bajguz and Hayat, 2009; Senthil-Kumar et al., 2013). For instance, in rice it was reported that the addition of BRs promoted the cell elongation of seedlings at 15 °C (Fujii and Saka, 2001) probably by modulating the gibberelin metabolism (Tong et al., 2014).

3.4.6 Genetic information processing response

The regulation of functions regarding genetic information processing, like DNA replication and repair, transcription, post-transcription, translation, protein folding and degradation, vesicular transport, and cytoskeleton are known to be of great importance in a stress response, as it was shown up in the enrichment analysis (Table 3-1). All these processes were found more regulated at the expression level in IR50 than in Koshihikari (Figure 3-4). IR50 showed most of DEGs regarding these functions upregulated, while Koshihikari downregulated the majority. IR50 downregulated UIP1, the transcript of a protein associated with post-transcriptional regulation of the Rubisco S subunit mRNA. UIP1 overexpression is known for contributing to rice tolerance against abiotic stresses, including cold stress (Park et al., 2012). Therefore, the downregulation of this gene together with the implication on the carbohydrate metabolism and the photosynthesis apparatus might have negative effects on the synthesis of starch and CO_2 fixation in the sensitive cultivar.

As it was commented in the previous section, low temperature is known to affect hormone homeostasis (Miura and Furumoto, 2013; Eremina et al., 2016). According to our results, there were evidences that hormone-related genes were regulated in response to ST. Among them, a transcriptional repressor gene related with indolacetic acid hormone was upregulated in IR50, AUX/IAA (Figure 3-4). This gene is known to regulate the expression of genes that alter plant morphology and development (Liscum and Reed, 2002; Jain et al., 2006) through the induction of auxin responsive factor (ARF; Jain and Khurana, 2009; Lyzenga and Stone, 2011; Vanneste and Friml, 2012). Besides the downregulation of the ET biosynthesis pathway described above, IR50 also downregulated CTR1. CTR1 is a regulator of the ET cascade that inhibits the induction of EIN3, a transcription factor that ultimately induces NAC proteins and was related with hypersensitivity to freezing (Eremina et al., 2016). In consequence, DEGs from NAC proteins (OsNAC1 and NAC131) were upregulated in this cultivar. NAC transcription factors were related with transcriptional reprogramming associated with the stress response (Nuruzzaman et al., 2013). However, WRKY DEGs that also form part of the ET signaling cascade, were downregulated (OsWRKY50 and WRKY). This genes have been related with tolerance against multiple abiotic stresses in several plants (Banerjee and Roychoudhury, 2015). In rice, enhanced WRKY50 expression was also related to higher tolerance to abiotic and biotic stresses (Kumar and Sinha, 2014).

However, the complex connection between the stress signaling cascades and the abiotic stresses cannot be completely understood without analyzing the circadian clock. Cold affects the expression of circadian clock genes (Hofmann, 2012) where key responses to abiotic stresses are gated by the clock at specific times of the day (Seo and Mas, 2015). The transcript factors, late elongated hypocotyl (LHY) and timing of cab expression 1 (TOC1) form the core of the rice circadian clock (Murakami et al., 2003) were described in the stomatal closure signaling process (Pokhilko et al., 2013; Zhang et al., 2013; Grundy et al., 2015). Besides, LHY indirectly regulates positively the Cold Regulated Genes (COR) in the canonical cold response pathway (Gilmour et al., 1998; Dong et al., 2011; Lee and Thomashow, 2012) and rhythmic changes of JA (Goodspeed et al., 2012; Zhang et al., 2013), whereas TOC1 regulates the ABA response through the ABA-binding protein ABAR (Grundy et al., 2015). ABA is also usually related with cold tolerance in different species as it triggers stomatal closure (Robertson et al., 2009; Shi and Yang, 2014). On the other hand, calmodulin/calmodulin like (CaMs/CMLs) genes that code for Ca^{2+} fluxes sensors play a role under chilling condition during stomatal closure, among other functions (Miura

and Furumoto, 2013). In turn, it has been shown that a calmodulin-like protein from *Arabidopsis thaliana* (AtCML9) is involved in abiotic stress tolerance through its effects on the ABA-mediated pathways (Magnan et al., 2008). Our results showed differences between both cultivars regarding ST-induced changes in the expression of LHY and TOC1 genes, and genes of the ABA and CaMs/CMLs signaling cascades. Taken together, these results put forward the notion that different crosstalk's among genes involved in the circadian clock and in ABA and Ca^{2+} signal cascades could take place in Koshihikari and IR50.

Besides, membrane transport and catalysis showed many upregulated genes in IR50, mainly regarding ions and peptides transport, as also pointed out in the enrichment analysis (Figure 3-3). Koshihikari also displayed some upregulated DEGs under this category but less than IR50 (Figure 3-2). Receptor kinases were found repressed in both cultivars, accordingly with the enrichment.

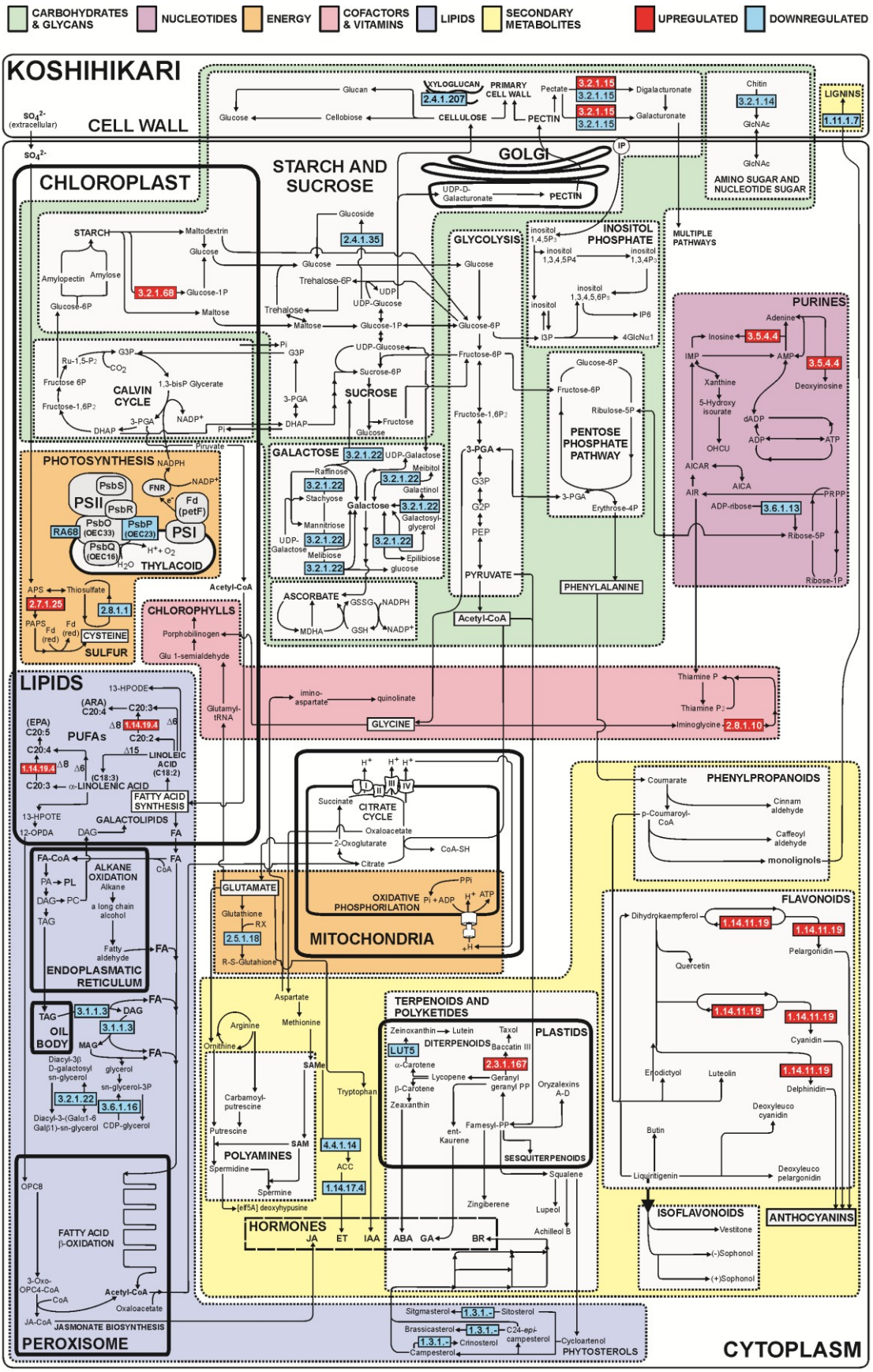

Figure 3-2. Schematic distribution of DEGs in subpathways of the KEGG pathway Metabolism in Koshihikari.

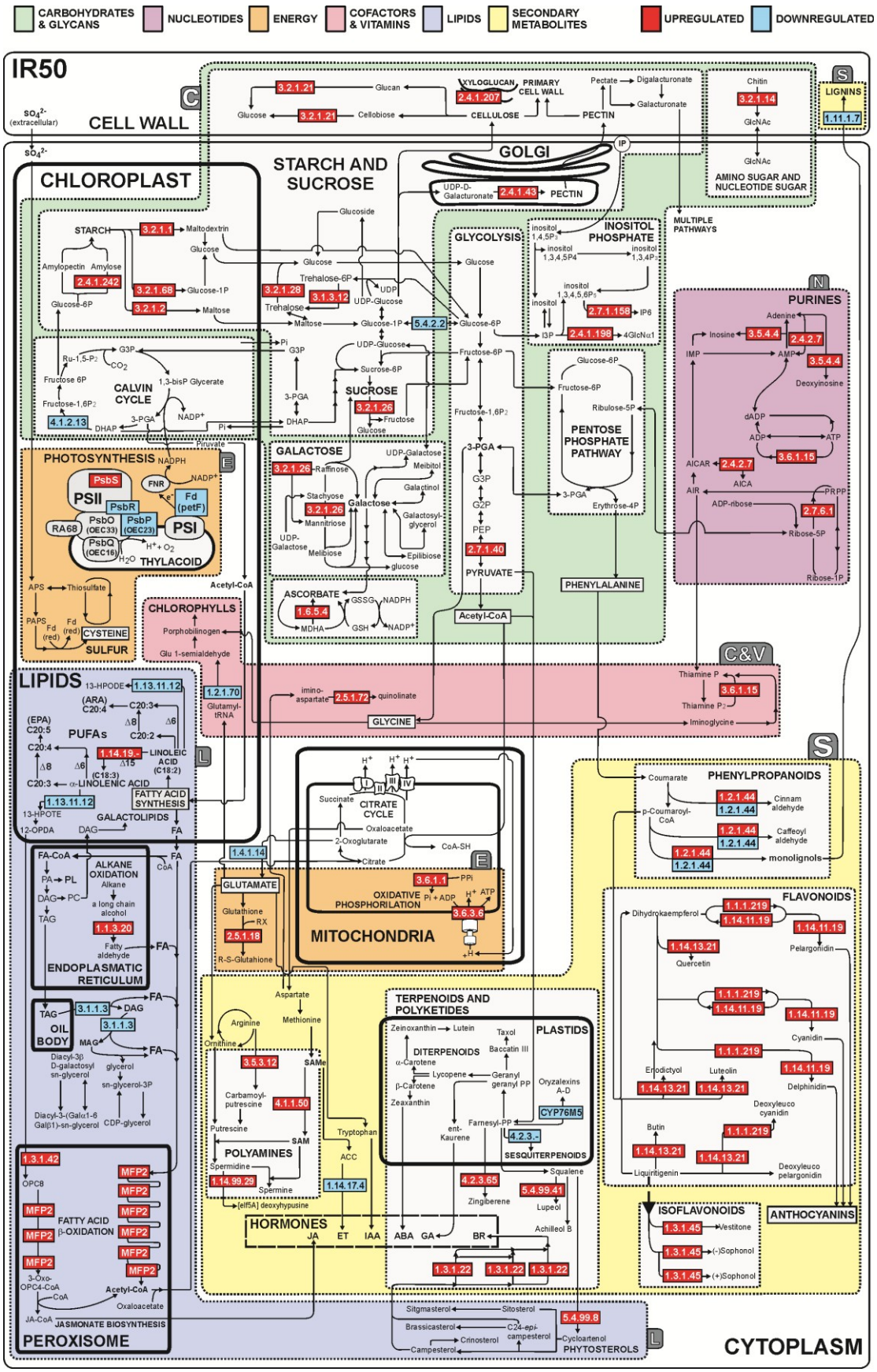

Figure 3-3. Schematic distribution of DEGs in subpathways of the KEGG pathway Metabolism in IR50.

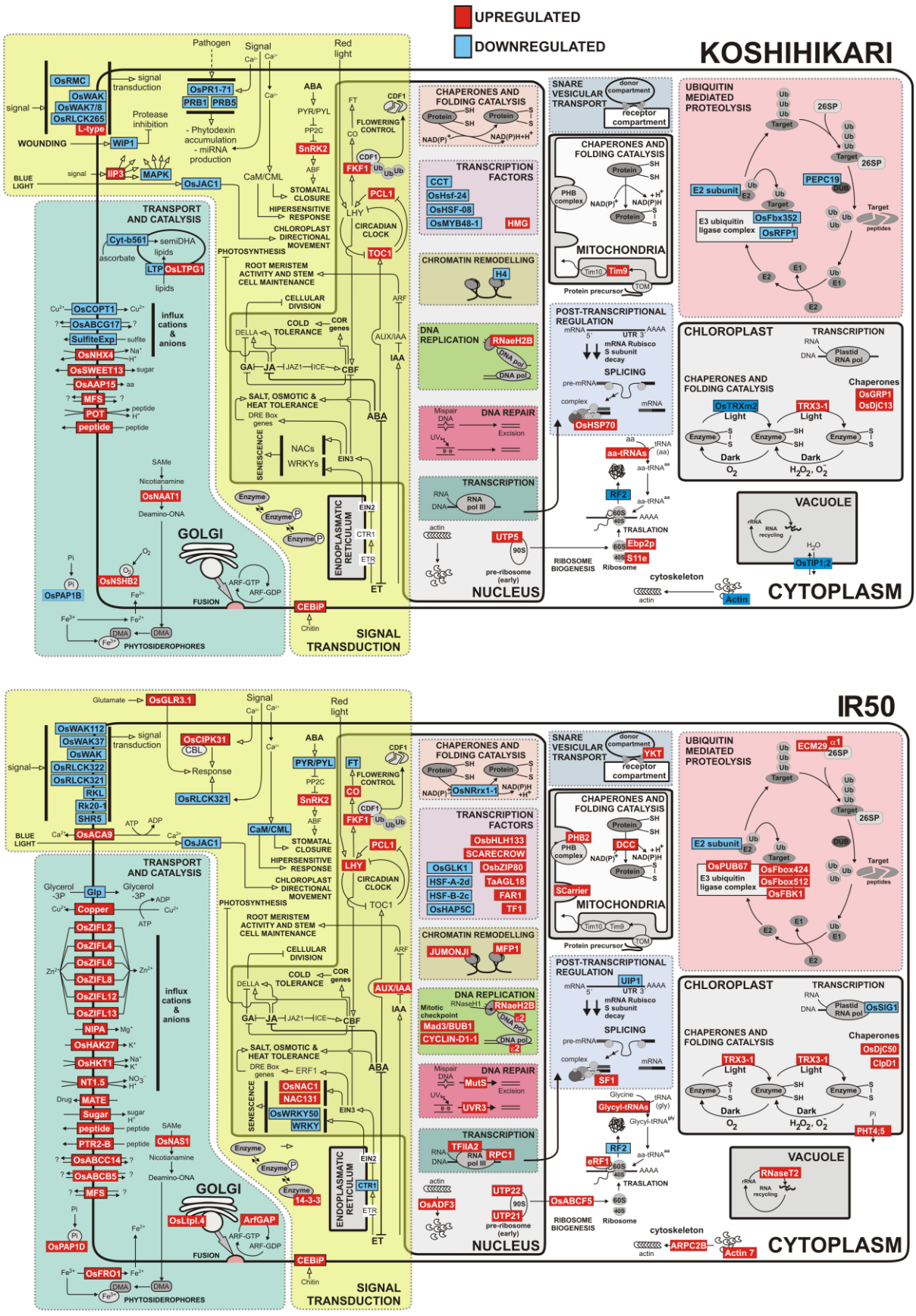

Figure 3-4. Schematic distribution of DEGs in subpathways of the KEGG pathways: Genetic Information Processing. *Environmental Information Processing. Cellular Processes and*

Environmental Adaptation. A portion of the subpathways of each KEGG pathway was organized in two large groups delimited by dashed lines: Transport and catalysis and Signal transduction. The other subpathways, also delimited by dashed lines, were located in different organelles and cellular compartments.

3.5 CONCLUSIONS

Our results provide evidence that both cultivars presented contrasting early responses at the transcriptional level. The metabolism of carbohydrates was highly regulated. Both cultivars upregulated the degradation of starch in response to ST. Besides, IR50 upregulated DEGs related with the saccharides catabolism probably as a strategy to obtain extra energy to counteract the energy imbalance resulting from PSII damage evidenced at the transcript level and mitigate the ST stress effects. Furthermore, the upregulation of the peroxisomal β-oxidation pathway could be another strategy for obtaining energy to maintain the cellular homeostasis. Koshihikari upregulated a α-galactosidase related with the accumulation of raffinose that was described to confer cold tolerance. A transformation of the cell wall was also suggested in both cultivars from the transcriptome analysis. Finally, differences in tolerance to the ST condition between both cultivars could be assigned in part to variations in crosstalk's among genes involved in the circadian clock, and in ET, ABA and Ca^{2+} signal cascades.

CHAPTER 4: Proteome analysis of the response to suboptimal temperatures in rice cultivars with contrasting sensitivity

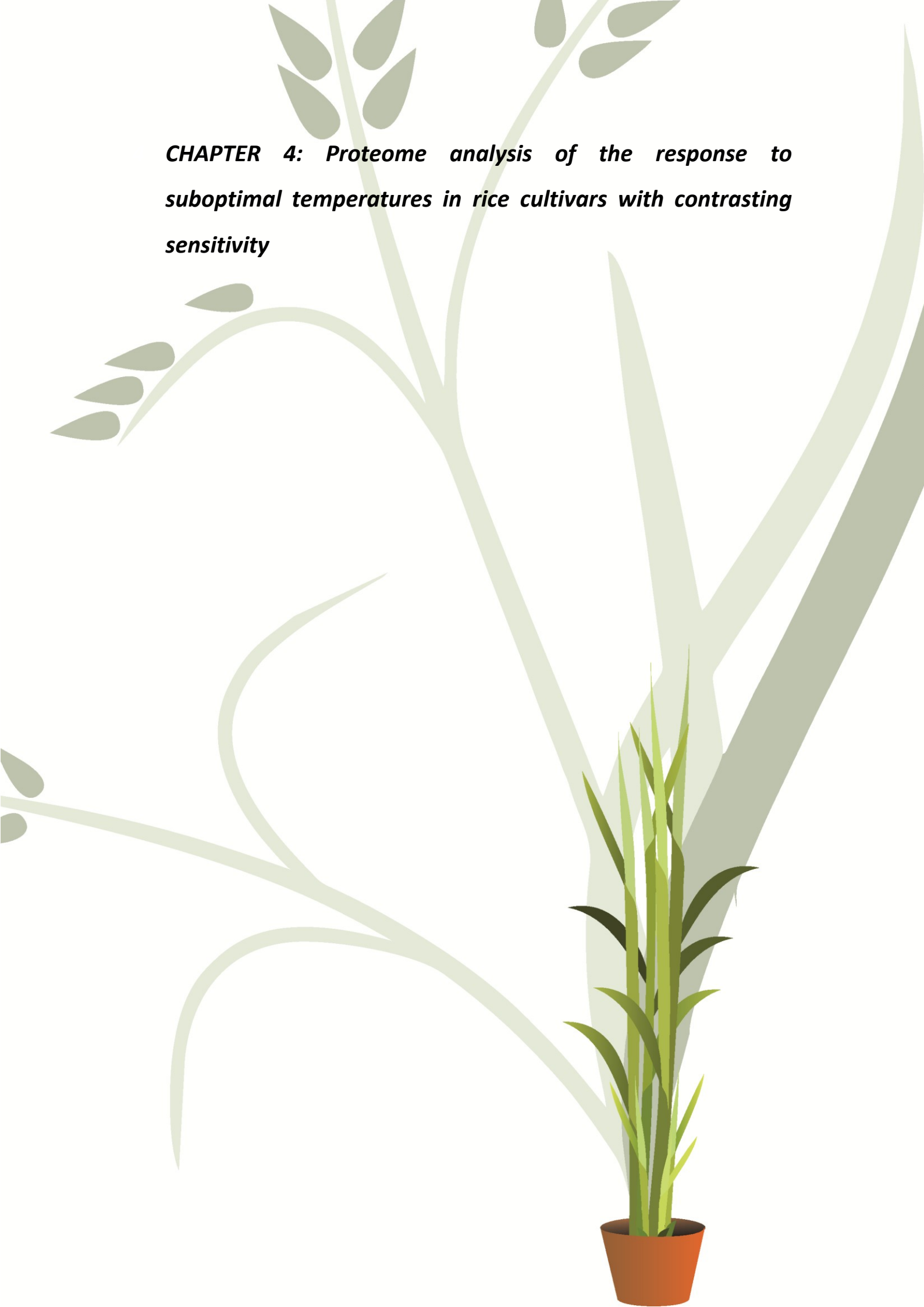

4.1 INTRODUCTION

Adverse environmental conditions alter various physiological processes which are directly controlled by genes and achieved by changes at the proteome level (Kosová et al., 2011; Hakeem et al., 2012; Barkla et al., 2013). Therefore, comparing the proteome changes in genotypes with contrasting responses to a stress could lead to identification of genes and their encoded proteins underlying the observed differences between tolerant and sensitive cultivars. Rice has advantages over other crops regarding transcriptome and proteome analyses, because its whole genome has been sequenced and databases of proteins sequences are available (Kosová et al., 2011; Singh and Jwa, 2013). Although proteome analyses have been done on rice seedlings subjected to cold stresses, they were mostly focused on chilling temperatures or in root response (Yan et al., 2006; Hashimoto and Komatsu, 2007; Komatsu et al., 2009; Lee et al., 2009; Chen et al., 2012; Neilson et al., 2013). However, three studies analyzed the proteome composition of the rice leaf at the seedling stage subjected to short periods of suboptimal temperatures similar to the ones we are focused here (Cui et al., 2005; Gammulla et al., 2011; Neilson et al., 2011).

In chapter 2 we showed that ST stress strongly inhibits leaf growth by decreasing leaf elongation rate. At the cellular level, division and expansion in the leaf growth zones determined the leaf growth under ST. Moreover, the ST effect on the growth parameters was different in cultivars with contrasting sensitivity to the stress being more aggressive on the sensitive cultivars. Hence, here we choose to sample by position, as opposed to entire organ, in order to identify specific changes related to the inhibition of cell division and expansion. Analogous to the previous growth (chapter 2) and transcriptome (chapter 3) analyses, rice seedlings were subjected to control temperatures (24/28 °C, day/night, OT treatment) and suboptimal temperatures of growth (13/21 °C, day/night, ST treatment) and samples of the meristem and the elongation zone of the fourth leaf were taken during the steady-state growth. Other proteome studies have shown sampling by position to be successful in maize leaves (Majeran et al., 2010; Facette et al., 2013; Ponnala et al., 2014) and roots (Marcon et al., 2015), and also in the study of the drought stress response (Avramova, 2016). To our knowledge this is the first attempt at using proteomics to capture proteome gradients associated with cell development transitions between proliferation and expansion related to the ST response and sensitivity in rice.

4.2 AIMS

Here we analyzed the regulation of two contrasting cultivars against ST at the proteomic level to complement the previous chapters of this Thesis in which a physiological and transcriptomical response were analyzed. Moreover, the sampling is done by position and not in the entire organ to see if differences in the proteome associated with cell division and expansion can be identified along the growth zone of the rice leaf in response to ST, and if they can be associated with sensitivity.

4.3 MATERIALS AND METHODS

4.3.1 Plant material and growth conditions

Rice seeds (Oryza sativa) from cultivars Koshihikari and IR50 were kindly provided by the Rice Breeding Program on the Universidad Nacional de La Plata, Argentina. Seeds of these cultivars were placed within Petri plates on two layers of Whatman N° 5 filter paper rinsed with 7 mL carbendazim 0.025 %p/v (Yoshida, 1981) and incubated in growth chamber at 30 °C in darkness until germination. The germinated seedlings were transplanted to peat potting medium (Jiffy, The Netherlands; volume of the pots: 1.6 l, dimensions: 13 cm tall and 5" of diameter) and saturated with water. The seedlings were then grown in a growth chamber under controlled conditions (Conviron, Adaptis A1000) with 12 h photoperiod, 80% humidity and 350 µmol photons m^{-2} s^{-1} of photosynthetically active radiation (PAR). Day and night temperatures for optimal temperatures of growth treatment (OT) were 28 and 24 °C (d/n), respectively. When the third leaf (Yoshida, 1981) emerged, day and night temperatures for the suboptimal temperatures of growth treatment (ST) were modified to 21 and 13 °C (d/n), respectively. Two days after emergence of the fourth leaf, 10 randomly chosen plants from each cultivar and treatment were harvested and the growth zone of the fourth leaf of each plant was cut in five segments as follows according to the results on Chapter 2: from the base of the leaf 4 mm (meristem), 3 mm (transition between meristem and elongation zone), 18 mm (elongation zone), 5 mm (transition between elongation and mature zone), and 20 mm (mature zone) were consecutively cut from plants under OT conditions; from the base of the leaf 3 mm (meristem), 3 mm (transition between meristem and elongation zone), 10 mm (elongation zone), 4 mm (transition between elongation and mature zone), and 20 mm (mature zone) were consecutively cut from plants under ST conditions (Figure 4-1). Samples were stored at -80 °C for further protein extraction. Only the meristem (M) and the elongation zone (EZ) were used for the analysis, the transition zones and the mature zone (Mat) were discarded. The

remaining plants (10) were used to determine the length of the fourth leaf until it reach maturity.

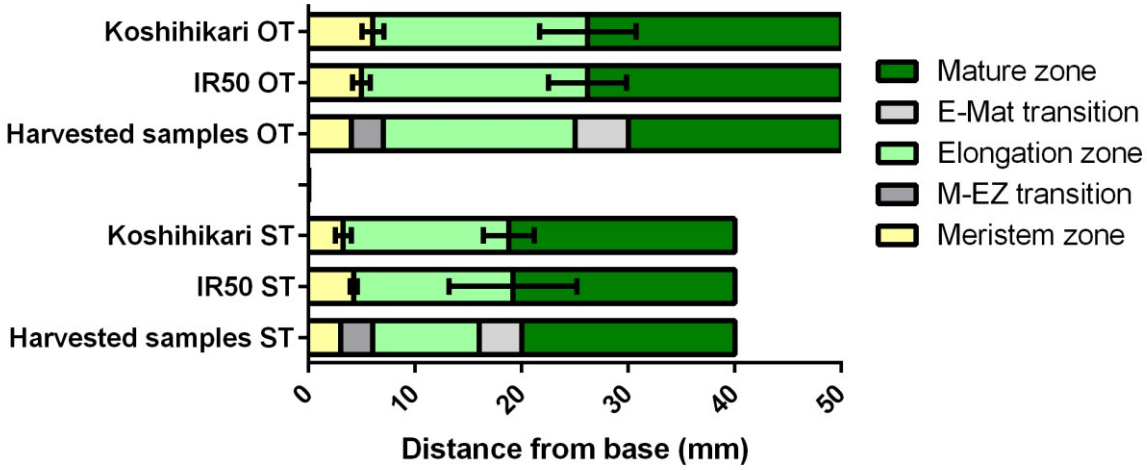

Figure 4-1. Length of the developmental zones of Koshihikari and IR50 under optimal and suboptimal temperatures. The length of each developmental zone (meristem, elongation, mature) and the transition zones (M-EZ transition, E-Mat transition) is marked for each condition (OT for optimal temperatures, ST for suboptimal temperatures) and each cultivar (Koshihikari, IR50). Harvested samples OT and ST show how the sampling was done for the proteome analysis for each treatment/genotype combination. Data are averages ± SD (n=5).

4.3.2 Protein extraction and digestion

Three isobaric tags for relative and absolute quantification (iTRAQ)-labeled sample pools were prepared for this study. Each of the pools contained 8 biological samples of 10 leaf sections, labeled with an 8-plex iTRAQ kit. Proteins extracts were prepared according to Méchin et al. (2007) with modifications. Samples were ground in liquid nitrogen and 10 volumes of 0.07% 2-β-mercapto-ethanol and 10% trichloroacetic acid in cold acetone were added. After overnight incubation at -20 °C, samples were centrifuged 30 min at 4 °C and 10,000 g and two consecutive acetone washings were made. Protein pellets were dissolved in 0.5 M triethylammonium bicarbonate (TEAB). Protein concentrations were determined by Pierce BCA Protein Assay Kit (Thermo Fisher Scientific. Belgium) using a NanoDrop 2000 spectrophotometer (Thermo Fisher Scientific. Belgium). From each sample, a total of 100 µg of protein were denaturized and reduced with reagents supplied with the iTRAQ labeling kit (AB Sciex), in a volume of 20 µl of 100 nM TEAB and incubated at 60 °C for 1 h. After cysteine-blocking by treating with Cysteine Blocking Reagent from the same kit for 10 min in the dark, 6 volumes of cold acetone were added and samples were incubated overnight at -20 °C. After centrifugation, proteins were dissolved in 20 µl of 100 nM TEAB and digested with

MS-grade Trypsin Gold (enzyme:protein ratio = 1:10; Promega) overnight at 37 °C according to the manufacturer's instructions. The next day samples were desalted with Pierce C18 Spin Columns according to the manufacturer's instructions (Thermo Scientific) before labeling was performed.

4.3.3 iTRAQ protein labeling

iTRAQ Reagents-8plex kit (AB Sciex) was used for the labeling of the samples. For the reconstitution of the tags, iTRAQ labels were dissolved in 50 µl of isopropanol according to the manufacturer's protocol. Subsequently, digested peptides were labeled with the iTRAQ reagents and incubated for 2 h at ambient temperature. A pooled sample was prepared based on the labeled samples (Table 4-1) with an equimolar peptide concentration ratio for all samples.

Table 4-1. Experimental design of iTRAQ proteome analysis of Koshihikari and IR50 rice cultivars. A total of three pools of samples were used for mass spectrometry analysis. Each pool contained eight samples (each in turn comprising 10 plants) that were marked with the contrasting 8-plex iTRAQ labels. *M,* mersitem zone. *EZ*, elongation zone. *OT*, optimal temperatures treatment. *ST*, suboptimal temperatures treatment.

iTRAQ label	Pool 1	Pool 2	Pool 3
113	IR50 M OT	IR50 EZ OT	IR50 M OT
114	IR50 M OT	IR50 EZ OT	IR50 M ST
115	IR50 M ST	IR50 EZ ST	Koshihikari M OT
116	IR50 M ST	IR50 EZ ST	Koshihikari M ST
117	Koshihikari M OT	Koshihikari EZ OT	IR50 EZ OT
118	Koshihikari M OT	Koshihikari EZ OT	IR50 EZ ST
119	Koshihikari M ST	Koshihikari EZ ST	Koshihikari EZ OT
121	Koshihikari M ST	Koshihikari EZ ST	Koshihikari EZ ST

4.3.4 Nano-reverse phase liquid chromatography and mass spectrometry

To reduce the overall complexity of the iTRAQ-labeled samples, a reverse phase chromatography on Easy-nLCsystem (Thermo Scientific) was done. A RP-C18 PepMap trap column 3 µm, 100 Å, 75x20 mm and an analytical column RP-C18 PepMap 2 µm, 100 Å, 50x150 mm were used. 1 µg of iTRAQ labeled peptide dissolved in 10 µl of mobile phase A, containing 2% acetonitrile and 0.1% formic acid, was loaded. A linear gradient of mobile phase B (98% acetonitrile and 0.1% formic acid) in mobile phase A from 2 to 40% in 300 min was used at a flow rate of 400 nl.min^{-1}. The nano-LC was coupled online with the mass spectrometer Q-Exactive Plus Hybrid Quadrupole-Orbitrap (Thermo Scientific). The equipment was set up in a MS/MS mode

where a full scan spectrum (350 – 2000 m/z) was done. Peptide ions were selected for further interrogation by tandem MS as the five most intense peaks of a full scan mass spectrum. Fragmentation was set to High Energy Collision Activated Dissociation (HCD) scans on the Orbitrap.

4.3.5 Proteome data analysis

Proteome Discoverer 1.3.0.339 software (Thermo Scientific) was used to perform database searching against the *Uniprot Oryza sativa subsp. Indica* (39946) and *Uniprot Oryza sativa subsp. Japonica* (39947) databases using both SEQUEST and Mascot (Matrix Science) algorithms with the following settings: mass spectrum range of 300 – 8000 Da, precursor mass tolerance of 10 ppm, and fragment mass tolerance of 0.01 Da. Trypsin was specified as digesting enzyme and 2 missed cleavages were allowed. iTRAQ 8-plex (N-terminus and lysine residues) and Methylthio (C) were defined as fixed modifications, and methionine oxidation and iTRAQ 8-plex tyrosine were variable modifications. The results were filtered for confident peptide-to-spectrum matches (PSMs) based on a non-concatenated target decoy database. The decoy database is a reversed version of the target database. Only first ranked peptides with a global FDR smaller than 1% were included in the results. All the sequences and reporter ion intensities of the PSMs that match the confidence requirements were exported to a comma-separated-values spreadsheet for further data-analysis (Supplementary Data 2). Data from the three iTRAQ samples were normalized together with the CONSTANd method (Maes et al., 2016) so peptides could be compared within and between the multiplex experiment without the need of a reference sample in each of them. For statistical and bioinformatic analysis as well as visualization Perseus 1.5.5.3 open software (Tyanova et al., 2016) was used. All peptides listed with multiple accessions were removed and only peptides sequences belonging to single protein identifications were kept for further analysis. Peptide relative abundances were $\log_2$ – transformed and missing values were replaced from normal distribution with default settings, width of 0.3 and down shift of 1.8 as described. IR50 data were further analyzed based on *Uniprot Oryza sativa subsp. Indica* (39946) database, and Koshihikari data based on *Uniprot Oryza sativa subsp. Japonica* (39947) database. All peptides matching to the same protein were averaged and a two-way ANOVA analysis was done in each cultivar using *treatment* and *zones* as factors with the built-in ANOVA functions of Perseus and False Discovery Rate (FDR) was applied as a multiple testing correction.

For overall description of the proteomes, the resulting significant proteins in each factor and the interaction with uncorrected *p*-values<0.05 were normalized with Z-score

normalization and clustered using Euclidean distance, average linkage, preprocess with K-means, number of clusters 300, maximal number of iterations 10, and number of restarts 1 in Perseus. An enrichment analysis was done in each cluster using Perseus and Perseus annotations files downloaded from http://annotations.perseus-framework.org/. For Koshihikari proteome's analysis the annotation file for japonica cultivars was used, and for IR50 the file for indica cultivar was used (dated on 20/06/2015). An extra annotation file was manually prepared with KEGG and MapMan BIN annotation, for this purpose the protein sequences of the significant proteins were downloaded from GrameneMart tool of the Gramene database with IRGSP (in Koshihikari case) or BGI (in IR50 case) databases or, in case they were missing, from Uniprot. KEGG Orthology assignment (Tanabe and Kanehisa, 2012) was made using KAAS web application (Moriya et al., 2007), search of protein sequences was made against *Oryza sativa* japonica KEGG database (no specific database is currently designed for indica cultivars) using the bi-directional best hit BBH algorithm. MapMan BINs (Thimm et al., 2004) were assigned with the Mercator web application (Lohse et al., 2014) and searched against Arabidopsis TAIR proteins (release 10), Swiss Prot/UniProt Plant Proteins, TIGR5 rice proteins, Cluster of orthologous eukaryotic genes, and Conserve Domain database, blast cut-off was set in 80, and multiple bin assignments were allowed. In the case of proteins that changed its abundance in response to the stress in each zone an enrichment study was carried out by PageMan (Usadel et al., 2009) with the Wilcoxon test .

For detailed descriptions, proteins with FDR<0.10 were further analyzed using information from the terms listed above and two extra searches were made: Batch web Conserved Domain-search tool from NCBI website (Marchler-Bauer et al., 2011) was used to search protein sequences obtained from GrameneMart and obtain conserved domains of the proteins, E-Value cut-off was set in 0.01, composition-corrected scoring was allowed, low-complexity filter was not apply, maximum number of hits was set on 500 and the search was made against CDD 48963 PSSMs database (v 3.15); TargetP 1.1 Server web application (http://www.cbs.dtu.dk/services/TargetP/; Emanuelsson et al., 2007) was used to assigned subcellular localization of the proteins sequences , no cut-off was used.

4.4 RESULTS AND DISCUSSION

4.4.1 Proteome profiling

8-plex iTRAQ labeling was used to compare proteome of cultivars (IR50 and Koshihikari), treatments (OT and ST), and zones (meristem and elongation). In order to obtain more accurate protein identification, the peptides for each cultivar were analyzed according to its specific database, *i.e.*, Koshihikari proteome was analyzed with the results from japonica Uniprot database and IR50 proteome was analyzed with the results from indica Uniprot database. After normalization, 1909 and 1874 unique peptides were identified when japonica and indica Uniprot databases were used, respectively (Supplementary Data 3). The peptides that listed multiple accessions (94 in each database) were removed and only peptide sequences belonging to single protein identifications were kept for further statistical analysis to increase the confidence of the quantification. Some peptides sequences did not have an accession in the database and so they were also ignored (200 in japonica database, and 303 in indica database). Missing values were imputed from a Gaussian distribution with a down sift of 1.8 and a width of 0.3 at the peptide level (Supplementary Figures 8 and 9; Lazar et al., 2016; Tyanova et al., 2016). The peptides obtained after filtering and imputation matched to a maximum number of 558 (Supplementary Table 7) and 541 (Supplementary Table 8) identified proteins in japonica and indica databases, respectively. Although most of the proteins were shared across zones and treatments in both cultivars (Figure 4-2), many were only present exclusively in the meristem (11 and 8 for Koshihikari and IR50, respectively) or in the elongation zone of each cultivar (48 and 13 for Koshihikari and IR50, respectively). Thus, differences between the zones are partially attributable to proteins absent from the meristem and present in the elongation zone, and vice versa. Besides, Koshihikari had a few proteins that were only present in the ST condition (Figure 4-2 A) while IR50 showed one exclusively in the OT treatment (Figure 4-2 B). Thus, differences in treatments might remain in the abundance of proteins rather than the absence/presence.

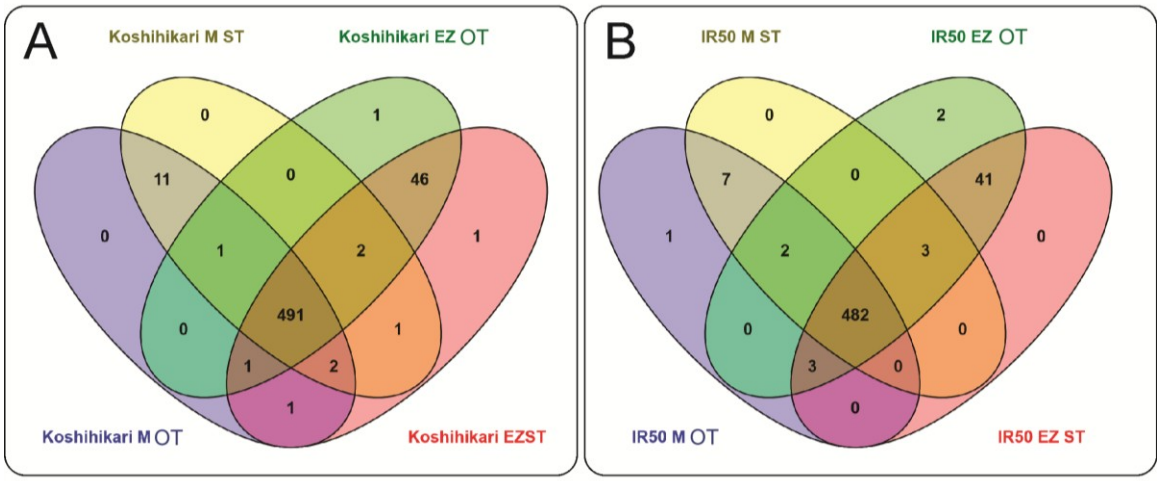

Figure 4-2. Venn diagram of all proteins detected in the analyses. "Present" is defined as being detected in at least one replicate. Label of each sample is marked as follows: name of the cultivar (Koshihikari or IR50), zones (M: meristem; EZ: elongation zone), treatments (OT: optimal temperatures; ST: suboptimal temperatures). **A)** Koshihikari proteomes. **B)** IR50 proteomes.

A two-way ANOVA analysis was performed for each cultivar using as factors treatments (OT and ST) and zones (meristem and elongation; Supplementary Table 7 and Supplementary Table 8). When FDR correction was applied to the *P*-values of the ANOVA analyses and a LSD Fisher *post-hoc* test to the proteins that showed interaction between factors, only a small number of proteins changed their abundance in response to the stress. When using the liberal FDR<0.10, 11 proteins changed their abundance in Koshihikari leaf (Supplementary Table 9), 7 proteins increased their abundance in both zones in response to the stress, 3 were repressed, and one increased only in the elongation zone. In the case of IR50 (Supplementary Table 9) 8 proteins abundances changed significantly: 6 upregulated in both zones in response to the stress, and 2 were repressed. To characterize the global protein expression patterns using functional overrepresentation, a lower selection stringency was applied to the two-way ANOVA so proteins with uncorrected *p*-value<0.05 were used for the analysis. Koshihikari proteome analysis resulted in 46 changed protein abundances in response to the stress, 142 along the growth zone, and 50 that interacted between factors. IR50 showed 47 proteins that changed in response to ST, 198 along the growth zone, and 21 that interacted. It is noteworthy that the effect of the zone was greater than the effect of the treatment in both cultivars proteome.

4.4.1.1 The zone effect

To identify enriched proteins in each zone, we performed a hierarchical clustering and enrichment analysis of proteins with uncorrected *p*-value<0.05 in the *zones* factor for each cultivar (Figure 4-3). Proteins from Koshihikari were clustered in 5 different profiles (Figure 4-3 A). The first cluster grouped 64 proteins upregulated in the elongation zone that were related with membrane parts. The second cluster showed 35 proteins more abundant in the meristem that represented mainly ribonucleoproteins terms. IR50 proteins were also classified in 5 different profiles (Figure 4-3 B). The first cluster with 143 upregulated proteins in the elongation zone was significantly enriched in terms related with chloroplast and its components and a second cluster grouped 42 proteins more abundant in the meristem related with ribonucleoproteins. The rest of the clusters did not show any enriched terms. Thus, both cultivars showed enriched terms related with ribonucleoproteins in the meristem, which is consistent with cells in this zone undergoing active division. The elongation zone was more related with membranes and chloroplast parts, which is related with cell expansion and differentiation in this zone. This partially validates our analysis because proteins distinguished between the zones and agrees with previous proteomes analyses from the growth zone of maize leaves (Majeran et al., 2010; Facette et al., 2013; Ponnala et al., 2014).

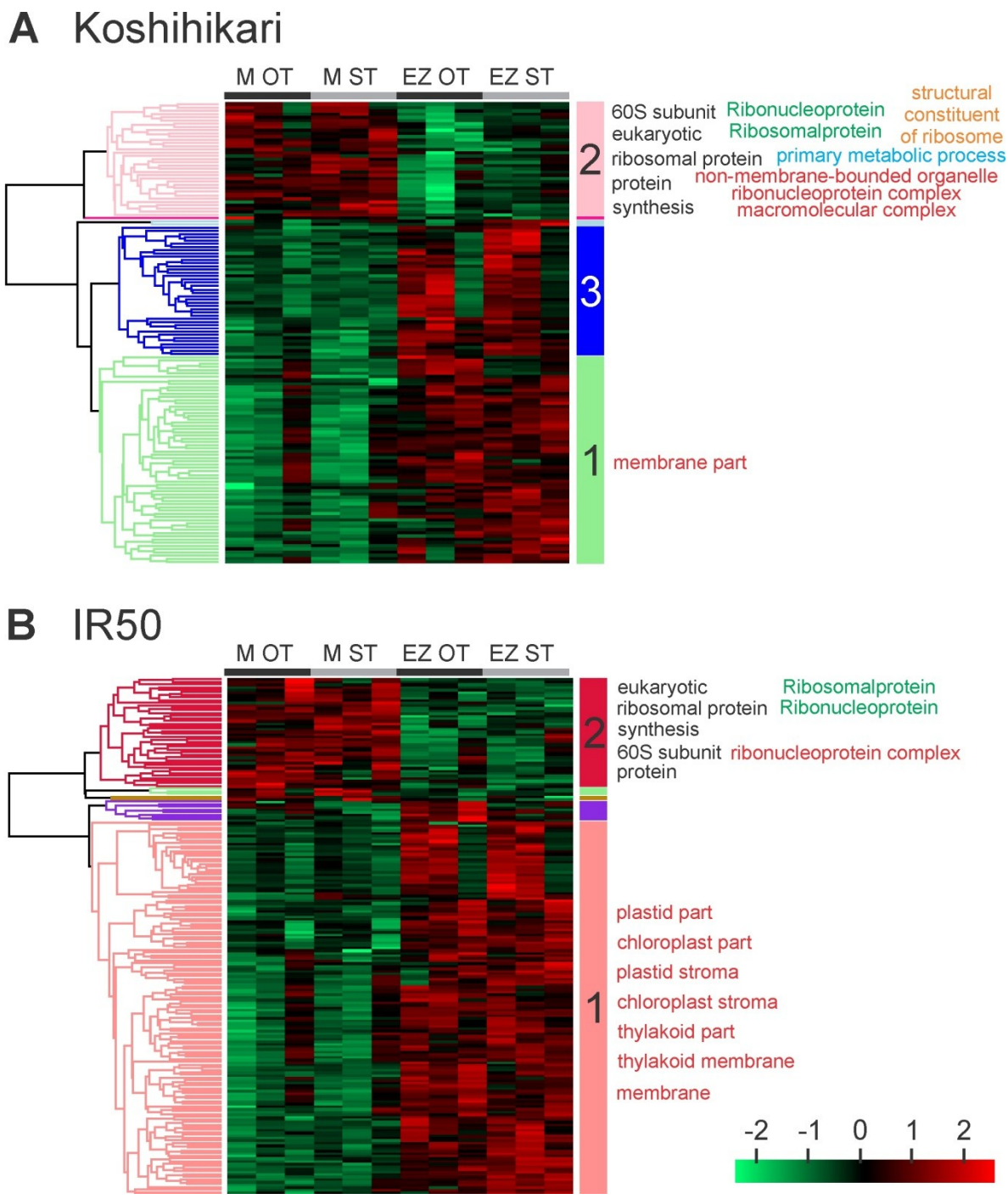

Figure 4-3. Heatmap and hierarchical clustering of significant proteins according to the *zones* effect of the two-way ANOVA (uncorrected *p*-value<0.05) between the meristem (M) and elongation zone (EZ) in each cultivar. Samples are labeled on the top representing zones (M: meristem; EZ: elongation zone) and treatments (OT: optimal temperatures; ST: suboptimal temperatures). Each sample name clusters three biological samples. Color scale at the bottom of the figure represents the abundance of proteins after normalization with Z-scoring across rows for the heatmap. The biggest clusters are numbered and enriched terms are written at the right each color representing a term category: GO Biological Processes in light blue, GO Molecular Function in orange, GO Cellular Component in red, MapManBIN in black, and Uniprot

Keywords in green. Enrichment was done with Perseus software, FDR<0.15. **A)** Hierarchical clustering of Koshihikari proteins, distance threshold of 3.43. **B)** Hierarchical clustering of IR50 proteins, distance threshold of 3.58.

4.4.1.2 The treatment effect

We performed hierarchical clusterings for proteins with uncorrected *p*-value<0.05 in response to the *treatments* factor or in the interaction *treatments*zones* for each cultivar (Figures 4-4 and 4-5). In order to identify the major processes represented by the protein profiles in the different clusters a protein enrichment analysis was performed. Koshihikari showed 16 clusters profiles for the proteins that interacted (Figure 4-4 A). Cluster 1 grouped 17 proteins that were exclusively upregulated in the elongation zone in response to ST and were overrepresented in chloroplast parts (plastid part, chloroplast part, and plastid stroma). Cluster 3 grouped 5 proteins that were downregulated in the meristem and upregulated in the elongation zone in response to the stress and were related to transcription regulation and primary metabolic processes. The rest of the clusters did not show enriched terms. When proteins that responded equally in the meristem and the elongation zone in response to ST were analyzed, 8 clusters were distinguished (Figure 4-4 B). The biggest cluster grouped 18 proteins that were upregulated in response to the stress and represented nucleotide binding proteins. Cluster 5 grouped 3 proteins downregulated in response to ST in both zones that were characterized by histones, synthesis/chromatin structure and DNA related proteins. The rest of the clusters did not have enriched terms. In the case of IR50, the interaction showed 6 clusters with different profiles (Figure 4-5 A). Only the largest cluster containing 7 proteins that were upregulated in the elongation zone in the OT condition showed enriched terms. Ion binding proteins and primary metabolism terms were overrepresented in this cluster. The analysis done for proteins that showed the same pattern in the meristem and the elongation zone depicted 8 clusters (Figure 4-5 B). Cluster 1 had 8 proteins downregulated in response to ST in both zones. The enrichment analysis of this cluster showed an overrepresentation of proteins related with organelles, the nucleus and interactions with DNA. The rest of the clusters did not show enriched terms.

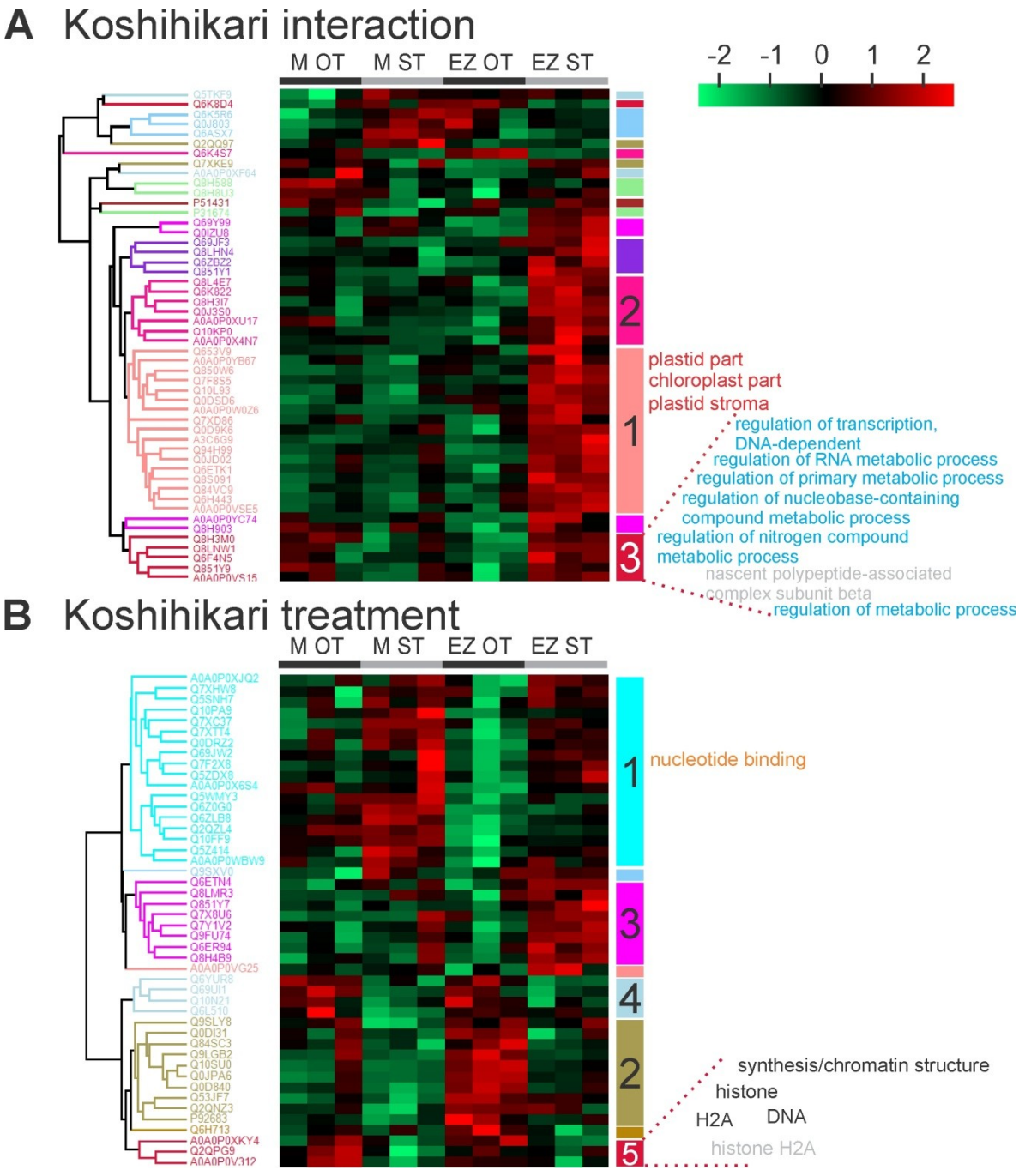

Figure 4-4. Heatmap and hierarchical clustering of significant proteins according to the *treatments*zones* or *treatments* factors of the two-way ANOVA (uncorrected *p*-value<0.05) of Koshihikari. Samples are labeled on the top same as in figure 4-3. Each sample clusters three biological samples. Uniprot IDs are marked for each protein. Color scale at the top of the figure represents the abundance of proteins after normalization with Z-scoring across rows for the heatmap. The biggest clusters are numbered and enriched terms are written at the right each color representing a term category: GO Biological Processes in light blue, GO Molecular Function in orange, GO Cellular Component in red, MapManBIN in black, and KEGG function in gray. Enrichment was done with Perseus software, FDR<0.15. **A)** Hierarchical clustering of Koshihikari proteins that interacted between zones and treatment, distance threshold of 2.58. **B)**

Hierarchical clustering of Koshihikari proteins that were significant only for the treatment effect, distance threshold of 3.15.

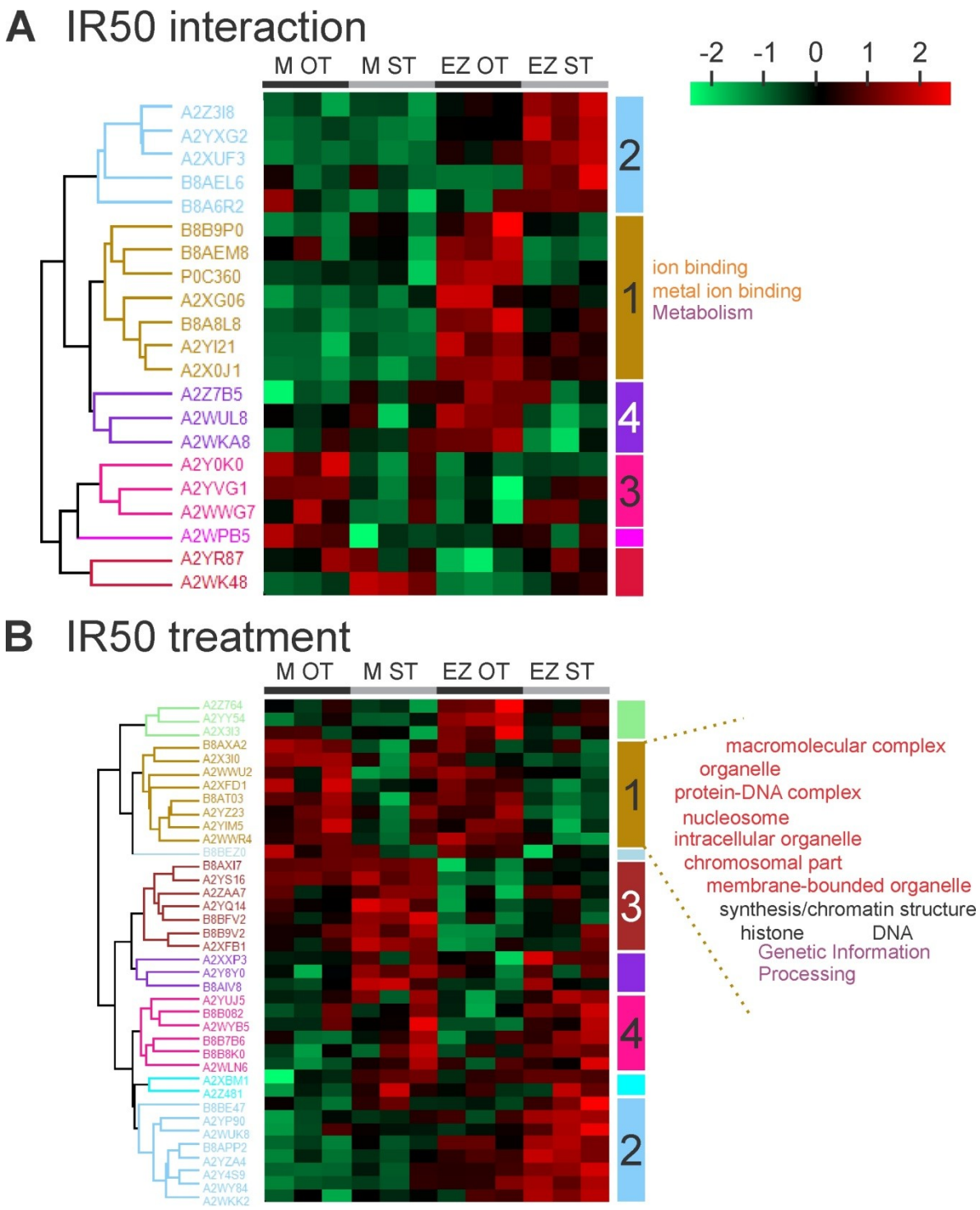

Figure 4-5. Heatmap and hierarchical clustering of significant proteins according to the *treatments*zones* or *treatments* factors of the two-way ANOVA (uncorrected *p*-value<0.05) of IR50. Samples are labeled on the top same as in figure 4-3. Each sample clusters three biological samples. Uniprot IDs are marked for each protein. Color scale at the top of the figure represents the abundance of proteins after normalization with Z-scoring across rows for the heatmap. The biggest clusters are numbered and enriched terms are written at the right each color representing a term category: GO Molecular Function in orange, GO Cellular Component in red, MapManBIN in black, and KEGG network in purple. Enrichment was done with Perseus

software, FDR<0.15. **A)** Hierarchical clustering of IR50 proteins that interacted between zones and treatment, distance threshold of 3.31. **B)** Hierarchical clustering of IR50 proteins that were significant only for the treatment effect, distance threshold of 3.43.

Overall, not many enriched terms were found, possibly because the low number of differentially expressed proteins in both cultivars. However, both cultivars showed proteins related to DNA, chromatin structure and histones downregulated in both zones in response to ST that could be reflecting the reduced cell division rate (chapter 2 part 2). Another report made on rice seedlings subjected to cold temperatures of 12-14 °C for three days indicated that histones play a role in the cold response as they were downregulated in the leaf (Neilson et al., 2011). The downregulation of histones was also reported in other species subjected to cold stress like petunia (Zhang et al., 2016). Chromatin regulation and histones and its modification play a major role in the transcription regulation in the response to environmental stresses so they could be a primary target to initiate the stress response (Kim et al., 2015; Asensi-Fabado et al., 2017).

4.4.2 Different response of the cultivars

For viewing global trends in protein function in response to ST, proteins that showed positive interaction *treatments*zones* where tested with a *post-hoc* Fisher test (*p*-value<0.05) for differences between treatment in each zone and cultivar, and were summed to proteins that responded to the *treatment* effect to constitute the list of proteins that changed in response to the stress (Supplementary Tables 10 and 11).

To describe the effect of the stress in each zone and cultivar, a functional classification of all this proteins was done according to MapMan terms (Figure 4-6). Some differences between the cultivars and zone responses could be detected. Terms related with photosynthesis were found downregulated in the elongation zone of IR50 in response to ST. This agrees with previous results from chapter 1 where IR50 showed a poor performance of the PSII when exposed to ST and from chapter 3 where the transcriptome analysis also depicted some detriment of the photosynthetic apparatus, while Koshihikari could maintain enhanced photosynthesis as many tolerant plants (Kosová et al., 2011). Mitochondrial electron transport proteins were upregulated in both zones of IR50 and downregulated in both zones of Koshihikari. Lipid metabolism showed the same pattern. Hormone metabolism terms were upregulated only in the elongation zone of IR50. Peroxiredoxin term was only upregulated in the elongation zone of Koshihikari. Terms related with protein synthesis were upregulated in the elongation zone of Koshihikari while IR50 mainly downregulated them. Finally,

terms related with cell, and particularly cell division, were only upregulated in Koshihikari.

An enrichment analysis of the protein functions was done for each zone and cultivar to test if some functions were overrepresented in the response to ST (asterisk in Figure 4-6). Downregulation of photosynthesis in IR50 elongation zone showed to be an enriched term. RNA processing and binding were also enriched terms and they were upregulated in the meristem of Koshihikari and the elongation zone of IR50. Terms related with DNA, chromatin and histones were enriched and downregulated in the meristem of both cultivars as discussed above. Ribosomal proteins were enriched and downregulated in both zones of IR50 and the elongation zone of Koshihikari while synthesis initiation was enriched and upregulated in the meristem of IR50.

Overall, this analysis showed that ST and developmental stage induce reprogramming of the rice leaf proteome differently depending on the cultivar sensitivity.

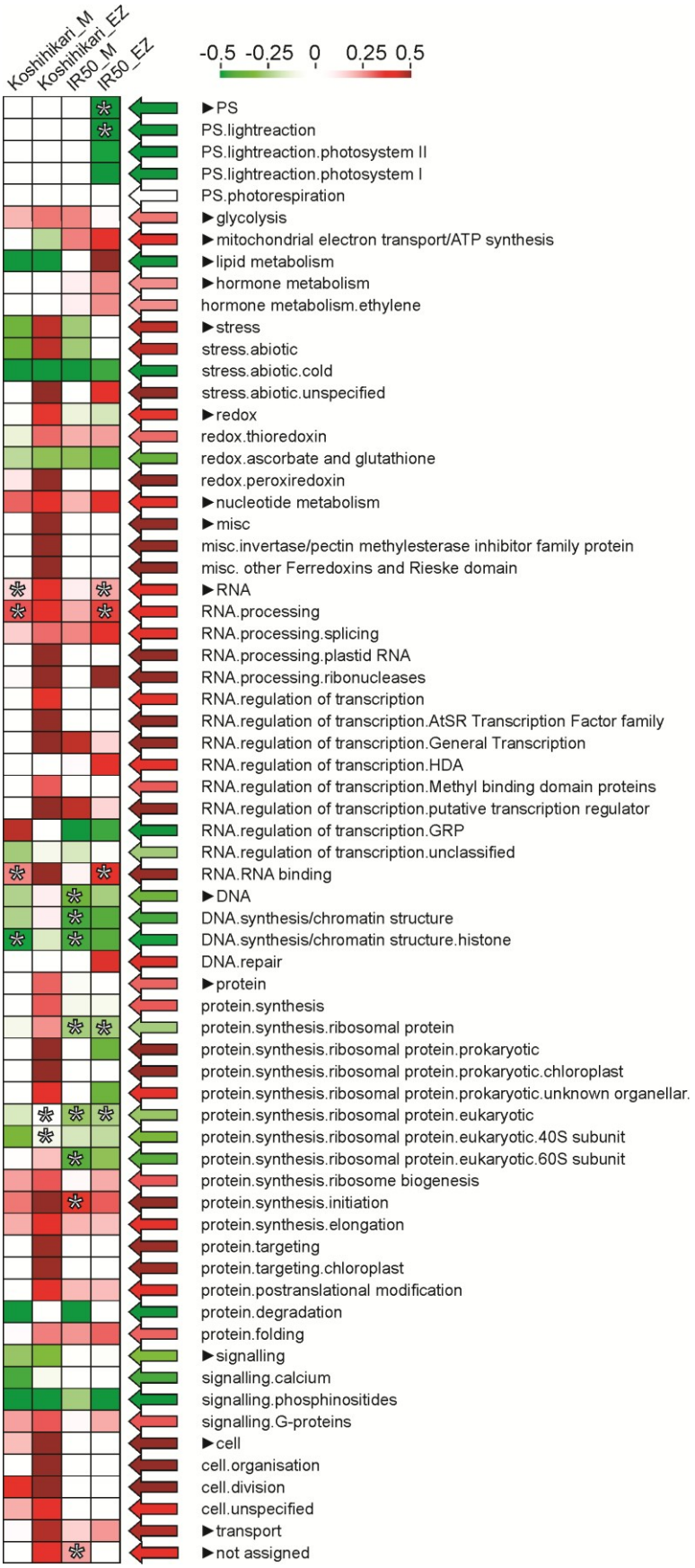

Figure 4-6. Functional categories of proteins identified in the meristem and the elongation zone of Koshihikari and IR50 leaves which abundance changed in response to the stress according to MapMan terms. Categories are averaged. Samples are named on the top: fold change of proteins from the meristem of IR50 (IR50_M); fold change of proteins from the elongation zone of IR50 (IR50_EZ); fold change of proteins from the meristem of Koshihikari (Koshihikari_M); fold change of proteins from the elongation zone of Koshihikari (Koshihikari_EZ). Main categories are marked with an arrowhead. Color scale on the top represents fold changes of proteins. Enriched terms according to Wilcoxon test done in PageMan are marked with an asterisk when corresponds.

4.4.3 Redox homeostasis was differentially regulated in the cultivars

Under stress conditions the reducing power produced by photosynthesis usually exceeds the demand of the Calvin cycle so energy is release as heat or electrons are captured by other metabolites leading to the generation of ROS that ultimately damage proteins and lipids, detoxifying strategies then act as sink of this extra energy (Ensminger et al., 2006; You and Chan, 2015). The description of the proteomes done above denoted differences in the effect of ST on photosynthetic proteins of each cultivar (Figure 4-6) that could have lead to an imbalance of the energy state of the plant and, thus, a redox deregulation. IR50 showed enriched terms related with photosynthesis in the elongation zone. In a more detail look, the downregulated proteins belong to subunits of the PSI and to proteins of the oxygen evolving complex (OEC; Table 4-2). Although the effect on PSII performance in this cultivar was already described in chapter 1 and has been widely reported in cold sensitive species (Huner et al., 1998), little is known about PSI. Under stressful conditions PSI is irreversibly affected and this could cause secondary damage generated by ROS (Sonoike, 2011). Secondly, the downregulation of the OEC proteins was also reported at the transcriptome level in the analysis done in chapter 3 and at the proteome level in other species subjected to cold stress (Kosová et al., 2011). Overall, the photosynthesis pathway in IR50 was affected at the protein level. On the contrary, Koshihikari did not show any effect of the photosystems at the protein level supporting the hypothesis that part of its tolerance to ST is due to the capacity of maintain a healthy and active photosynthetic apparatus. Although two proteins related with photosynthesis that belong to the glycine cleavage system of photorespiration pathway changed their abundance in Koshihikari, the implication in the response will be discussed below.

The response of the redox system in plants can be generally described with the next strategies (Voss et al., 2013): (*i*) the prevention of the limitation of the acceptor by the malate valve system; (*ii*) in case there is an acceptor limitation at the PSI then it prevents reactive oxygen species (ROS) accumulation by activating the cycle electron flow decreasing that way the generation of NADPH and increasing ATP; (*iii*) in the case ROS is already at high levels then detoxifying systems are activated, *i.e.*, ascorbate-glutathion pathway, NADPH-thioredoxin reductase (NTRC), and photorespiration; (*iv*) ROS signaling triggers other strategies leading to acclimation to the stress. Koshihikari and IR50 showed different responses at the protein level related with different strategies of redox homeostasis especially regarding strategy *iii*. Due to the relevance of the antioxidant regulation for stress responses in general and in response to low

temperature stress, we looked more specifically at ROS related protein expression in our dataset (Table 4-2).

Table 4-2. Fold change and description of proteins belonging to the photosynthesis (PS) and redox MapMan terms. Only fold changes with uncorrected *p*-value<0.05 for the factor *treatments*, and the interaction *treatments*zones* subjected to *post-hoc* Fisher test (*p*-value<0.05) are shown in the table. Proteins which FDR<0.10 are marked in bold.

Cultivar	Protein ID	FC Meristem	FC Elongation zone	Protein description
PS				
Koshihikari	**A3C6G9**		0,66549333	glycine cleavage system H protein
	Q6H713	-0,07592	-0,70802	putative glycine cleavage system H protein
IR50	P0C360		-1,43531	photosystem I subunit VII
	B8A8L8		-0,636163	photosystem II oxygen-evolving enhancer protein 1
	A2YI21		-0,339493	photosystem II oxygen-evolving enhancer protein 2
	A2YY54	-0,0550467	-0,42299	photosystem I subunit II
Redox				
Koshihikari	Q6ER94	0,24247667	0,70296	*BAS1*, 2-Cys peroxiredoxin BAS1, chloroplastic
	Q7F8S5		0,80441333	*PRXIIE-2*, Peroxiredoxin-2E-2, chloroplastic
	Q8S091		0,99011	Thioredoxin F, chloroplastic
	Q0D840	-0,26354	-0,39242333	*OsTrx23*, thioredoxin H1, cytosolic
	Q10N21	-0,22205333	-0,29684667	L-ascorbate peroxidase
IR50	**A2WY84**	0,214233	0,236643	Thioredoxin F, chloroplastic
	A2XFC7	-0,140213	-0,282367	*OsAPX1,* L-ascorbate peroxidase
	A2XFD1	-0,446577	-0,489693	*OsAPX1,* L-ascorbate peroxidase

Both cultivars downregulated cytosolic L-ascorbate peroxidases in both zones in response to ST. There are eight ascorbate peroxidases (APX) described in japonica rice from which two were found in the cytosol, *OsAPX1* (Accession: Q10N21) and *OsAPX2* (Accession: Q9FE01; Teixeira et al., 2006). Indica cultivars have two homologous for *OsAPX1* (Accessions: A2XFC7 and A2XFD1) and one for *OsAPX2* (Accession: B8B6B6; http://gramene.org/). *OsAPX2* were detected in both cultivars proteomes (see Supplementary Tables 7 and 8) but they did not change their abundance, while all homologous from *OsAPX1* were downregulated in Koshihikari and IR50. Many studies were done with cytosolic APX knockdown rice mutants and evidence of compensation from other pathways were found, for instance, photorespiration proteins were incremented, other peroxidases responded in the

absence of cytosolic APX (Rosa et al., 2010; Bonifacio et al., 2011; Carvalho et al., 2014). In that way, two chloroplastic peroxiredoxin were upregulated in the tolerant cultivar. *PRXIIE-2* was found upregulated only in the elongation zone (Q7F8S5) while *BAS1* (Q6ER94) was upregulated in both zones. This particular type of thioredoxins is known to play a role in the context of photosynthesis in the detoxification of photochemically produced H_2O_2, less reactive than other ROS but that could be reduced to more harmful ROS (Rhee et al., 2001; Dietz et al., 2006; Pérez-Ruiz et al., 2006). The peroxiredoxin pathway presents an alternative to the water/water cycle and protects proteins of the stroma associated with the inner envelope membrane from probable peroxides that escaped from thylakoids or enter from the cytoplasm, acting that way as an antioxidant (Dietz et al., 2002). Koshihikari also increased the abundance of a crucial protein that forms part of the glycine cleavage system (GCS), the *GDCSH* (A3C6G9), in both zones in response to the stress (Douce et al., 2001). This protein takes part in the photorespiration pathway. Photorespiration helps to minimize ROS production by using directly or indirectly ATP and NADPH when re-assimilating NH_4^+ from glycine by the GCS in C_3 plants, protecting the plant from photoinhibition (Peterhansel et al., 2010; Voss et al., 2013; Keech et al., 2016). A knockdown of this protein in rice displayed a photorespiration-deficient phenotype with induced ROS (Zhou et al., 2013). Because the low temperatures increases the solubility of oxygen more than carbon dioxide and cold stress can cause ROS production, the photorespiration would be working as a sink of the extra reducing power (Huang et al., 2013). Another putative protein H from the GCS was downregulated in both zones of Koshihikari (Q6H713) but its activity has not been proven.

Koshihikari also downregulated a thioredoxin *h*, *OsTrx23,* in the meristem as well as in the elongation zone (Q0D840). This protein was found in the cytosol but it was also described to be the major protein in the phloem sap being synthesized in the companion cells prior to being transferred by mediating its own cell-to-cell transport through plasmodesmata to the sieve-tubes of the mature phloem (Ishiwatari et al., 1995; Ishiwatari et al., 1998). It was also found in the apoplastic space where the generation of ROS is required for inducing the stomata closure by the absicic acid signal (Zhang et al., 2011; Sierla et al., 2013; Kaushik and Roychoudhury, 2014). *OsTrx23* interacts with the NADPH/thioredoxin system that generates ROS in the apoplast required for inducing the stomata closure by the absicic acid signal (Zhang et al., 2011; Shaykholeslam Esfahani and Shahpiri, 2015). The importance of *OsTrx23* in stomata closure was proven when overexpressing lines were found sensitive to salt

stress because they could not accumulate ROS in the apoplast. This suggests that *OsTrx23* actively participates in the ROS regulation of the apoplastic space and its repression would allow ROS signaling to trigger stomatal closure in Koshihikari in response to the low temperature stress. This hypothesis is supported by the previous description of different cultivar regarding the stomata conductance in Chapter 1. There, when rice cultivars were subjected to low temperatures the stomata conductance was lower in the tolerant cultivars, including Koshihikari, than in the sensitive cultivars response, including IR50 (Figures 1-10 and 1-12), evidencing the stomata closure in the tolerant ones. It was reported an upregulation of *OsTrx23* in a japonica rice cultivar in response to 12 °C treatment at the transcript level and no evidence at the protein level was studied (Xie et al., 2009; Xie et al., 2012). Besides, a thioredoxin *f* in the chloroplast was upregulated in both cultivars, in the elongation zone in the case of Koshihikari (Q8S091) and in both zones in the case of IR50 (A2WY84). Thioredoxin *f* family is known to regulate the enzymes of the Calvin cycle and associated processes activating the carbon metabolism (Balmer et al., 2003; Nuruzzaman et al., 2008), acting this way as redox signaling mechanism (Michelet et al., 2005). Thioredoxins would be participating in the strategy *iv* of the ROS system.

4.4.4 Regulation of transcription, translation and protein folding

Transcriptional and translational regulations are key to the response of plants to cold stress (Heidarvand and Maali Amiri, 2010) and so terms related to these processes were found enriched in both cultivars (Figure 4-6). Terms related to DNA interaction were enriched specially in the meristem response of both cultivars. These proteins corresponded mainly to histones and were downregulated in both cultivars and zones (Table 4-3). As commented above, histones are known to be modified under cold stress because they are involved in transcription regulation and its downregulation has been reported and could be a consequence of a reduced cell division rate.

Table 4-3. Fold change and description of proteins belonging to DNA MapMan terms. Only fold changes with uncorrected *p*-value<0.05 for the factor *treatments*, and the interaction *treatments*zones* subjected to *post-hoc* Fisher test (*p*-value<0.05) are shown in the table. Proteins which FDR<0.10 are marked in bold.

Cultivar	Protein ID	FC Meristem	FC Elongation zone	Protein description
DNA				
Koshihikari	Q69JW2	0.26127666	0.6381767	template-activating factor I
	A0A0P0V312	-0.48028	-0.25429666	histone H2A
	Q2QPG9	-0.50226665	-0.07192	histone H2A
IR50	A2YVG1		0.43288	UV excision repair protein RAD23
	B8AXA2	-0.5685833	-0.16455667	histone H2A
	A2WWU2	-0.46364668	-0.42670667	histone H2B
	A2WWR4	-0.32943332	-0.7050267	Histone H4

Proteins associated with ribosomes were upregulated in both cultivars (Table 4-4), as well as RNA-binding proteins and splicing factors. This was already reported in other species subjected to cold stress (Kosová et al., 2011) since transcriptional and posttranscriptional regulation of RNA metabolism is an essential step for fine regulation of gene expression (Kwanuk and Hunseung, 2016). The cold shock protein *OsCSP1* was repressed in both zones in Koshihikari (Q6YUR8). Although this protein appears to be capable of binding to nucleic acids and to complement an *E. coli* strain with quadruple deletion of cold shock domain proteins (CSD proteins) when exposed to low temperatures, it was not upregulated in response to chilling treatment of rice japonica cultivar seedlings and its transcript induction was only transitional during the first half hour of treatment (Chaikam and Karlson, 2008). *OsCSP1* was found accumulated in reproductive tissues which is in line with the fact that the reproductive stage of rice is also sensitive to low temperatures (Imin et al., 2004; Chaikam and Karlson, 2008). Unlike rice, in winter wheat cultivar, CSD protein *WCSP1* was highly expressed in crown tissue under chilling stress (Karlson et al., 2002), although only transiently in the leaf (Radkova et al., 2014). It might be possible that in rice *OsCSP1* has a role in the later stages, or that CSD proteins are not capable to confer low temperature acclimation in rice as they do in winter wheat.

Table 4-4. Fold change and description of proteins belonging to RNA MapMan terms. Only fold changes with uncorrected *p*-value<0.05 for the factor *treatments*, and the interaction *treatments*zones* subjected to *post-hoc* Fisher test (*p*-value<0.05) are shown in the table. Proteins which FDR<0.10 are marked in bold.

Cultivar	Protein ID	FC Meristem	FC Elongation zone	Protein description
RNA				
Koshihikari	Q10PA9	0.69879	0.28461334	small nuclear ribonucleoprotein D3
	Q6ETN4	0.48309666	0.99534	small nuclear ribonucleoprotein F
	Q0J803	0.43197		small nuclear ribonucleoprotein E
	Q5ZDX8	0.37218666	0.73875	Heterogeneous nuclear ribonucleoprotein A2/B1-like
	Q2QQ97	0.52638		heterogeneous nuclear ribonucleoprotein A1/A3
	Q69JF3		0.75412333	ribonuclease T2
	Q5TKF9	1.0235367		U6 snRNA-associated Sm-like protein LSm8
	Q0DRZ2	0.26336	0.26721334	splicing factor, arginine/serine-rich 1/9
	Q2QZL4	0.073026665	0.32748666	Splicing factor U2af large subunit B
	Q8L4E7		0.6348067	SAP-like protein BP-73
	Q8H4B9	0.11618666	0.5620033	Putative translational inhibitor protein
	Q851Y9		0.56799	Nascent polypeptide-associated complex subunit beta
	Q8LNW1		0.67068	Nascent polypeptide-associated complex subunit beta
	A0A0P0VS15		0.9220267	Nascent polypeptide-associated complex subunit beta
	Q10KP0		0.79014665	nucleolin
	A0A0P0XJQ2	0.14323667	0.37117666	polyadenylate-binding protein
	Q6H443		0.6674567	polyadenylate-binding protein
	Q6F4N5		0.70558	Aspartyl protease 25
	Q851Y1		0.5225833	Ankyrin repeat domain protein 2, putative, expressed
	Q6ASX7	0.46618667		Glycine-rich RNA binding protein
	Q0J3S0		0.76565665	Similar to Nucleic acid-binding protein precursor
	Q7F2X8	0.5113533	0.5370567	
	Q8LHN4		0.64607334	
	A0A0P0YC74		0.31729665	
	Q6YUR8	-0.7245233	-0.7200633	Cold shock protein, *OsCSP1*
	Q10SU0	-0.32459	-1.05496	
IR50	B8AIV8	0.82024	0.45398667	small nuclear ribonucleoprotein F
	A2YR87		0.40006	small nuclear ribonucleoprotein E
	A2Z3I8		0.85685664	ribonuclease T2
	B8APE3	0.26823333	0.39204332	Serine/arginine rich splicing factor, mitochondrial
	A2YZA4	0.18809	0.35664666	polyadenylate-binding protein
	B8AEL6		0.2619	far upstream element-binding protein

	A2XBM1	0.46166667	0.15539333	Nascent polypeptide-associated complex subunit beta
	B8B082	0.0567	0.33499667	plasminogen activator inhibitor 1 RNA-binding protein
	B8AXI7	0.06073	0.41566333	
	A2WUK8	0.09325667	0.42326668	
	A2WYB5	0.20530333	0.46652666	
	B8B9P0		-0.38203666	polyadenylate-binding protein
	B8AGK8	-0.5329267	-0.46398333	plasminogen activator inhibitor 1 RNA-binding protein

Koshihkari and IR50 differentially regulated proteins that participate in the translation processes (Table 4-5). Koshihikari increased the level of various subunit ribosomal proteins in both zones in response to the stress while IR50 downregulated them. This kind of proteins has different responsive elements in the promoter including low temperature responsiveness elements. The particular effect on cold stress could be to enhance the polypeptide synthesis at low temperatures (Kim et al., 2004). Cellular proteins in the chloroplast could be damaged because of increments in ROS that escaped the scavenging system and so chaperones would have to act to ensure the correct folding of the proteins (Wang et al., 2004). A few chaperonins were upregulated in the elongation zone of Koshihikari and in both zones of the sensitive cultivar. The correct folding of proteins for well functionality of the cell is crucial for the growth of the plant and this was evidenced in upregulation of chaperonins in both cultivars in response to the stress. The sensitive cultivar also overexpressed two translation initiation factors in both zones known as translation initiation factor 5A *eIF5A* (B8B833 and A2YHI1; Table 4-5). *eIF5A* proteins participate in different steps from the translation initiation, a limiting-step in this process (Dutt et al., 2015). Chou et al. (2004) analyzed two *eIF5A* from rice and found that its expression at the transcript level was higher in older leaves, they were more expressed in the division and elongation zone than in the mature part, and they were upregulated in response to different environmental stresses. In some plants *eIF5A* seemed to be related with premature senescence induced by environmental stresses by facilitating the translation of mRNA species required for programmed cell death (Wang et al., 2001; Thompson et al., 2004; Parkash et al., 2014). On the other hand, *eIF5A* was also related with plant adaptation to changing environmental conditions and xylogenesis in *Arabidopsis* (Liu et al., 2008; Ma et al., 2010; Xu et al., 2011; Wang et al., 2012).

Table 4-5. Fold change and description of proteins belonging to Proteins MapMan terms. Only fold changes with uncorrected *p*-value<0.05 for the factor *treatments*, and the interaction *treatments*zones* subjected to *post-hoc* Fisher test (*p*-value<0.05) are shown in the table. Proteins which FDR<0.10 are marked in bold.

Cultivar	Protein ID	FC Meristem	FC Elongation zone	Protein description
Proteins				
Koshihikari	Q10L93		0.52825665	large subunit ribosomal protein L6
	A0A0P0VSE5		0.61778	large subunit ribosomal protein L11
	Q653V9		0.72164667	large subunit ribosomal protein L24
	Q5WMY3	0.34140667	0.25058666	large subunit ribosomal protein L18e
	Q6ZLB8	0.40118	0.42088667	60S ribosomal protein L4/L1
	Q0DSD6		0.38768	small subunit ribosomal protein S1
	Q850W6		0.64033	small subunit ribosomal protein S5
	Q7XHW8	0.31454	0.32609335	translation initiation factor 2 subunit 2
	Q7Y1V2	0.32786	0.95992	translation initiation factor 1A
	Q6Z0G0	0.37155333	0.17052333	molecular chaperone GrpE
	Q69Y99		0.55468	chaperonin GroES
	Q8H3I7		0.39826667	chaperonin GroES
	Q8H903		0.27647	chaperonin GroEL
	Q8LMR3	0.21553333	0.37254667	nascent polypeptide-associated complex subunit alpha
	Q6K5R6	0.67737		
	Q7XTT4	0.23430666	0.32001	
	Q0JD02		0.49144334	
	Q6K822		0.6341633	
	Q69UI1	-0.67852664	-0.40966332	small subunit ribosomal protein S13e
	Q8H588	-0.5328067		small subunit ribosomal protein S18e
	P51431	-0.8020167		small subunit ribosomal protein S27Ae
	Q6L510	-0.60182333	-0.10566	large subunit ribosomal protein L36e
	Q6K8D4		-0.38052332	peptidylprolyl isomerase
IR50	A2Y8Y0	0.37901	0.08707	small subunit ribosomal protein S20e
	B8B7B6	0.24657667	0.29134333	small subunit ribosomal protein S12e
	A2XXP3	0.07485667	0.21757667	nucleolin
	A2YS16	0.06128	0.22338	nucleolin
	A2YHI1	0.35956	0.34610334	Eukaryotic translation initiation factor 5A, *eIF5A*
	B8B833	0.26076666	0.39830333	Eukaryotic translation initiation factor 5A, *eIF5A*
	B8B8K0	0.20676	0.18975	elongation factor 1-beta
	B8B537	0.19935	0.19505666	chaperonin GroES
	A2XAA0	0.30108333	0.29007667	chaperonin GroES
	B8B9V2	0.24317667	0.43737	molecular chaperone GrpE
	A2WLN6	0.46192333	0.19885333	
	B8BAC6	-0.61974	-0.51312333	40S ribosomal protein S13-2, *rps13*

	A2Z764	-0.22964333	-0.39825332	small subunit ribosomal protein S17e
	A2YIM5	-0.32617334	-0.40566334	small subunit ribosomal protein S18e
	A2XIT5	-0.30577	-0.18207666	large subunit ribosomal protein L13e
	A2YZ23	-0.18497667	-0.4671	large subunit ribosomal protein L17e
	A2X3I0	-0.39258	-0.23938666	large subunit ribosomal protein L27e
	B8AT03	-0.48683667	-0.59354335	large subunit ribosomal protein L35e
	A2Y0K0	-0.74587667		large subunit ribosomal protein L18e
	A2WPB5	-0.69289666		small subunit ribosomal protein S27Ae
	A2XG06		-0.3706	small subunit ribosomal protein S1
	A2WUL8		-0.54714	small subunit ribosomal protein S24e

4.5 CONCLUSIONS

The proteomic analysis of the ST stress response across the growth zone showed differences between contrasting rice cultivars. The majority of the proteins that changed their abundance in response to the stress were related with genetic information processes. Although the total number of proteins that changed their abundance against ST did not differ that much between Koshihikari and IR50, their functions did. The overrepresentation analyses showed big differences between the zones in Koshihikari. Proteins related with transcription and splicing in the meristem and with parts of the chloroplast and the phospholipids metabolite pathway in the elongation zone were overexpressed. IR50 also showed some differences between the zones responses: in the meristem ribosomal and organelle related proteins were repressed in the elongation zone proteins related with photosynthesis and ribosomes were repressed. These results suggested differences between the response of the cultivars, especially regarding photosynthetic apparatus and, in consequence, redox homeostasis.

CHAPTER 5: Biochemical analysis of contrasting rice cultivars in response to suboptimal temperatures

5.1 INTRODUCTION

Results from previous chapters triggered the necessity of studying particular metabolic processes that could explain the response of rice to ST stress and the differences between representative contrasting rice cultivars, Koshihikari and IR50. Photosynthetic performance proved to be a key difference in ST stress sensitivity at long exposures (chapter 1) and this was also denoted in the omics analyses (chapters 3 and 4). The transcriptome analysis done after 24 h of exposure to ST at the whole shoot level showed that the OEC was regulated suggesting that the effect of ST on the PSII might have started from the beginning. At the leaf growth zone level the proteome analysis also showed that proteins from the OEC were actually downregulated in the sensitive cultivar. Since the performance of the PSII was already evaluated (chapter 1) it rests to check whether the OEC was one of the first systems to be affected as the transcriptome and proteome analyses suggested in IR50.

Several symptoms of the ST stress suggested that differences at the ultrastructural level of photosynthetically active cells could be also implied in the different response of Koshihikari and IR50. The transcriptome analysis depicted differences in the photosynthetic apparatus at short term (Chapter 3) between cultivars, and long term exposures (Chapter 1) showed that Koshihikari was able to maintain a healthy photosystem that allowed it to growth better than IR50 under stress conditions (see Chapter 1 and 2). It is known that the chloroplast is commonly the earliest ultrastructure affected by chilling stress (Kimball and Salisbury, 1973; Kratsch and Wise, 2000) so it makes sense to analyze whether these differences are visible in ST stress or not, particularly at the long term when PSII performance was proved to be affected in the sensitive cultivars. Besides, both transcriptome (Chapter 3) and proteome (Chapter 4) analyses were enriched in terms regarding chloroplast parts, membranes, and carbohydrates metabolism in the stress responses and they showed differences between Koshihikari and IR50.

Fatty acid composition can be altered by cold stress because of the need of remodeling the membrane fluidity (Upchurch, 2008). The transcriptome analysis suggested that different balance of fatty acids could be part of the cultivars response to ST (Chapter 3) since desaturases were upregulated in both cultivars and lipids degradation was upregulated in IR50. To see if the transcriptional regulation sorted effect on the membranes, a lipidomic analysis at longer exposures to ST stress in both cultivars needs to be done.

That the photosynthetic apparatus is damaged as a consequence of the ST stress has been discussed all along the manuscript. The extra reducing power that this system generates and do not use for the growth of the plant necessary needs to be released as heat or electrons need to be used by alternative pathways (Ensminger et al., 2006). Many evidences that the redox homeostasis was altered in response to ST have been described at the transcriptome (chapter 3) and the proteome levels (chapter 4). The growth (chapter 2) and the proteome analyses showed that Koshihikari and IR50 had different response depending on the zone sampled from the leaf, so an analysis of metabolites and enzymes related to redox should be done across the growth zone of both cultivars.

Different environmental stresses are known to also alter plant secondary metabolites since they play a major role in the adaptation to the environment (Ramakrishna and Ravishankar, 2011). Secondary metabolism also represented a great percentage of DEGs in both cultivars transcriptome response (Chapter 3). Particularly, DEGs of polyamines pathway were differentially expressed only in IR50. Since polyamines are known to be related in many abiotic stress and its biosynthesis is known to be primary at the transcriptiome level (Calzadilla et al., 2014; Liu et al., 2015), a more detailed analysis of these metabolites should be done.

5.2 AIMS

This chapter looks forward to study specific metabolic processes to gain some evidences about the different response between tolerant and sensitive rice cultivars against the ST stress that were proposed in studies done at different levels in previous chapters.

5.3 MATERIALS AND METHODS

5.3.1 Plant material and growth conditions

Rice cultivars Koshihikari and IR50 were kindly provided by the Rice Breeding Program of the Universidad Nacional de La Plata, Argentina. Seeds were placed within Petri plates on two layers of Whatman Nº 5 filter paper rinsed with 7 mL Carbendazim 0.025 %p/v (Yoshida. 1981) and incubated in growth chamber at 30 ºC in darkness until germination. Seedlings were transplanted to plastic net frames placed over a 4 L black tray containing 3 L distilled water (hydroponic culture) or to peat potting medium (Jiffy, The Netherlands; volume of the pots: 1.6 l, dimensions: 13 cm tall and 5” of diameter) and saturated with water (soil culture). Hydroponic cultures of both cultivars

were placed in the Percival E-30B chamber (Percival E-30B, Percival Scientific, IA, USA) and soil cultures of both cultivars were placed in the Conviron chamber (Conviron, Adaptis A1000). All chambers were set with same condition: 12 h photoperiod, 80% humidity, and 400 µmol photons m^{-2} s^{-1} of photosynthetically active radiation (PAR). Day and night temperatures for optimal temperatures of growth treatment (OT) were 28 and 24 °C, respectively. After three days of culture, the water of the hydroponic cultures was replaced by 3 L Yoshida solution (Rachoski et al., 2015). Therein, the Yoshida solution was renewed every three days until the end of the experiment. When the third leaf (Yoshida, 1981) emerged, day and night temperatures of one chamber were modified to 21 and 13 ºC, respectively (suboptimal temperatures; ST). Seedlings were further cultivated and harvested at different times depending on the analysis.

5.3.2 Determination of decoupling of oxygen evolving complex and quinone B reducing centers

Decoupling of Oxygen Evolving Complex (OEC) and quinone B (Q_B) reducing centers were determined by non-invasive chlorophyll fluorescence fast-transient test (JIP test) using a fluorometer (Handy PEA fluorometer, Hansatech Instruments® Ltd., King's Lynn, Norfolk, UK) in seedlings from the hydroponic cultures. The PEA software (PEA plus v1.1, Hansatech Instrument Ltd., UK) was used according to Chen et al., (2014). After 24 h of treatment, a blade section of the third leaf in expansion was covered with leaf clips to adapt them to darkness for 20 min. Then, leaf clips were opened and initial fluorescence (F_O) was determined at 20 µs (Step O). Samples were then exposed during 1 s to a first pulse of saturating red light (650 nm, 3000 µmol photons m^{-2} s^{-1}). Fast-transient chlorophyll fluorescence was determined at: 20 ms (F_j; step J or V_J), 300 µs (F_K; step K), 30 ms (F_I; Step I); Maximal fluorescence intensity (F_M) is equal to F_P (Step P) since the light pulse was saturating. The fluorescence kinetics was normalized by F_O and F_J as W_{OJ} from the equation:

$$W_{OJ} = (F_t - F_0)/(F_J - F_0)$$

and ΔW_{OJ} was calculated from the equation:

$$\Delta W_{OJ} = W_{OJ(treated)} - W_{OJ(control)}$$

K band was determined as the difference kinetics ΔW_{OJ}. After Step P, samples were kept for 10 s in darkness and then exposed during 1 s to a second pulse of red

light. The reaction center fraction called slow or non-Q_B reducing centers (ΔV_0) was calculated as following:

$$\Delta V_0 = [1-(F_0/F_M)_{(2^o \text{ exposure})}/\ 1-(F_0/F_M)_{(1^o \text{ exposure})}]$$

and Q_B reducing centers was calculated from the equation:

$$Q_B \text{ reducing centers} = 1- \Delta V_0$$

5.3.3 Ultrastuctural analysis

The mature part of the last fully expanded leaf (third or fourth leaf) from each cultivar and treatment grown in soil during 10 or 24 d was harvested 5 h after the start of the photoperiod and cut in pieces of 2 mm^2. The samples were fixed in 2% glutaraldehyde in a potassium phosphate buffer pH 7.2-7.4 for 2 h at 4 °C. A secondary fixation was done with 1% (w/v) osmium tetroxide for 1 h at 4 °C. Then, the samples were dehydrated in an increasing series of alcohols (from 50% to 100%) in a vacuum chamber and included in Spurr resin. Ultrathin sections (90 nm) were contrasted with uranyl acetate and lead citrate, examined with a transmission electron microscope (TEM) JEM 1200 EX II (JEOL Ltd., Tokio, Japón) and photographed with a digital camera Erlangshen ES1000W (Model 785, Gatan Inc., Pleasanton, California, USA) at the *Central de Microscopía Electrónica* from the *Facultad de Ciencias Veterinarias* (UNLP, Argentina).

5.3.4 Lipidomic analysis

Total lipid extraction and purification was done according Bligh et al., (1959) with modifications in seedlings from the hydroponic culture. 3 seedlings shoots were harvested at 6 d of treatment and pooled, constituting a biological replicate. 5 pools from each treatment and cultivar were analyzed. Samples were ground with mortar in liquid N_2 and 100 mg of the powder were mixed with chloroform:methanol 1:2 v/v, and 15 ppm of the internal standard (IS) pentadecanoic acid (SIGMA). After centrifuging at 6000 g for 5 m, supernatant was kept apart and lipids from the pellet were re-extracted with 0.3 mL of chloroform:methanol 1:2 v/v and 0.08 mL of KCl 1 %. Both supernatants were mixed and 0.2 mL chloroform and 1.2 mL KCl 1% were added. The sample was centrifuged 5 min at 10000 g and 150 µL of the organic phase were dried with liquid nitrogen.

Preparation of fatty acid methyl esters for gas-liquid chromatography was made according to Ichihara and Fukubayashi, (2010) mild methanolysis/methylation. The

sample was dissolved with 0.05 mL of toluene and 0.375 mL methanol and 0.075 mL HCl 8% were added. After mixing, the solution was transferred into 5 mL screw-capped tubes and incubated at 45 °C over night. After cooling, the sample was mixed with 0.25 mL hexane and 0.25 mL dH_2O. The tube was homogenized with vortex, and then the hexane layer was analyzed by GC/MS (Clarus SQ 8. Perkin Elmer. MA. USA), in SIM mode, using a DB-23 column (30 m X 0.250 mm X 0.25 µm), He as a gas carrier (1.5 mL min^{-1}), split mode injection (270 °C, ratio 50:1), and temperature ramp 130 °C 1 min, 6.5 °C min^{-1} till 170 °C, 2.75 °C min^{-1} till 215 °C, 40 °C min^{-1} till 230 °C 3 min. The quantification was made according to the IS method. A standard mix of fatty acids (Accustandard) was used for standard curves. The fatty acids analyzed with their respective retention times are shown in the Supplementary Table 12.

5.3.5 Measurements related with redox state of the plants

Two days after emergence of the fourth leaf of seedlings in the soil cultures, 10 randomly chosen plants from each cultivar and treatment were harvested and the growth zone of the fourth leaf of each plant was cut in five segments as follows according to the results on Chapter 2 (Figure 4-1): from the base of the leaf 4 mm (meristem), 3 mm (transition between meristem and elongation zone), 18 mm (elongation zone), 5 mm (transition between elongation and mature zone), and 20 mm (mature zone) were consecutively cut from plants under OT conditions; from the base of the leaf 3 mm (meristem), 3 mm (transition between meristem and elongation zone), 10 mm (elongation zone), 4 mm (transition between elongation and mature zone), and 20 mm (mature zone) were consecutively cut from plants under ST conditions. For each cultivar and treatment, three pools of each segment (each pool from 10 plants) weighing between 15 and 100 mg were homogenized with 500 µl of K-Phosphate buffer (0.05 M pH 7.0), containing 2% w/v polyvinyl pyrrolidone, EDTA (0.4 mM) and PMSF (0.2 mM), by using a MagNALyser (Roche, Vilvoorde, Belgium). Homogenates were centrifuged (14000 g, 45 min). An aliquot of 25 µl of supernatant was separated for the FRAP assay and ascorbic acid (1 mM) was added to the rest. Samples were stored at -80 °C for the following determinations. The remaining plants were used to determine the length of the fourth leaf until it reach maturity.

5.3.5.1 Determination of H_2O_2

For H_2O_2 determination, 25 µl of xylenol orange dye reagent (Bellincampi et al., 2000) were added to 25 µl of supernatant. After 45 min incubation, the Fe^{3+}-xylenol orange complex was measured at 600 nm. Standard curves of H_2O_2 were obtained by

adding variables amounts of H_2O_2 to the xylenol orange dye reagent. Data were normalized and expressed as µM H_2O_2 per gram of fresh weight tissue.

5.3.5.2 Determination of malondialdehyde

Malondialdehyde (MDA) was indirectly measured through the substances that react with thiobarbituric acid (TBA; Hodges et al., 1999). 25 µl of supernatant were heated with 25 µl of 0.5% (w/v) TBA in 20% (w/v) tricloroacetic acid (TCA) at 95 °C for 1 h. Samples were centrifuged, placed in a 96-well plate and the absorbance measured at 440, 532 and 600 nm in a microplate reader Synergy H1 (BioTek). Data were expressed as MDA equivalents (nmol/g FW) according to Du and Bramlage, (1992).

5.3.5.3 Non-enzymatic antioxidant capacity

The Ferric Reducing Ability of Plasma (FRAP) assay was used to estimate the antioxidant capacity of plant extracts (Benzie and Strain, 1996). 25 µl of supernatant were mixed with equal amount of 0.3 M acetate-buffer (pH 3.6), containing 10 mM 2,4,5-Tris-(2-pyridil)-*s*-triazine (TPTZ) and 200 mM $FeCl_3$. The absorbance was measured at 600 nm in a microplate reader (Synergy H1, BioTeK). 6-hydroxy-2,5,7,8-tetramethylchroman-2-carboxylic acid (Trolox) was used for the standard curve. Data were expressed as Trolox equivalents (µM/g FW).

5.3.5.4 Polyphenol concentration

Polyphenol concentration was determined by using Folin-Ciocalteu reagent (Zhang et al., 2006). Absorbance was measured at 765 nm in a microplate reader (Synergy H1, BioTeK). Gallic acid (GA) was used for preparing standard curves. Data were expressed as GA equivalents (mg/g FW).

5.3.5.5 Flavonoid concentration

Estimation of total flavonoid content was done by mixing 20 µl of supernatant with 60 µl absolute ethanol, 10 µl 10% (w/v) aluminium chloride, 10 µl 1M potassium acetate and 120 µl distilled water. After mixing and incubating at room temperature for 30 min, absorbance was measured at 415 nm in a microplate reader (Synergy H1, BioTeK). Quercetin (QE) was used for standard curve preparation. Data was expressed as equivalents of QE (µg/g FW) according to Chang et al., (2002).

5.3.5.6 Ascorbate and glutathione concentration

Ascorbate (ASC) and glutathione (GSH) levels were determined by HPLC analysis (Potters et al., 2004). Antioxidants were separated on a reverse-phase column (100 x

4.6 mm Polaris C_{18}-A, 3 mm particle size; 40 °C) with an isocratic flow rate of 1 ml.min^{-1} of elution buffer (2 mM KCl, pH 2.5 adjusted with *O*-phophoric acid). The components were quantified using a custom-made electrochemical detector and the purity and identity of the peaks was confirmed using an in-line DAD (SPD-M10AVP, Shimadzu). ASC was measured at 242 nm and GSH at 196 nm. Chromatogram analysis was performed with the Class VP software package (ClassVP 5.0, Shimadzu). Reduced antioxidant concentration was determined after reducing with 0.04 DTT.

5.3.5.7 Enzyme extraction and enzyme activity assays

Peroxidase (POX) activity was measured by monitoring the production of purpurogallin at 430 nm (Kumar and Khan, 1982). Catalase (CAT) activity was calculated out of the decrease in H_2O_2 concentration, measured at 240 nm (Aebi, 1984). Measuring the inhibition of NBT reduction at 550 nm was used to assay superoxide dismutase (SOD) activity (Dhindsa et al., 1981). The activity of ascorbate peroxidase (APX), glutathione reductase (GR), glutathione peroxidase (GPX), monodehydroascorbate reductase (MDAR), and dehydroascorbate reductase (DHAR) were assayed according to Murshed et al., (2008). Glutaredoxin (GRx) activity was measured monitoring the reduction of GSH in the presence of NADPH (Lundberg et al., 2001). Thioredoxin (TRx) activity was indirectly measured as the ability of reduce the NADP-malate dehydrogenase, which activity was measured as the capacity of reducing NADPH, previously TRx was reduced with dithiothreitol (Wolosiuk et al., 1979). All determinations were scaled to do them with 25 µl of supernatant and to be measured in a microplate reader (Synergy H1, BioTek).

5.3.5.8 Soluble protein content

Soluble protein was determined according to Lowry method (Lowry et al., 1951) with a microplate reader (Synergy H1, BioTek).

5.3.6 Determination of free polyamines

Rice free polyamines of seedlings from the hydroponic cultures were determined according to Rodríguez et al., (2009) with modifications. To extract free polyamines, six shoots of plants subjected to six days of treatment were frozen in liquid N_2 and homogenized. The homogenate (50 mg) was resuspended in 150 µL of PCA 5% (v/v), incubated in ice for 30 min and centrifuged at 15000 g (15 min). The pellet was discarded and the supernatant was kept at -20 °C. For dansylation, 60 µL of supernatant were added to 6 µL of 0.1 mM heptanodiamine (internal standard, ICN Biomedicals, Costa Mesa, CA) plus 60 µL saturated Na_2CO_3 and 75 µL dansyl chloride-

acetone 1% (w/v). After 90 min at 70 °C in the dark, 20 µL of proline 10% (w/v) was added to stop the reaction. Dansyl-derived polyamines were extracted with 200 µL toluene. The organic phase (175 µL) was evaporated under vacuum and resuspended in 40 µL acetonitrile. Dansyl-derived polyamines were separated by HPLC (HPLC, Waters 1525 Binary HPLC Pump, Milford, MA, USA) with a reverse phase column Sephasil C18 (Amersham Pharmacia) and detected with a spectrofluorometer (Waters 2475, Multi λ Fluorescence Detector). The solvent mix was obtained with a flow of 1.5 mL min^{-1} as follows: 0-4.5 min, acetonitrile:H_2O 70:30 v/v; 4.5-9 min, acetonitrile 100; 9-15 min, acetonitrile:H_2O 70:30 v/v. Peak areas were integrated, normalized to heptanodiamine and interpolated into a polyamine standards calibration curve.

5.3.7 Statistical analysis

Data was analyzed with InfoStat statistical software package (Di Rienzo et al., 2016).

5.4 RESULTS AND DISCUSSION

5.4.1 The tolerant cultivar can maintain a healthy photosynthetic apparatus

A possible damage of the photosynthetic apparatus caused by ST stress could have led to a decoupling and inactivation of the oxygen evolving complex (OEC). This was evidenced with the downregulation of transcripts at the short term in the whole shoot (chapter 3) and the downregulation of proteins at the elongation zone of the fourth leaf (chapter 4) that constitute part of the OEC in IR50. The OEC is in charge of the oxidation of water to molecular O_2 in PSII and it is the main energy transforming structure of the chloroplast (Shutilova, 2010). Decoupling of OEC can be identified by the presence of positive slope of K band through a non-invasive OJIP test (Chen et al., 2014; Gururani et al., 2015). A JIP test at short exposure to ST (24 h) determined that only IR50 presented a K band with increased slope (Figure 5-1 A). Chen et al., (2014), also indicated that the decoupling of OEC is accompanied by a reduction of reaction centers of PSII able to reduce Q_B. This fraction of reaction centers, also the most active fraction in water oxidation by OEC, is denominated Q_B reducing centers (Mamedov et al., 2000). The OJIP test also indicated that Q_B reducing centers decreased only in IR50 under ST respect to the control condition (Figure 5-1 B).

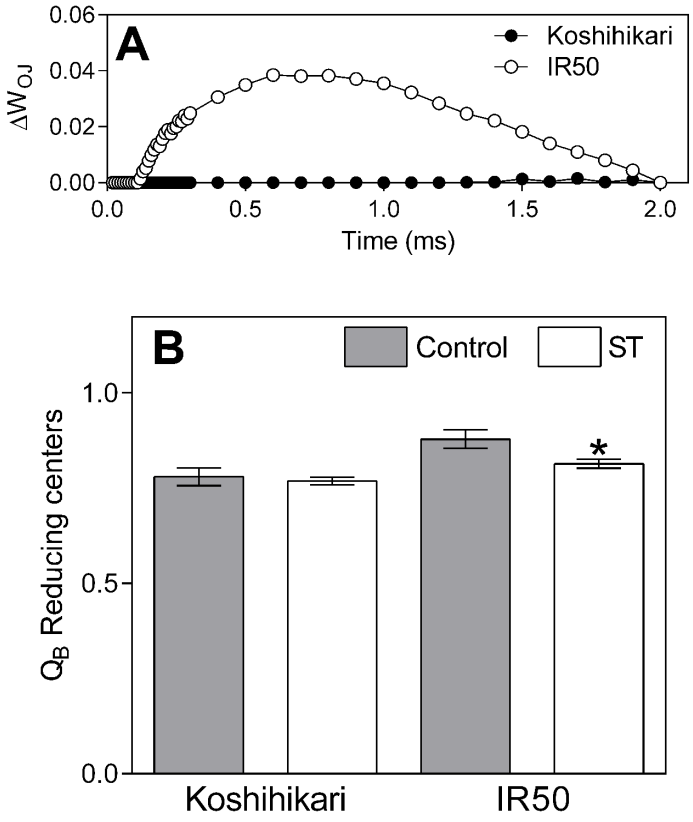

Figure 5-1. Determination of decoupling of oxygen evolving complex and quinone B reducing centers. Seedlings were grown under optimal and ST conditions during 24 h. Decoupling of OEC and Q_B reducing centers were determined by non invasive OJIP test. **A)** Decoupling of OEC was detected by the presence of positive slope of K band determined as the difference kinetics ΔW_{OJ}. **B)** Q_B reducing centers was calculated 10 seconds in darkness posterior Step P by a second pulse of red light during 1 s. Asterisks represent significant differences between treatments (T test; $P < 0.05$; $n = 9$).

5.4.2 Consequences on the ultrastructure of mesophyll cells

Fully expanded leaves from Koshihikari and IR50 treated for 10 or 24 d under OT or ST conditions were sliced and ultrathin sections obtained, 5 h after the photoperiod had started. Cells from the mesophyll of the apical part of the leaf were observed under TEM in order to describe ultrastructural changes in response to long exposures to ST at the seedling stage. Under optimal temperatures at 10 d, micrographs of both cultivars revealed healthy cells with many regular, oval or elongated mitochondrias and dense layer of chloroplasts along the cell wall (Figures 5-2 A and 5-3 A). Chloroplasts were well developed, showed no starch granules, grana thylakoids were highly stacked, and small plastoglobules were visible between thylakoids (Figures 5-2 B and 5-3 B). After 24 d under OT treatment both cultivars showed normal cells, similar to the ones found at 10 d, with the difference that small starch grains appeared in the chloroplasts (Figures 5-2 C and D, and Figures 5-3 C and D). Cells of seedlings from Koshihikari grown for 10 d under ST stress (Figure 5-2 E) were also healthy with organelles like mitochondrias and peroxisomes closed to the chloroplasts located around the cell wall. Contrasting with the OT condition at 10 d, chloroplasts showed some small starch granules and grana had usually less thylakoid disks, but the

presence of plastoglobules was similar to that in OT (Figure 5-2 F). The sensitive cultivar IR50 showed healthy cells at 10 d under ST stress (Figure 5-3 E) and the chloroplasts had highly stacked grana. Unlike cells in OT and Koshihikari, lots of big starch granules were found in the chloroplasts (Figure 5-3 E and F). At 24 d under ST, Koshihikari cells contained densely packed organelles and the presence of middle size starch grains, grana with small number of thylakoid disks and dark stroma (Figures 5-2 G and H), whereas IR50 cells also showed densely packed organelles but its chloroplasts had many and big starch grains and grana with many thylakoid disks and dark stroma (Figures 5-3 G and H).

Species that are adapted to chilling stress usually show densely packed organelles and plastoglobule clusters, as Koshihikari under ST, so metabolic interactions between organelles can happen and energy expenditure in long distance transport in the cell is avoided (Lütz, 2010; Gielwanowska et al., 2014; Giełwanowska et al., 2015). The presence of more grana with lower number of thylakoids and the decrease of large grana was also described in a wheat chilling tolerant variety (Venzhik et al., 2013). This could be a strategy to avoid damage since grana thylakoids are more sensitive than stroma thylakoids and, hence, are the first to undergo disintegration potentiated by ROS that are produced in cells under stress (Holá et al., 2008). Besides, Koshihikari chloroplasts had more densely stacked grana in response to ST probably contributing to its higher photosynthetic capacity, since it is well established that PSII is exclusively localized in the compressed regions of the grana (Armond and Arntzen, 1977; Daum et al., 2010).

Plants must achieve a balance between carbon assimilation, carbon storage and growth. The ultrathin slides showed that in the long term both cultivars accumulate starch but IR50 showed more and bigger starch grains. Species that are sensitive to cold stress usually accumulate starch granules while the ones that can tolerate this stress reduce their size and ultimately eliminates them after prolonged exposure, probably because of an efficient transport and hydrolysis of photosynthetic products (Ma et al., 1990; Mostowska, 1999; Peng et al., 2015). Besides, rice subjected to chilling during 24 h also accumulated many big starch grains while a phytochrome-B deficient mutant tolerant to chilling stress did not accumulate them and its PSII performed better under the stress (Yang et al., 2013). The availability of starch in the leaves is essential for the plant growth since it provides carbon source during the night when the plant cannot photosynthesize but still needs to keep growing (Smith and Stitt, 2007). A study done on maize leaves revealed that lines that could maintain high

growth rates (LER) during longer period of times (T_{LE}) had a modified balance between carbon supply and growth compared with other lines since they correlated with genes involved in starch biosynthesis (Baute et al., 2015; Baute et al., 2016). Moreover, T_{LE} was the main the parameter that could distinguish between tolerant and sensitive rice cultivars in the determination of the final length of the fourth leaf (chapter 2). Therefore, the greater LER and T_{LE} of Koshihikari compared to IR50 could be associated to a better management of the carbohydrates being used during the day for growth and the synthesis of starch to provide carbon supply for the subsequent night.

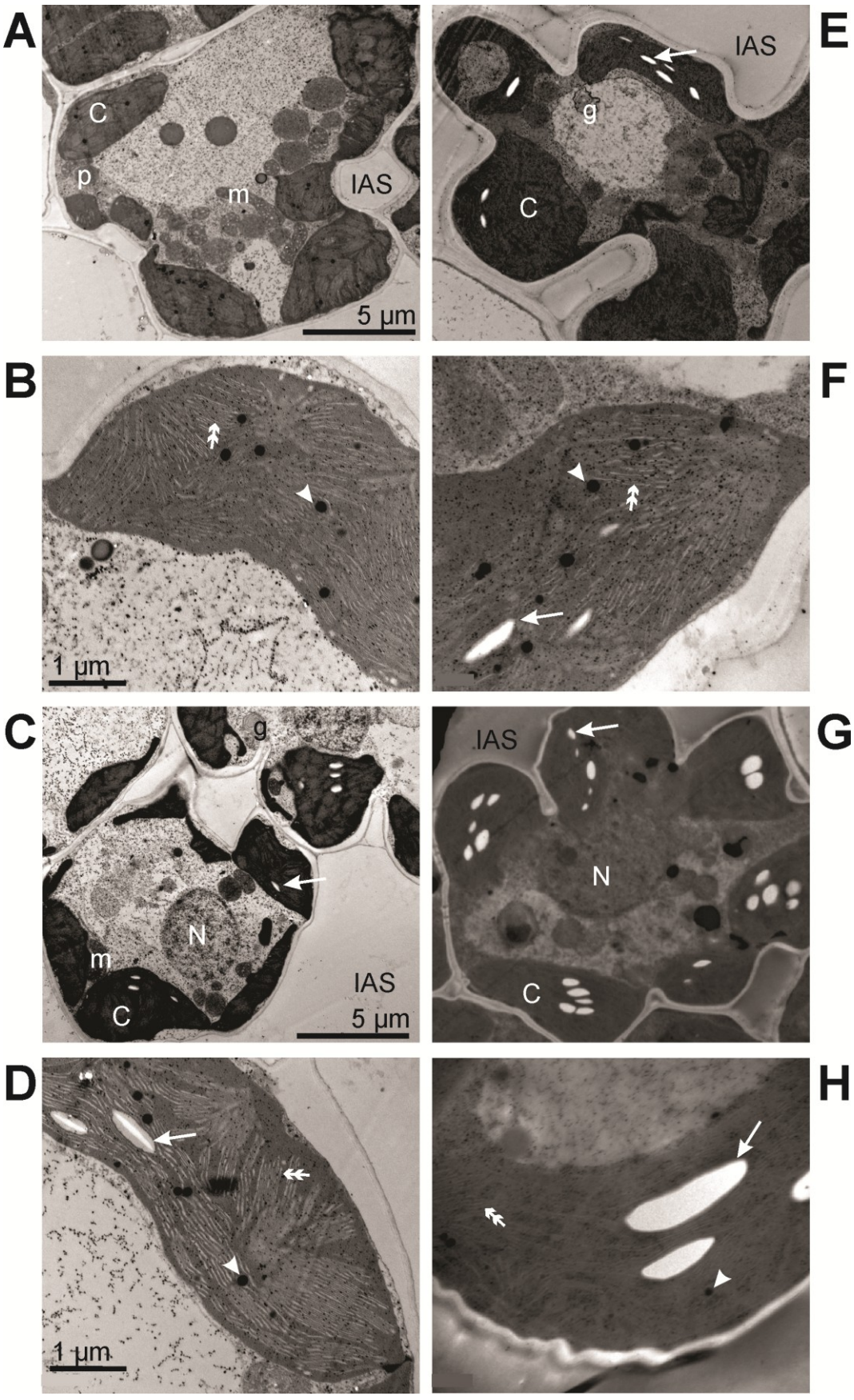
A
C
p
m
IAS
5 µm
E
IAS
g
C
B
1 µm
F
C
g
N
m
C
IAS
5 µm
G
IAS
N
C
D
1 µm
H

Figure 5-2. Transmission electron micrographs of transverse sections from a fully expanded leaf of Koshihikari subjected to optimal temperatures (A, B, C, and D) or suboptimal temperatures (E, F, G, and H) during 10 d (A, B, E, and F) or 24 d (C, D, G, and H). Scale bar of pictures on the left (A, B, C, and D) correspond also to its respective neighbors on the right (E, F, G, and H). Plastoglobules are indicated by arrowheads, starch granules by arrows, and grana thylakoids by double arrowheads. Chloroplasts (C), mitochondria (m), peroxisomes (p), nucleus (N) and Golgi apparatus (g) are located on the interior of the cells. Intercellular air space (IAS) is also marked.

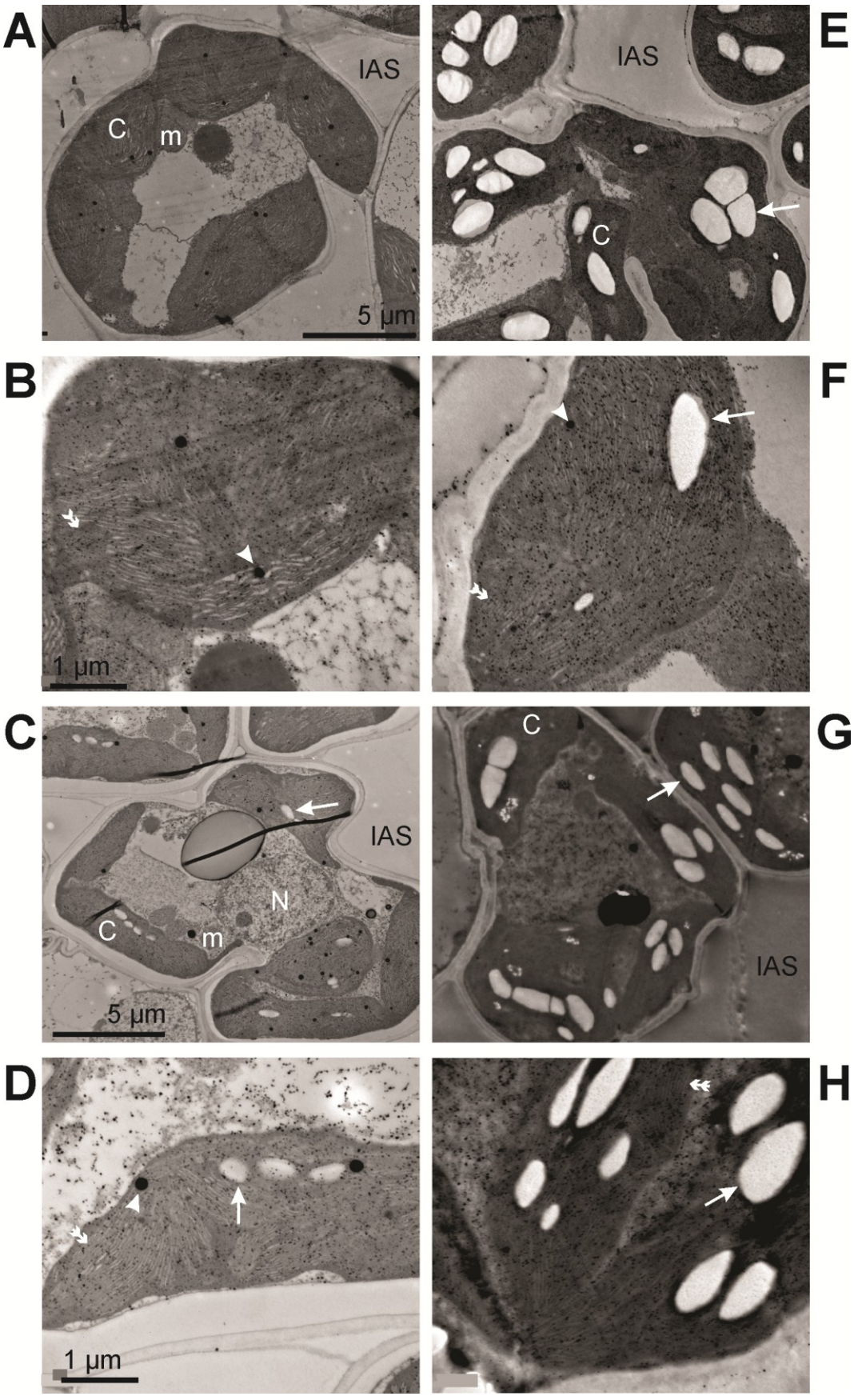
A
IAS
C
m
5 µm
E
IAS
C
B
1 µm
F
C
IAS
N
C
m
5 µm
G
C
IAS
D
1 µm
H

Figure 5-3. Transmission electron micrographs of transverse sections from a fully expanded leaf of IR50 subjected to optimal temperatures (A, B, C, and D) or suboptimal temperatures (E, F, G, and H) during 10 d (A, B, E, and F) or 24 d (C, D, G, and H). Scale bar of pictures on the left (A, B, C, and D) correspond also to its respective neighbors on the right (E, F, G, and H). Plastoglobules are indicated by arrowheads, starch granules by arrows, and grana thylakoids by double arrowheads. Chloroplasts (C), mitochondria (m), peroxisomes (p), nucleus (N) and Golgi apparatus (g) are located on the interior of the cells. Intercellular air space (IAS) is also marked.

5.4.3 The effect of suboptimal temperatures stress on lipid composition

The lipid composition of the cultivars was analyzed after 6 d under OT and ST conditions. The analysis revealed that only total saturated fatty acids diminished in the sensitive cultivar under ST respect to the control (Table 5-1) but no change was observed regarding total unsaturated fatty acids. However, Koshihikari showed no changes in saturated or unsaturated fatty acids. These results disagree partially with Pereira da Cruz et al. (2010), who reported no cold (10°C) -induced changes in the proportion of saturated fatty acids for the tolerant rice cultivar, although there was an increase of this proportion for the sensitive one. Besides, many authors reported that cold tolerance in rice is related to an increase in unsaturated fatty acids (Majumder et al., 1989; Bertin et al., 1998; Maeda et al., 1999). Moreover, a positive relationship between the unsaturated fatty acid composition of the chloroplast membrane and the photosynthetic tolerance to chilling was reported (Peoples et al., 1978; Ariizumi et al., 2002; Zhu et al., 2007).

Table 5-1. Total saturated and unsaturated fatty acid contents. Seedlings were grown under OT and ST conditions during 6 days. The fatty acids contents were calculated from the lipidomic analysis data. Numbers are expressed in µg per g of fresh weight. Asterisks represent significant differences between treatments (t-test; $P < 0.05$; $n = 5$).

	OT	ST
	Saturated fatty acids	
Koshihikari	128 ± 32	149 ± 14
IR50	151 ± 10	**131 ± 15 ***
	Unsaturated fatty acids	
Koshihikari	372 ± 74	422 ± 32
IR50	417 ± 24	397 ± 25

However, changes in some particular fatty acids were found (Figure 5-4). Although total unsaturated fatty acids did not change in Koshihikari, one particular unsaturated fatty acid, oleic acid (18:1), increased 30% in response to ST (Figure 5-4 A). Rice thylakoid membranes are rich in oleic acid (Jing et al., 2006) so its increment could be contributing to conserve its capacity of photosynthesis through the maintenance of membrane fluidity at long term. This result therefore agrees with the analysis done in Chapter 1, where a higher PSII performance in Koshihikari plants grown under ST during 24 d was reported, in contrast with IR50.

On the other hand, IR50 reduced eicosatrienoic acid (20:3), detected in trace amounts (0.02% of total fatty acids), and palmitic acid (16:0; Figure 5-4 B). Palmitic acid has been reported as the major saturated fatty acid and one of the most abundant fatty acids in rice (Bertin et al., 1998; Ariizumi et al., 2002; Cheah et al., 2013). The reduction of palmitic acid (Figure 5-4 B) in IR50 could be related with the upregulation of DEGs from fatty acid degradation within β-oxidation and alkane oxidation pathways (Chapter 3). Furthermore, through the peroxisomal β-oxidation pathway extra energy can be obtained for maintaining cellular homeostasis as it was described for starch-depleted Arabidopsis under extended darkness (Kunz et al., 2009). Besides, palmitic is one of the main fatty acids of thylakoid membranes along with oleic, stearic, linoleic and linolenic acids (Jing et al., 2006; Ping et al., 2006) so the degradation of palmitic acid may have a negative effect on thylakoid membrane stability at long term.

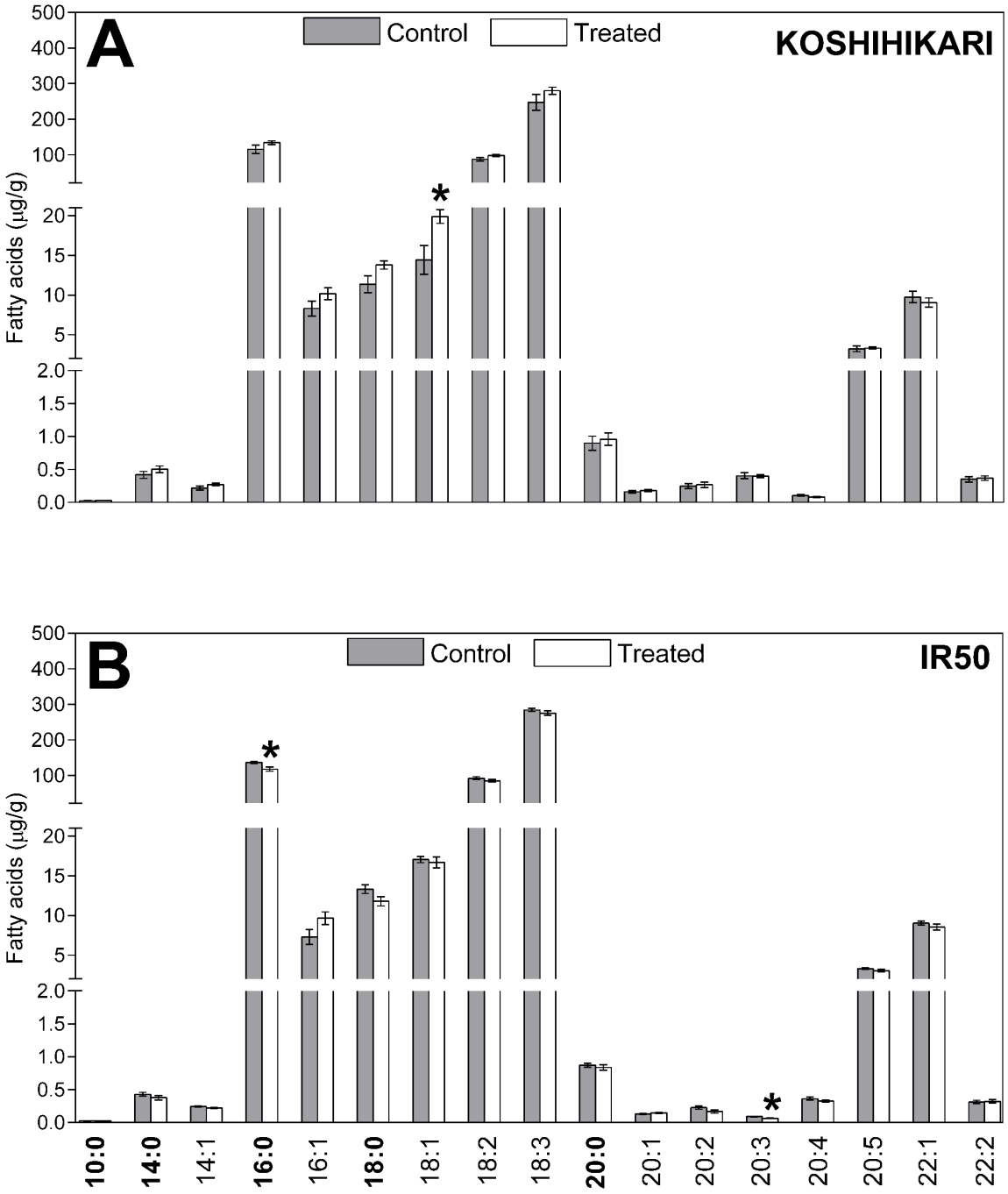

Figure 5-4. Lipidomic analysis. Seedlings were grown under optimal and ST conditions during 6 d. Fatty acids composition in Koshihikari (**A**) and IR50 (**B**) was determined by GC/MS in shoots. Asterisks represent significant differences between treatments (T test; $P < 0.05$; $n = 5$).

5.4.4 The redox system

A consequence of the aerobic metabolism is the production of reactive oxygen species (ROS; Sharma et al., 2012). In chapter 4, the proteomic analysis showed that Koshihikari and IR50 modified the abundance of some proteins related to the redox response. Koshihikari showed incremented thioredoxin and peroxiredoxins in the elongation zone and a peroxiredoxin in the meristem, while IR50 only incremented a thioredoxin in both zones (Table 4-2). Besides, both cultivars downregulated cytosolic ascorbate peroxidases (APXs) in both zones. Overall, a differentiated response of the cultivars and the zones in the redox system response to ST was evidenced and hence it was here studied. For this analysis the growth zone of the fourth leaf was harvested during its steady state growth and samples from the meristem, elongation zone, mature zone, and the transitions zones between them were taken. Different metabolites and enzymes activities related to the redox system were quantified and a three-way ANOVA with the factors *cultivar*, *treatment* and *zone* was done testing also all the interactions of these factors. A *post-hoc* Duncan test was done when a positive interaction was found. All details of the statistic analysis are omitted in the figures because of the extensivity of the analysis and can be found in Supplementary Table 13.

Hydrogen peroxide represents a well-established indicator of the oxidative stress of the cells generated by the photosystem and other primary processes accuring in the cell (Shulaev and Oliver, 2006). Hydrogen peroxide was measured in each zone of the fourth leaf to see if ST increased the level of ROS and if this was localized in particular zones of the cultivars (Figure 5-5 A). No difference was found between the cultivars when H_2O_2 was measured in OT conditions and small differences appeared between the zones. When subjected to ST stress concentrations of this metabolite increased in all zones, with the exception of the mature zone (MaZ). Besides, big differences were found between the cultivars in the meristem (M) and the transition zone between the meristem and the elongation zone (M-EZ) being much higher in the sensitive cultivar than in the tolerant one. If production and removal of ROS is not strictly controlled oxidative damaged can occur and important biomolecules can be affected (Sharma et al., 2012). Lipid peroxidation was here measured by the detection of a secondary metabolite, malondialdehyde (MDA), generally accepted as a good marker of oxidative stress (Shulaev and Oliver, 2006). MDA did not show big differences between the cultivars and the zones in the OT conditions but its level was incremented in response to the stress in both cultivars although IR50 showed higher levels in the transition between the elongation zone and the mature zone (EZ-MaZ) than Koshihikari (Figure

5-5 B). Overall, oxidative stress and, in consequence, oxidative damage was present in response to ST in both cultivars and it showed to be localized in the different zones of the leaf with higher impact in the sensitive cultivar than in the tolerant one. Although ROS is needed for cell division (Livanos et al., 2012) and expansion (Schmidt et al., 2016) to trigger signaling pathways, its imbalance can cause cell damaged, as here described. In the meristem, this damage caused by ROS has been associated with interferences with the nuclear envelope dynamics, disorganization of tubulin cytoskeleton, and avoidance of chromosome movements (Livanos et al., 2012). This is in line with the downregulation of proteins related with DNA binding, chromatin structure and histones (chapter 4) and the fact that leaf elongation rate was highly reduced as a consequence of a lower cell production rate (chapter 2). The difference between H_2O_2 and MDA could be associated with fact that MDA (damage) is relatively permanent and cells from the basal part of the leaf move to more distal regions carrying the damage incurred in the high H_2O_2 basal regions with them.

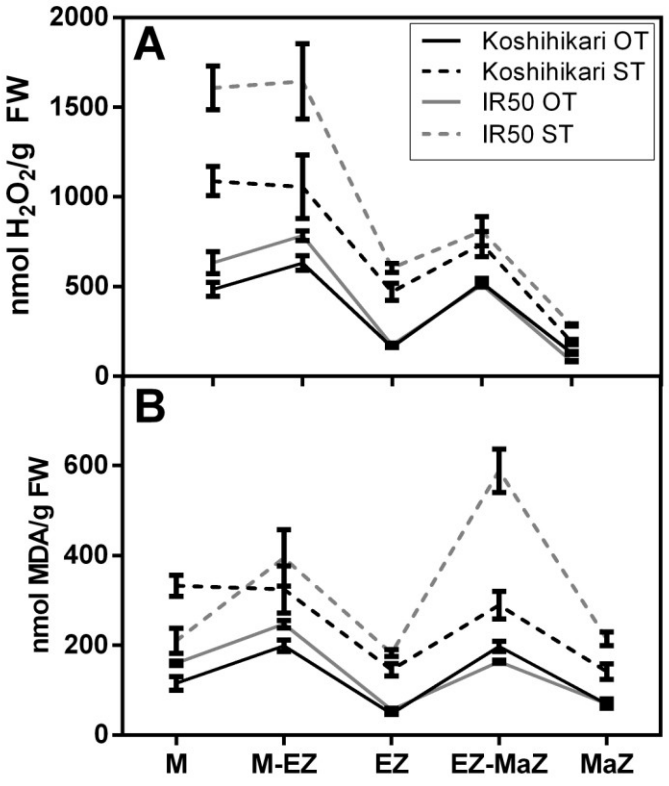

Figure 5-5. Measurement of oxidative stress indicators along the growth zone of two contrasted rice cultivars in OT and ST conditions. Metabolite concentrations were determined in each part of the growth zone of the fourth leaf: M, mersitem; M-EZ, transition zone between the meristem and the elongation zone; EZ, elongation zone; EZ-MaZ, transition zone between EZ and the mature zone; MaZ, mature zone. Legend on figure A corresponds also to figure B. **A)** hydrogen peroxide (H_2O_2) contents. **B)** Malondialdehyde (MDA) contents. Data are averages ± SE (n=3).

ROS levels need to be controlled by the plants so efficient antioxidant strategies are usually triggered including both non-enzymatic and enzymatic systems (Sharma et al., 2012). For measuring the total non-enzymatic antioxidant power, the ferric reducing

ability of plasma (FRAP; Benzie and Strain, 1996) was quantified in each zone (Figure 5-6 A). In control conditions, no differences were found between cultivars or zones, but an increment in the transition EZ-MaZ appeared in response to the stress in both cultivars, this increment was higher in the tolerant cultivar that also rose in EZ and MaZ. Among non-enzymatic scavenging systems, polyphenols were described as powerful antioxidants that represent the major class of plant antioxidant molecules (Sharma et al., 2012) so they were here measured (Figure 5-6 B). The amount of total polyphenols decreased along the growth zone from M to MaZ in both cultivars with no differences between them. When subjected to the stress, polyphenols increased in Koshihikari compared to the OT condition showing similar amounts across the growth zone while IR50 only did it in EZ. Flavonoids, a particular class of polyphenols known to participate in controlling ROS stress (Di Ferdinando et al., 2012), showed same patterns between cultivars under OT condition with lower amounts in EZ and MaZ (Figure 5-6 C). In response to ST, flavonoids were increased in the M-EZ and EZ in Koshihikari and in EZ and EZ-MaZ in IR50 showing similar profiles between the cultivars. Overall, flavonoids and polyphenols played a role from the EZ till the MaZ in both cultivars but they did not explain completely the differences found between cultivars in the FRAP assay (Figure 5-6 A). The transcriptome analyses already displayed the upregulation of many DEGs related with flavonoids in response to the stress, although this was at the whole shoot and at short exposures (chapter 3). The presence of secondary metabolites antioxidants in the part of the leaf where cells are differentiating or already mature agrees with an analysis that showed that proteins related with secondary metabolism were increased towards the mature part of the maize leaf (Majeran et al., 2010). Besides, differentiating and mature cells are capable of produce secondary metabolites but not cells from the meristem that are meant to focus only on division.

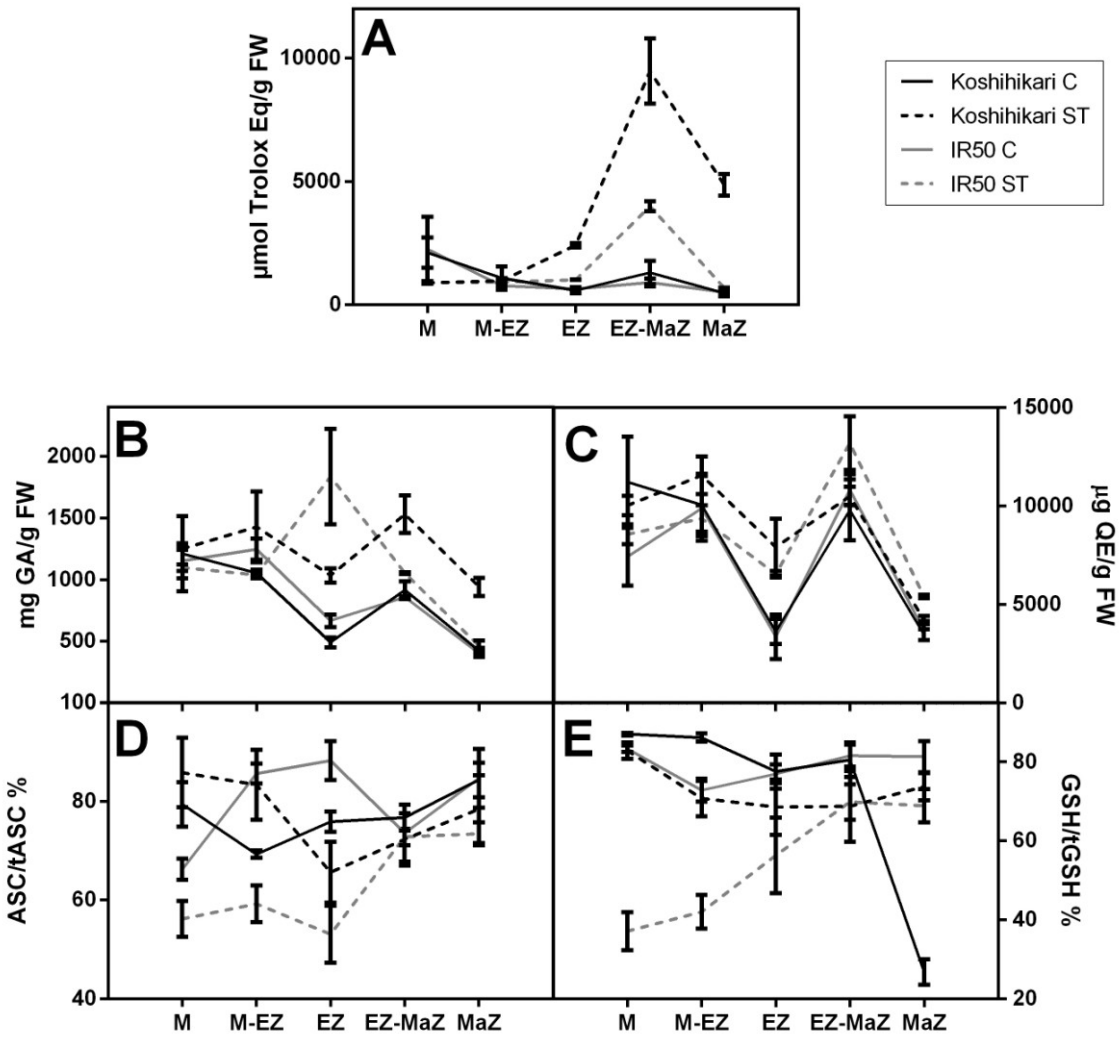

Figure 5-6. Measurement of non-enzymatic antioxidants along the growth zone of two contrasted rice cultivars in OT and ST conditions. Metabolite concentrations were determined in each part of the growth zone of the fourth leaf: M, mersitem; M-EZ, transition zone between the meristem and the elongation zone; EZ, elongation zone; EZ-MaZ, transition zone between EZ and the mature zone; MaZ, mature zone. Legend for all graphs is on the right up corner. **A)** Ferric Reducing Ability of Plasma (FRAP). **B)** Polyphenols contents as equivalents of galic acid (GA). **C)** Flavonoids contents as equivalents of quercetin (QE). **D)** Reduced ascorbate (ASC) and total ascorbate (tASC) relation. **E)** Reduced glutathione (GSH) and total glutathione (tGSH) relation. Data are averages ± SE (n=3).

Ascorbate (ASC) and glutathione (GSH) are low molecular weight antioxidants that play a key role in the scavenging of ROS. When levels are sufficiently high, the balance between its reduced forms, ASC and GSH, and the oxidized forms, monodehydroascrobate (MDHA) and dehydroascorbate (DHA) for ASC and glutathione disulfide (GSSC) for GSH, are central in maintaining cellular redox state (Sharma et al.,

2012). Here the relationships between ASC and GSH contents before (ASC, GSH) and after reduction (tASC, tGSH) were quantified (Figures 5-6 D and E). In OT conditions the cultivars did not show big differences between them or the zones regardless the MaZ of Koshihikari that showed lower GSH/tGSH% than the rest and IR50 showed a bit higher percentages of ASC/tASC near EZ. When subjected to ST conditions big differences between the cultivars appeared, while Koshihikari did not show big responses besides the increment of GSH/tGSH% in MaZ, IR50 diminished the percentages of ASC/tASC and GSH/tGSH from the M to EZ, with the lowest values of percentages in the meristem. While ASC stimulates cell division by mediating the transition to the S-phase, its oxidized forms blocks the cell cycle (Potters et al., 2002). Although GSH was also linked to cell division, its contribution was not that clear. Overall, the response of ASC and GSH and its oxidized partners in the meristem of IR50 could be linked to a greater effect of ST on the cell production that ultimately reduced the final leaf length while Koshihikari was less affected (chapter 2).

Besides the non-enzymatic antioxidant metabolites, the redox status of the leaf depends on the activity of the redox-regulating enzymes such as superoxide dismutase (SOD), catalase (CAT), glutathione peroxidase (GPX), ascorbate peroxidase (APX), peroxidases (POX), monodehydroascorbate reductase (MDHAR), dehydroascorbate reductase (DHAR), glutathione reductase (GR), glutaredoxins (GRx), and thioredoxins (TRx) that were here studied (Sharma et al., 2012; Kaushik and Roychoudhury, 2014). SOD catalyzes the dismutation of superoxide ($O_2^{\cdot -}$) to oxygen (O_2) and hydrogen peroxide (H_2O_2) and it constitutes the first line of defense against ROS (Gill and Tuteja, 2010; Sharma et al., 2012). In OT conditions SOD showed low activity in all zones in both cultivars (Figure 5-7 A). When subjected to ST the sensitive cultivar did not respond and Koshihikari showed high activity of SOD in the M and the transition M-EZ. CAT is indispensable for ROS detoxification under stress conditions since it has a fast turnover (Gill and Tuteja, 2010; Sharma et al., 2012). This enzyme showed a similar pattern than the one found for SOD with no difference between zones or cultivars in the OT condition but with high activity in the M and the transition M-EZ in Koshihikari in response to ST (Figure 5-7 B). GPX, a group of enzymes that use GSH to reduce hydrogen peroxide and other peroxides (Gill and Tuteja, 2010), also depicted the same pattern as SOD and CAT (Figure 5-7 C). POX constitute a large family of enzymes that usually has as an optimal substrate hydrogen peroxide and so they are usually related to ROS scavenging (Smith and Veitch, 1998; Sharma et al., 2012). POX activity was similar in all zones and in both cultivars when they were under OT conditions (Figure 5-7 D). When subjected to ST conditions, POX activity was found increased in M and

M-EZ in both cultivars although Koshihikari showed higher levels of activity besides also increasing the activity in the MaZ.

The ratios of ASC/tASC and GSH/tGSH described above are regulated by the cycle ASC-GSH that also detoxifies hydrogen peroxide and so it is crucial for the redox homeostasis (Gill and Tuteja, 2010; Sharma et al., 2012). This cycle can be described by the activities of APX, MDHAR, DHAR and GR that were here measured (Figure 5-7 E, F, G, and H). APX showed the same profile of activity than SOD, CAT and GPX (Figure 5-7). Although the proteomic analysis showed one cytosolic APX downregulated in both M and EZ, its activity was actually upregulated in response to the stress in the M of Koshihikari. No differences were found in the activity of MDHAR regarding zones or cultivars under OT conditions, while ST stress highly incremented its activity in the intersection M-EZ and it also increased in the MaZ of Koshihikari (Figure 5-7 F). DHAR displayed the same profile for Koshihikari as MDHAR in both conditions, while IR50 showed an increment in its activity from the M to the MaZ in OT conditions and also in ST with no difference between the treatments in each zone (Figure 5-7 G). GR showed differences in activity in OT conditions in the transition EZ-MaZ of Koshihikari but in general no big differences were found between zones or cultivars in this condition (Figure 5-7 H). In response to the stress, only Koshihikari incremented GR activity in the zones M-EZ and MaZ while IR50 slightly incremented it in MaZ.

Peroxiredoxins, thioredoxins (TRx), and glutaredoxins (GRx) also play an important role as scavengers of hydrogen peroxide as an alternative to the water-water cycle where ASC and GSH are involved (Dietz et al., 2006; Miyake, 2010; Dietz, 2016). The activity of GRx and TRx were here measured, no big differences were found in their activities between zones or cultivars under OT conditions although GRx was slightly increased in the MaZ of IR50 in both conditions (Figures 5-7 I and J). Under ST stress, GRx activity was found increased in the transition M-EZ and the MaZ in Koshihikari with higher level in the MaZ than in the others, while IR50 showed no response regarding this enzyme (Figure 5-7 I). TRx activity was highly increased in the M-EZ of Koshihikari in response to the stress and no modification was found in IR50 (Figure 5-7 J).

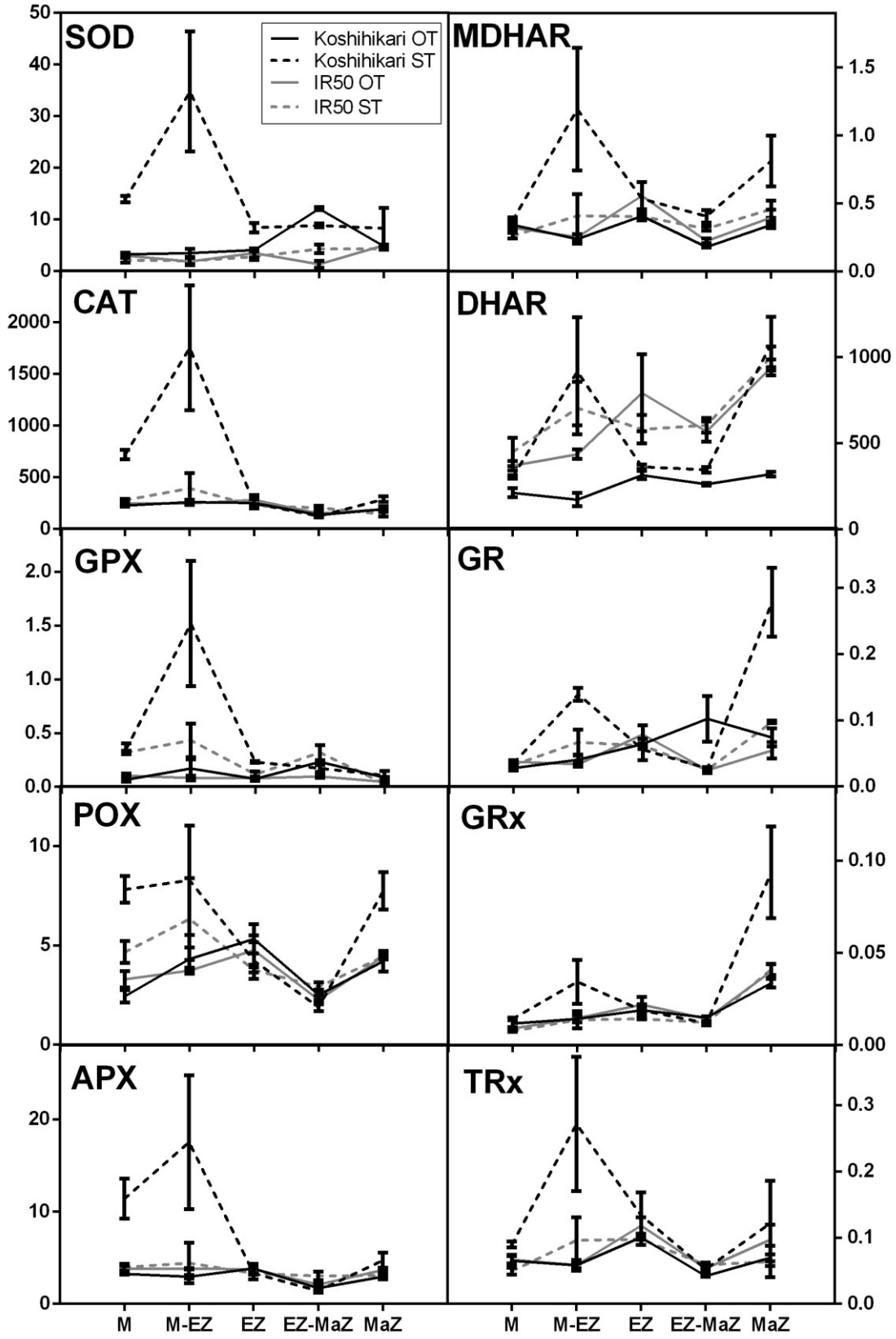

Figure 5-7. Measurement of enzymatic antioxidants along the growth zone of two contrasted rice cultivars in OT and ST conditions. Enzyme activities were determined in each

part of the growth zone of the fourth leaf: M, mersitem; M-EZ, transition zone between the meristem and the elongation zone; EZ, elongation zone; EZ-MaZ, transition zone between EZ and the mature zone; MaZ, mature zone. Measurements are units of enzymes UE.mg $prot^{-1}.min^{-1}$. The measured enzyme is named in each panel: superoxide dismutase (SOD), catalase (CAT), glutathione peroxidase (GPX), peroxidases (POX), ascorbate peroxidase (APX), monodehydroascorbate reductase (MDHAR), dehydroascorbate reductase (DHAR), glutaredoxins (GRx), thioredoxins (TRx). Legend in the figure of SOD panel is the same for the rest of the panels. Data are averages ± SE (n=3).

5.4.5 Polyamines

Polyamines were measured at the whole shoot level on Koshihikari and IR50 seedlings subjected to OT and ST conditions during 6 days. The analysis indicated that IR50 increased 90% the total free polyamines content under ST in comparison with the control treatment after 6 d (Figure 5-8). This increment was attributed principally to putrescine (+190%) and spermidine (+80%). However, the spermine level decreased 30%. In the case of Koshihikari, the spermidine level was increased 47% under ST with respect to the control. Whereas some authors have related chilling or freezing tolerance to high levels of putrescine (Nadeau et al., 1987; Lee et al., 1997; Cuevas et al., 2008), others have associated it with high levels of spermine (Bodapati et al., 2005) or spermidine (Kasukabe et al., 2004). Furthermore, it has been suggested that polyamines function in stress tolerance play a major role in the ROS homeostasis by inhibiting the auto-oxidation of metals and by modifying the antioxidant system (Liu et al., 2015). If this was the case, then the increase of polyamines in IR50 would be part of the response against ROS accumulation while Koshihikari did not suffer as much as IR50 the redox damaged, as described above. Besides, several studies showed that tolerant abiotic stresses genotypes usually accumulated more spermidine and spermine while sensitive ones from the same species accumulated putrescine (Liu et al., 2015). This led to the hypothesis that since spermidine and spermine contain additional amino groups, they would be more efficient in executing protective functions.

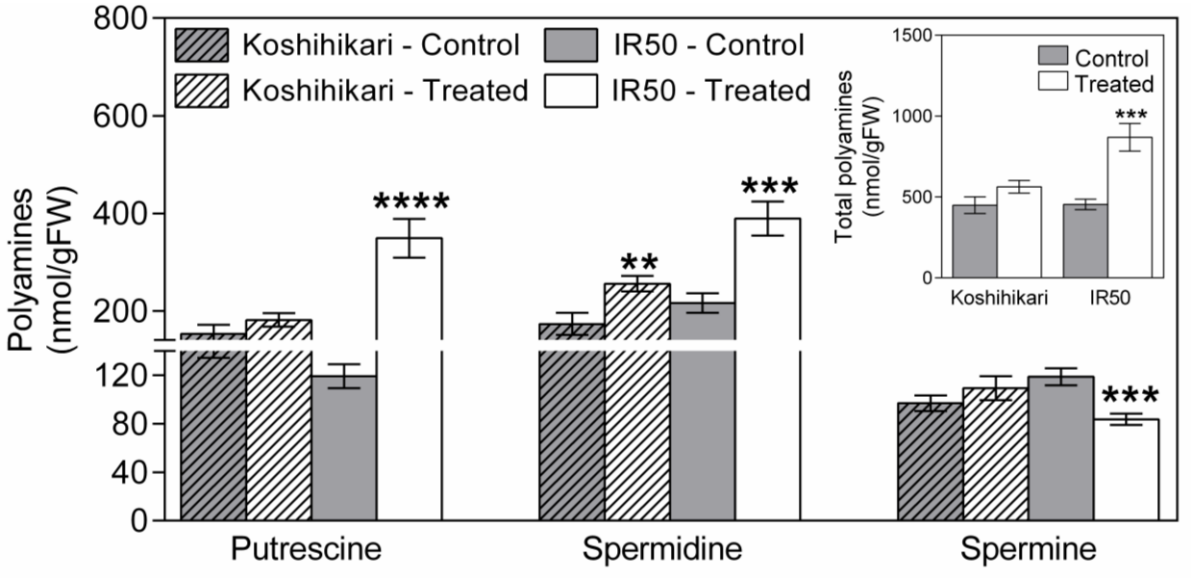

Figure 5-8. Determination of free polyamines content. Seedlings were grown under optimal and ST conditions during 6 days. Free polyamines composition was determined by HPLC in shoots. Inset shows total polyamines. Asterisks represent significant differences between treatments (T test; $P < 0.05$; $n = 5$).

5.5 CONCLUSIONS

In this chapter some hypothesis made in previous chapters were further investigated. The balance of carbohydrates showed to be differentially regulated by Koshihikari and IR50 at the short term, as the transcriptome analysis indicated. At the short term Koshihikari increased starch level at expenses of free sugars. However, at long ST exposures the ultrastructural images showed that Koshihikari apparently maintained the starch with time while IR50 increased its granules in high amount having a negative effect on leaf growth rate as described above. The main effect of ST stress seemed to be on the photosynthetic apparatus since even at short ST exposures the sensitive cultivar already showed effects the OEC that at long exposures lead to a worst PSII performance. On the contrary, Koshihikari was able to maintain the energy equilibrium by sustaining PSII efficiency. The ability of Koshihikari to protect its photosynthetic apparatus could be due to more compact grana thylakoids and densely packed organelles besides the maintenance of the thylakodis membranes fluidity by the increase of oleic acid.

As seen in the proteome analysis, different balance of the redox state in the zones of the leaf was described in each cultivar. Although oxidative damage was present in both cultivars, the sensitive one presented much higher levels when subjected to ST stress with different level of damage according to the growth zone. When antioxidants

systems were analyzed, Koshihikari responded more strongly than IR50 in all aspects. The non-enzymatic antioxidant power was highly incremented in the tolerant cultivar especially from EZ-MaZ transition till MaZ according to the FRAP assay, being partly attributed to polyphenols. The enzymatic system was mainly activated in the zones nearby the meristem, where SOD, CAT, GPX, POX and the ASC-GSH cycle showed higher levels in Koshihikari under ST stress. GRx and TRx were increase in the transition M-EZ and in the MaZ of Koshihikari in response to the stress. In general, the data indicated that enzymatic antioxidant power was upregulated to protect the zone nearby the meristem, particularly the transition M-EZ, while non-enzymatic antioxidant power was upregulated in the mature part of the leaf.

Finally, polyamines showed to be differently regulated by the cultivars in response to the stress. The total amount of polyamines was increase only in the sensitive cultivar suggesting a protective role against the oxidative damage triggered by ST. Besides, the transcriptome analysis showed upregulation of DEGs related with the biosynthesis of flavonoids and other antioxidants at the short term and in fact the amount of polyphenols and flavonoids increased under ST conditions along the growth zone of the fourth leaf. This was in line with the increase of polyamines, particularly in IR50. Moreover, the tolerant cultivar increased the level of spermidine, a polyamine with more amino groups than putrescine that has been related with protective functions.

GENERAL CONCLUSIONS

In order to test the hypothesis *"there is a differential response to suboptimal temperatures among seedlings from different rice cultivars (Oryza sativa* L.*)"* the effects of suboptimal temperatures (ST) stress at the seedling stage at different levels on contrasting rice cultivars were for first time studied. Here, the main characteristics of the response were described and some conclusions about possible tolerance mechanisms could be made.

Effects of suboptimal temperatures on rice seedlings

The effect of ST typical of rice cultures from the south-central area of Entre Ríos, Argentina, were studied on rice seedlings. It is noteworthy that the assays done in growth chambers under conditions that were in our control were highly comparable with the effects seen in the field, pointing out that the lab system was able to predict what happened in the field and works as a model system of the stress.

The first visible characteristic of ST stress at the whole plant response was the inhibition of shoot growth, described in chapter 1, and particularly in the leaf growth, described in chapters 1 and 2. Even at the first days of stress retardation of leaf growth could be detected since leaves three and four reduced their growth rate about 70 -80%, and the effect on the whole plant at the long term could be correlated at with results from the field. At the leaf level, the reduction of 41% of the fourth leaf final length was attributed to a strong reduction in the leaf growth rate of about 76% partly compensated by the time the leaf was elongation. Since such a high compensation by the time of elongation was only described in other kind of cold stresses and not in other abiotic stresses, we can suggest that this is a particular characteristic of the cold stresses. Kinematic analysis of the leaf growth showed that this effect on the leaf elongation rate was due to a strong inhibition of cell production rate caused by a strong inhibition of the cell division rate rather than a reduction in the expansion of the cells, although the final cell length was reduced 25%.

The proteome and redox analyses done across the growth zone of the fourth leaf showed some characteristics of each zone that could be related with the processes ongoing there. In the meristem, proteins related with DNA, chromatin structure and histones were downregulated as a consequence of the reduced cell division, suggesting that a major response at the transcriptome level was being triggered. Moreover, H_2O_2 increased across the growth zone in response to ST showing the higher levels in the meristem zone. The presence of ROS caused damage since MDA also increased, agreeing with the repression of cell division in the meristem. Hence, the

enzymatic antioxidants were upregulated around the meristem in order to protect this zone and allow cell division.

Other physiological processes also contributed to the diminution of shoot growth in response to the stress. For instance, the PSII was affected after long periods of ST (10-24 d), as the results from the JIP-test suggested. This test showed that F_V/F_M and RC/ABS, two parameters related to the performance of PSII, diminished their values, while the dissipation of energy evidenced by DI_0/RC increased in response to the stress showing a detriment of the photosynthetic system. This was associated with reductions in the amount of active chlorophyll that works as reaction centers. The transcriptional analysis at short term exposures (24 h) in the whole shoot showed that changes in the genes response were ongoing. The detriment of PSII was evidenced at this level too, since many genes related with the photosystem structure were downregulated. Particularly, genes related with the complex in charge of oxidizing water molecules, the OEC, were affected. The damage of the photosynthetic apparatus was also evidenced when rice seedlings grown under OT condition were subjected to a range of low temperatures and showed, as a consequence, a decrease in Pn and Gs.

The balance between carbon source and storage is tightly managed in the plant to assure growth. The transcriptome analysis showed that DEGs from the carbohydrate metabolism were regulated after 24 h of stress, suggesting that carbohydrate sensing and signaling mechanisms were already triggered to further modulate plant growth. Rice seedlings induced enzymes from the starch degradation. However, the analyzed transversal slides of the leaf done at longer times of exposure showed that starch began to accumulate in big granules during the day. It could be suggested that problems in the transport and hydrolysis of photosynthetic products could exist that do not permit the plant to use the stored carbohydrates to grow during the night. However, it could also be a response of the plant that tried to accumulate starch to store carbon so it can grow when the stress is over.

Secondary metabolism also plays an important role in a stress response since they usually participate in the plant defense system (Ramakrishna and Ravishankar, 2011). The transcriptome analysis at short term showed an upregulation of DEGs related with secondary metabolites biosynthesis like flavonoids. When the fourth leaf was studied, flavonoids and polyphenols measurements increased near the mature part of the leaf being part of the redox response.

Tolerant vs. sensitive cultivars

Although rice is a sensitive species to cold temperatures, a wide range of variability between the germoplasm accessions could be found. Our analysis of 18 cultivars revealed a great variation in the ST induced growth inhibition. Two groups with different response could be detected at short term exposures to ST and used to further describe the differences between them based in the growth of the third leaf. Among the most tolerant group were Koshihikari and Bombilla, two japonica cultivars, while in the more sensitive group were IR50 and IR24, described as from the indica subspecies. Though, our results suggest that japonica cultivars probably performed better than indica cultivars under ST at the seedling stage, as it was also described under chilling stress. The screening method here designed has its advantages for ST screening at the seedling stage over other methods usually used in the literature, *e.g.*, Standard Evaluation System. First, because it was specially design for testing ST stress using temperatures that are commonly measured in the field. Second, because it is a quick method, easy to schedule in a growth chamber where many cultivars can be fit at once, saving time and space. Finally, it is a quantitative method that does not depend on the observer. Overall, this screening method can be used to rapidly detect possible tolerant cultivars that afterward could be tested in the field or with other screening methods, *e.g.*, marker assisted breeding.

The inhibition of the seedling growth differed among cultivars, as discussed above. In order to analyze which processes at the cell level were differentially affected between cultivars, the growth of the fourth leaf was studied. Although the differences in reduction of the elongation rate of the leaf were not that big between tolerant and sensitive cultivars (5% difference), the compensation by duration of its elongation was greatly distinct between them so at the end final leaf length was reduced by half in the sensitive cultivars and only a third in tolerant ones. The higher increase of duration of elongation in response to ST in the tolerant cultivars could be associated with the better performance of the PSII and also a better balance between carbon assimilation and usage. Under the thermal time theory, the sensitive cultivars appeared to have higher base temperatures than the tolerant ones and, hence, different behavior in a range of temperatures could be supposed. However, the differences in leaf elongation rate were further related with differences in the inhibition of the cell production, strictly linked to cell division processes. Besides, this is in line with what the transcriptome analysis at 24 h showed, since jasmonic acid biosynthesis pathway was upregulated in the sensitive cultivar and it was described in other studies to inhibit cell division.

Moreover, H_2O_2 increased in the meristem and the transition to elongation zone of the sensitive cultivar more than in the tolerant one causing damage evidenced by MDA measurements. Instead, the tolerant cultivar triggered the enzymatic antioxidants system in the meristem and increased its non-enzymatic antioxidants (flavonoids and polyphenols among others) from the elongation till the mature zones protecting these zones from ROS. The strong inhibition of cell production in the sensitive cultivar was also in line with the higher amount of the oxides forms of ASC and GSH in the meristem, related with the blocking of the cell cycle.

The response of the tolerant and sensitive cultivars was highly distinct regarding other physiological processes as well. Our results showed that at long exposures (10 and 24 d) big differences in PSII performance could be detected. Tolerant cultivars were able to maintain an acceptable F_V/F_M while dissipating some energy. On the contrary, sensitive cultivars showed low F_V/F_M probably caused by the inactivation of many reaction centers and the high dissipation of energy. The different detriment of the photosynthetic apparatus between cultivars was also evidenced in the ultrastructure of the cells. The tolerant cultivar denoted less grana thylakoids and more densely stacked grana than the sensitive one in response to ST, probably contributing to its higher photosynthetic performance here described. Our results suggested that the effects on the photosynthetic apparatus began early in the stress since the transcriptome analysis done at 24 h showed many genes downregulated related with the PSII structure and the OEC, and a post-transcriptional regulator of the Rubisco S subunit mRNA in the sensitive cultivar. However, the tolerant cultivar also showed some genes from the photosystem affected. The proteomic analysis done on the fourth leaf also supported what was described at the transcriptome level since the sensitive cultivar downregulated proteins that were part of the OEC and from the PSI in the elongation zone. Moreover, the tolerant genotype upregulated chloroplastic peroxiredoxins closely related with detoxification of photochemically produced H_2O_2 and, hence, the protection of the photosynthetic apparatus. This was evidenced with the double-hit JIP test performed in a tolerant and a sensitive cultivar that demonstrated that only the sensitive one decoupled its OEC and affected the fraction of reaction centers with the ability to reduce Q_B after only 24 h of treatment.

The differences between the cultivars were also evidenced when they were subjected to a range of decreasing temperatures. All cultivars diminished Gs and Pn in response to this treatment but tolerant ones had much lower Gs values over the whole range. Although this could be explain in regard to intrinsic differences such as

differences in the stomatal density and stomata aperture, the difference between the cultivars was increased when lowering the temperature. This suggested that other mechanisms were triggered that allowed tolerant cultivars to respond faster than the sensitive ones. In line with this, the downregulation of a particular thioredoxin protein detected in the fourth leaf growth zone of the tolerant cultivar would allow ROS signaling to trigger stomata closure in response to ST and in that way lower the Gs. It is possible that tolerant cultivars that had a higher ability to reduce Gs in response to low temperatures, were able to improved water balance, as WUE_i proved, and in consequence were able to sustain plant growth.

The balance between carbon assimilation and its utilization is crucial in order to maintain a sustainable plant growth. In this regard, rice showed an upregulation of transcripts of enzymes from the starch degradation pathway at short exposures to ST. However, the sensitive cultivar also depicted upregulation of transcripts related with the degradation of disaccharides probably to be used as an energy source. The tolerant cultivar downregulated a α-galactosidase tightly related with raffinose and galactinol increase, metabolites which accumulation was described to confer low temperatures tolerance in rice and other species. These metabolites confer tolerance apparently due to its roles as osmoprotectants, stabilizers of cell membranes, and scavengers of ROS. However, the ultrastructural analysis at long exposures to ST (10 and 24 d) showed that the sensitive cultivar accumulated starch in big granules while the tolerant one did it but in less proportion. This could be indicating a better management of carbohydrates usage and accumulation by the tolerant cultivar that, in turned, could be related with its higher growth rates and the ability to maintain them for longer periods as described above.

Some differences regarding membranes lipid composition in response to ST were detected between contrasting cultivars. At the transcriptome level, both cultivars upregulated desaturases suggesting that unsaturated fatty acid should increase in response to ST. Besides, IR50 showed an upregulation of the β-oxidation of fatty acids. The lipidomic analysis done after 6 d of exposure to the stress showed that this did not translate in higher unsaturated fatty acids content or in a diminish of total fatty acids in IR50. On the contrary, saturated fatty acids were diminished in the sensitive cultivar. However, the increase of oleic acid in Koshihikari was probably associated with the better photosynthesis performance. On the other hand, IR50 reduced the major fatty acid in rice and one of the mains in thylakoids membranes, palmitic acid, so could be partly explaining the effect on the photosystem.

Secondary metabolism also showed differences between the contrasting cultivars. At the transcriptional level IR50 upregulated genes related with polyamine biosynthesis that agreed with polyamine measurements done at longer time of exposures (6 d). Particularly, it almost doubled the content of putrescine in response to the stress, typical from sensitive genotypes. This cultivar also reduced the spermine levels. However, Koshihikari only increased the level of spermidine that could be related with its higher tolerance since its additional amino groups would be more efficient in protective functions. In general, the response of IR50 regarding polyamines could be linked to its necessity to counteract the ROS generated by the stress that could not be dismissed by other means as seen in the redox analysis on the fourth leaf growth zone.

Therefore, an enhanced tolerance to ST stress could be related with the capacity of maintaining high photosynthetic efficiency and to regulate carbon assimilation, storage and usage. Besides, the induction of several antioxidant systems against ROS across the growth zone protected cell process necessary to the growth of the leaf, especially in the meristem were cell division occurs. Hence, the plant is able to maintain sufficient rates of several metabolic processes, particularly those associated with energy metabolism, and so cell production is not as inhibited as in other cultivars. The maintenance of the photosynthetic apparatus is crucial for the plant to counteract the stress, since acclimation processes needs energy to synthesize metabolites and enzymes from the antioxidant system that help to avoid damage.

Final conclusions and future perspectives

It has been suggested that tolerance against an abiotic stress can only be achieved after pyramiding several characteristics in a single genotype (Mittler, 2006). Hence, acquiring information about the effects of the stress being studied is important to describe those strategies that would be related with tolerance. ST stress was for first time here described in detail and some possible tolerance mechanism could be distinguished. However, many points remained to be further analyzed to unravel the mechanism. Some of the described strategies can be measured with simple techniques, *e.g.*, LER, F_V/F_M, double-hit JIP analysis. Luckily, many open access information about thousands of rice cultivars and its seeds are freely available now (Crowell et al., 2016; McCouch et al., 2016). A genome-wide association study could be done with the named parameters and the genotyping information of the cultivars in order to detect allelic variants that are related with tolerance. New marker assisted breeding programs could be created that help to create new genotypes with high yield characteristics and ST seedling tolerance.

REFERENCES

Achard P, Gusti A, Cheminant S, Alioua M, Dhondt S, Coppens F, Beemster GTS, Genschik P (2009) Gibberellin Signaling Controls Cell Proliferation Rate in Arabidopsis. Curr Biol **19**: 1188–1193

Aebi H (1984) Catalase in vitro. Methods Enzymol **105**: 121–126

Agati G, Mazzinghi P, Fusi F, Ambrosini I (1995) The F685/F730 chlorophyll fluorescence ratio as a tool in plant physiology: response to physiological and environmental factors. J Plant Physiol **145**: 228–238

Aghaee A, Moradi F, Zare-Maivan H, Zarinkamar F, Irandoost HP, Sharifi P (2011) Physiological responses of two rice (Oryza sativa L.) genotypes to chilling stress at seedling stage. African J Biotechnol **10**: 7617–7621

Allen DJ, Ort DR (2001) Impacts of chilling temperatures on photosynthesis in warm-climate plants. Trends Plant Sci **6**: 36–42

Andaya VC, Mackill DJ (2003) Mapping of QTLs associated with cold tolerance during the vegetative stage in rice. J Exp Bot **54**: 2579–2585

Andriankaja M, Dhondt S, DeBodt S, Vanhaeren H, Coppens F, DeMilde L, Mühlenbock P, Skirycz A, Gonzalez N, Beemster GTS, et al (2012) Exit from Proliferation during Leaf Development in Arabidopsis thaliana: A Not-So-Gradual Process. Dev Cell **22**: 64–78

Arguissain G (2006) Ecofisiología del cultivo de arroz. El Arroz su Cultiv. y sustentabilidad en Entre Ríos.

Ariizumi T, Kishitani S, Inatsugi R, Nishida I, Murata N, Toriyama K (2002) An increase in unsaturation of fatty acids in phosphatidylglycerol from leaves improves the rates of photosynthesis and growth at low temperatures in transgenic rice seedlings. Plant Cell Physiol **43**: 751–8

Armond PA, Arntzen CJ (1977) Localization and characterization of photosystem II in grana and stroma lamella. Plant Physiol **59**: 398–404

Aroca R, Porcel R, Ruiz-Lozano JM (2011) Regulation of root water uptake under abiotic stress conditions. J Exp Bot **63**: 43–57

Aroca R, Vernieri P, Irigoyen JJ, Sánchez-Díaz M, Tognoni F, Pardossi A (2003) Involvement of abscisic acid in leaf and root of maize (Zea mays L.) in avoiding chilling-induced water stress. Plant Sci **165**: 671–679

Asensi-Fabado MA, Amtmann A, Perrella G (2017) Plant responses to abiotic

stress: The chromatin context of transcriptional regulation. Biochim Biophys Acta **1860**: 106–122

Ashikari M, Matsuoka M, Yano M (2007) Application of functional genomics tools for crop improvement. *In* NM Upadhyaya, ed, Rice Funct. Genomics challenges, Prog. Prospect. Springer, New York, United States of America, pp 411–423

Avramova V (2016) An integrated approach to unravel the growth response of maize leaves to drought. Universiteit Antwerpen

Avramova V, AbdElgawad H, Zhang Z, Fotschki B, Casadevall R, Vergauwen L, Knapen D, Taleisnik E, Guisez Y, Asard H, et al (2015) Drought Induces Distinct Growth Response, Protection, and Recovery Mechanisms in the Maize Leaf Growth Zone. Plant Physiol **169**: 1382–96

Bajguz A, Hayat S (2009) Effects of brassinosteroids on the plant responses to environmental stresses. Plant Physiol Biochem **47**: 1–8

Balmer Y, Koller A, del Val G, Manieri W, Schürmann P, Buchanan BB (2003) Proteomics gives insight into the regulatory function of chloroplast thioredoxins. Proc Natl Acad Sci U S A **100**: 370–375

Balzarini M, Di Rienzo J (2012) InfoGen v.2012. http://www.info-gen.com.ar,

Banerjee A, Roychoudhury A (2015) WRKY Proteins: Signaling and Regulation of Expression during Abiotic Stress Responses. Sci World J 17

Barkla BJ, Vera-Estrella R, Pantoja O (2013) Progress and challenges for abiotic stress proteomics of crop plants. Proteomics **13**: 1801–1815

Barrôco RM, Peres A, Droual A-M, De Veylder L, Nguyen LSL, De Wolf J, Mironov V, Peerbolte R, Beemster GT, Inzé D, et al (2006) The Cyclin-Dependent Kinase Inhibitor Orysa;KRP1 Plays an Important Role in Seed Development of Rice 1. Plant Physiol **142**: 1053–1064

Baskin TI (2000) On the constancy of cell division rate in the root meristem. Plant Mol Biol **43**: 545–554

Basu S, Roychoudhury A (2014) Expression Profiling of Abiotic Stress-Inducible Genes in response to Multiple Stresses in Rice (Oryza sativa L.) varieties with contrasting level of stress tolerance. Biomed Res Int 12

Basuchaudhuri P (2014) Cold Tolerance in Rice Cultivation. CRC Press, New York, United States of America

Baute J, Herman D, Coppens F, De Block J, Slabbinck B, Dell'Acqua M, Pè ME, Maere S, Nelissen H, Inzé D (2015) Correlation analysis of the transcriptome of growing leaves with mature leaf parameters in a maize RIL population. Genome Biol **16**: 168

Baute J, Herman D, Coppens F, De Block J, Slabbinck B, Dell'Aqcua M, Pè ME, Maere S, Nelissen H, Inzé D (2016) Combined large-scale phenotyping and transcriptomics in maize reveals a robust growth regulatory network. Plant Physiol **170**: pp.01883.2015

Beemster GTS, Baskin TI (1998) Analysis of Cell Division and Elongation Underlying the Developmental Acceleration of Root Growth in Arabidopsis thaliana. Plant Physiol **116**: 1515–1526

Beemster GTS, Fiorani F, Inzé D (2003) Cell cycle: the key to plant growth control? Trends Plant Sci **8**: 154–158

Beemster GTS, Masle J (1996) Effects of soil resistance to root penetration on leaf expansion in wheat (Triticum aestivum L): kinematic analysis of leaf elongation. J Exp Bot **47**: 1651–1662

Beemster GTS, Masle J, Williamson RE, Farquhar GD (1996) Effects of soil resistance to root penetration on leaf expansion in wheat (Triticum aestivum L): kinematic analysis of leaf elongation. J Exp Bot **47**: 1651–1662

Bellincampi D, Dipierro N, Salvi G, Cervone F, De Lorenzo G (2000) Extracellular H(2)O(2) induced by oligogalacturonides is not involved in the inhibition of the auxin-regulated rolB gene expression in tobacco leaf explants. Plant Physiol **122**: 1379–1385

Benavidez R (2006) Análisis de conjunto para el diagnóstico del sistema arrocero. El Arroz su Cultiv. y sustentabilidad en Entre Ríos.

Benzie IF, Strain JJ (1996) The ferric reducing ability of plasma (FRAP) as a measure of "antioxidant power": the FRAP assay. Anal Biochem **239**: 70–6

Berberich T, Sagor G, Kusano T (2015) Polyamines in plant stress response. *In* T Kusano, H Suzuki, eds, Polyamines. Springer, Japan, pp 155–168

Bertin P, Bullens P, Bouharmont J, Kinet J (1998) Somaclonal variation and chilling tolerance improvement in rice : changes in fatty acid composition. 31–41

Bertin P, Kinet J, Bouharmont J (1996) Evaluation of chilling sensitivity in different rice varieties. Relationship between screening procedures applied during germination and vegetative growth. Euphytica **89**: 201–210

Bilsborough GD, Runions A, Barkoulas M, Jenkins HW, Hasson A, Galinha C (2011) Model for the regulation of Arabidopsis thaliana leaf margin development. PNAS **108**: 3424–3429

Bizet F, Hummel I, Bogeat-Triboulot M-B (2014) Length and activity of the root apical meristem revealed in vivo by infrared imaging. J Exp Bot 1–9

Bligh EG, Dyer WJW, Blygh E, Dyer WJW (1959) A rapid method of total lipid extraction and purification. Can J Biochem Physiol **37**: 911–917

Bloom AJ, Zwieniecki MA, Passioura JB, Randall LB, Holbrook NM, St. Clair DA (2004) Water relations under root chilling in a sensitive and tolerant tomato species. Plant, Cell Environ **27**: 971–979

Bodapati N, Gunawardena T, Fukai S (2005) Increasing cold tolerance in rice by selecting for high polyamine and gibberellic acid content. RIRDC, Autralian Government

Bolhàr-Nordenkampf HR, Long SP, Baker NR, Oquist G, Schreiber U, Lechner EG (1989) Chlorophyll fluorescence as a probe of the photosynthetic competence of leaves in the field: A review of current instrumentation. Funct Ecol **3**: 497–514

Bonhomme R (2000) Bases and limits to using "degree day" units. Eur J Agron **13**: 1–10

Bonifacio A, Martins MO, Ribeiro CW, Fontenele A V., Carvalho FEL, Margis-Pinheiro M, Silveira JAG (2011) Role of peroxidases in the compensation of cytosolic ascorbate peroxidase knockdown in rice plants under abiotic stress. Plant, Cell Environ **34**: 1705–1722

Bonnecarrère V, Borsani O, Díaz P, Capdevielle F, Blanco P, Monza J (2011) Response to photoxidative stress induced by cold in japonica rice is genotype dependent. Plant Sci Shannon Irel **180**: 726–732

Bos HJ, Tijani-Eniola H, Struik PC (2000) Morphological analysis of leaf growth of maize: responses to temperature and light intensity. NJAS - Wageningen J Life Sci **48**: 181–198

Brizuela A (2006) Síntesis climática de Entre Ríos, descripción y efectos. El Arroz su Cultiv. y sustentabilidad en Entre Ríos.

Brouns SJJ, Smits N, Wu H, Ambrosius PL, Wright PC, Vos WM De, Van J, Snijders APL, Oost J Van Der (2006) Identification of a Novel α - Galactosidase from the Hyperthermophilic Archaeon Sulfolobus solfataricus Identification of a Novel alpha -Galactosidase from the Hyperthermophilic Archaeon Sulfolobus solfataricus †. J Bacteriol **188**: 2392–2399

Brunoud G, Wells DM, Oliva M, Larrieu A, Mirabet V, Burrow AH, Beeckman T, Kepinski S, Traas J, Bennett MJ, et al (2012) A novel sensor to map auxin response and distribution at high spatio-temporal resolution. Nature **482**: 103–6

Bultynck L, Fiorani F, Van Volkenburgh E, Lambers H (2003) Epidermal cell division and cell elongation in two Aegilops species with contrasting leaf

elongation rates. Funct Plant Biol **30**: 425–432

Calzadilla PI, Gazquez A, Maiale SJ, Ruiz OA, Bernardina MA (2014) Polyamines as Indicators and Modulators in the Abiotic Stress in Plants. Plant Adapt. to Environ. Chang. significance Amin. acids their Deriv. pp 109–128

Camacho C, Coulouris G, Avagyan V, Ma N, Papadopoulos J, Bealer K, Madden TL (2009) BLAST plus: architecture and applications. BMC Bioinformatics **10**: 1

Carvalho FEL, Ribeiro CW, Martins MO, Bonifacio A, Staats CC, Andrade CMB, Cerqueira J V., Margis-Pinheiro M, Silveira JAG (2014) Cytosolic APX knockdown rice plants sustain photosynthesis by regulation of protein expression related to photochemistry, Calvin cycle and photorespiration. Physiol Plant **150**: 632–645

Chaikam V, Karlson D (2008) Functional characterization of two cold shock domain proteins from Oryza sativa. Plant, Cell Environ **31**: 995–1006

Chang A, Scheer M, Grote A, Schomburg I, Schomburg D (2009) BRENDA, AMENDA and FRENDA the enzyme information system: New content and tools in 2009. Nucleic Acids Res **37**: 588–592

Chang C-C, Yang M-H, Wen H-M, Chern J-C (2002) Estimation of Total Flavonoid Content in Propolis by Two Complementary Colorimetric Methods. J Food Drug Anal **10**: 178–182

Cheah TW, Ismail I, Sidek NM, Wagiran A, Abdullah R (2013) Biosynthesis of very long polyunsaturated Omega-3 and Omega-6 fatty acids in transgenic Japonica rice (Oryza sativa L). **7**: 1227–1234

Chen J, Tian L, Xu H, Tian D, Luo Y, Ren C, Yang L, Shi J (2012) Cold-induced changes of protein and phosphoprotein expression patterns from rice roots as revealed by multiplex proteomic analysis. Plant Omics **5**: 194–199

Chen S, Strasser RJ, Qiang S (2014) In vivo assessment of effect of phytotoxin tenuazonic acid on PSII reaction centers. Plant Physiol Biochem **84**: 10–21

Chen W, Xu Z, Zhang L, Yang S (1990) Comparative Studies on Stomatal Density and Its Relations to Gas Diffusion Resistance and Net Photosynthetic Rate in Rice Leaf. Chinese J Rice Sci **4**: 163–168

Cheng C (2006) Semi-global Analysis of the Early Cold Stress Response Transcriptome of Developing Seedlings of Rice (Oryza sativa L., japonica). The University of Maine, Orono, ME, USA

Chou WC, Huang YW, Tsay WS, Chiang TY, Huang DD, Huang HJ (2004) Expression of genes encoding the rice translation initiation factor, eIF5A, is

involved in developmental and environmental responses. Physiol Plant **121**: 50–57

Counce PA, Siebenmorgen TJ, Ambardekar AA (2015) Rice reproductive development stage thermal time and calendar day intervals for six US rice cultivars in the Grand Prairie, Arkansas, over 4 years. Ann Appl Biol **167**: 262–276

Cox J, Mann M (2012) 1D and 2D annotation enrichment: a statistical method integrating quantitative proteomics with complementary high-throughput data. BMC Bioinformatics **13**: S12

Crowell S, Korniliev P, Falcão A, Ismail A, Gregorio G, Mezey J, McCouch S (2016) Genome-wide association and high-resolution phenotyping link Oryza sativa panicle traits to numerous trait-specific QTL clusters. Nat Commun **7**: 10527

Cuevas JC, López-Cobollo R, Alcázar R, Zarza X, Koncz C, Altabella T, Salinas J, Tiburcio AF, Ferrando A (2008) Putrescine is involved in Arabidopsis freezing tolerance and cold acclimation by regulating abscisic acid levels in response to low temperature. Plant Physiol **148**: 1094–1105

Cui S, Huang F, Wang J, Ma X, Cheng Y, Liu J (2005) A proteomic analysis of cold stress responses in rice seedlings. Proteomics **5**: 3162–3172

Czesnick H, Lenhard M (2015) Size Control in Plants — Lessons from Leaves and Flowers. Cold Spring Harb Perspect Biol 1–17

Das G, Rao GJN (2015) Molecular marker assisted gene stacking for biotic and abiotic stress resistance genes in an elite rice cultivar. Front Plant Sci **6**: 698

Daum B, Nicastro D, Austin J, McIntosh JR, Kühlbrandt W (2010) Arrangement of photosystem II and ATP synthase in chloroplast membranes of spinach and pea. Plant Cell **22**: 1299–1312

Dhindsa R, Plumbdhindsa P, Thorpe T (1981) Leaf senescence correlated with increased levels of membrane permeability and lipid peroxidation, and decreased levels of superoxide dismutase and catalase. J Exp Bot **32**: 93–101

Dietz K-J (2016) Thiol-Based Peroxidases and Ascorbate Peroxidases: Why Plants Rely on Multiple Peroxidase Systems in the Photosynthesizing Chloroplast? Mol Cells **39**: 20–5

Dietz KJ, Horling F, König J, Baier M (2002) The function of the chloroplast 2-cysteine peroxiredoxin in peroxide detoxification and its regulation. J Exp Bot **53**: 1321–1329

Dietz KJ, Jacob S, Oelze ML, Laxa M, Tognetti V, De Miranda SMN, Baier M,

Finkemeier I (2006) The function of peroxiredoxins in plant organelle redox metabolism. J Exp Bot **57**: 1697–1709

Dong MA, Farre EM, Thomashow MF (2011) CIRCADIAN CLOCK-ASSOCIATED 1 and LATE ELONGATED HYPOCOTYL regulate expression of the C-REPEAT BINDING FACTOR (CBF) pathway in Arabidopsis. Proc Natl Acad Sci **108**: 7241–7246

Donnelly PM, Bonetta D, Tsukaya H, Dengler RE, Dengler NG (1999) Cell cycling and cell enlargement in developing leaves of Arabidopsis. Dev Biol **215**: 407–19

Douce R, Bourguignon J, Neuburger M, Rébeillé F (2001) The glycine decarboxylase system: A fascinating complex. Trends Plant Sci **6**: 167–176

Du H, Liu H, Xiong L (2013) Endogenous auxin and jasmonic acid levels are differentially modulated by abiotic stresses in rice. Front Plant Sci **4**: 397

Du Z, Bramlage W (1992) Modified thiobarbituric acid assay for measuring lipid oxidation in sugar-rich plant tissue extracts. J Agric Food Chem **40**: 1566–1570

Dutt S, Parkash J, Mehra R, Sharma N, Singh B, Raigond P, Joshi A, Chopra S, Singh BP (2015) Translation initiation in plants: roles and implications beyond protein synthesis. Biol Plant **59**: 401–412

Eckardt N a (2000) Sequencing the Rice Genome. Plant Cell **12**: 2011–2017

Emanuelsson O, Brunak S, von Heijne G, Nielsen H (2007) Locating proteins in the cell using TargetP, SignalP and related tools. Nat Protoc **2**: 953–971

Ensminger I, Busch F, Huner NPA (2006) Photostasis and cold acclimation: Sensing low temperature through photosynthesis. Physiol Plant **126**: 28–44

Eremina M, Rozhon W, Poppenberger B (2016) Hormonal control of cold stress responses in plants. Cell Mol Life Sci **73**: 797–810

Facette MR, Shen Z, Björnsdóttir FR, Briggs SP, Smith LG (2013) Parallel proteomic and phosphoproteomic analyses of successive stages of maize leaf development. Plant Cell **25**: 2798–812

FAO (2016) Food and Agriculture Organization of the United Nations Statistics Division. http://faostat3.fao.org/home/E

Di Ferdinando M, Brunetti C, Fini A, Tattini M (2012) Flavonoids as Antioxidants in Plants Under Abiotic Stresses. *In* P Ahmad, M Prasad, eds, Abiotic Stress Responses Plants Metab. Product. Sustain. Springer New York, New York, USA, pp 159–179

Ferjani A, Horiguchi G, Yano S, Tsukaya H (2007) Analysis of leaf development in fugu mutants of Arabidopsis reveals three compensation modes that modulate cell expansion in determinate organs. Plant Physiol **144**: 988–99

Ferreira PCG, Hemerly IAS, Engler DA, Montagu M Van, Engler G (1994) Developmental Expression of the Arabidopsis Cyclin Gene cyclAt. Plant Cell **6**: 1763–1774

Fiorani F, Beemster GT, Bultynck L, Lambers H (2000) Can Meristematic Activity Determine Variation in Leaf Size and Elongation Rate among Four Poa Species? A Kinematic Study. Plant Physiol **124**: 854–855

Fiorani F, Beemster GTS (2006) Quantitative analyses of cell division in plants. Plant Mol Biol **60**: 963–79

Flachsbarth I, Willaarts B, Xie H, Pitois G, Mueller ND, Ringler C, Garrido A (2015) The role of Latin America's land and water resources for global food security: Environmental trade-offs of future food production pathways. PLoS One **10**: 1–24

Fracheboud Y, Haldimann P, Leipner J, Stamp P (1999) Chlorophyll fluorescence as a selection tool for cold tolerance of photosynthesis in maize (Zea mays L.). J Exp Bot **50**: 1533–1540

French AP, Wilson MH, Kenobi K, Dietrich D, Voß U, Ubeda-tomás S, Pridmore TP, Wells DM (2012) Identifying biological landmarks using a novel cell measuring image analysis tool : Cell-o-Tape. Plant Methods 8:

Fujii S, Saka H (2001) The promotive effect of brassinolide on lamina joint-cell elongation, germination and seedling growth under low-temperature stress in rice (Oryza sativa L.). Plant Prod Sci **4**: 210–214

Gammulla CG, Pascovici D, Atwell BJ, Haynes PA (2011) Differential proteomic response of rice (Oryza sativa) leaves exposed to high- and low-temperature stress. Proteomics **11**: 2839–2850

Gao D, Jln Z, Huang Y, Zhang D (1992) Rice clock model - a computer model to simulate rice development. Agric For Meteorol **60**: 1–16

Gesch RW, Heilman JL (1999) Responses of photosynthesis and phosphorylation of the light-harvesting complex of photosystem II to chilling temperature in ecologically divergent cultivars of rice. Environ Exp Bot **41**: 257–266

Ghosh N, Singh MRK (1983) IR24 selections for cold tolerance. Int Rice Res News **4**: 8

Giarrocco LE, Marassi MA, Salerno GL (2007) Assessment of the genetic diversity in Argentine rice cultivars with SSR markers. Crop Sci **47**: 853–860

Giełwanowska I, Pastorczyk M, Kellmann-Sopyła W, Górniak D, Górecki RJ (2015) Morphological and Ultrastructural Changes of Organelles in Leaf Mesophyll Cells of the Arctic and Antarctic Plants of Poaceae Family Under Cold Influence. Arctic, Antarct Alp Res **47**: 17–25

Gielwanowska I, Pastorczyk M, Lisowska M, Wegrzyn M, Górecki RJ (2014) Cold stress effects on organelle ultrastructure in polar Caryophyllaceae species. Polish Polar Res **35**: 627–646

Gill SS, Tuteja N (2010) Reactive oxygen species and antioxidant machinery in abiotic stress tolerance in crop plants. Plant Physiol Biochem **48**: 909–930

Gilmour SJ, Zarka DG, Stockinger EJ, Salazar MP, Houghton JM, Thomashow MF (1998) Low temperature regulation of the Arabidopsis CBF family of AP2 transcriptional activators as an early step in cold-induced COR gene expression. Plant J **16**: 433–442

Gonzalez N, De Bodt S, Sulpice R, Jikumaru Y, Chae E, Dhondt S, Van Daele T, De Milde L, Weigel D, Kamiya Y, et al (2010) Increased leaf size: different means to an end. Plant Physiol **153**: 1261–1279

Gonzalez N, Vanhaeren H, Inzé D (2012) Leaf size control: Complex coordination of cell division and expansion. Trends Plant Sci **17**: 332–340

González Moreno S, Perales Vela H, Salcedo Alvarez MO (2008) La fluorescencia de la clorofila a como herramienta en la investigación de efectos tóxicos en el aparato fotosintético de plantas y algas. Rev Educ Bioquímica **27**: 119–129

Goodspeed D, Chehab EW, Min-Venditti A, Braam J, Covington MF (2012) Arabidopsis synchronizes jasmonate-mediated defense with insect circadian behavior. Proc Natl Acad Sci U S A **109**: 4674–7

Goodwin RH, Stepka W (1945) Growth and differentiation in the root tip of Phleum pratense. Am J Bot **32**: 36–46

Granier C, Massonnet C, Turc O, Muller B, Chenu K, Tardieu F (2002) Individual leaf development in Arabidopsis thaliana: A stable thermal-time-based programme. Ann Bot **89**: 595–604

Granier C, Tardieu F (1998a) Is thermal time adequate for expressing the effects of temperature on sunflower leaf development? Plant, Cell Environ **21**: 695–703

Granier C, Tardieu F (1998b) Spatial and Temporal Analyses of Expansion and Cell Cycle in Sunflower Leaves. Plant Physiol **116**: 991–1001

Greaves J a (1996) Improving suboptimal temperature tolerance in maize - The

search for variation. J Exp Bot **47**: 307–323

Green P (1976) Growth and cell pattern formation on an axis: critique of concepts, terminology and modes of study. Bot Gaz **137**: 187–202

Gregorio GB, Senadhira D, Mendoza RD (1997) Screening Rice for Salinity Tolerance. IRRI **22**: 30

Grieneisen VA, Xu J, Marée AFM, Hogeweg P, Scheres B (2007) Auxin transport is sufficient to generate a maximum and gradient guiding root growth. Nature **449**: 1008–1013

GRiSP (2013) Rice Almanac, 4th ed. International Rice Research Institute, Los Baños, Philippines

Grundy J, Stoker C, Carré IA (2015) Circadian regulation of abiotic stress tolerance in plants. Front Plant Sci. doi: 10.3389/fpls.2015.00648

Guo-li W, Zhen-fei G (2005) Effects of Chilling Stress on Photosynthetic Rate and Chlorophyll Fluorescence Parameter in Seedlings of Two Rice Cultivars Differing in Cold Tolerance. Rice Sci **12**: 187–191

Guo M, Rupe MA, Wei J, Winkler C, Goncalves-Butruille M, Weers BP, Cerwick SF, Dieter JA, Duncan KE, Howard RJ, et al (2014) Maize ARGOS1 (ZAR1) transgenic alleles increase hybrid maize yield. J Exp Bot **65**: 249–260

Das Gupta M, Nath U (2015) Divergence in Patterns of Leaf Growth Polarity Is Associated with the Expression Divergence of miR396. Plant Cell **27**: 2785–2799

Gururani MA, Venkatesh J, Ganesan M, Strasser RJ, Han Y, Kim J-I, Lee H-Y, Song P-S (2015) In Vivo Assessment of Cold Tolerance through Chlorophyll-a Fluorescence in Transgenic Zoysiagrass Expressing Mutant Phytochrome A. PLoS One **10**: e0127200

Hakeem KR, Chandna R, Ahmad P, Iqbal M, Ozturk M (2012) Relevance of Proteomic Investigations in Plant Abiotic Stress Physiology. Omi A J Integr Biol **16**: 621–635

Hasan MM, Rafii MY, Ismail MR, Mahmood M, Rahim HA, Alam MA, Ashkani S, Malek MA, Latif MA (2015) Marker-assisted backcrossing: A useful method for rice improvement. Biotechnol Biotechnol Equip **29**: 237–254

Hashimoto M, Komatsu S (2007) Proteomic analysis of rice seedlings during cold stress. Proteomics **7**: 1293–1302

Hassibi P, Nabipour M, Moradi F (2011) The glucose-intermediate role in ABA signalling and its influence on several physiological characteristics of rice (Oryza sativa L.) seedlings during low temperature stress. Int J Agric **1**: 381–

389

van Heerden PDR, Tsimilli-Michael M, Kruger GHJ, Strasser RJ (2003) Dark chilling effects on soybean genotypes during vegetative development: parallel studies of CO2 assimilation, chlorophyll a fluorescence kinetics O-J-I-P and nitrogen fixation. Physiol Plant **117**: 476–491

Heidarvand L, Maali Amiri R (2010) What happens in plant molecular responses to cold stress? Acta Physiol Plant **32**: 419–431

Hisanaga T, Ferjani A, Horiguchi G, Ishikawa N, Fujikura U, Kubo M, Demura T, Fukuda H, Ishida T, Sugimoto K, et al (2013) The ATM-dependent DNA damage response acts as an upstream trigger for compensation in the fas1 mutation during Arabidopsis leaf development. Plant Physiol **162**: 831–41

Hodges DM, DeLong JM, Forney CF, Prange RK (1999) Improving the thiobarbituric acid-reactive-substances assay for estimating lipid peroxidation in plant tissues containing anthocyanin and other interfering compounds. Planta **207**: 604–611

Hofmann NR (2012) Alternative Splicing Links the Circadian Clock to Cold Tolerance. Plant Cell **24**: 2238

Holá D, Kutík J, Kočová M, Rothová O (2008) Low-temperature induced changes in the ultrastructure of maize mesophyll chloroplasts strongly depend on the chilling pattern/intensity and considerably differ among inbred and hybrid genotypes. Photosynthetica **46**: 329–338

Horiguchi G, Tsukaya H (2011) Organ Size Regulation in Plants: Insights from Compensation. Front Plant Sci **2**: 1–6

Huang S, Raman AS, Ream JE, Fujiwara H, Cerny RE, Brown SM (1998) Overexpression of 20-Oxidase Confers a Gibberellin- Overproduction Phenotype in Arabidopsis. Plant Physiol **118**: 773–781

Huang S, Shingaki-Wells RN, Taylor NL, Millar AH (2013) The rice mitochondria proteome and its response during development and to the environment. Front Plant Sci **4**: 16

Huner NPA, Öquist G, Sarhan F (1998) Energy balance and acclimation to light and cold. Trends Plant Sci **3**: 224–230

Ichihara K, Fukubayashi Y (2010) Preparation of fatty acid methyl esters for gas-liquid chromatography. J Lipid Res **51**: 635–40

Imin N, Kerim T, Rolfe BG, Weinman JJ (2004) Effect of early cold stress on the maturation of rice anthers. Proteomics **4**: 1873–1882

International Rice Genome Sequencing Project (2005) The map-based

sequence of the rice genome. Nature **436**: 793–800

Ioio R Dello, Nakamura K, Moubayidin L, Perilli S, Taniguchi M, Morita MT, Aoyama T, Costantino P, Sabatini S (2008) A Genetic Framework for the Control of Cell Division and Differentiation in the Root Meristem. Science (80-) **322**: 1380–1384

IRRI (1988) Standard Evaluation System for Rice. Los Baños, Philippines

Ishida S, Morita KI, Kishine M, Takabayashi A, Murakami R, Takeda S, Shimamoto K, Sato F, Endo T (2011) Allocation of absorbed light energy in PSII to thermal dissipations in the presence or absence of PsbS subunits of rice. Plant Cell Physiol **52**: 1822–1831

Ishiwatari Y, Fujiwara T, McFarland KC, Nemoto K, Hayashi H, Chino M, Lucas WJ (1998) Rice phloem thioredoxin h has the capacity to mediate its own cell-to-cell transport through plasmodesmata. Planta **205**: 12–22

Ishiwatari Y, Honda C, Kawashima I, Nakamura S ichi, Hirano H, Mori S, Fujiwara T, Hayashi H, Chino M (1995) Thioredoxin h is one of the major proteins in rice phloem sap. Planta **195**: 456–463

Jackson SA (2016) Rice: The First Crop Genome. Rice **9**: 1–3

Jain M, Kaur N, Garg R, Thakur JK, Tyagi AK, Khurana JP (2006) Structure and expression analysis of early auxin-responsive Aux/IAA gene family in rice (Oryza sativa). Funct Integr Genomics **6**: 47–59

Jain M, Khurana JP (2009) Transcript profiling reveals diverse roles of auxin-responsive genes during reproductive development and abiotic stress in rice. FEBS J **276**: 3148–3162

Janowiak F, Markowski A (1994) Changes in leaf water relations and injuries in maize seedlings induced by different chilling conditions. J Agron Crop Sci **172**: 19–28

Jena K, Hardy B (2012) Advances in temperate rice research. International Rice Research Institute, Los Baños, Philippines

Jena KK, Mackill DJ (2008) Molecular markers and their use in marker-assisted selection in rice. Crop Sci **48**: 1266–1276

Jeong SW, Choi SM, Lee DS, Ahn SN, Hur Y, Chow WS, Park Y-I (2002) Differential susceptibility of photosynthesis to light-chilling stress in rice (Oryza sativa l.) depends on the capacity for photochemical dissipation of light. Mol Cells **13**: 419–28

Jing W, Cheng-jun Z, Guo-xiang C, Ping W, Da-wei L (2006) Responses of Photosynthetic Functions to Low Temperature in Flag Leaves of Rice

Genotypes at the Milky Stage. Rice Sci **13**: 113–119

Kabaki N (1983) Physiological Analysis of Growth Retardation of Rice Seedlings Caused by Low Temperature. Japan Agric Res Q **17**: 161–165

Kagale S, Divi UK, Krochko JE, Keller WA, Krishna P (2007) Brassinosteroid confers tolerance in Arabidopsis thaliana and Brassica napus to a range of abiotic stresses. Planta **225**: 353–364

Kalve S, Fotschki J, Beeckman T, Vissenberg K, Beemster GTS (2014a) Three-dimensional patterns of cell division and expansion throughout the development of Arabidopsis thaliana leaves. J Exp Bot **65**: 6385–6397

Kalve S, De Vos D, Beemster GTS (2014b) Leaf development: a cellular perspective. Front Plant Sci **5**: 362

Karlson D, Nakaminami K, Toyomasu T, Imai R (2002) A cold-regulated nucleic acid-binding protein of winter wheat shares a domain with bacterial cold shock proteins. J Biol Chem **277**: 35248–35256

Kasprzewska A, Carter R, Swarup R, Bennett M, Monk N, Hobbs JK, Fleming A (2015) Auxin influx importers modulate serration along the leaf margin. Plant J **83**: 705–718

Kasukabe Y, He L, Nada K, Misawa S, Ihara I, Tachibana S (2004) Overexpression of spermidine synthase enhances tolerance to multiple environmental stresses and upregulates the expression of various stress-regulated genes in transgenic Arabidopsis thaliana. Plant Cell Physiol **4**: 712–722

Kaushik D, Roychoudhury A (2014) Reactive oxygen species (ROS) and response of antioxidants as ROS-scavengers during environmental stress in plants. Front Environ Sci **2**: 53 (1-13)

Kavanová M, Lattanzi FA, Grimoldi AA, Schnyder H (2006) Phosphorus deficiency decreases cell division and elongation in grass leaves. Plant Physiol **141**: 766–75

Kazama T, Ichihashi Y, Murata S, Tsukaya H (2010) The mechanism of cell cycle arrest front progression explained by a KLUH/CYP78A5-dependent mobile growth factor in developing leaves of arabidopsis thaliana. Plant Cell Physiol **51**: 1046–1054

Keech O, Gardeström P, Kleczkowski LA, Rouhier N (2016) The redox control of photorespiration: From biochemical and physiological aspects to biotechnological considerations. Plant, Cell Environ 1–17

Kim J-M, Sasaki T, Ueda M, Sako K, Seki M (2015) Chromatin changes in

response to drought, salinity, heat, and cold stresses in plants. Front Plant Sci **6**: 1–12

Kim KY, Park SW, Chung YS, Chung CH, Kim JI, Lee JH (2004) Molecular cloning of low-temperature-inducible ribosomal proteins from soybean. J Exp Bot **55**: 1153–1155

Kim S-I, Kim D, Tai TH (2012) Evaluation of Rice Seedling Tolerance to Constant and Intermittent Low Temperature Stress. Rice Sci **19**: 295–308

Kim S-I, Tai TH (2011) Evaluation of seedling cold tolerance in rice cultivars: a comparison of visual ratings and quantitative indicators of physiological changes. Euphytica **178**: 437–447

Kimball SL, Salisbury FB (1973) Ultrastructural changes of plants exposed to low temperatures. Bot Soc Am **60**: 1028–1033

Komatsu S, Yamada E, Furukawa K (2009) Cold stress changes the concanavalin A-positive glycosylation pattern of proteins expressed in the basal parts of rice leaf sheaths. Amino Acids **36**: 115–123

Körner C, Menendez-Riedl SP, John PCL (1989) Why are Bonsai Plants Small ? A Consideration of Cell Size. Aust J Plant Physiol **16**: 443–448

Kosová K, Vítámvás P, Prášil IT, Renaut J (2011) Plant proteome changes under abiotic stress - Contribution of proteomics studies to understanding plant stress response. J Proteomics **74**: 1301–1322

Kratsch HA, Wise RR (2000) The ultrastructure of chilling stress. Plant, Cell Environ **23**: 337–350

Kumar K, Khan P (1982) Peroxidase and polyphenol oxidase in excised Ragi (Eleusine-Coracana Cv Pr 202) leaves during senescence. Indian J Exp Biol **20**: 412–416

Kumar K, Sinha AK (2014) Genome-wide transcriptome modulation in rice transgenic lines expressing engineered mitogen activated protein kinase kinase 6. Plant Signal Behav **9**: e28502

Kunz H, Scharnewski M, Feussner K, Feussner I, Flügge U-I, Fulda M, Gierth M, Flugge UI, Fulda M, Gierth M (2009) The ABC transporter PXA1 and peroxisomal beta-oxidation are vital for metabolism in mature leaves of Arabidopsis during extended darkness. Plant Cell **21**: 2733–2749

Kurata N, Yamazaki Y (2006) Oryzabase. An integrated biological and genome information database for rice. Plant Physiol **140**: 12–17

Kwanuk L, Hunseung K (2016) Emerging Roles of RNA-Binding Proteins in Plant Growth, Development, and Stress Responses. Mol Cells **39**: 179–185

Laurance WF, Sayer J, Cassman KG (2014) Agricultural expansion and its impacts on tropical nature. Trends Ecol Evol **29**: 107–116

Lazar C, Gatto L, Ferro M, Bruley C, Burger T (2016) Accounting for the Multiple Natures of Missing Values in Label-Free Quantitative Proteomics Data Sets to Compare Imputation Strategies. J Proteome Res **15**: 1116–1125

Lee C-M, Thomashow MF (2012) Photoperiodic regulation of the C-repeat binding factor (CBF) cold acclimation pathway and freezing tolerance in Arabidopsis thaliana. Proc Natl Acad Sci U S A **109**: 15054–9

Lee DG, Ahsan N, Lee SH, Lee JJ, Bahk JD, Kang KY, Lee BH (2009) Chilling stress-induced proteomic changes in rice roots. J Plant Physiol **166**: 1–11

Lee J (1979) Screening methods for cold tolerance at Crop Experiment Station Phytotron and at Chuncheon. Rep. a Rice Cold Toler. Work. International Rice Research Institute, Los Baños, Philippines, pp 77–90

Lee T-M, Lur H-S, Chu C (1997) Role of abscisic acid in chilling tolerance of rice (Oryza sativa L.) seedlings. II. Modulation of free polyamine levels. Plant Sci **126**: 1–10

Li QF, Sun SSM, Yuan DY, Yu HX, Gu MH, Liu QQ (2010a) Validation of candidate reference genes for the accurate normalization of real-time quantitative RT-PCR data in rice during seed development. Plant Mol Biol Report **28**: 49–57

Li X, Cao K, Wang C, Sun Z, Yan L (2010b) Variation of photosynthetic tolerance of rice cultivars (Oryza sativa L .) to chilling temperature in the light. J Biotechnol **9**: 1325–1337

Ling Q, Trösch R, Jarvis P (2013) The Ins and Outs of Chloroplast Protein Transport. *In* B Biswal, K Krupinska, U Biswal, eds, Plast. Dev. Leaves Dur. Growth Senescence, Adv. Photosynth. Respir. Springer Science + Business Media, pp 239–280

Liscum E, Reed JW (2002) Genetics of Aux / IAA and ARF action in plant growth and development. Plant Mol Biol 387–400

Liu H, Frankel LK, Bricker TM (2009) Characterization and complementation of a psbR mutant in Arabidopsis thaliana. Arch Biochem Biophys **489**: 34–40

Liu J-H, Wang W, Wu H, Gong X, Moriguchi T (2015) Polyamines function in stress tolerance: from synthesis to regulation. Front Plant Sci **6**: 827

Liu Z, Duguay J, Ma F, Wang TW, Tshin R, Hopkins MT, McNamara L, Thompson JE (2008) Modulation of eIF5A1 expression alters xylem abundance in Arabidopsis thaliana. J Exp Bot **59**: 939–950

Livanos P, Apostolakos P, Galatis B (2012) Plant cell division: ROS homeostasis

is required. Plant Signal Behav **7**: 771–778

Livore A (2006a) La genética del arroz. El Arroz su Cultiv. y sustentabilidad en Entre Ríos.

Livore A (2006b) Los cultivares de arroz. El Arroz su Cultiv. y sustentabilidad en Entre Ríos.

Lohse M, Nagel A, Herter T, May P, Schroda M, Zrenner R, Tohge T, Fernie AR, Stitt M, Usadel B (2014) Mercator: a fast and simple web server for genome scale functional annotation of plant sequence data. Plant Cell Environ **37**: 1250–8

Long S, Humphries S (1994) Photoinhibition of photosynthesis in nature. Annu Rev Plant Physiol Plant Mol Biol **45**: 633–662

Lowry O, Resebgough N, Farr A, Randall R (1951) Protein measurements with the Folin Phenol reagent. J Biol Chem **193**: 265–275

Lundberg M, Johansson C, Chandra J, Enoksson M, Jacobsson G, Ljung J, Johansson M, Holmgren A (2001) Cloning and Expression of a Novel Human Glutaredoxin (Grx2) with Mitochondrial and Nuclear Isoforms. J Biol Chem **276**: 26269–26275

Luo L, Zhou WQ, Liu P, Li CX, Hou SW (2012) The development of stomata and other epidermal cells on the rice leaves. Biol Plant **56**: 521–527

Lütz C (2010) Cell physiology of plants growing in cold environments. Protoplasma **244**: 53–73

Lyzenga W, Stone S (2011) Protein Ubiquitination: An Emerging Theme in Plant Abiotic Stress Tolerance. Am J Plant Sci Biotechnol **52**: 1–11

Ma F, Liu Z, Wang TW, Hopkins MT, Peterson CA, Thompson JE (2010) Arabidopsis eIF5A3 influences growth and the response to osmotic and nutrient stress. Plant, Cell Environ **33**: 1682–1696

Ma SF, Lin CY, Chen YM (1990) Comparative studies of chilling stress on alterations of chloroplast ultrastructure and protein synthesis in the leaves of chilling - sensitive (mungbean) and - insensitive (pea) seedlings. Bot Bull Acad Sin **31**: 263–272

Mackill DJ, Xiaomao L (1997) Genetic Variation for Traits Related to Temperate Adaptation of Rice Cultivars. Crop Sci **37**: 1340–1346

Maeda S, Horibata A, Yamagata H (1999) Cold tolerance at seedling stage in Japonica rice varieties. Relatsh. cold Toler. with Temp. React. fatty-acid Compos. Breeding Research, p 86

Maes E, Hadiwikarta WW, Mertens I, Baggerman G, Hooyberghs J, Valkenborg D (2016) CONSTANd : a normalization method for isobaric labeled spectra by constrained optimization. Mol Cell Proteomics 2779–2790

Magnan F, Ranty B, Charpenteau M, Sotta B, Galaud JP, Aldon D (2008) Mutations in AtCML9, a calmodulin-like protein from Arabidopsis thaliana, alter plant responses to abiotic stress and abscisic acid. Plant J **56**: 575–589

Majeran W, Friso G, Ponnala L, Connolly B, Huang M, Reidel E, Zhang C, Asakura Y, Bhuiyan NH, Sun Q, et al (2010) Structural and metabolic transitions of C4 leaf development and differentiation defined by microscopy and quantitative proteomics in maize. Plant Cell **22**: 3509–42

Majumder MK, Seshu D V, Shenoy V V (1989) Implication of fatty acids and seed dormancy in a new screening procedure for cold tolerance in rice. Crop Sci **29**: 1298–1304

Mamedov F, Stefansson H, Albertsson PA, Styring S (2000) Photosystem II in different parts of the thylakoid membrane: A functional comparison between different domains. Biochemistry **39**: 10478–10486

Marchler-Bauer A, Lu S, Anderson JB, Chitsaz F, Derbyshire MK, DeWeese-Scott C, Fong JH, Geer LY, Geer RC, Gonzales NR, et al (2011) CDD: A Conserved Domain Database for the functional annotation of proteins. Nucleic Acids Res **39**: 225–229

Marcon C, Malik WA, Walley JW, Shen Z, Paschold A, Smith LG, Piepho H-P, Briggs SP, Hochholdinger F (2015) A high-resolution tissue-specific proteome and phosphoproteome atlas of maize primary roots reveals functional gradients along the root axes. Plant Physiol **168**: 233–46

Maruyama S, Tajima K (1990) Leaf conductance in japonica and indica rice varieties. I. Size, frequency, and aperture of stomata. Japan J Crop Sci **59**: 801–808

McCouch SR, Wright MH, Tung C-W, Maron LG, McNally KL, Fitzgerald M, Singh N, DeClerck G, Agosto-Perez F, Korniliev P, et al (2016) Open access resources for genome-wide association mapping in rice. Nat Commun **7**: 10532

Méchin V, Damerval C, Zivy M (2007) Total Protein Extraction with TCA-Acetone. Plant Proteomics. pp 1–8

Menéndez A, Rodríguez A, Maiale S, Rodríguez Kessler M, Jimenez Bremont J, Ruiz O (2013) Polyamines contribution to the improvement of crop plants tolerance to abiotic stress. *In* N Tuteja, S Gill, eds, Crop Improv. Under Advers. Cond. Springer, New York, USA, pp 113–136

Michelet L, Zaffagnini M, Marchand C, Collin V, Decottignies P, Tsan P, Lancelin J-M, Trost P, Miginiac-Maslow M, Noctor G, et al (2005) Glutathionylation of chloroplast thioredoxin f is a redox signaling mechanism in plants. Proc Natl Acad Sci U S A **102**: 16478–16483

Mittler R (2006) Abiotic stress, the field environment and stress combination. Trends Plant Sci **11**: 15–19

Miura K, Furumoto T (2013) Cold signaling and cold response in plants. Int J Mol Sci **14**: 5312–5337

Miyake C (2010) Alternative electron flows (water-water cycle and cyclic electron flow around PSI) in photosynthesis: Molecular mechanisms and physiological functions. Plant Cell Physiol **51**: 1951–1963

Moriya Y, Itoh M, Okuda S, Yoshizawa AC, Kanehisa M (2007) KAAS: An automatic genome annotation and pathway reconstruction server. Nucleic Acids Res **35**: 182–185

Morsy MR, Almutairi AM, Gibbons J, Yun SJ, De Los Reyes BG (2005) The OsLti6 genes encoding low-molecular-weight membrane proteins are differentially expressed in rice cultivars with contrasting sensitivity to low temperature. Gene **344**: 171–180

Morsy MR, Jouve L, Hausman JF, Hoffmann L, Stewart JM (2007) Alteration of oxidative and carbohydrate metabolism under abiotic stress in two rice (Oryza sativa L.) genotypes contrasting in chilling tolerance. J Plant Physiol **164**: 157–167

Mostowska A (1999) Response of chloroplast structure to photodynamic herbicides and high oxygen. Verlag der Zeitschrift fur Naturforsch - Sect C J Biosci **54**: 621–628

Moubayidin L, Perilli S, Dello Ioio R, Di Mambro R, Costantino P, Sabatini S (2010) The rate of cell differentiation controls the arabidopsis root meristem growth phase. Curr Biol **20**: 1138–1143

Murakami M, Ashikari M, Miura K, Yamashino T, Mizuno T (2003) The Evolutionarily Conserved OsPRR Quintet: Rice Pseudo-Response Regulators Implicated in Circadian Rhythm. Plant Cell Physiol **44**: 1229–1236

Murshed R, Lopez-Lauri F, Sallanon H (2008) Microplate quantification of enzymes of the plant ascorbate-glutathione cycle. Anal Biochem **383**: 320–322

Nadeau P, Delaney S, Chouinard L (1987) Effects of Cold Hardening on the Regulation of Polyamine Levels in Wheat (Triticum aestivum L.) and Alfalfa (Medicago sativa L.). Plant Physiol **84**: 73–77

Negrão S, Oliveira MM, Jena KK, Mackill D (2008) Integration of genomic tools to assist breeding in the japonica subspecies of rice. Mol Breed **22**: 159–168

Neilson K a., Mariani M, Haynes P a. (2011) Quantitative proteomic analysis of cold-responsive proteins in rice. Proteomics **11**: 1696–1706

Neilson KA, Scafaro AP, Chick JM, George IS, Van Sluyter SC, Gygi SP, Atwell BJ, Haynes PA (2013) The influence of signals from chilled roots on the proteome of shoot tissues in rice seedlings. Proteomics **13**: 1922–1933

Nelissen H, Gonzalez N, Inzé D (2016) Leaf growth in dicots and monocots: So different yet so alike. Curr Opin Plant Biol **33**: 72–76

Nelissen H, Rymen B, Jikumaru Y, Demuynck K, Van Lijsebettens M, Kamiya Y, Inzé D, Beemster GTS (2012) A local maximum in gibberellin levels regulates maize leaf growth by spatial control of cell division. Curr Biol **22**: 1183–1187

Neuner G, Larcher W (1990) Determination of Differences in Chilling Susceptibility of 2 Soybean Varieties By Means of Invivo Chlorophyll Fluorescence Measurements. J Agron Crop Sci **164**: 73–80

Nishizawa a., Yabuta Y, Shigeoka S (2008) Galactinol and raffinose constitute a novel function to protect plants from oxidative damage. Plant Physiol **147**: 1251–1263

Noir S, Bömer M, Takahashi N, Ishida T, Tsui T, Balbi V, Shanahan H, Sugimoto K, Devoto A (2013) Jasmonate Controls Leaf Growth by Repressing Cell Proliferation and the Onset of Endoreduplication while Maintaining a Potential Stand-By Mode. Plant Physiol **161**: 1930–1951

Nuruzzaman M, Gupta M, Zhang C, Wang L, Xie W, Xiong L, Zhang Q, Lian X (2008) Sequence and expression analysis of the thioredoxin protein gene family in rice. Mol Genet Genomics **280**: 139–151

Nuruzzaman M, Sharoni AM, Kikuchi S (2013) Roles of NAC transcription factors in the regulation of biotic and abiotic stress responses in plants. Front Microbiol **4**: 1–16

Ohsumi A, Kanemura T, Homma K, Horie T, Shiraiwa T (2007) Genotypic variation of stomatal conductance in relation to stomatal density and length in rise (Oryza sativa L.). Plant Prod Sci **10**: 322–328

Pagter M, Liu F, Jensen CR, Petersen KK (2008) Effects of chilling temperatures and short photoperiod on PSII function, sugar concentrations and xylem sap ABA concentrations in two Hydrangea species. Plant Sci **175**: 547–555

De Palma M, Grillo S, Massarelli I, Costa A, Balogh G, Vigh L, Leone A (2007) Regulation of desaturase gene expression, changes in membrane lipid

composition and freezing tolerance in potato plants. Mol Breed **21**: 15–26

Pardossi a, Vernieri P, Tognoni F (1992) Involvement of Abscisic Acid in Regulating Water Status in Phaseolus vulgaris L. during Chilling. Plant Physiol **100**: 1243–1250

Park S-H, Chung PJ, Juntawong P, Bailey-Serres J, Kim YS, Jung H, Bang SW, Kim Y-K, Do Choi Y, Kim J-K (2012) Posttranscriptional Control of Photosynthetic mRNA Decay under Stress Conditions Requires 3' and 5' Untranslated Regions and Correlates with Differential Polysome Association in Rice. Plant Physiol **159**: 1111–1124

Parkash J, Vaidya T, Kirti S, Dutt S (2014) Translation initiation factor 5A in Picrorhiza is up-regulated during leaf senescence and in response to abscisic acid. Gene **542**: 1–7

Peng S, Ismail A (2004) Physiological basis of yield and environmental adaptation in rice. *In* H Nguyen, A Blum, eds, Physiol. Biochem. Integr. plant Breed. Marcel Dekker, New York, USA, pp 83–140

Peng X, Teng L, Yan X, Zhao M, Shen S (2015) The cold responsive mechanism of the paper mulberry: decreased photosynthesis capacity and increased starch accumulation. BMC Genomics **16**: 898

Pennycooke JC (2003) Down-Regulating -Galactosidase Enhances Freezing Tolerance in Transgenic Petunia. Plant Physiol **133**: 901–909

Peoples TR, Koch DW, Smith SC (1978) Relationship between Chloroplast Membrane Fatty Acid Composition and Photosynthetic Response to a Chilling Temperature in Four Alfalfa Cultivars. Plant Physiol **61**: 472–3

Pereira da Cruz R, Golombieski JI, Bazana MT, Cabreira C, Silveira TF, Picolli da Silva L (2010) Alterations in fatty acid composition due to cold exposure at the vegetative stage in rice. Brazilian Soc Plant Physiol **22**: 199–207

Pérez-Bueno ML, Horton P (2008) The role of lutein in the acclimation of higher plant chloroplast membranes to suboptimal conditions. Physiol Plant **134**: 227–236

Pérez-Ruiz JM, Spínola MC, Kirchsteiger K, Moreno J, Sahrawy M, Pe JM, Cejudo FJ (2006) Rice NTRC Is a High-Ef ciency Redox System for Chloroplast Protection against Oxidative Damage. Plant Cell **18**: 2356–2368

Perilli S, Di Mambro R, Sabatini S (2012) Growth and development of the root apical meristem. Curr Opin Plant Biol **15**: 17–23

Peterhansel C, Horst I, Niessen M, Blume C, Kebeish R, Kürkcüoglu S, Kreuzaler F (2010) Photorespiration. Arab B 1–24

Pettkó-Szandtner A, Cserháti M, Barrôco RM, Hariharan S, Dudits D, Beemster GTS (2015) Core cell cycle regulatory genes in rice and their expression profiles across the growth zone of the leaf. J Plant Res **128**: 953–974

Ping W, Cheng-Jun Z, Guo-Xiang C, Jing W, Da-Wei S, Chuan-Gen L (2006) Effects of Low Temperature on Lipid Peroxidation and Fatty Acid Composition of Flag Leaf in Rice (Oryza sativa L.). Acta Agron Sin **32**: 568–572

Pokhilko A, Mas P, Millar AJ (2013) Modelling the widespread effects of TOC1 signalling on the plant circadian clock and its outputs. BMC Syst Biol **7**: 1–12

Ponnala L, Wang Y, Sun Q, Van Wijk KJ (2014) Correlation of mRNA and protein abundance in the developing maize leaf. Plant J **78**: 424–440

Potters G, De Gara L, Asard H, Horemans N (2002) Ascorbate and glutathione: Guardians of the cell cycle, partners in crime? Plant Physiol Biochem **40**: 537–548

Potters G, Horemans N, Bellone S, Caubergs RJ, Trost P, Guisez Y, Asard H (2004) Dehydroascorbate Influences the Plant Cell Cycle through a Glutathione-Independent Reduction Mechanism. Plant Physiol **134**: 1479–1487

Powell AE, Lenhard M (2012) Control of organ size in plants. Curr Biol **22**: R360–R367

Quintero C (2009) Factores limitantes para el crecimiento y productividadd del arroz en Entre Ríos, Argentina. Universidade da Coruña

Rabbani MA, Maruyama K, Abe H, Khan MA, Katsura K, Ito Y, Yoshiwara K, Seki M, Shinozaki K, Shinozaki KY (2003) Monitoring Expression Profiles of Rice Genes under Cold, Drought, and High-Salinity Stresses and AbscisicAcid Application Using cDNA Microarray and RNAGel-Blot Analyses. Plant Physiol **133**: 1755–1767

Rachoski M, Gazquez A, Calzadilla P, Bezus R, Rodriguez A, Ruiz O, Menendez A, Maiale S (2015) Chlorophyll fluorescence and lipid peroxidation changes in rice somaclonal lines subjected to salt stress. Acta Physiol Plant **37**: 1–12

Radkova M, Vítámvás P, Sasaki K, Imai R (2014) Development- and cold-regulated accumulation of cold shock domain proteins in wheat. Plant Physiol Biochem **77**: 44–48

Ramakrishna A, Ravishankar GA (2011) Influence of abiotic stress signals on secondary metabolites in plants. Plant Signal Behav **6**: 1720–1731

Renaut J, Hoffmann L, Hausman JF (2005) Biochemical and physiological mechanisms related to cold acclimation and enhanced freezing tolerance in

poplar plantlets. Physiol Plant **125**: 82–94

Rhee SG, Kang SW, Chang TS, Jeong W, Kim K (2001) Peroxiredoxin, a novel family of peroxidases. IUBMB Life **52**: 35–41

Di Rienzo J, Casanoves F, Balzarini M, Gonzalez L, Tablada M, Robledo C (2016) InfoStat.

Ripullone F, Lauteri M, Grassi G, Amato M, Borghetti M (2004) Variation in nitrogen supply changes water-use efficiency of Pseudotsuga menziesii and Populus x euroamericana; a comparison of three approaches to determine water-use efficiency. Tree Physiol **24**: 671–679

Robertson FC, Skeffington AW, Gardner MJ, Webb AAR (2009) Interactions between circadian and hormonal signalling in plants. Plant Mol Biol **69**: 419–427

Rodríguez AA, Maiale SJ, Menéndez AB, Ruiz OA (2009) Polyamine oxidase activity contributes to sustain maize leaf elongation under saline stress. J Exp Bot **60**: 4249–4262

Rosa SB, Caverzan A, Teixeira FK, Lazzarotto F, Silveira JAG, Ferreira-Silva SL, Abreu-Neto J, Margis R, Margis-Pinheiro M (2010) Cytosolic APx knockdown indicates an ambiguous redox responses in rice. Phytochemistry **71**: 548–558

Rymen B, Coppens F, Dhondt S, Fiorani F, Beemster GTS (2010) Kinematic analysis of cell division and expansion. *In* L Hennig, C Köhler, eds, Plant Dev. Biol. Methods Mol. Biol. Humana Press, Totowa, NJ, pp 203–227

Rymen B, Fiorani F, Kartal F, Vandepoele K, Inzé D, Beemster GTS (2007) Cold nights impair leaf growth and cell cycle progression in maize through transcriptional changes of cell cycle genes. Plant Physiol **143**: 1429–38

Sabatini S, Beis D, Wolkenfelt H, Murfett J, Guilfoyle T, Malamy J, Benfey P, Leyser O, Bechtold N, Weisbeek P, et al (1999) An Auxin-Dependent Distal Organizer of Pattern and Polarity in the Arabidopsis Root. Cell **99**: 463–472

Saito M, Yoshida M (2011) Expression analysis of the gene family associated with raffinose accumulation in rice seedlings under cold stress. J Plant Physiol **168**: 2268–2271

Sakai H, Lee SS, Tanaka T, Numa H, Kim J, Kawahara Y, Wakimoto H, Yang CC, Iwamoto M, Abe T, et al (2013) Rice annotation project database (RAP-DB): An integrative and interactive database for rice genomics. Plant Cell Physiol **54**: 1–11

Sánchez B, Rasmussen A, Porter JR (2014) Temperatures and the growth and

development of maize and rice: A review. Glob Chang Biol **20**: 408–417

Schmidt R, Kunkowska AB, Schippers JHM (2016) Role of Reactive Oxygen Species during Cell Expansion in Leaves. Plant Physiol **172**: 2098–2106

Schruff MC, Spielman M, Tiwari S, Adams S, Fenby N, Scott RJ (2006) The AUXIN RESPONSE FACTOR 2 gene of Arabidopsis links auxin signalling, cell division, and the size of seeds and other organs. Development **133**: 251–261

Seidler A (1996) The extrinsic polypeptides of photosystem II. Biochim Biophys Acta - Bioenerg **1277**: 35–60

Sengupta S, Mukherjee S, Basak P, Majumder AL (2015) Significance of galactinol and raffinose family oligosaccharide synthesis in plants. Front Plant Sci **6**: 1–11

Senthil-Kumar M, Wang K, Mysore K (2013) AtCYP710A1 gene-mediated stigmasterol production plays a role in imparting temperature stress tolerance in Arabidopsis thaliana. Plant Signal Behav 2013; 8: Plant Signal Behav **8**: 2

Seo PJ, Mas P (2015) STRESSing the role of the plant circadian clock. Trends Plant Sci **20**: 230–237

Sharma P, Jha AB, Dubey RS, Pessarakli M (2012) Reactive Oxygen Species, Oxidative Damage, and Antioxidative Defense Mechanism in Plants under Stressful Conditions. J Bot **2012**: 1–26

Shaykholeslam Esfahani E, Shahpiri A (2015) Thioredoxin h isoforms from rice are differentially reduced by NADPH/thioredoxin or GSH/glutaredoxin systems. Int J Biol Macromol **74**: 243–248

Shi Y, Yang S (2014) ABA regulation of the cold stress response in plants. *In* D-P Zhang, ed, Abscisic Acid Metab. Transp. Signal. Springer Netherlands, pp 337–363

Shimamoto K, Kyozuka J (2002) Rice as a model for comparative genomics of plants. Annu Rev Plant Biol **53**: 399–419

Shimono H, Okada M, Kanda E, Arakawa I (2007) Low temperature-induced sterility in rice: Evidence for the effects of temperature before panicle initiation. F Crop Res **101**: 221–231

Shimosaka E, Ozawa K (2015) Overexpression of cold-inducible wheat galactinol synthase confers tolerance to chilling stress in transgenic rice. Breed Sci **65**: 363–371

Shulaev V, Oliver DJ (2006) Metabolic and Proteomic Markers for Oxidative Stress. New Tools for Reactive Oxygen Species Research. Plant Physiol **141**:

367–372

Shutilova NI (2010) The oxygen-evolving complex of chloroplast membranes. Biochem Suppl Ser A Membr Cell Biol **4**: 125–133

Sierla M, Rahikainen M, Salojärvi J, Kangasjärvi J, Kangasjärvi S (2013) Apoplastic and chloroplastic redox signaling networks in plant stress responses. Antioxid Redox Signal **18**: 2220–39

Silk WK, Erickson RO (1979) Kinematics of plant growth. J Theor Biol **76**: 481–501

Singh R, Jwa N (2013) Understanding the Responses of Rice to Environmental Stress Using Proteomics. J Proteome Res **12**: 4652–4669

Smith AM, Stitt M (2007) Coordination of carbon supply and plant growth. Plant, Cell Environ **30**: 1126–1149

Smith AT, Veitch NC (1998) Substrate binding and catalysis in heme peroxidases. Curr Opin Chem Biol **2**: 269–278

Sonoike K (2011) Photoinhibition of photosystem I. Physiol Plant **142**: 56–64

Sthapit B, Witcombe J, Wilson J (1993) Methods of Selection for Chilling Tolerance in Nepalese Rice by Chlorophyll Fluorescence Analysis. Crop Sci **35**: 90–94

Stirbet A, Govindjee (2011) On the relation between the Kautsky effect (chlorophyll a fluorescence induction) and Photosystem II: Basics and applications of the OJIP fluorescence transient. J Photochem Photobiol B Biol **104**: 236–257

Strasser RJ, Srivastava A, Govindjee (1995) Polyphasic Chlorophyll a Fluorescence Transient in Plants and Cyanobacteria. Photochem Photobiol **61**: 32–42

Strasser RJ, Srivastava A, Tsimilli-Michael M (2000) The fluorescence transient as a tool to characterize and screen photosynthetic samples. *In* M Yunus, P Uday, M Prasanna, eds, Probing Photosynth. Mech. Regul. Adapt. Taylor and Francise, pp 445–483

Strauss AJ, Krüger GHJ, Strasser RJ, Heerden PDR Van (2006) Ranking of dark chilling tolerance in soybean genotypes probed by the chlorophyll a fluorescence transient O-J-I-P. Environ Exp Bot **56**: 147–157

Strauss AJ, Krüger GHJ, Strasser RJ, Van Heerden PDR (2007) The role of low soil temperature in the inhibition of growth and PSII function during dark chilling in soybean genotypes of contrasting tolerance. Physiol Plant **131**: 89–105

Suorsa M, Sirpiö S, Allahverdiyeva Y, Paakkarinen V, Mamedov F, Styring S, Aro EM (2006) PsbR, a missing link in the assembly of the oxygen-evolving complex of plant photosystem II. J Biol Chem **281**: 145–150

Swarup R, Kramer EM, Perry P, Knox K, Leyser HMO, Haseloff J, Beemster GTSS, Bhalerao R, Bennett MJ, Leyser O, et al (2005) Root gravitropism requires lateral root cap and epidermal cells for transport and response to a mobile auxin signal. Nat Cell Biol **7**: 1057–1065

Świątek A, Lenjou M, Van Bockstaele D, Inzé D, Van Onckelen H (2002) Differential Effect of Jasmonic Acid and Abscisic Acid on Cell Cycle Progression in Tobacco BY-2 Cells. Plant Physiol **128**: 201–211

Takanashi J, Maruyama S, Kabaki N, Tajima K (1987) Temperature dependency of protein synthesis by cell-free system constructed with polysomes from rice radicle. Japan J Crop Sci **56**: 44–50

Takeuchi Y, Hayasaka H, Chiba B, Tanaka I, Shimano T, Yamagishi M, Nagano K, Takuji S, Yano M (2001) Mapping quantitative trait loci controlling cool-temperature tolerance at booting stage in temperate japonica rice. Breed Sci **51**: 191–197

Tanabe M, Kanehisa M (2012) Using the KEGG database resource. Curr Protoc Bioinforma. doi: 10.1002/0471250953.bi0112s38

Teixeira FK, Menezes-Benavente L, Galvão VC, Margis R, Margis-Pinheiro M (2006) Rice ascorbate peroxidase gene family encodes functionally diverse isoforms localized in different subcellular compartments. Planta **224**: 300–314

The 3000 Rice Genomes Project . (2014) The 3,000 rice genomes project. Gigascience **3**: 7

Thimm O, Bläsing O, Gibon Y, Nagel A, Meyer S, Krüger P, Selbig J, Müller L a., Rhee SY, Stitt M (2004) Mapman: a User-Driven Tool To Display Genomics Data Sets Onto Diagrams of Metabolic Pathways and Other Biological Processes. Plant J **37**: 914–939

Thompson JE, Hopkins MT, Taylor C, Wang TW (2004) Regulation of senescence by eukaryotic translation initiation factor 5A: Implications for plant growth and development. Trends Plant Sci **9**: 174–179

Tong H, Xiao Y, Liu D, Gao S, Liu L, Yin Y, Jin Y, Qian Q, Chu C (2014) Brassinosteroid Regulates Cell Elongation by Modulating Gibberellin Metabolism in Rice. Plant Cell **26**: 4376–4393

Trudgill DL, Honek a, Li D, Van Straalen NM, Straalen NM, Honěk A, Li D, Van Straalen NM (2005) Thermal time – concepts and utility. Ann Appl Biol **146**:

1–14

Tsiantis M, Brown MIN, Skibinski G, Langdale JA (1999) Disruption of Auxin Transport Is Associated with Aberrant Leaf Development in Maize. Plant Physiol **121**: 1163–1168

Tsukagoshi H, Busch W, Benfey PN (2010) Transcriptional regulation of ROS controls transition from proliferation to differentiation in the root. Cell **143**: 606–616

Tsukaya H (2002) Interpretation of Mutants in Leaf Morphology: Genetic evidence for a Compensatory System in Leaf Morphogenesis That Provides a New Link between Cell and Organismal Theories. Int Rev Citol **217**: 1–39

Tyanova S, Temu T, Sinitcyn P, Carlson A, Hein MY, Geiger T, Mann M, Cox J (2016) The Perseus computational platform for comprehensive analysis of (prote)omics data. Nat Methods **13**: 731–40

Ubeda-Tomás S, Swarup R, Coates J, Swarup K, Laplaze L, Beemster GTS, Hedden P, Bhalerao R, Bennett MJ (2008) Root growth in Arabidopsis requires gibberellin/DELLA signalling in the endodermis. Nat Cell Biol **10**: 625–628

Uehara Y (2003) Improving field resistance to blast and eating quality in Japanese rice varieties. *In* GS Khush, DS Brar, B Hardy, eds, Adv. Rice Genet. IRRI, Manila,Phillipines, pp 41–44

Uematsu K, Suzuki N, Iwamae T, Inui M, Yukawa H (2012) Increased fructose 1,6-bisphosphate aldolase in plastids enhances growth and photosynthesis of tobacco plants. J Exp Bot **63**: 3001–3009

Upchurch RG (2008) Fatty acid unsaturation, mobilization, and regulation in the response of plants to stress. Biotechnol Lett **30**: 967–977

Usadel B, Poree F, Nagel A, Lohse M, Czedik-Eysenberg A, Stitt M (2009) A guide to using MapMan to visualize and compare Omics data in plants: a case study in the crop species, Maize. Plant Cell Environ **32**: 1211–29

Vanneste S, Friml J (2012) Plant signaling: Deconstructing auxin sensing. Nat Chem Biol **8**: 415–416

Venzhik Y V., Titov a. F, Talanova V V., Miroslavov E a., Koteeva NK (2013) Structural and functional reorganization of the photosynthetic apparatus in adaptation to cold of wheat plants. Cell tissue biol **7**: 168–176

Villanova G, Albornoz E (2006) La economía del cultivo de arroz. El Arroz su Cultiv. y sustentabilidad en Entre Ríos.

Voorend W, Lootens P, Nelissen H, Roldán-ruiz I, Inzé D, Muylle H (2014)

LEAF-E : a tool to analyze grass leaf growth using function fitting. Plant Methods **10**: 37

De Vos D, Vissenberg K, Broeckhove J, Beemster GTS (2014) Putting Theory to the Test: Which Regulatory Mechanisms Can Drive Realistic Growth of a Root? PLoS Comput Biol. doi: 10.1371/journal.pcbi.1003910

Voss I, Sunil B, Scheibe R, Raghavendra AS (2013) Emerging concept for the role of photorespiration as an important part of abiotic stress response. Plant Biol **15**: 713–722

Wand M, Jones M (1995) Kernel Smoothing. Chapman & Hall/CRC.

Wang J, Lin X, Sun Q, Jena KK (2013) Evaluation of cold tolerance for japonica rice varieties from different country. Adv J Food Sci Technol **5**: 54–56

Wang L, Xu C, Wang C, Wang Y (2012) Characterization of a eukaryotic translation initiation factor 5A homolog from Tamarix androssowii involved in plant abiotic stress tolerance. BMC Plant Biol **12**: 118

Wang TW, Lu L, Wang D, Thompson JE (2001) Isolation and Characterization of Senescence-induced cDNAs Encoding Deoxyhypusine Synthase and Eucaryotic Translation Initiation Factor 5A from Tomato. J Biol Chem **276**: 17541–17549

Wang W, Chen Q, Hussain S, Mei J, Dong H, Peng S, Huang J, Cui K, Nie L (2016) Pre-sowing Seed Treatments in Direct-seeded Early Rice: Consequences for Emergence, Seedling Growth and Associated Metabolic Events under Chilling Stress. Sci Rep **6**: 19637

Wang W, Vinocur B, Shoseyov O, Altman A (2004) Role of plant heat-shock proteins and molecular chaperones in the abiotic stress response. Trends Plant Sci **9**: 244–252

van der Weele CM, Jiang HS, Palaniappan KK, Ivanov VB, Palaniappan K, Baskin TI (2003) A New Algorithm for Computational Image Analysis of Deformable Motion at High Spatial and Temporal Resolution Applied to Root Growth . Roughly Uniform Elongation in the Meristem and Also , after an Abrupt Acceleration , in the Elongation Zone. Plant Physiol **132**: 1138–1148

Wery J, Silim SN, Knights EJ, Malhotra RS, Cousin R (1994) Screening Techniques and Sources of Tolerance To Extremes of Moisture and Air-Temperature in Cool-Season Food Legumes. Euphytica **73**: 73–83

West G, Inze D, Inzé D, Beemster G, Inze D (2004) Cell cycle modulation in the response of the primary root of Arabidopsis to salt stress. Plant Physiol **135**: 1050–1058

Wijerathna YMAM (2015) Marker Assisted Selection: Biotechnology Tool for Rice

Molecular Breeding. Adv Crop Sci Technol. doi: 10.4172/2329-8863.1000187

Wingler A (2015) Comparison of signaling interactions determining annual and perennial plant growth in response to low temperature. Front Plant Sci **5**: 1–9

Wolosiuk A, Crawford A, Yee C, Buchanan B (1979) Isolation of Three Thioredoxins from Spinach Leaves. J Biol Chem **254**: 1627–1632

Xie G, Kato H, Imai R (2012) Biochemical identification of the OsMKK6-OsMPK3 signalling pathway for chilling stress tolerance in rice. Biochem J **443**: 95–102

Xie G, Kato H, Sasaki K, Imai R (2009) A cold-induced thioredoxin h of rice, OsTrx23, negatively regulates kinase activities of OsMPK3 and OsMPK6 in vitro. FEBS Lett **583**: 2734–2738

Xu J, Zhang B, Jiang C, Ming F (2011) RceIF5A, encoding an eukaryotic translation initiation factor 5A in Rosa chinensis, can enhance thermotolerance, oxidative and osmotic stress resistance of Arabidopsis thaliana. Plant Mol Biol **75**: 167–178

Yan S-P, Zhang Q-Y, Tang Z-C, Su W-A, Sun W-N (2006) Comparative proteomic analysis provides new insights into chilling stress responses in rice. Mol Cell Proteomics **5**: 484–96

Yang JC, Li M, Xie XZ, Han GL, Sui N, Wang BS (2013) Deficiency of phytochrome B alleviates chilling-induced photoinhibition in rice. Am J Bot **100**: 1860–1870

Yoshida S (1981) Fundamentals of rice crop science. IRRI, Los Baños, Laguna, Philippines

You J, Chan Z (2015) ROS regulation during abiotic stress responses in crop plants. Front Plant Sci **6**: 1092

Youssef C, Aubry C, Montrichard F, Beucher D, Juchaux M, Ben C, Prosperi JM, Teulat B (2016) Cell length instead of cell number becomes the predominant factor contributing to hypocotyl length genotypic differences under abiotic stress in Medicago truncatula. Physiol Plant **156**: 108–124

Yu Y, Huang Y, Zhang W (2012) Changes in rice yields in China since 1980 associated with cultivar improvement, climate and crop management. F Crop Res **136**: 65–75

Zhang C-J, Zhao B-C, Ge W-N, Zhang Y-F, Song Y, Sun D-Y, Guo Y (2011) An Apoplastic H-Type Thioredoxin Is Involved in Stress Response Through Regulation of the Apoplastic Reactive Oxygen Species in Rice. Plant Physiol **157**: 1884–1899

Zhang C, Xie Q, Anderson RG, Ng G, Seitz NC, Peterson T, McClung CR, McDowell JM, Kong D, Kwak JM, et al (2013) Crosstalk between the

Circadian Clock and Innate Immunity in Arabidopsis. PLoS Pathog. doi: 10.1371/journal.ppat.1003370

Zhang Q, Zhang J, Shen J, Silva A, Dennis DA, Barrow CJ (2006) A simple 96-well microplate method for estimation of total polyphenol content in seaweeds. J Appl Phycol **18**: 445–450

Zhang T, Zhao X, Wang W, Pan Y, Huang L, Liu X, Zong Y, Zhu L, Yang D, Fu B (2012) Comparative transcriptome profiling of chilling stress responsiveness in two contrasting rice genotypes. PLoS One **7**: e43274

Zhang W, Zhang H, Ning L, Li B, Bao M (2016) Quantitative Proteomic Analysis Provides Novel Insights into Cold Stress Responses in Petunia Seedlings. Front Plant Sci **7**: 1–13

Zhang Z, Sang J, Ma L, Wu G, Wu H, Huang D, Zou D, Liu S, Li A, Hao L, et al (2014) RiceWiki: A wiki-based database for community curation of rice genes. Nucleic Acids Res **42**: 1222–1228

Zhao W, Wang J, He X, Huang X, Jiao Y, Dai M, Wei S, Fu J, Chen Y, Ren X, et al (2004) BGI-RIS: an integrated information resource and comparative analysis workbench for rice genomics. Nucleic Acids Res **32**: 377–382

Zhou Q, Yu Q, Wang Z, Pan Y, Lv W, Zhu L, Chen R, He G (2013) Knockdown of GDCH gene reveals reactive oxygen species-induced leaf senescence in rice. Plant, Cell Environ **36**: 1476–1489

Zhu S, Yu C, Liu X, Ji B, Jiao D (2007) Changes in Unsaturated Levels of Fatty Acids in Thylakoid PSII Membrane Lipids During Chilling-induced Resistance in Rice. J Integr Plant Biol **49**: 463–471

Zorrilla G, Martínez C, Berrío L, Corredor E, Carmona L, Pulver E (2013) Improving Rice Production Systems in Latin America and the Caribbean. Eco-efficiency From Vis. to Real. pp 161–170

Supplementary material

Supplementary tables

Supplementary Table 1. Root growth parameters extracted from published data used for meta-analysis. ***This table is available upon asking to ayelen@gazquez.com.ar.***

Supplementary Table 2. *Graminae* leaf growth parameters extracted from published data used for meta-analysis. ***This table is available upon asking to ayelen@gazquez.com.ar.***

Supplementary Table 3. Eudicotyledonous leaf growth parameters extracted from published data used for meta-analysis. ***This table is available upon asking to ayelen@gazquez.com.ar.***

Supplementary Table 4. Kinematic analysis parameters describing the effect of ST stress on the fourth leaf growth of six contrasting cultivars. Data are average ± SD (n=23 for LER; n=10 for FLL and TLE; n=5 for the rest of the parameters). A t-test was used to test differences between treatments. Percentage change of ST over OT data is shown for each cultivar and parameter, *** *p*-value <0.0001, ** 0.001<*p*-value<0.0001, * 0.05<*p*-value<0.001, not significant (NS) if *p*-value<0.05. Parameters: FLL, final leaf lengths; TLE, time that leaf was elongating; LER, leaf elongation rate; lmat, mature cell length; P, cell production; D, average cell division rate; TC, cell cycle duration; Ndiv, number of cells in the meristem; Tdiv, time of cells in the meristem; Tel, time of cells in the elongation zone; RER, relative elongation rate; ldiv, length of the cells leaving the mersitem; Lmer, length of the meristem; Lel, length of the elongation zone; Lgr, length of the growth zone; Nel, number of cells in the elongation zone; Ngr, number of cells in the growth zone.

Parameter	Koshihikari		
	OT	ST	% change
FLL (cm)	30.01 ± 3.1547	20.16 ± 1.6985	**-33*** **
T_{LE} (d)	5.7 ± 0.8233	14.2 ± 0.6325	**149*** **
LER ($mm.h^{-1}$)	2.617 ± 0.2786	0.6978 ± 0.0913	**-73*** **
l_{mat} (µm)	70.0095 ± 5.5663	50.3642 ± 3.3979	**-28** **
P ($cells.h^{-1}$)	35.351 ± 2.641	13.939 ± 0.9777	**-61*** **
D ($cells.cells^{-1}.h^{-1}$)	0.0687 ± 0.0085	0.0467 ± 0.0174	**-32***
T_c (h)	10.2382 ± 1.5048	16.2303 ± 4.8215	**58***
N_{div} (cells)	522.9047 ± 92.0759	327.0345 ± 95.9572	**-37***
T_{div} (h)	92.5425 ± 16.224	136.4169 ± 46.4452	NS
T_{el} (h)	13.9115 ± 2.3671	48.3369 ± 10.562	**248***
RER ($\mu m.\mu m^{-1}.h^{-1}$)	0.0955 ± 0.0168	0.0332 ± 0.0042	**-65***
l_{div} (µm)	19.2295 ± 4.0517	10.7004 ± 3.0432	**-44***
L_{mer} (mm)	6.0552 ± 1.0025	3.2733 ± 0.73	**-46***
L_{el} (mm)	20.1448 ± 4.5306	15.5267 ± 2.4093	NS
L_{gr} (mm)	26.2 ± 4.0249	18.8 ± 2.9496	**-28***
N_{el} (cells)	489.4516 ± 75.877	678.6639 ± 170.8433	NS
N_{gr} (cells)	1012.3563 ± 59.4005	1005.6984 ± 256.7088	NS

Parameter	CT-6742-10-10-1		
	OT	ST	% change
FLL (cm)	47.97 ± 1.6918	30.85 ± 2.4346	**-36*** **
T_{LE} (d)	7.1 ± 0.9944	14.3 ± 1.3375	**101*** **
LER ($mm.h^{-1}$)	3.9526 ± 0.3267	0.9639 ± 0.1426	**-76*** **
l_{mat} (µm)	82.6583 ± 7.1997	66.2669 ± 9.451	**-20***
P ($cells.h^{-1}$)	45.3358 ± 4.163	14.5111 ± 3.0134	**-68*** **
D ($cells.cells^{-1}.h^{-1}$)	0.0667 ± 0.0105	0.0316 ± 0.005	**-52****
T_c (h)	10.5808 ± 1.5463	22.4003 ± 3.5259	**112****
N_{div} (cells)	687.2374 ± 77.6726	459.6158 ± 69.1811	**-33***
T_{div} (h)	99.7956 ± 15.7554	197.7945 ± 31.0317	**98****
T_{el} (h)	17.0901 ± 2.286	64.9701 ± 12.9308	**280***
RER ($µm.µm^{-1}.h^{-1}$)	0.106 ± 0.0109	0.0271 ± 0.0048	**-74*** **
l_{div} (µm)	13.7821 ± 1.7535	11.8898 ± 1.481	NS
L_{mer} (mm)	6.3834 ± 0.8674	4.7282 ± 0.5366	**-26***
L_{el} (mm)	28.0166 ± 3.6257	25.0718 ± 3.0945	NS
L_{gr} (mm)	34.4 ± 3.5777	29.8 ± 2.6833	NS
N_{el} (cells)	770.3258 ± 85.5864	913.7764 ± 70.3037	**-19***
N_{gr} (cells)	1457.5632 ± 105.5855	1373.3923 ± 104.2043	NS

Parameter	General Rossi		
	OT	ST	% change
FLL (cm)	38.77 ± 1.5826	25.42 ± 1.0809	**-35*****
T_{LE} (d)	7.2 ± 0.6325	14.7 ± 1.0593	**104*****
LER ($mm.h^{-1}$)	3.3013 ± 0.2578	0.8717 ± 0.1464	**-74*****
l_{mat} (µm)	74.263 ± 5.8384	59.6561 ± 3.5294	**-20***
P ($cells.h^{-1}$)	44.6998 ± 3.1151	14.9528 ± 1.9061	**-67*****
D ($cells.cells^{-1}.h^{-1}$)	0.0929 ± 0.0152	0.0379 ± 0.0139	**-59****
T_c (h)	7.6208 ± 1.2052	20.3925 ± 7.2895	**168***
N_{div} (cells)	488.7138 ± 62.5774	425.8272 ± 110.8495	NS
T_{div} (h)	68.1643 ± 11.9798	179.3997 ± 70.5899	**163****
T_{el} (h)	18.7555 ± 3.3755	52.7433 ± 8.1737	**118*****
RER ($\mu m.\mu m^{-1}.h^{-1}$)	0.0939 ± 0.0135	0.0301 ± 0.0037	**-68****
l_{div} (µm)	13.2357 ± 1.1282	12.4733 ± 1.4643	NS
L_{mer} (mm)	4.9035 ± 0.7556	4.8643 ± 0.9654	NS
L_{el} (mm)	29.0965 ± 5.0875	20.5357 ± 1.7755	**-29***
L_{gr} (mm)	34 ± 5.0498	25.4 ± 1.8166	**-25***
N_{el} (cells)	840.0054 ± 176.9085	777.6307 ± 46.1389	NS
N_{gr} (cells)	1328.7192 ± 148.3811	1203.458 ± 100.5426	NS

Parameter	IR50		
	OT	ST	% change
FLL (cm)	29.83 ± 2.6767	14.42 ± 0.8702	**-52*** **
T_{LE} (d)	7.2 ± 0.9189	12.8 ± 1.2293	**78*** **
LER ($mm.h^{-1}$)	2.5978 ± 0.2437	0.5591 ± 0.078	**-79*** **
l_{mat} (µm)	71.1071 ± 6.6093	56.376 ± 4.0943	**-21***
P ($cells.h^{-1}$)	35.9218 ± 4.7807	10.091 ± 1.6581	**-72*** **
D ($cells.cells^{-1}.h^{-1}$)	0.0542 ± 0.0091	0.0246 ± 0.0052	**-55****
T_c (h)	13.0472 ± 2.0126	29.2503 ± 6.4417	**124***
N_{div} (cells)	665.6667 ± 35.6515	417.3304 ± 66.4547	**-37****
T_{div} (h)	122.4369 ± 19.6403	254.9268 ± 60.6683	**108***
T_{el} (h)	21.0352 ± 2.564	55.2615 ± 28.764	NS
RER ($µm.µm^{-1}.h^{-1}$)	0.0893 ± 0.0095	0.0322 ± 0.0131	**-64*** **
l_{div} (µm)	11.0677 ± 0.9678	13.1162 ± 3.7451	NS
L_{mer} (mm)	4.991 ± 0.8284	4.2443 ± 0.3143	NS
L_{el} (mm)	21.209 ± 3.6458	14.9557 ± 5.9793	NS
L_{gr} (mm)	26.2 ± 4.0866	19.2 ± 5.7619	NS
N_{el} (cells)	761.276 ± 183.6129	528.8427 ± 227.7546	NS
N_{gr} (cells)	1426.9427 ± 176.0434	946.1731 ± 278.5743	**-34***

Parameter	IR24		
	OT	ST	% change
FLL (cm)	28.51 ± 2.162	13.83 ± 0.8782	**-51*** **
T_{LE} (d)	6.3 ± 0.483	10.9 ± 0.9944	**73*** **
LER ($mm.h^{-1}$)	2.7026 ± 0.2627	0.5548 ± 0.0988	**-80*** **
l_{mat} (µm)	85.962 ± 4.6833	55.0762 ± 3.3776	**-36*** **
P ($cells.h^{-1}$)	32.4218 ± 2.9573	10.4786 ± 1.3581	**-68*** **
D ($cells.cells^{-1}.h^{-1}$)	0.0779 ± 0.0113	0.0386 ± 0.0157	**-50***
T_c (h)	9.043 ± 1.2236	19.8785 ± 6.1344	**120***
N_{div} (cells)	422.1449 ± 63.2508	306.8456 ± 118.2353	NS
T_{div} (h)	78.9231 ± 12.2362	165.238 ± 60.4262	**109***
T_{el} (h)	17.2225 ± 4.1621	51.703 ± 9.5059	**200** **
RER ($µm.µm^{-1}.h^{-1}$)	0.1087 ± 0.0238	0.0285 ± 0.0063	**-74***
l_{div} (µm)	14.397 ± 2.7991	13.2614 ± 1.527	NS
L_{mer} (mm)	4.0306 ± 0.7193	3.7072 ± 0.5926	NS
L_{el} (mm)	23.3694 ± 6.4192	14.0928 ± 2.6621	**-40***
L_{gr} (mm)	27.4 ± 6.8775	17.8 ± 3.0332	**-35***
N_{el} (cells)	555.4778 ± 122.9777	534.2144 ± 69.8178	NS
N_{gr} (cells)	977.6227 ± 167.2911	841.06 ± 129.6149	NS

Parameter	Honezhaosen		
	OT	ST	% change
FLL (cm)	26.14 ± 0.9686	13.45 ± 1.2039	**-49*****
T_{LE} (d)	6.7 ± 0.6749	12.6 ± 1.7127	**88*****
LER (mm.h^{-1})	2.4583 ± 0.1954	0.54 ± 0.0745	**-78*****
l_{mat} (µm)	69.048 ± 8.2535	50.5883 ± 4.6861	**-27***
P (cells.h^{-1})	36.5468 ± 5.0818	12.5027 ± 2.0467	**-66*****
D (cells.$cells^{-1}$.h^{-1})	0.1117 ± 0.0203	0.0324 ± 0.0077	**-71*****
T_c (h)	6.3879 ± 1.2775	22.3652 ± 5.158	**250***
N_{div} (cells)	335.1183 ± 66.8189	395.8887 ± 78.6964	NS
T_{div} (h)	53.6588 ± 12.3091	193.3376 ± 49.6597	**260***
T_{el} (h)	18.6512 ± 4.5697	50.9218 ± 10.7211	**173****
RER (µm.$µm^{-1}$.h^{-1})	0.0759 ± 0.0136	0.0326 ± 0.0058	**-57****
l_{div} (µm)	18.7259 ± 10.075	10.1992 ± 2.2315	NS
L_{mer} (mm)	4.2328 ± 1.0458	3.5913 ± 0.5656	NS
L_{el} (mm)	23.3672 ± 3.8587	15.0087 ± 2.5196	**-36***
L_{gr} (mm)	27.6 ± 3.5777	18.6 ± 2.4083	**-33***
N_{el} (cells)	696.4601 ± 253.5035	627.5186 ± 123.1999	NS
N_{gr} (cells)	1031.5784 ± 267.4337	1023.4073 ± 98.1969	NS

Supplementary Table 5. Primers of selected genes for quantitative PCR used for microarray validation.

RJpGene-1_0-st array:					
IRGSP 1.0 Gene ID	BGI Gene ID	MSU 7 Gene ID	RJpGene-1_0-st Transcript Cluster ID	Left primer 5' → 3'	Right primer 5' → 3'
Os01g0128200	BGIOSGA002698	LOC_Os01g03730	16096632	AATTCTCGTCACCAGCAAGG	AACATCAGGCTCTCCGTCAG
Os01g0922700	BGIOSGA000229	LOC_Os01g69840	16132742	CCAGAGCAGCCCTTCTGTAA	CTCTGACGGCCAAGATGTAAG
Os01g0702000	BGIOSGA000953	LOC_Os01g50622	16126263	TACGTTTGGTGCGGATTACA	GAACCTTACACCGGAAAGCA
Os12g0586100	BGIOSGA035923	LOC_Os12g39630	16174270	CAGAAGCAACAATTCCAGCA	GTCCGAGTCCATATCCTCCA
Os09g0489200	BGIOSGA029547	LOC_Os09g31380	16359971	GGCTCAGCATCCCTTGTTT	GTGCAATGGTGTCACTGTCC
Os12g0493900	BGIOSGA037422	LOC_Os12g31000	16165506	GCAGCAATGTGGTTGAGAAA	AGCAAGGAGCTCCAGAATGA
Os11g0525700	BGIOSGA035363	LOC_Os11g32270	16152261	GTGCAACCAGAACCTGGACT	CCAGAGAAGGTGCAGTAGGG
Os03g0133400	BGIOSGA011785	LOC_Os03g04110	16209190	GCGCCTACAGTGGTTACTCC	TGCAAGGCTGGTTTGTATGA
Os12g0638300	BGIOSGA035754	LOC_Os12g44110	16175694	GCCAACGTCTGCTACTTCCT	TGGTGGTGTTCTTGAACCTG
Os06g0306300	BGIOSGA022766	LOC_Os06g20150	16293838	AGCTCCGCGTCGACTACTAC	GCCGATGATCTTCTCCATCT
Os04g0684800	BGIOSGA017384	LOC_Os04g58800	16255114	TTCTGCGACAAGGACTACCC	CATGTTGATCCTGGAGTGGA
Os04g0688100	BGIOSGA014042	LOC_Os04g59150	16267762	CTTCTTCCACGACTGCTTCC	TATCTCACCCAGCTCGCTTT
Os07g0663800	BGIOSGA026332	LOC_Os07g46852	16319789	TACGTCAACGGGCATAACCT	ATGCGATTGTCGTCTCCTTT
Os08g0103000	BGIOSGA027812	LOC_Os08g01270	16339955	AGGGATTTCGCTTGGAGATT	CAGGATCTTCGTCCCAACAC
Os12g0583300	BGIOSGA037682	LOC_Os12g39360	16167170	AAGCTGTTCGTTCTCGTGCT	CAAGTAATTAGGGCGGTGGT
Os11g0256900	BGIOSGA015677	LOC_Os11g15040	16150447	GGAGCGACTACACCACCATC	TCTCCATGCATCTCATCTGG
Os03g0161900	BGIOSGA011916	LOC_Os03g06630	16210166	TGAATGATGAGCCTGCAAAG	TCGTCGGTTAACTCGGTTTC
Os12g0247700	BGIOSGA037221	LOC_Os12g14440	16164162	ATACCACGGCTGGTCTGTTG	GACCTGCCTTGTGCTTCTCT

RCnGene-1_0-st array:

IRGSP 1.0 Gene ID	BGI Gene ID	MSU 7 Gene ID	RCnGene-1_0-st Transcript Cluster ID	Left primer 5' → 3'	Right primer 5' → 3'
Os01g0128200	BGIOSGA002698	LOC_Os01g03730	16381715	AATTCTCGTCACCAGCAAGG	AACATCAGGCTCTCCGTCAG
Os09g0489200	BGIOSGA029547	LOC_Os09g31380	16558706	GGCTCAGCATCCCTTGTTT	GTGCAATGGTGTCACTGTCC
Os12g0493900	BGIOSGA037422	LOC_Os12g31000	16427933	GCAGCAATGTGGTTGAGAAA	AGCAAGGAGCTCCAGAATGA
Os01g0702000	BGIOSGA000953	LOC_Os01g50622	16401551	TACGTTTGGTGCGGATTACA	GAACCTTACACCGGAAAGCA
Os03g0133400	BGIOSGA011785	LOC_Os03g04110	16456567	GCGCCTACAGTGGTTACTCC	TGCAAGGCTGGTTTGTATGA
Os12g0586100	BGIOSGA035923	LOC_Os12g39630	16434013	CAGAAGCAACAATTCCAGCA	GTCCGAGTCCATATCCTCCA
Os11g0525700	BGIOSGA035363	LOC_Os11g32270	16419297	GTGCAACCAGAACCTGGACT	CCAGAGAAGGTGCAGTAGGG
Os07g0283050	BGIOSGA024476	LOC_Os07g18230	16534260	CAGGTGCGATTAGCACAAGA	AGGTCTTGGAACGAGGCTTT
Os04g0688100	BGIOSGA014042	LOC_Os04g59150	16495207	CTTCTTCCACGACTGCTTCC	TATCTCACCCAGCTCGCTTT
Os04g0684800	BGIOSGA017384	LOC_Os04g58800	16486700	TTCTGCGACAAGGACTACCC	CATGTTGATCCTGGAGTGGA
Os07g0663800	BGIOSGA026332	LOC_Os07g46852	16531335	TACGTCAACGGGCATAACCT	ATGCGATTGTCGTCTCCTTT
Os08g0103000	BGIOSGA027812	LOC_Os08g01270	16544769	AGGGATTTCGCTTGGAGATT	CAGGATCTTCGTCCCAACAC
Os11g0256900	BGIOSGA015677	LOC_Os11g15040	16487219	GGAGCGACTACACCACCATC	TCTCCATGCATCTCATCTGG
Os06g0306300	BGIOSGA022766	LOC_Os06g20150	16513232	AGCTCCGCGTCGACTACTAC	GCCGATGATCTTCTCCATCT
Os03g0161900	BGIOSGA011916	LOC_Os03g06630	16457253	TGAATGATGAGCCTGCAAAG	TCGTCGGTTAACTCGGTTTC
Os12g0583300	BGIOSGA037682	LOC_Os12g39360	16429063	AAGCTGTTCGTTCTCGTGCT	CAAGTAATTAGGGCGGTGGT
Os12g0247700	BGIOSGA037221	LOC_Os12g14440	16427159	ATACCACGGCTGGTCTGTTG	GACCTGCCTTGTGCTTCTCT

Housekeeping for both arrays:

IRGSP 1.0 Gene ID	BGI Gene ID	MSU 7 Gene ID	Housekeeping name	Left primer 5' → 3'	Right primer 5' → 3'
OS03G0718100	BGIOSGA013463	LOC_Os03g50885	Actin-1	AGGAATGGAAGCTGCGGGTAT	GCAGGAGGACGGCGATAACA

Supplementary Table 6. Microarray results from IR50 and Koshihikari seedlings. ***This table is available upon asking to ayelen@gazquez.com.ar.***

Supplementary Table 7. Proteomic results from Koshihikari. ***This table is available upon asking to ayelen@gazquez.com.ar.***

Supplementary Table 8. Proteomics results from IR50. ***This table is available upon asking to ayelen@gazquez.com.ar.***

Supplementary Table 9. Description of proteins that significantly changed their abundance in response to ST (FDR<0.10). ***This table is available upon asking to ayelen@gazquez.com.ar.***

Supplementary Table 10. Functional description of protein identified in the meristem and elongation zone of Koshikari that changed their abundance in response to ST. ***This table is available upon asking to ayelen@gazquez.com.ar.***

Supplementary Table 11. Functional description of protein identified in the meristem and elongation zone of IR50 that changed their abundance in response to ST. ***This table is available upon asking to ayelen@gazquez.com.ar.***

Supplementary Table 12. The fatty acids analyzed with their respective retention times.

FAME		t_R (min)
Caproic acid	C6	2.02
Caprylic acid	C8	2.76
Capric acid	C10	4.31
Undecylic acid	C11	5.46
Lauric acid	C12	6.79
Tridecylic acid	C13	8.25
Myristic acid	C14	9.78
Myristoleic acid	C14(n:9)	10.39
Pentadecylic acid	C15	11.32
cis-10-Pentadecanoic acid	C15(n:10)	11.95
Palmitic acid	C16	12.88
Palmitoleic acid	C16(n:9)	13.31
Margaric acid	C17	14.36
cis-10-Heptadecanoic acid	C17(n:10)	14.81
Stearic acid	C18	15.83
Elaidic acid	trans C18(n:9)	16.03
Oleic acid	cis C18(n:9)	16.18
Linolelaidic acid	trans C18(n:9.12)	16.53
Linoleic acid	cis C18(n:9.12)	16.85
g-Linolenic acid	gC18(n:6.9.12)	17.24
Linolenic acid	C18(n:9.12.15)	17.72
Arachidic acid	C20	18.58
cis-11-Eicosenoic acid	C20(n:11)	18.92
cis-11,14-Eicosodienoic acid	C20(n:11,14)	19.6
methyl-cis-8,11,14-Eicosatrienoic acid	C21(n:8,11,14)	19.89
Heneicosylic acid	C21	19.98
Arachidonic acid	C20(n:5,8,11,14)	20.21
cis-11,14,17-Eicosatrienoic acid	C20(n:11,14,17)	20.42
cis-5,8,11,14,17-Eicosapentaenoic acid	C20(n:5,8,11,14,17)	21.03
Behenic acid	C22	21.15
Erucic acid	C22(n:13)	21.48
cis-13,16-Docosadienoic acid	C22(n:13,16)	22.14
Tricosylic acid	C23	22.34
Lignoceric acid	C24	23.53
cis-4,7,10,13,16,19-Docosahexanoic acid	C22(n:4,7,10,13,16,19)	23.81

Supplementary Table 13. Results of the three-way ANOVA done for the redox system analysis on data discussed in section 5.4.4. ***This table is available upon asking to ayelen@gazquez.com.ar.***

Supplementary figures

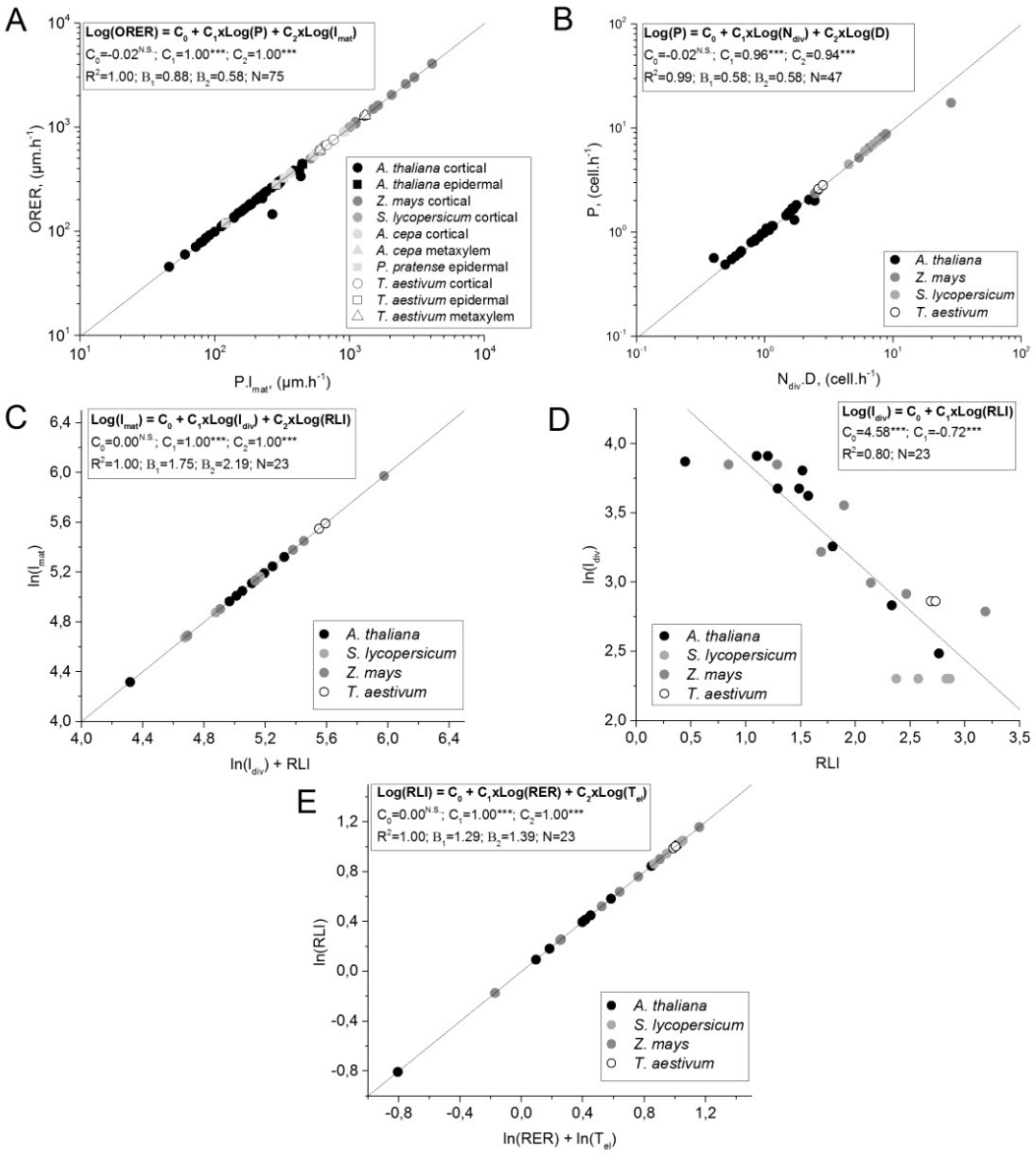

Supplementary Figure 1. Regressions with full models of the cellular basis of differences in root growth rate across a range of species. **A)** the relationship between root elongation rate (ORER), cell production (P) and mature cell length (l_{mat}). **B)** the relationship between P, number of cells in the meristem (N_{div}) and average cell division rate (D). **C)** the relationship between mature cortical cell length (l_{mat}), length of cells at the end of the meristem (l_{div}) and relative length increase (RLI). **D)** the relationship between l_{div} and RLI. **E)** the relationship between RLI, relative elongation rate (RER) and time in elongation zone (T_{el}). Details of the regression parameters are shown in the figure: C_0, C_1, and C_2 are the partial coefficients; R^2, coefficient of correlation; B_1 and B_2, Beta standardized coefficients; N, number of samples.

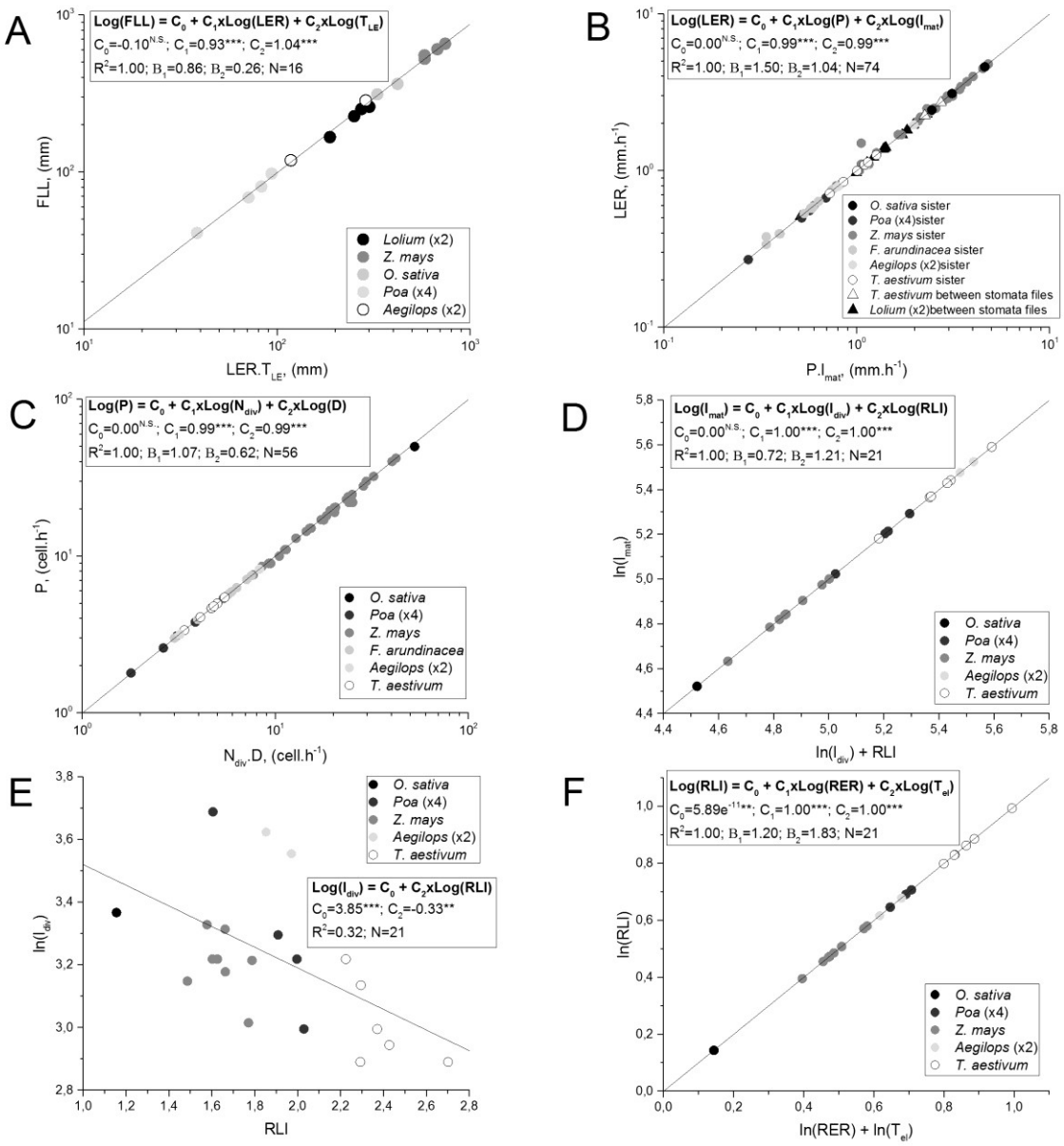

Supplementary Figure 2. Quantitative analysis of the whole organ growth pattern and in the cellular basis of leaf elongation rate that determine leaf size across a range of *Graminae*. **A)** the relationship between final leaf length (FLL), leaf elongation rate (LER) and duration of leaf expansion (T_{LE}). **B)** the relationship between LER, cell production (P) and mature cell length (l_{mat}). **C)** the relationship between P of sister cells, the number of cells in the meristem (N_{div}) and average cell division rate (D). **D)** the relationship between l_{mat} of sister cells, length of cells at the end of the meristem (l_{div}) and relative length increase (RLI). **E)** the relationship between l_{div} and relative length increase (RLI) of sister cells. **F)** the relationship between RLI, relative elongation rate (RER) and time in elongation zone (T_{el}) of sister cells. Details of the regression parameters are shown in the figure: C_0, C_1, and C_2 are the partial coefficients; R^2, coefficient of correlation; B_1 and B_2, Beta standardized coefficients; N, number of samples.

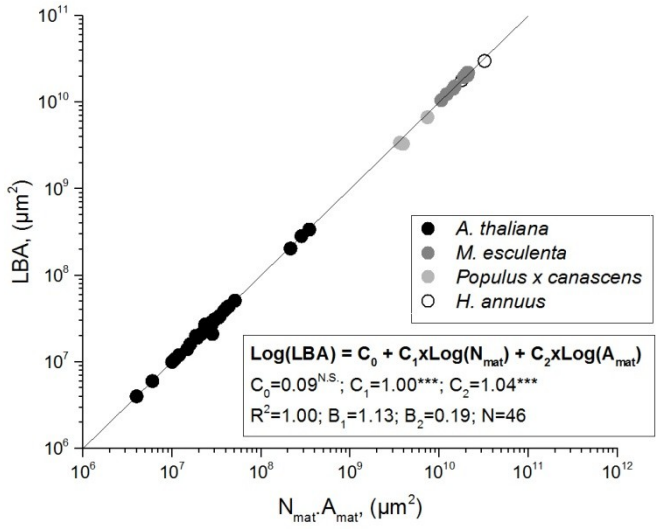

Supplementary Figure 3. Full model of the cellular basis of differences in leaf size across a range of Eudicotyledonous species. The correlation between leaf blade area (LBA), mature cell area (A_{mat}) and number of cells (N_{mat}) for epidermal cells of dicotyledonous leaves. Details of the regression parameters are shown in the figure: C_0, C_1, and C_2 are the partial coefficients; R^2, coefficient of correlation; R^2, coefficient of correlation; B_1 and B_2, Beta standardized coefficients; N, number of samples.

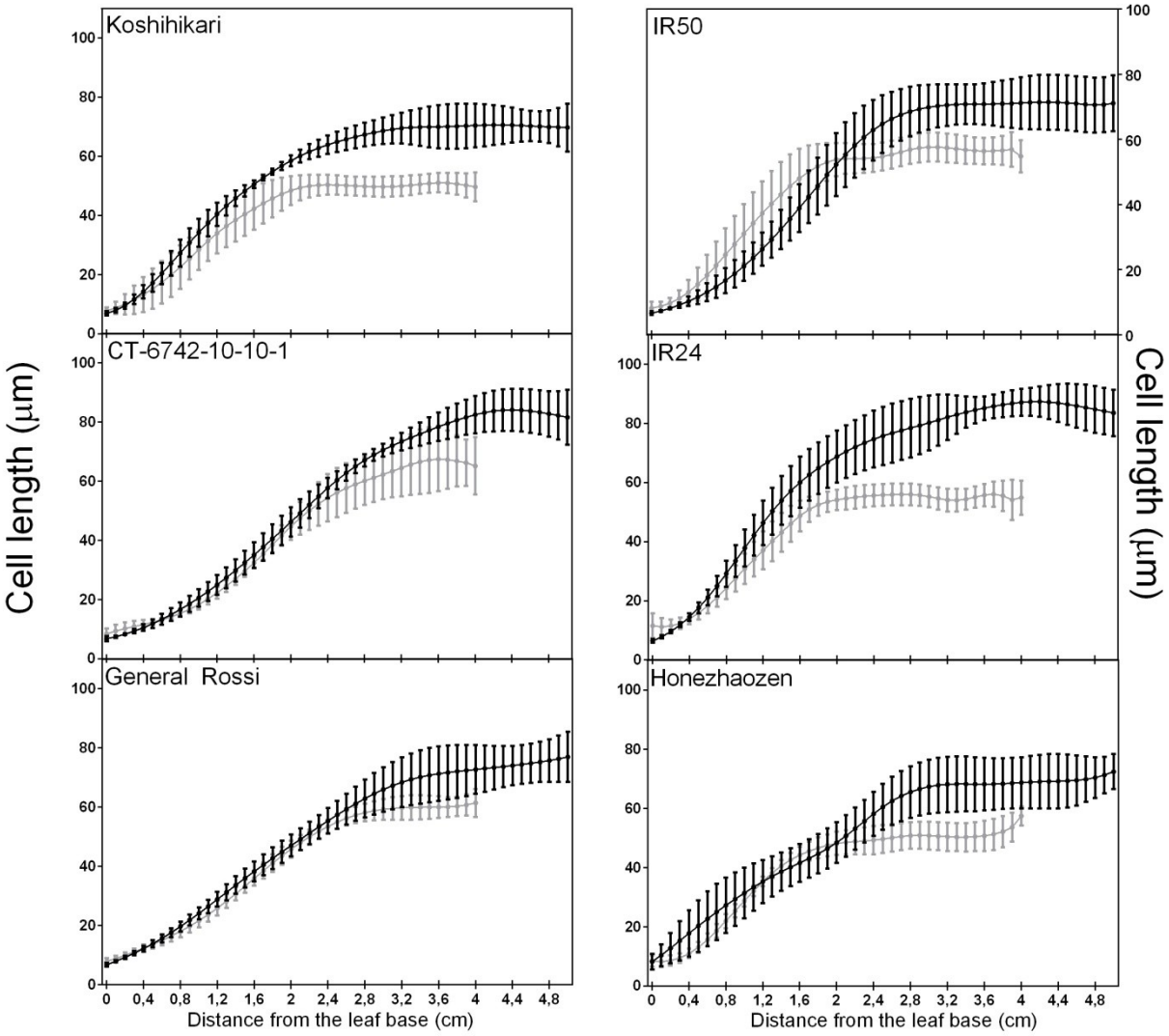

Supplementary Figure 4. The effect of ST on the cell length profile. Cell length from the base of the leaf was measure in six cultivars in OT (black line) and ST (grey line) conditions every one mm. Data was plotted as mean ± SD. n=5.

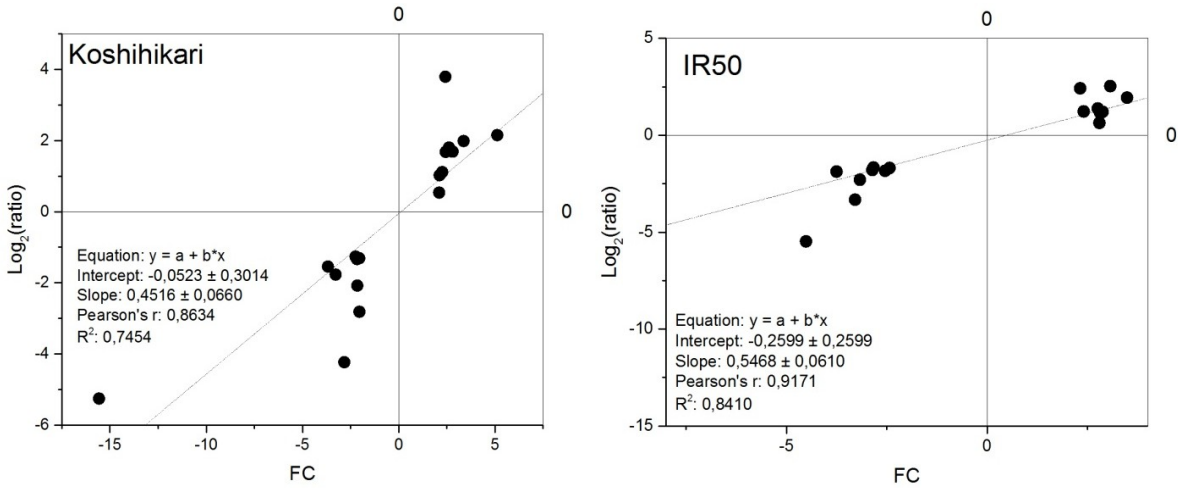

Supplementary Figure 5. Regression analysis and Pearson correlation for the validation of the results obtain in the microarray. Scatter plot showing the relative expression of the genes obtained from the microarray analysis (X axis) and from the qPCR (Y axis). In the graphs information about the linear regression and the correlation is showed.

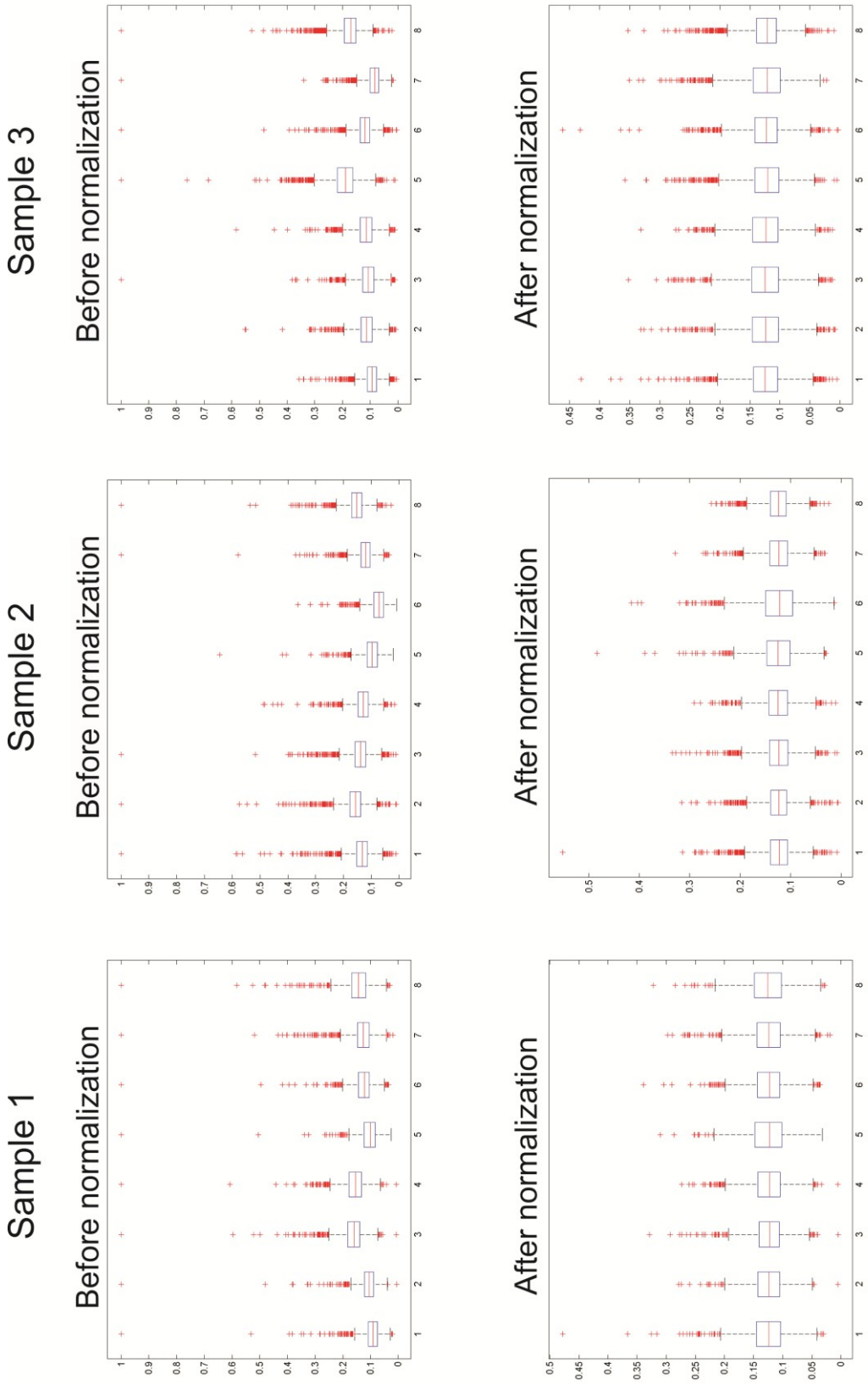

Supplementary Figure 6. Boxplots of raw data of the three multiplex iTRAQ-labeled samples using Uniprot *O. sativa* japonica subspecies (39947) for database searching before

and after CONSTANd normalization. Boxplots displays median value, upper and lower quartiles, largest/smaller non-outliers, and outliers.

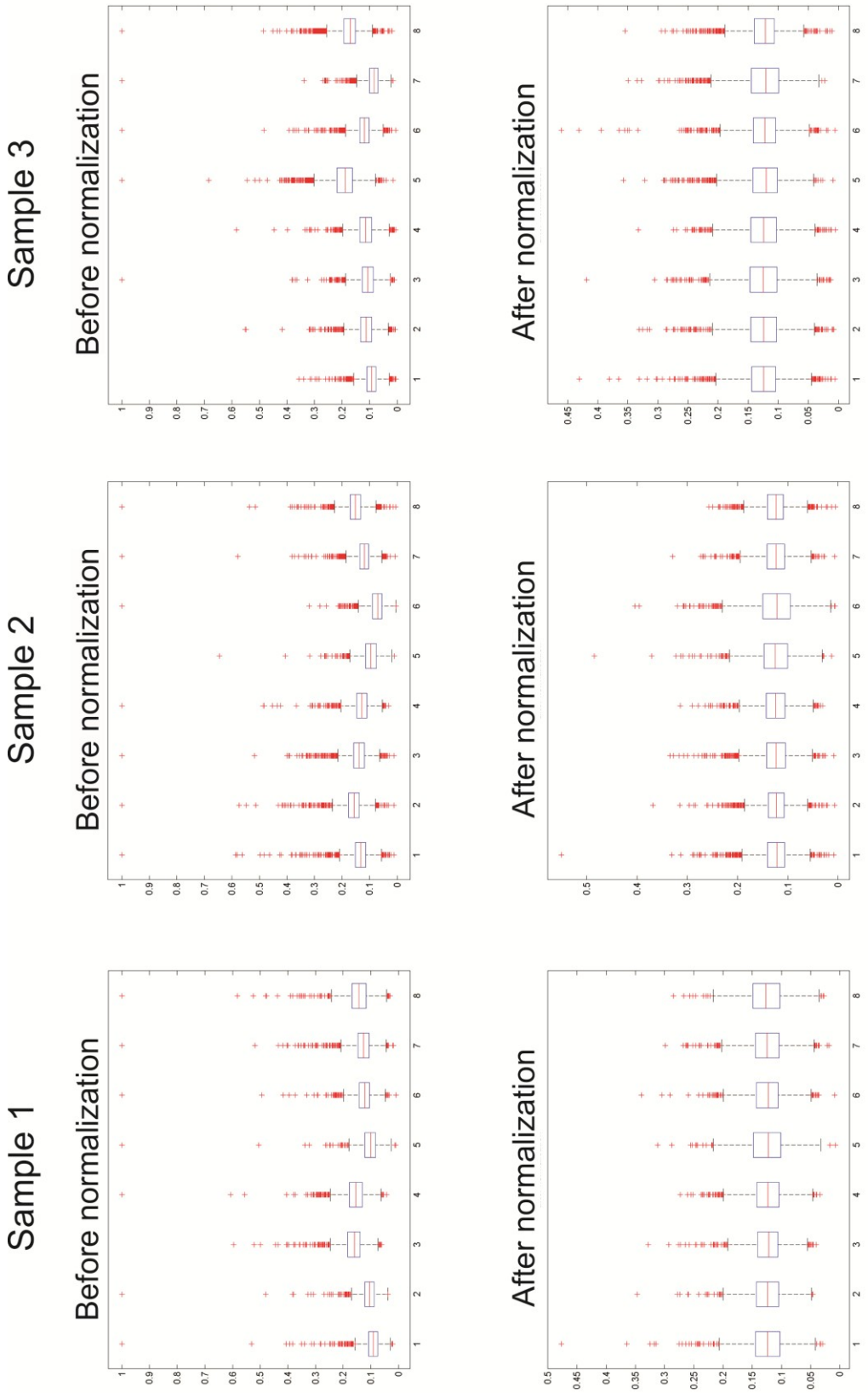

Supplementary Figure 7. Boxplots of raw data of the three multiplex iTRAQ-labeled samples using Uniprot *O. sativa* indica subspecies (39946) for database searching before and after CONSTANd normalization. Boxplots displays median value, upper and lower quartiles, largest/smaller non-outliers, and outliers.

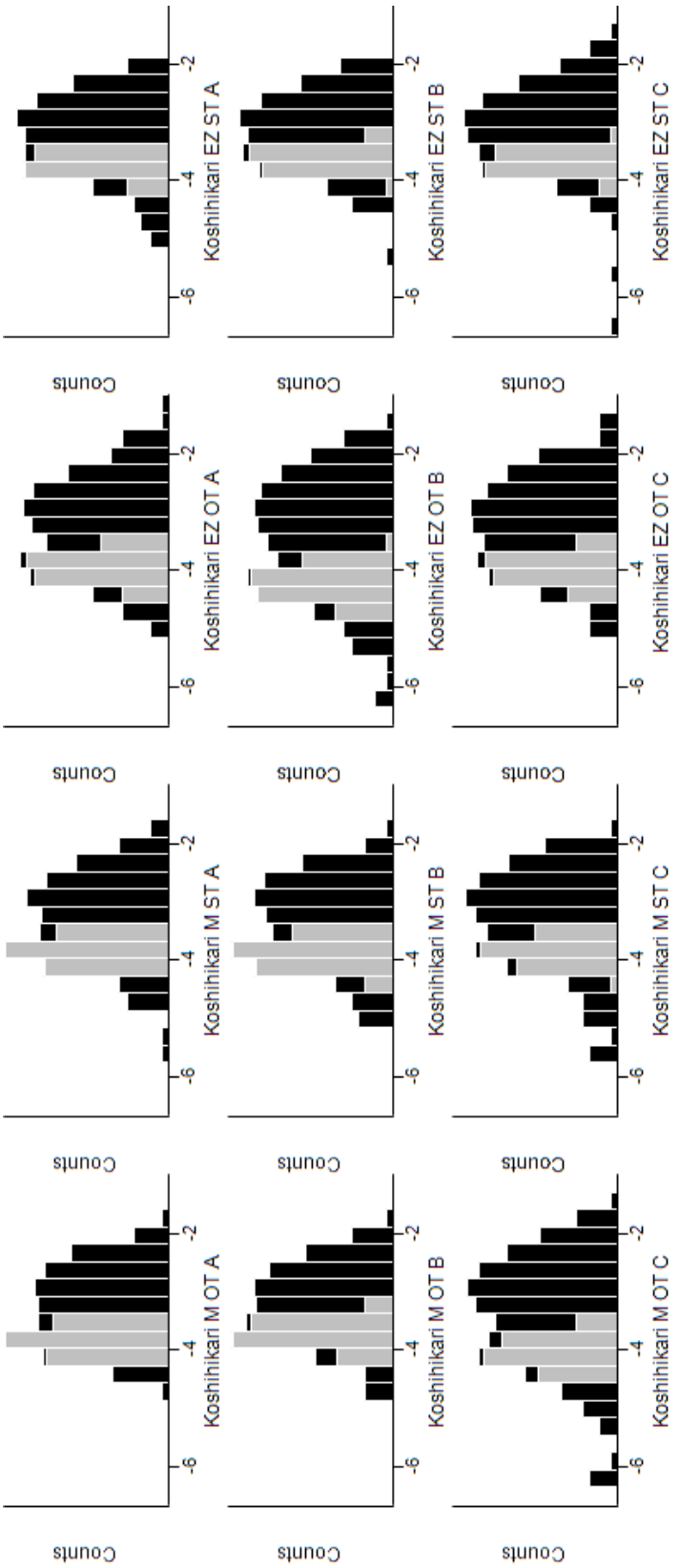

Supplementary Figure 8. Distribution of the peptide abundance data displayed as histograms for each sample of Koshihikari analyzed based on japonica proteins database. Data

is in scaled; in black is the whole data, in grey imputed missing values. Label of each sample is marked as follows: name of the cultivar (Koshihkari), zones (M: meristem; EZ: elongation zone), treatments (OT: optimal temperatures; ST: suboptimal temperatures), and sample pool (A, B, or C).

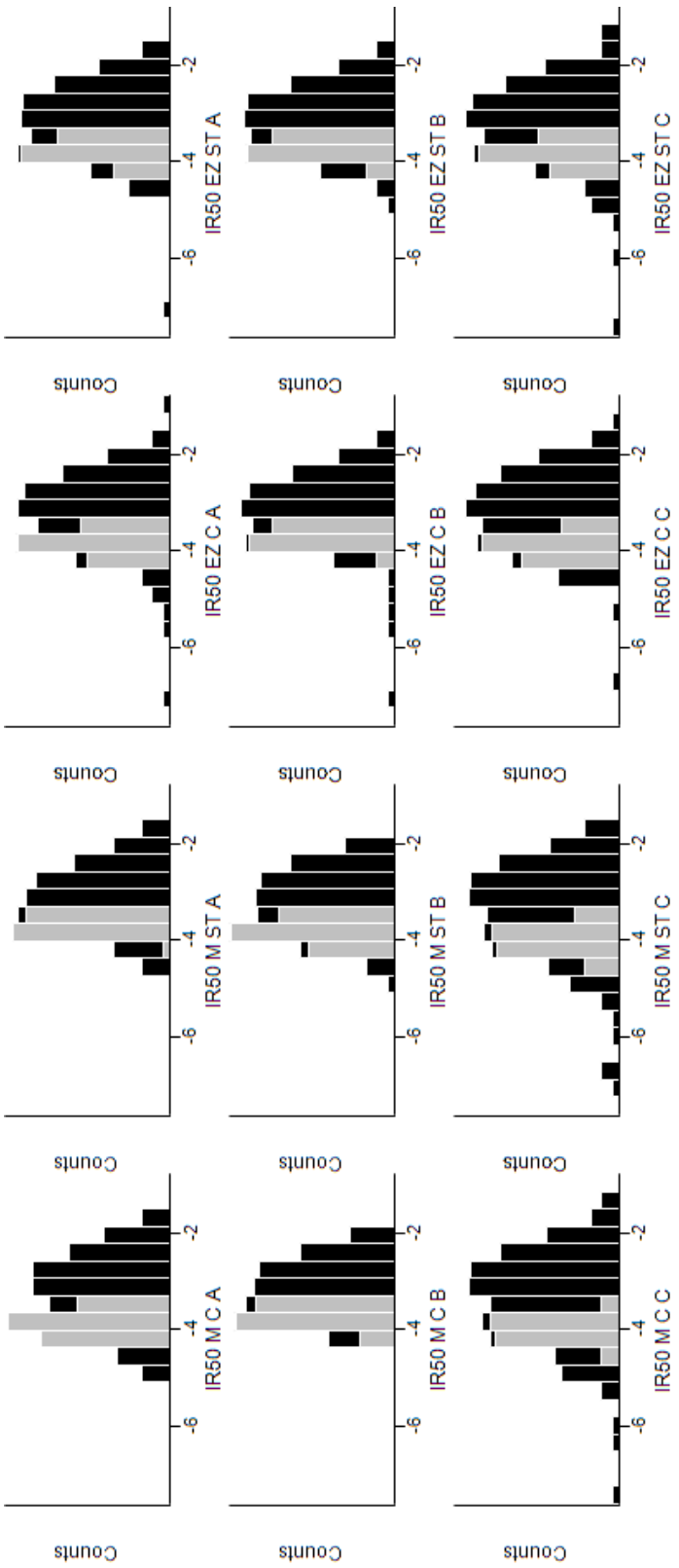

Supplementary Figure 9. Distribution of the peptide abundance data displayed as histograms for each sample of IR50 analyzed based on indica proteins database. Data is in-scaled; in black is the whole data, in grey imputed missing values. Label of each sample is marked as follows: name of the cultivar (IR50), zones (M: meristem; EZ: elongation zone),

treatments (OT: optimal temperatures; ST: suboptimal temperatures), and sample pool (A, B, or C).

Supplementary data

The supplementary data will be given as extra files upon asking to ayelen@gazquez.com.ar since the data do not fit in this Thesis. The supplementary data available correspond to:

Supplementary Data 1. Raw data of the transcriptome analysis in .CEL files.

Supplementary Data 2. Data from peptides detected in the proteome analysis before statistical analysis.

Supplementary Data 3. Peptide abundances in each sample after CONSTANd normalization. Empty spaces means the reporter ion was below the detection limit or missing. Zero means that peptide could not match across the different runs.